Chapter 18
Industrial Applications of Thermal Spraying Technology

Abbreviations

ACP	Amorphous Calcium Phosphate
APS	Atmospheric Plasma Spraying
BAG	Bioactive Glass
BOF	Basic Oxygen Furnace
BRT	Burner Rig Test
CMAS	Acronym of each oxide deposits CaO, MgO, Al_2O_3, and SiO_2
CNT	Carbon Nano-tubes
CFRP	Carbon Fiber-Reinforced Plastics rolls
C-SS-CS	Composite surface of Stainless Steel and Carbon Steel welded together
CTE	Coefficient of Thermal Expansion
C-W	Corrosion and Wear
dBA	decibel Authorized
d.c.	direct current
D-gun	Detonation-gun
DRC	Diamond-Reinforced Composite
EAF	Electric Arc Furnace
EBC	Environmental Barrier Coating
EB-PVD	Electron Beam-Physical Vapor Deposition
E–C	Erosion–Corrosion
EHC	Electrolytic Hard Chrome
EIS	Electrochemical Impedance Spectroscopy
FAC	Fe-based Alloy Coatings
FBC	Fluidized-Bed Combustor
fcc	Face Center Cubic
FG	Functionally Graded
FGC	Functionally Graded Coating
GDC	$Ce_{0.8}\ Gd_{0.2}\ O_{1.9}$
GS	Gas Shroud

P.L. Fauchais et al., *Thermal Spray Fundamentals: From Powder to Part*,
DOI 10.1007/978-0-387-68991-3_18, © Springer Science+Business Media New York 2014

HA	Hydroxyapatite $Ca_{10}(PO_4)_6(OH)_2$
HAT	HA Top coating
HB	Hardness Brinell
HCC	Hard Chromium Coating
HEPS	High-Energy Plasma Spray
HIP	Hot Isostatically Pressed
HPAL	High-Pressure Acid-Leach
HTBC	50 vol. % HA and 50 vol. % TiO_2 (HT)
HTH	(HA)/HA + TiO_2 bond coat composite
HVAF	High-Velocity Air Flame
HVLF	High-Velocity Liquid Fuel
HVOF	High-Velocity Oxy-fuel Flame
HVPS	High-Velocity Plasma Spray
HVSFS	High-Velocity Suspension Flame Spraying
IACS	International Annealed Copper Standard
IPS	Induction plasma spraying
LaMA	La $MgAl_{11}O_{19}$
LTA	$LaTi_2Al_9O_{19}$
LSCF	$La_{0.6}\ Sr_{0.4}\ Co_{0.2}\ Fe_{0.8}\ O_{32-\delta}$
M	Mole unit
MMCs	Metal Matrix Composites
MSWI	Municipal Solid Waste Incinerators
NTSRS	Net Thermal Spraying Residual Stress
ODS	Oxide-Dispersion Strengthened
OEM	Original Equipment Manufacturer
PA-12	Polyamide 12
PAH	Progressive Abradability Hardness
PECVD	Plasma Enhanced Chemical Vapor Deposition
PEEK	Poly-Ether-Ether-Ketone
PEI	Poly Ether Imide
PGDS	Pulsed Gas Dynamic Spraying
PS	Plasma Sprayed
PS-PVD	Plasma-Sprayed-Plasma Vapor Deposition
PTA	Plasma-Transferred Arc
PVD	Physical Vapor Deposition
QC	Quality Control
r.f.	Radio Frequency
RFC	Rolling Contact Fatigue
RH	Relative air Humidity
SBF	Simulated Body Fluid
SER	Specific Energy Requirement
SLPS	Super solidus Liquid Phase Sintering
SPS	Spark Plasma Sintering
SPS	Suspension Plasma Spraying

SPPS	Solution Precursor Plasma Spraying
SS	Stainless Steel
SSC	Sm0.5 Sr0.5 Co O3
STS	Special Treatment Steel
SW-SS	Spot-Welded Stainless Steel
TBC	Thermal Barrier Coating
TCF	Thermal Cycling Fatigue
TCHT	Thermo Chemical Heat Treatment
TCP	Tricalcium Phosphate
TCR	Temperature Coefficient of Resistance
TF-LPPS	Thin Film-Low Pressure Plasma Spraying
TGO	Thermally Grown Oxide
TSR	Thermal Shock Rig
TTCP	Tetra-Calcium Phosphate
UHTC	Ultrahigh Temperature Ceramics
VIPS	Vacuum Induction Plasma Spraying
VPS	Vacuum Plasma Spraying
WA	Wire Arc
YPSZ	Yttria Partially Stabilized Zirconia
YSZ	Yttria-Stabilized Zirconia
ZFA	ZrO_2–CaF_2–Ag_2O composite coating

18.1 Introduction

At its early stages of development, thermal spray technology was mostly used for the repair, rebuilding, retrofitting, and for surface protection against corrosion, erosion, and wear [1]. Up to the early 1980s, the basic phenomena involved in most of thermal spray processes were poorly understood, with the process parameters based more on the operator experience and skill, rather than on a solid scientific understanding of the phenomena involved. This often resulted in unsatisfactory process reproducibility and reliability. The wider acceptance of the technology for industrial-scale production has started in the late 1980s and early 1990s, with applications limited to high-added value components in the aeronautic and nuclear industry. These were mostly driven by the fact that no alternate viable solutions were available, and design engineers and scientists were used to work with rather complex processes.

Over the past decade, a wide range of industrial-scale surface modification processes became available. These are presently accepted for applications ranging from tribological and wear-resistant applications including lubricity and low-friction surfaces, to resistance to corrosion and/or oxidation, thermal protection, freestanding components, electrical and optical components, electromagnetic shielding, electrical insulation, abradable seals, biomedical applications, superconducting oxides, components with coefficient of thermal expansion tailored

to service conditions, magnetic coatings, solid oxide fuel cells, replacement of hard chromium, as well as ornamental applications. The choice of a specific coating and/or thermal spray process, for a given service condition, depends, however, on the expectation of the user and the cost that could be tolerated for the application. This affected, in turn, the selection of the material to be applied for the coating and the spray process to be used. The coating design process is often complicated by the fact that, in practice, components are not always devoted to a single requirement such as wear or corrosion or electrical insulation or thermal insulation. In most cases, coatings must resist to different combined needs: for example, wear is often linked to corrosion.

The different available spray processes are generally complementary and not competitive and any overlap between them in terms of application is not very broad. To choose one of them, it is important to know the advantages and limitation of each of these processes and to make the proper decision of the best process for each application. A review is given in Sect. 18.2 of the principal characteristics and limitations of different thermal spray processes and the criteria for their selection. The different applications will be briefly described in Sect. 18.3 together with the expected material properties adapted to each one. In Sect. 18.4 current applications of thermal-sprayed coatings by industry are described. As pointed out previously, the cost of the coating plays an important role in the final choice of the spray process. An economic analysis of the different thermal spray processes is presented in Sect. 18.5. A listing of the range of materials that can be used for different applications is provided in the appendix of this chapter.

18.2 Advantages and Limitations of the Different Spray Processes

In the following advantages and limitations of the different processes are presented. A comparative economic analysis of each of these processes is given in Sect. 18.5.

18.2.1 Flame Spraying

Two techniques are used: powder on the one hand and wire, cord, or rod on the other. With powders, the melting temperature of the material can be at best about 70 % of the flame temperature, while with rods or cords, it corresponds to 90–95 % of the flame temperature. The combustion process uses gaseous fuels, and the mean power of a torch is around 40 kW.

18.2.1.1 Powders

(a) As-Sprayed Coating

Sprayed materials are mainly metals or polymers, which are rather easy to melt and spray. Particles are axially injected into the flame. Coatings present a high porosity (>10 vol. %) and a low adhesion (<30 MPa). Powder feed rates is typically between 2 and 10 kg/h, depending on sprayed material and torch used. The deposition efficiency is around 50 %. In-flight oxidation of the powder occurs during processing (oxide content between 6 and 12 wt%). They are used for wear abrasion under low load and wear adhesion under low load. For details see Sect. 5.2.1. Substrate and coating must be cooled during spraying. Flame spraying is generally rather noisy (90–125 dBA).

(b) Remelted Coating (Flame, Furnace, Induction)

Self-fluxing alloys (see Sect. 5.2.2.2) contain Si and B (for example, CrBFeSiCNi) which are used as deoxidizers. When the coating is heat treated at about 1,030 °C they diffuse toward the coating surface trapping the oxygen. It results in coatings with almost no porosity, an excellent adhesion by diffusion at the substrate–coating interface. It is also very easy to deposit materials of brazing type, and composite coatings are possible. Of course these coatings are limited to substrates that can tolerate the fusing temperature (steel and not aluminum for example) and possibly any induced distortion. Such coatings are used against abrasion (friction, erosion) and corrosion (cold or hot).

18.2.1.2 Wire, Rod, or Cord

A compressed air jet atomizes the melted tip of the wire (metallic and ductile) or cored wires (containing ceramics or non-ductile materials), rod, or cord (for ceramics). Due to the compressed gas atomization, the noise level is not negligible. For details see Sect. 5.2.3. Compared to powders, the variety of materials that can be sprayed as wires, rods, or cords are larger. Wires of self-fluxing alloys can also be sprayed. Oxides are of course generated during the process, but less than with powders (about 4–8 wt%), and the deposition efficiency is better (around 70 %). Compared to powders the material flow rate varies from 5 to 25 kg/h. With wires the coating adhesion is slightly better than that obtained with powders. The porosity is similar to that obtained with powders except for ceramic materials that are more porous but present an excellent wear resistance. Generally the metal or alloy coatings are used against wear, especially abrasion or adhesion under low load,

for example, in rotating heavy equipments, piston rings and synchronizing rings, and atmospheric corrosion: bridges, large steel structures, galvanized tubing, ships, . . . The wire flame spray noise level is between 118 and 122 dBA, while with rods it is about 125 dBA. For details see Sect. 5.2.3.

18.2.2 D-Gun Spraying

This process is pulsed at a frequency between 6 and 100 Hz. Particle velocities are due to the energy of a detonation (explosion) (for details see Sect. 5.4.1). The resulting deposit is extremely hard, dense, and tightly bonded to the substrate. The process is the noisiest of all the thermal spray processes (more than 145 dBA). Coatings porosity is low (below 1 vol. %) and its oxygen content is between 0.1 and 0.5 wt%. The deposition efficiency is around 90 %, but powder flow rates are limited to the 1–2 kg/h range. Sprayed materials are mainly powders of metals, alloys, and cermets. Some oxides can also be sprayed by this technique as long as particle sizes are below 20 μm. The main applications are abrasion and adhesion (friction) under low load as well as corrosion. Substrate and coating must be cooled during spraying. For more details see Sect. 5.4.1.

18.2.3 HVOF–HVAF Spraying

HVOF and HVAF are also combustion-driven processes with internal combustion at pressure below 1 MPa for those with gaseous fuel and slightly higher for those with liquid fuels. They produce very high-velocity gas streams, thanks to a convergent–divergent nozzle following the combustion chamber (see Sect. 5.3.1.1). In most cases, particles are axially injected but radial injection is possible with some guns. Power levels for HVOF guns working with gaseous fuels are in the range of 100–120 kW, with a noise level of 125–135 dBA. For those working with liquid fuels, the power can reach 300 kW with a noise level of 133 dBA or more. The actual trend is to increase particle velocities and reduce their temperatures in order to limit their oxidation (see Sect. 5.3.1.5), the high-kinetic energy of particles compensating for the lower temperature. This was first realized with HVAF guns working with air and where the noise level was 133 dBA or more. In the high-power guns, especially designed for that, high quantities (up to 2,000 slm) of nitrogen are injected in the combustion chamber to reduce gas temperature and increase its velocity. Globally this process, working mainly with metals, alloys, and cermets (one of their most successful application) has deposition efficiencies of about 70 % for powder flow rates up to 7.2 kg/h for gaseous-fuel guns, and up to 12 kg/h for liquid-fuel guns with deposition efficiencies roughly of 60–80 %. Resulting coating porosities are a few vol. %, with a good adhesion (>50–60 MPa) and low oxygen content (between 0.5 and a few wt%). Due to shot-peening effect, stresses are compressive and rather

thick coatings can be achieved (up to 6.4 mm). Of course the process is noisy, dusty, and requires special safety precautions for the handling of large flow rates of explosive gases. As with D-guns, the main applications of HVOF and HVAF spraying guns are against wear and corrosion. The wear resistance: sliding/adhesive wear, fretting, erosion or cavitation, of course depending on the material and process parameters chosen, is generally excellent. The corrosion resistance is also very good with the high density of coatings and, according to the sprayed material, they are used for hot corrosion, oxidation, against acidic or alkaline atmospheres and liquids. Substrate and coating must be cooled during spraying. A few processes have been developed to spray wires but in most cases powders are used. For details see Sects. 5.3.1 and 5.3.2

18.2.4 Wire Arc Spraying

Two wires or cored wires are continuously fed to a point where the arc striking at their tips melts them and an atomizing gas form the superheated spray droplets accelerating them toward the substrate. The high-droplet temperatures produce metallurgical interactions or diffusion zones or both after impact with the substrate or previously deposited layers. The maximum arc current, can vary from 200 to 1,500 A. This process spray rates between 5 and 30 kg/h, with deposition efficiency of about 80 %, are higher than most other spray processes. Consequently, it is one of the most economical processes, as long as the materials to be sprayed can be obtained in the form of wires or cored wires. The noise level is similar to that of wire flame process: 118–122 dBA. The oxide content depends strongly on the sprayed materials but is rather high, over 25 wt% for Al, for example. Using nitrogen instead of air as atomizing gas can reduce the oxidation level in the deposit, but depending on the required gas flow rates (around 1.0 m^3/min or more) the process becomes expensive. Porosity is usually over 10 vol. % and the coatings adhesion is medium in the 40 MPa range. An advantage is the minimal heating of the substrate, while the divergence of the spray pattern is a disadvantage. As other spray processes it is noisy and dusty. Coatings can be used for abrasion and adhesion (friction) under low load but their main use is for atmospheric or marine corrosion protection and a broad range of electrical applications. For more details see Sects. 9.2, 9.7, and 9.8.

18.2.5 Plasma Spraying

With temperatures over 8,000 K any material whether metallic or ceramic can be melted. At conventional spray distances, 10–12 cm, the heat flux to the substrate is among the highest ($\approx$2 MW/m^2) and the substrate as well as the coating must be cooled. To avoid oxidation, spraying must be performed under controlled atmosphere or soft vacuum conditions.

18.2.5.1 Air Plasma Spraying

The heat source is a direct current (d.c.) arc through which flows a nonoxidizing and/or non-carburizing gas. In most cases powder injection is radial. For plasma spray torches with one-stick type cathode, power levels range from 30 to 90 kW. For power levels in the range 40–50 kW, the powder flow rate is between 3 and 6 kg/h, the deposition efficiency around 50 %, and the torch noise level between 110 and 125 dBA. With high-power torches (250 kW), powder flow rates as high as 15–20 kg/h can be reached. With tri-cathode torches, torch power varies from 40 to 80 kW. Plasma torches developed by Mettech comprise three-plasma jets converging in a nozzle which length and diameter can be varied; particles are axially injected between the three converging plasma jets and power levels reach 150 kW.

Plasma-sprayed coating porosities are between 2 and 8 vol. %, the oxygen content of metal or alloy coatings being between 1 and 5 wt% and their adhesion is good (>40–50 MPa). They are mainly used to spray oxides. However they present good resistance to abrasive, adhesive, fretting, or sliding wear. They also produce thermally conductive or resistant surfaces. They are used for salvage and restoration of worn surfaces. For details see Sects. 7.3 and 7.8.

18.2.5.2 Inert Atmosphere Plasma Spraying

When oxidation is a problem, metals with high-melting temperature and non-oxide ceramics can be sprayed only in inert atmosphere (chamber filled with argon), at atmospheric pressure or slightly over. The technique is mostly used to melt materials with high-melting temperature, such as TaC, which has a melting temperature close to 4,000 °C. The controlled atmosphere chamber must be water cooled if its volume is below 10 m^3, and industrial scale production of such coatings requires using antechambers (connecting zones) to introduce and remove parts from the chamber, without allowing for air penetrating the main chamber. The noise level is that of the surrounding pumps, fans, and power supply. With all the equipment required, including that of argon gas recycling (see Sect. 17.4.3), the equipment cost is rather high compared to that of air plasma spraying.

18.2.5.3 Vacuum d.c. Plasma Spraying (VPS)

In this case the controlled atmosphere is at a pressure below atmospheric (in the tens of kPa range, see Sects. 17.4.1 and 7.9) and can even be below the 0.1 kPa range, for vapor deposition (see Sect. 17.4.2). According to the plasma jet expansion, the mean ambient temperature in the chamber is over 200 °C. The noise level is similar to that of inert atmosphere spraying. The equipment is more complex than that of inert atmospheric pressure spraying and consequently is the most expensive of all spray processes. One of the advantages of the process, besides the significant

reduction of oxidation, is the possibility to remove the oxide layer from the substrate. This is achieved with a transferred arc etching the surface of the substrate prior to deposition, the part to be coated being in a reversed polarity (cathode of transferred arc). During the deposition step, the part is heated to a sufficiently high temperature to achieve diffusion bonding between the sprayed metal or alloy and substrate, the part being then the anode of the transferred arc. This process is used for high-added value parts, such as turbine blades.

18.2.5.4 Induction Plasma Spraying (VIPS)

Induction plasma spraying is usually carried out under controlled atmosphere at atmospheric pressure (IPS), or soft vacuum conditions, down to 10 kPa (VIPS) (for more details see Sects. 8.2 and 8.5). The process is essentially similar to d.c. vacuum plasma spraying (VPS), with the exception that the torch is fixed with respect to the chamber walls, while the substrate has to be translated in a linear or rotating movement across the stream of molten droplets immerging from the torch at the required spraying distance. With torches i.d. of a few tens of mm, against below 10 mm for d.c. ones, the plasma jet velocity is considerably lower (<100 m/s) than that of a corresponding d.c. plasma jet, at a comparable power rating. It allows spraying bigger particles (up to 200–250 μm) than those sprayed with d.c. torches. Typical plasma power ratings for VIPS installations are in the 50–400 kW range, with corresponding powder feed rates of 2–10 kg/h, depending on the sprayed material. Induction plasma spraying is mostly used for the spraying of metals and ceramics on small parts with a high-added value and coating densities close to 98 % of the theoretical value. VIPS is used on an industrial production scale for the deposition of high purity silica on fiber optics performs and refractory metals on X-Ray targets. However one of their main applications is powder spheroidization to produce powders with an excellent flow ability that are used for many applications not necessarily linked to spray processes. For more details on VIPS equipment, design, and operating conditions see Sect. 8.5.

18.2.6 Plasma-Transferred Arcs (PTA)

The process is a combination of welding and thermal spraying process that requires electrically conductive substrates acting mostly as the anode. The feedstock is wires or powders with particle sizes in 100 μm range. Metals, alloys, and cermets are sprayed using PTA techniques. The different guns are characterized by the maximum current varying from 200 to 600 A. The coatings are thicker than those of other spray processes; they can be 10 mm thick or more, and a metallurgical bond with the substrate is achieved. The substrate must be kept as horizontal as possible during spraying. No porosity is observed and the deposition efficiency is over 90 %.

Powder flow rate can be as high as 18 kg/h or even more with high power devices. The resistance to wear is excellent as well as that to high temperature corrosion. These coatings are used to achieve high-quality rebuild surface, to coat large and heavy parts without cracks or deformation, to produce smooth and highly wear-resistant surfaces. PTA coatings are used against wear in different industries: mining, pulp and paper, oil and gas, power, . . .

18.2.7 Plasma Transferred Arc

The process is significantly different from the other coating processes as the substrate is part of the electrical circuit that delivers the power for the coating process. As the substrate in most of the cases serves as the anode of the arc transferred from the torch it must consist of an electrically conducting material. The stability of the arc is improved when using a "pilot arc" between the cathode and the nozzle of the transferred arc, which becomes the anode of the transferred arc. It requires a two-stage power supply or two independent power supplies. The powder, bigger than with most other spray processes (typically 50 to 150 μm), is introduced into the arc plasma though two or more orifices located on a ring surrounding the exit of the nozzle. A further annular slot surrounding the powder injection ring provides the shield gas flow, necessary to avoid reaction of the molten metal pool with the environmental air. The coating is different from those obtained from other thermal spray coating processes because the arc melts to some degree the substrate material, and the molten powder of the coating material is mixing with the molten substrate material. The consequence is that a good metallurgical bond or fusion bond is achieved, and that the porosity is very low, however, the heat penetration region and in particular the region where the coating material is mixed with the substrate material can change the properties of both the substrate and the coating. This mixing region is expressed in terms of the "dilution". Torches used are divided into three different categories according to the deposition rate and the power used: Micro PTA with deposition rates of 0.1–2 kg/h, used for small components, or components with complex shapes, regular PTA for deposition rates of 2–10 kg/h, and high power PTA for deposition rates between 10 and 20 kg/h.

Compared to other coating processes, the substrate must be metals or alloys, coatings are also metals or alloys with the possibility to achieve cermet coatings, the deposited metal must be compatible with that of substrate. Coatings are also different because they are generally fully dense and considerably thicker than other coatings (up to a few cm). Their main use is for wear and corrosion resistance applications. For more details see Chap. 10.

18.2.8 Cold Spray

Cold spray is mostly used for the spraying of metals on virtually any substrate, with the main advantage of avoiding the in-flight oxidation of the powder and achieving high coating densities. With this spray process, the oxide content of the coating is limited to that of the sprayed powder (for example, less than 100 ppm for copper). After optimization of the spray parameters and proper choice of powder characteristics, the mechanical and electrical properties of as-sprayed coatings are remarkably close to those of bulk materials, especially with very good tensile properties. However the ductility of cold-sprayed coatings can be rather low due to the important work hardening inherent to the process. Coatings are made of pure metals, ferrous, and nonferrous metal alloys, composites, and cermets; provided, they are ductile (at least the matrix for cermets). The noise level is about 110 dBA. For more details see Sect. 6.2. The drawback of the process is the high nitrogen or helium (or both) flow rates needed. With flows in the few m^3/min range within the de Laval-type nozzle, particles achieve very high impact velocities (up to 1,200–1,500 m/s). Recycling helium requires to spray in a controlled atmosphere with the chamber adapted to the part size, and if necessary antechambers to introduce it, and use pumps, filters, and tanks to recycle the gas, thus increasing the investment. In this case, the noise level is that of the surrounding equipment. The deposition rates are in the 2–10 kg/h with deposition efficiency in the 40–90 % range depending strongly of sprayed materials. The first and very successful application was copper metallization, then the selective protection of localized areas against corrosion, rapid tooling repair, electromagnetic shielding, and repair of magnesium components. It is also used for metal restoration and sealing, engine blocks, castings, molds and dies, refrigeration equipment, heat exchangers, for aluminum piston heads, manifolds, disc brakes, for heat sinks for microelectronics (Al and Cu), for solid lubricant matrix with base metals, for electronically conductive coatings (Cu or Al on ceramic or polymeric components), for localized corrosion protection (Zn or Al coatings), . . .

18.3 Thermal-Sprayed Coating Applications

Of course the list presented below is far to be exhaustive and its goal is to emphasize the wide variety of thermal-sprayed coatings. However the reader must keep in mind that the sprayed materials (see Appendix) have mechanical, thermal, service properties different from those of bulk ones. They depend on the real contacts between layered splats, porosities, crack types and distributions, oxide inclusions, materials partial decomposition (WC for example). Coating morphologies and microstructure are linked to the spray process used, the morphology of the sprayed particles, depending on their manufacturing process, the spray parameters, the substrate used, the coating thickness and the possible post-treatments of coatings (annealing, laser, hot isostatic pressing, . . .). For each topic a few examples are given.

18.3.1 Wear Resistant Coatings

"Wear is the problem" and it occurs in almost all industries where thermal-sprayed coatings are used. In all cases, it is a progressive loss of material at the active surface due to the relative movement of another part or particles on this surface. The lifetime of the coating depends on its resistance to wear and its thickness, which can reach up to 10 mm with PTA coatings. The different types of wear are described below, according to [2–8]. For each type of wear, a few examples of coatings are presented.

18.3.1.1 Abrasive Wears

It corresponds to weight loss with grooves, pits, and scores at the surface due to cutting or deformation. It results from either two-body abrasion where the asperities or defects of one of the surface plough or abrade the counter face, or three-body abrasion where hard particles move freely between both surfaces or are imbedded in one of them (for more details see Sect. 15.9.1). The phenomena are promoted when temperature, humidity, aggressiveness of the environment (corrosion) increase. The three-body abrasion depends also on the shape, grain size, and hardness of the abrasive particles and the relative speed of the two bodies. As a general rule abrasion increases drastically as soon as the hardness of one metal or alloy becomes equal to that of the abrasive particles. If the abrasive belongs to the surrounding medium the contact must be protected from it and wear debris must be removed or trapped. At last the roughness of the harder surface must be reduced to the minimum. It must be emphasized that abrasion wear represents more than 50 % of wear. In most cases wear-resistant coatings are hard with a good resistance to heat and chemical attack; coating materials with such properties are [2]:

(a) Self-Fluxing Alloys

If their corrosion resistance is generally excellent, their hardness is not particularly high and they cannot compete with cermets for sliding wear resistance. Thus one can either spray them with hard particles or heat-treat them. This for example the solution proposed by Bolelli and Lusvarghi [9]. After HVOF spraying Co-28 %Mo-17 %Cr-3 %Si coatings, they studied them as-sprayed and after heat treatments at 200, 400, and 600 °C for 1 h. A significant degree of splat boundary oxidation existed in the as-sprayed coating, because of exothermic oxidative reaction occurring at $T > 810$ °C; thus, it had low hardness and toughness, resulting in poor tribological performance. The 600 °C treatment caused the appearance of submicrometric crystalline regions improving hardness and elastic modulus and the sliding wear performance at room temperature was improved. Kulu and Hailing [10] have flame-sprayed NiCrSiB self-fluxing alloy-base composite powders,

containing WC–Co hard metal powders (from 15 to 50 wt%) from used (recycled) hard metals. They compared them with D-gun-sprayed WC–Co particles. The wear resistance of coatings at small impact angles of abrasive particles increased with an increase in matrix phase hardness as well as with an increase in hard phase content in the composite. However the wear resistance of the self-fluxing alloy coatings, reinforced with hard metal particles, was low at straight impact. Sakata et al. [11] have flame-sprayed Co-based (Co–Cr–W–B–Si) self-fluxing alloy coating. The diffusion treatments of thermally sprayed Co-based self-fluxing alloy coating on steel substrate were carried out at 1,370–1,450 K for 600–6,000 s under an Ar gas atmosphere. The proper diffusion treatment precipitated two kinds of fine compounds in Co-based matrix: a chromium boride dissolving cobalt and a tungsten boride containing cobalt and chromium. The size of each precipitate became larger with increasing treatment temperature and time. A coating with the proper size borides showed a superior wear resistance. The diffusion treatment temperature of 1,397–1,406 K substantially improved the abrasion resistance. Otsubo et al. [12] fused flame-sprayed coatings of nickel-base self-fluxing alloy, containing chromium and boron, and also showed that they resulted in complex structures. Kulu and Pihl [13] have sprayed WC–Co systems and self-fluxing alloys, containing tungsten carbide-based hard metal particles [NiCrSiB-(WC-Co)], by the detonation gun, HVOF JP 5000 that they called "continuous detonation spraying," and spray fusion processes. They found that coatings must have the following properties: minimum porosity (less than 3 vol. %), hardness higher than that of the abrasive, and a metal matrix structure containing particles of WC–Co granules, or WC–Co particles to have a good resistance to oblique impact and normal impact. Miranda and Ramalho [14] studied coatings sprayed, with different proportion mixtures, two commercial alloys, a nickel self-fluxing alloy and a tungsten carbide–cobalt. Coatings were sprayed by HVOF and powder oxyacetylene flame processes. The effect of both hard-phase content and coating-spraying technique on abrasion resistance was studied in terms of the coatings' mechanical properties and microstructures. For coatings produced by powder flame spraying, the remelting after spraying led to increased adhesion to the substrate and also higher hardness, especially in the coatings with a larger WC + Co percentage. PTA is used against abrasive wear in petrochemical, mining and agricultural applications see Sect. 10.7.3 of Chap. 10.

(b) Cermet Coatings, Especially Those HVOF or HVAF Sprayed

Coating quality is strongly linked to the spray process and parameters, especially with WC particles. If corrosion problems are also to be considered, Cr is important in the metal matrix. For example, Schwetzke and Kreye [15] have sprayed different WC–Co and WC–Co–Cr powders with various high-velocity oxygen fuel spray systems (Jet Kote, Top Gun, Diamond Jet (DJ) Standard, DJ 2600 and 2700, JP-5000, Top Gun-K). Powders exhibited various degrees of phase transformation during the spray process depending on type of powder, spray system, and spray

parameters. Phase transformations increased when the injection of the powder occurred in a region where the flame temperature was highest, for example, into the combustion chamber of the Top Gun system. Decarburization of agglomerated and sintered WC–Co 83-17 powder ranged from 25 to 70 % for the various spray systems and fuels. When the carbon loss remained below 60 %, the properties of the coatings such as hardness and wear resistance were not influenced. The decarburization seemed to be compensated by the hardening with the formation of a solid solution of cobalt (tungsten, carbon) and hard W_2C and h-phases. If the wear resistance of WC–Co–Cr coatings were comparable to those of WC–Co, the corrosion resistance of WC–Co–Cr was considerably higher.

Kasparova et al. [16] have evaluated the abrasive wear resistance and adhesive strength of HVOF-sprayed WC–Co and the Cr_3C_2–NiCr coatings. They found that high-stress abrasive conditions change the coatings behavior very significantly, particularly that of the Cr_3C_2–NiCr coating. The high-plastic deformation and pulling out of entire splats or splat blocks, especially during abrading by the alumina sand, were detected under the high-stress abrasive conditions for both coatings, but much more with Cr_3C_2–NiCr. As shown by Houdkova et al. [17], the spraying angle is one of the deposition parameters that influence the quality of thermally sprayed coatings. They HVOF (TAFA JP-5000) sprayed WC–Co and Cr_3C_2–NiCr coatings with different spray angles. Their results showed that with a maximum 30° angle diversion from the normal spray direction for WC–Co and 15° angle diversion for Cr_3C_2–NiCr coatings wear resistance was not reduced. Tillmann et al. [18] used statistical design of experiments to identify the most relevant factors influencing the HVOF spraying of fine $75Cr_3C_2$–25(Ni20Cr) powders and find an optimum setting of these factors to produce coatings with improved morphological and mechanical properties. Fine structured coatings obtained showed an extremely dense and finely dispersed structure (porosity <2 vol. %), a high surface quality (Ra < 2 μm) and a high adhesive strength. These coatings showed a high potential to be used as wear-resistant coatings for large tools without any post treatment or surface finish.

Recently, considerable emphasis has been placed on HVOF thermal spraying of nanostructured WC/Co to achieve high hardness combined with excellent wear resistance. However, it appeared difficult to achieve dense coatings and avoid decarburization. Skandan et al. [19] have HVOF-sprayed homogeneously mixed powders. They consisted of WC/12 Co agglomerates in the range 15–40 μm with a carbide grain size of 2–5 μm (70 vol. % of the mixture) and WC/5 Co, forming particles in the range 0.1–0.5 μm with each particle composed of many WC nanometer-sized crystals (~30 nm in diameter). The coating was dense and had no decarburized phases. The abrasion wear resistance was at least 50 % better than that of a pure coarse-grained WC/Co coating. In their review Lima and Marple [20] have presented superior abrasion and sliding wear performance of nanostructured ceramic coatings (Al_2O_3, Al_2O_3–13 wt% TiO_2, Al_2O_3–3 wt% TiO_2, TiO_2, and YSZ) when compared to those of conventional coatings. By employing HVOF and nanosized ceramics, the abrasion wear levels could be reduced by up to 90 % in comparison with the wear performance of optimized APS conventional ceramic

coatings. It was generally observed that the nanostructured coatings were not harder than the conventional ones; however, they tended to be much tougher. Kim and Walker [21] have developed nanostructured titania coating specifically for ball valves destined for high-pressure acid-leach (HPAL) service. These coatings were compared to conventional ones. The nanostructured titania coating provided dramatically superior resistance against abrasive and erosive wear, better wear performance attributed to improved toughness.

Gawne et al. [22] have plasma-sprayed ball-milled mixture of glass and alumina powders to produce alumina–glass composite coatings. The alumina raised the mean hardness from 300 HV for pure glass coatings to 900 HV for a 60 wt% alumina–glass composite coating. The scratch resistance increased by a factor of 3 and the wear resistance by a factor of 5, maximum value obtained with 40–50 vol. % alumina. This alumina content corresponded to the change over from a glass matrix to an alumina matrix. Cipri et al. [23] produced thick alumino-silicate coatings by plasma-spray technique. Coatings, efficiently coupling to metallic substrates even after plastic deformation, exhibited very interesting performance in terms of mechanical properties and fracture toughness (elastic modulus of 43 GPa and K_{1c} of about 2 MPa $m^{1/2}$ for 850 μm thick coatings) and compliance. Thus they showed an excellent refractory behavior allowing a wide use as wear-resistant thermal barrier coatings in metallurgical and glass plants and in high-temperature heat exchangers. At last to illustrate the interest of such coatings, Kang et al. [24] used detonation gun to spray three different WC–Co–Cr, Cr_3C_2–NiCr, and Stellite-21 coatings on high-tensile steel rotavator blades. The wear rates of Cr_3C_2–NiCr and Stellite-21 coated blades showed significant superiority over the uncoated blade, but not as much as shown by WC–Co–Cr coated blade.

18.3.1.2 Erosive Wear

It occurs when hard particles carried by a fluid hit the surface (for details see Sect. 15.9.3). The impact angle plays an important role on the wear rate depending on the surface material: ductile, hard metal, ceramic, . . . [4, 5]. To reduce the wear, one must choose a coating material harder than the abrasive particles, with toughness high enough, especially for inclined impact angle between 30 and 45°, which must be avoided if possible, and the coating roughness must be reduced to the minimum. It is also important to avoid turbulences in service conditions because they increase erosion. The erosion is much more complex than abrasive wear in which the wear resistance is predominantly influenced by the hardness of the coatings. The erosion depends on the response behavior of coatings to the impact of erosive particles at high velocity. It is usually considered that the wear and erosion resistance of cermet coatings are predominating influenced by their microstructures including the splat size, carbide particle size, carbide content, and carbide distribution within a splat, and the cohesion between the splats [25, 26]. For example, Kim et al. [25] showed that inter-splat cohesive strength of coatings, measured by a simple bonding test, was the most significant factor relating to the wear rate of plasma-sprayed

WC-12 wt% Co coatings. As previously emphasized, the microstructure strongly depended on starting powder, spray system, and spray conditions. Other parameters, such as the influence of time, solid loading, impingement angle, temperature, particle velocity, as well as the erosion–corrosion mechanism must also be considered [27]. When comparing the influence of dry and slurry erosion on HVOF coatings, it was shown that erosion rates in dry particle impact were about three orders of magnitude higher than those in slurry systems. This difference probably reflects the real erodent target impact velocities, which are mitigated in the slurry test by the water medium [28]. A few examples are presented below. Ji et al. [29] have HVOF-sprayed Cr_3C_2–NiCr coatings and erosion tests were performed at different jet angles of abrasive particles. The erosion occurred dominantly by spalling of splats from the lamellar interfaces, spalling resulting from the propagation of cracks parallel to the interfaces between the lamellae exposed at the surface and underlying coating. The carbide particle size and content in the coating influenced significantly the erosion performance of Cr_3C_2–NiCr coatings. Yang et al. [30] have compared the high-temperature erosion behavior of HVOF-sprayed Cr_3C_2–NiCr coating with mild steel for circulating fluidized bed boiler tubes. The erosion rate of the HVOF-sprayed Cr_3C_2–NiCr coating was not influenced by the temperature in the range of 300–800 °C, while that of the mild steel at 800 °C was four times that at 300 °C at an erosion angle of 30°. Osawa et al. [31], for WC–Co HVOF-sprayed coatings, have shown that the substrate also played a role in coating erosion resistance. For the studied variety of steel substrates, the near-surface hardness of the substrate resulting from the work hardening caused by peening during the grit blasting and HVOF spraying played a dominant role. It improved the ability of the substrate to support the coating and thus the integrated coating-substrate performance during impact loading. Kulu et al. [32] sprayed, by detonation gun, HVOF JP 5000 spraying, and spray fusion process, tungsten carbide-based hard metal, nickel-based self-fluxing alloy, and composites NiCrSiB. For all of them the erosion was strongly affected by particle impact angle. For all materials tested, the erosion rate was 5–6 times higher at elevated temperature, but in that case, the influence of impact angle had no great effect. Ramesha et al. [33] have plasma-sprayed Inconel-718 (thicknesses of 200 μm and 250 μm) on mild steel. Increased coating thickness decreased the porosity and increased the hardness significantly. Inconel-718 coatings exhibited improved slurry (containing 3.5 vol. % NaCl) erosive wear resistance when compared to uncoated mild steel. The wear resistance increased with coating thickness. Higuera Hidalgo et al. [34] have compared the behavior of plasma- and flame-sprayed modified nickel–chromium alloy (with small aluminum and titanium additions) subjected to the action of simulated post-combustion gases from a coal-fired boiler combustor. With flame, the adherence was much lower even with a bond coat. High-temperature oxidation rate of nickel–chromium coatings in post-combustion gases from coal-fired boilers, (atmospheres with 3–3.5 vol. % of free oxygen) was low. The embedment of fly ash particles on the surface of coatings was especially important at higher temperatures (800 °C). The erosion behavior of nickel–chromium flame and plasma-sprayed coatings at medium temperatures (500 °C) was characterized by low erosion rates

and a ductile erosion mechanism. At 800 °C the wear was essentially corrosive. Krishnamurthy et al. [35] studied the erosion resistance of plasma-sprayed alumina and calcia-stabilized zirconia coatings on Al-6061 substrate. It was found that erosion of coating systems occurred through spalling of lamella exposed on coating surface resulting from cracking along the lamellar interface. Erosion wear was more at 45° angle of impact. Pores seemed to act as stress concentrators and decreased the load-bearing surface. At last, the promising behavior of unconventional nanoscale composite coatings must be underlined. Branagan et al. [36] have wire arc-sprayed amorphous SHS7170. Coatings were found to develop an amorphous matrix structure containing starburst-shaped boride and carbide crystallites with sizes ranging from 60 to 140 nm. The performance of the SHS7170 coatings in boiler environments was measured via elevated temperature erosion experiments conducted at 300, 450, and 600 °C using bed ash from an operating circulating fluidized-bed combustor boiler, and the results were compared with those for existing boiler coatings. The elevated temperature erosion resistance of the SHS7170 wire arc coatings was found to be superior, based on thickness loss, compared with the existing wire arc coatings that have been tested. SHS7170 coatings have resisted to erosion almost independently of contact angle.

18.3.1.3 Friction and Adhesive Wears

It occurs when particles are transferred from one interacting surface to the other. When different materials are in contact, particles are mainly transferred from the softer or weaker material onto the harder one. This wear is promoted when increasing the load and/or the temperature, and under dry friction, or poor lubrication (see Sect. 15.9.2). It depends on the structure, composition, hardness, and melting temperature of the material.

To reduce it, dry friction must be avoided and, if it is not possible, coatings containing solid lubricants or retaining lubricants must be used. The compatibility of materials is also important: the friction coefficient, f ($f = T/N$, $T =$ tangential force, $N =$ Normal force), depends on the couple of materials rubbing against each other. It is also linked to the load, P, (or more precisely the pressure, p), and the relative velocity, v, between both parts (in principle the product, $p \cdot v$, must be below 1 MPa m/s [3]) The roughness of surfaces into contact must be as low as possible and from a rough surface (Ra of a few μm) to a smooth one (Ra < 0.1 μm), f, can be reduced by 60 %. Dry friction, usually results in high local heating and, even with a very low relative velocity, the friction coefficient, f, increases with temperature. Low friction coefficients can be achieved with solid lubricants ($f = 0.001$–0.05), but the relative velocity must be low. Using materials with a high thermal conductivity (both coating and substrate) reduces the heating due to friction. As wear increases with the energy of adhesion, it is also important to avoid micro welding, i.e., to use materials with a low solubility and a narrow range of solid solution (ex: Fe/Al, Fe/Cu). The work of adhesion decreases with the

following couples: metal–metal, metal–ceramic, ceramic–ceramic, metal–polymer, ceramic–polymer, and polymer–polymer. A few examples are presented below.

High stress, due to too high average pressure or very high local pressure that exceed the elastic limit, might be favorable when it strengthens the material by work hardening, but it might result in surface embrittlement of surface layers reducing their fatigue strength. It is promoted by an increase of the friction coefficient or temperature. Here again the worst occurs when cracks propagate.

(a) Ceramic Materials

Pantelis et al. [37] have plasma sprayed a 450 μm thick Al_2O_3 coating deposited on cast iron substrate. Wear tests were carried out with normal force varying from 50 to 160 N, sliding speed of 1.40 m/s, and average relative humidity of 60 %, using as a counter-body a quenched D2 tool steel (D-type tool steels contain between 10 % and 18 % chromium and D2 is very wear resistant but not as tough as lower alloyed steels). The coating wear rate presented three stages. During the first one, the wear rate was decreasing rapidly and the wear of the coating proceeded via adhesion mechanism. During the second stage, wear rate remained almost constant and the wear of the coating was taking place via a combined "polishing/abrasion/fatigue" wear mechanism. During the last stage, wear rate increased rapidly until the total worn of the ceramic layer due to the "easy" removal of the completely cracked remained coating. The D2 tool steel counter-body was also worn out by a combination of wear mechanisms. Sanchez et al. [38] have plasma-sprayed Al_2O_3–13 %TiO_2 coatings on stainless steel substrates from conventional and agglomerated nanostructured powders. The wear resistance of conventional coatings was shown to be lower than that of nanostructured coatings. As already emphasized in Chap. 14, Darut et al. [39] found that the friction coefficient of Al_2O_3 coatings, suspension plasma sprayed (SPS), was decreased by a factor of 2 compared to that obtained with micrometer-sized particles; meanwhile, alumina was not a material suitable for friction layers. Moreover, wear rate was 30 times lower for SPS layers compared to the conventional ones. Bolelli et al. [40] have HVOF-sprayed alumina suspensions and compared them to coatings obtained with conventional powders sprayed with APS and HVOF. With the suspension, porosity is much lower and pores are smaller than in conventional coatings. Moreover, few inter-lamellar or intra-lamellar cracks exist, resulting in reduced pore interconnectivity (evaluated by electrochemical impedance spectroscopy). Such strong inter-lamellar cohesion favors much better dry sliding wear resistance at room temperature and at 400 °C. Ahn and Kwon [41] studied the tribological behavior of plasma-sprayed chromium oxide coatings against cast iron both in dry at 450 °C and lubricated wear tests at room temperature and 200 °C. Under dry sliding conditions, dispersed smooth surface films were formed by plastic deformation of compacted debris particles that adhered to the surface and these films strongly influenced the friction coefficient and wear rate of the coating. Considerable quantity of CrO_3 was detected at room temperature, whereas CrO_2 (more favorable

than CrO_3 in reducing friction) was detected at 450 °C. Under lubricated sliding conditions, tribochemical reaction films of different species of carbon–oxygen bond units were formed depending on the test temperature and they appeared to be effective in reducing friction and preventing wear. Pratap Singh et al. [42] studied the tribological behaviors of plasma-sprayed conventional and nanostructured (agglomerated nanoparticles) Cr_2O_3–3 %TiO_2 ceramic coatings. Samples coated with nanostructured powder exhibited better properties such as higher hardness and less porosity as compared to conventional powder coated samples. Dry sliding wear resistance of nanostructured powder under 60 N load was better than the wear resistance offered by conventional powder under 50 and 60 N load for similar testing conditions. In general, nanostructured powder exhibits a better wear resistance than conventional powder. Tao et al. [43] deposited Al_2O_3 and Cr_2O_3 coatings on stainless steel by atmospheric plasma spraying and tested their dry sliding tribological properties against copper alloy using a block-on-ring configuration at room temperature. The wear resistance of Al_2O_3 coating was superior to that of the Cr_2O_3 coating under these conditions. This was mainly attributed to the better thermal conductivity of Al_2O_3 coating (about 2.8 W/m K for alumina against 2.4 for chromia at 400 °C), which was considered to effectively facilitate the dissipation of tribological heat and alleviate the reduction of hardness due to the accumulated tribological heat. Bolelli et al. [44] plasma-sprayed ceramic coatings (Al_2O_3, Al_2O_3–13 wt% TiO_2, Cr_2O_3) and tested them through pin-on-disk and dry sand–steel wheel tests. The toughest coating (Al_2O_3) displayed the highest wear resistance, which in fact overcame HVOF-sprayed cermets and Cr electroplating, when a low number of wheel revolutions were considered. Against the alumina ball, Al_2O_3 and Al_2O_3–TiO_2 coatings showed high wear rates and friction coefficients (due to chemical affinity), while Cr_2O_3 had better wear resistance, lower friction coefficient, and inflicted less wear on the counterpart. Cr_2O_3 wear scar consisted in plastically deformed splats and debris forming a quite adherent protective tribofilm. In pin-on-disk tests, no coating underwent wear loss against the 100Cr6 ball that possessed lower hardness. Ramachandran et al. [45] studied the friction and wear behaviors of Yttria Stabilized Zirconia (YSZ) coatings, Lanthanum Zirconate (LZ) coatings, and Inconel 738 base material (BM) sliding under unlubricated conditions, against a sintered tungsten carbide surface in a pin-on-disc configuration. They found that the wear resistance of the ceramic coatings got deteriorated with the increase in the percentage volume of porosity.

(b) Cermets

Dallaire [46] studied a cored wire, referred to as Alpha 1800, developed to produce tailored arc-sprayed coatings that were tough enough to resist particle impacts at 90° and sufficiently hard to deflect eroding particles at low impact angles. Results showed that coatings produced with the new cored wire are at least 5 times more erosion resistant and 10 times more abrasion resistant than coatings produced by arc spraying commercial cored wires.

Yang et al. [47] sprayed by a HVOF system three-agglomerated WC–12 wt% Co powders with different carbide grain size distributions. Dry sliding friction and wear behavior of the WC–12 wt% Co coatings was investigated by using sintered alumina (Al_2O_3) as the mating material at 200 °C, 300 °C, and 400 °C. The specific wear rate of the coatings increased when increasing the carbide grain size at a given testing temperature. It decreased when increasing the temperature for a given carbide grain size. The specific wear rate was reduced by more than one order of magnitude when the test temperature was increased from room temperature to 400 °C. The tribofilm formed at higher temperature was denser and more adhesive to the underlying surface, thus providing more surface protection against wear. The results showed that the formation of dense and well-adhered tribofilms played an important role on the low sliding wear rate of the coatings at elevated temperatures.

Yandouzi et al. [48] sprayed by pulsed gas dynamic spraying (PGDS) process both cryo-milled particles made of an Al matrix reinforced with B_4C powders (Al5356 + 20 % B_4C) and conventional composite. The presence of homogeneously distributed fine B_4C reinforcement particles embedded within the nanostructured Al5356 matrix significantly improved the dry sliding wear resistance of the coating. Li et al. [49] cold-sprayed dense Al5356/TiN composites with TiN particles uniformly dispersed in the matrix (50 wt% TiN). The coating porosity was less than 1 vol. %. The deposited composite coating presented an excellent performance compared to that of the composite sprayed without using the ball-milled powder.

Qiao et al. [50] studied the resistance of the coatings to abrasive and un-lubricated sliding wear of 40 WC/Co coatings applied by HVOF, high-energy plasma spray (HEPS), and high-velocity plasma spray (HVPS), using commercial and nanostructured experimental powders. Phase analysis by X-ray diffraction revealed various amounts of decarburization in the coatings, some of which contained WC, W_2C, W, and h phase. The wear resistance was lowered by decarburization, which produced a hard but brittle phase. Jacobs et al. [51] investigated the microstructural properties of WC–Co–Cr and WC–Co coatings deposited by HVOF and HVAF processes. The HVAF-sprayed coatings showed better sliding wear resistance compared to the HVOF coatings. The prime wear mechanism in the WC–Co HVAF coatings was adhesive wear; the lubricious cobalt matrix resulted in very low wear rates and low debris generation. The WC–Co–Cr HVOF coatings wear was linked to "pullouts" that became trapped in the contact zone and acted as a third-body abrasive. The HVAF/WC–Co–Cr coatings exhibited better resistance. Bolelli et al. [52] studied the tribological performance of two Colferoloy Fe–Cr–Ni–Si–B–C coatings HVOF sprayed and they compared them to other coatings. Under sliding wear conditions, these coatings were a good alternative to Ni-based alloy coatings but they could not replace Cr_3C_2–NiCr cermets (best sliding wear). These coatings were unsuitable for dry particle abrasion conditions. At 400 °C, all coatings were softened and their sliding wear behavior was dominated by more severe abrasive grooving and all differences were reduced.

Alam et al. [53] studied the tribological characteristics of low-pressure plasma-sprayed aluminum bronze coatings against steel ball. Under optimum operating conditions, the test samples exhibited a dense microstructure with high hardness, low coefficient of friction, and high wear resistance. Ouyang et al. [54] studied the tribological properties of VPS ZrO_2–CaF_2–Ag_2O composite coating (ZFA). At 300–700 °C, the ZFA coating exhibited lower friction and wear than at room temperature, 200 °C or 800 °C. Ag_2O and CaF_2 acted as solid lubricants effectively at 300–400 and 600–700 °C, respectively. But with the increase of temperature up to 800 °C, the severe adhesive sliding caused more material transfer and tearing out of coating, and finally leads to a high friction and wear.

(c) Metals

Ahn et al. [55] studied the wear resistance of plasma sprayed, on a low-carbon steel substrate, molybdenum blend coatings consisting of powders of bronze and aluminum–silicon alloy powders mixed with molybdenum. The wear test results revealed that the wear rate of all coatings increased with rising wear load and that the blended coatings had better wear resistance than the pure molybdenum coatings, although the hardness was lower. The molybdenum coating blended with bronze and aluminum–silicon alloy powders exhibited excellent wear resistance because hard phases such as $CuAl_2$ and Cu_9Al_4 formed inside the coating. Bolelli et al. [52] studied the tribological performance of two Fe–Cr–Ni–Si–B–C (Colferoloy) alloy coatings manufactured by HVOF thermal spraying, through rubber-wheel dry particle abrasion test and ball-on-disk sliding wear tests. Colferoloy coatings were validated as alternatives to Ni-based alloys and electroplated chromium under sliding wear conditions, but appeared unsuitable for particle abrasion resistance. The different sliding wear behaviors of HVOF-sprayed coatings were explained by coupling micro and nano-hardness to scratch testing, which reflected cracking resistance and plastic deformability. Rodriguez et al. [56] compared NiCrBSi alloys sprayed by either plasma or flame but then fused for the latter. Four sets of specimens were tested varying the composition (with the presence or not of WC in the powders). Coatings were tested in a reciprocating pin on plate wear machine able to select loads ranging from 50 to 200 N and temperatures up to 500 °C. NiCrBSi alloys, deposited by thermally spray techniques, maintained their wear resistant performances up to bulk temperatures of 500 °C. The alloys deposited by flame spraying with fusion had better wear resistance than those deposited by plasma spraying. The presence of tungsten carbide in the powders was not a beneficial factor on the wear performance of thermally sprayed NiCrBSi coatings. PTA is used to increase wear resistance mainly in steel industry, see Sect. 10.7.2 of Chap. 10.

(d) Polymers

At last at low temperatures polymers can be used against friction. Niebuhr and Scholl [57] sprayed with high-energy plasma polymer–steel coatings for high-contact pressure rolling/sliding systems. Polymers were applied as a thin film (75–100 μm) over a thicker (250–750 μm) steel coating. Twin roller rolling/sliding tests were performed at 5 and 35 % creep and contact loads of 1,700 N on a 5 mm contact face. A lower coefficient of friction (0.10–0.15) with increased durability compared with that of AISI 1080 steel thermally sprayed coating (coefficient of friction of 0.46) was observed under these rolling–sliding contact conditions. Li et al. [58] deposited, using the flame spray process, PEEK coatings with three kinds of crystallinities. Investigations were performed under dry sliding conditions against a 100C6 counter-body. The average friction coefficients appeared to decrease while increasing the sliding velocity, but were insensitive to the applied load in the range of investigation. The higher was the crystallinity of the coating, the lower was its average friction coefficient. The wear mechanisms of the different coatings were explained in terms of plastic deformation, plough marks, and fatigue tearing. Li et al. [59] flame sprayed polyamide1010 (PA1010) and its composite with nanometer-sized silica (PA1010/n-SiO_2). The dry friction and wear behaviors of both coatings were investigated under dry sliding conditions. The results showed that the addition of nanometer-sized silica increased the crystallinity of the coatings and reduced friction and wear compared to pure PA1010. The nano-composite coatings, containing 1.5 wt% nanosized silica, displayed better properties.

18.3.1.4 Scuffing

It is a localized damage caused by the occurrence of solid-phase welding between sliding surfaces, without local melting [1]. Scuffing may result from missing of lubricating film and formation of adhesive contact between surfaces and finish with the macro-damage [60]. Żórawski and Kozerski [60] characterized the tribological properties of plasma- and HVOF-sprayed WC–12 Co and Cr_3C_2–25(Ni20Cr) coatings. The WC–12Co coating sprayed using HVOF method showed the best scuffing resistance and the most homogeneous structure. The resistance was better for coatings presenting lower friction coefficient, higher hardness, and being more homogeneous. Edrisy et al. [61] HVOF coated the inner surfaces of the engine blocks working in racetrack conditions. During the deposition of the HVOF 2.5 % Al coating, the gun traveled along the length of the bore as it rotated inside the cylinder and sufficient excess coating was applied so that about 30 % of the coating layer was removed subsequently. Then they studied scuffing damage mechanisms of the engine. The delamination of the tribolayers was the primary source of material removal during scuffing. This process was facilitated by crack formation at the $FeAlO_3$ inclusions as well as fracture along the FeO veins between the iron splats.

18.3.1.5 Cavitation Wear

Cavitation, where pits and pores are formed, results from sudden variations of pressure in the fluid resulting in the creation of shocks waves due to implosion (for more details see Sect. 15.9.3) inducing fatigue phenomenon. Cavitation occurs when the velocity difference between the liquid and solid becomes important. Cavitation can be reduced by a proper design to diminish the low-pressure area. Against it, high toughness alloys with a good resistance to micro-crack formation are mandatory. The surface polishing is also very important; a low Ra can reduce the wear by a factor 5. Of course the proper design of the different parts can reduce drastically cavitation.

Arc spraying has been extensively used against cavitation, but liquid corrosion phenomena must also be considered and thus results depend on hardness and internal coherency of coatings. For example, Kim and Lee [62] have arc sprayed ten different coatings. Stainless steel coatings with the highest hardness showed the best performance against the cavitation erosion. In Al-based coatings, Si addition improved both the hardness and bond strength, resulting in drastic increment of cavitation erosion resistance by about 40 times when adding 12 wt% Si. In terms of marine corrosion resistance, aluminum coating showed the best performance with the aid of the sacrificial anode effect; unfortunately, the addition of Si to Al-based coatings caused surface pitting similar to those of Zn-based coatings. In both the Cu- and Fe-based coatings, interfacial oxidation occurred in between the coating and steel substrate. Hahn and Fischer [63] have tested the cavitation resistance of FeC0.8 coating arc sprayed, FeC0.8 coating HVOF sprayed, and FeCr19C0.1B1.6 coating deposited by plasma-transferred arc fed with wire. They showed that for all coatings the weight loss immediately starts with the beginning of the test. The major acting wear mechanism within cavitation was surface fatigue with splat delamination and cracks propagation along splat interfaces, the worst being when coating had a very low ductility. Kumar et al. [64] have tested 21 different coatings thermal sprayed. The HVOF-sprayed coatings exhibited lower cavitation wear rates than the thermal spray coatings deposited by the plasma spray process. The lowest cavitation rate was for Stellite 6; however, its cavitation rate was 11.7 mg/h, while the corresponding cavitation rate for 308 stainless steel weld metal was 3.2 mg/h. But in slurry erosion wear testing, the volume loss for Stellite 6 coatings was 5.33 mm^3/h, less than half the volume loss of 11.17 mm^3/h for 304 stainless steel. Factor and Roman [65] have subjected a selection of WC–Co and Cr_3C_2–25 %NiCr coatings produced by plasma spray and HVOF deposition techniques to various wear tests designed to simulate abrasion, cavitation, sliding, and particle erosion type wear mechanisms. Cr_3C_2–25 wt% NiCr outperforms the WC–Co samples, and it appeared that the WC–12 wt% Co sample performed better than the WC–17 wt% Co samples. For all samples the wear loss mechanism was clearly that of the delamination of flakes of material. With WC–Co samples, corrosion mechanisms played an important role, possibly through enhanced corrosion resulting from the cavitation mechanisms causing pit corrosion or similar

behavior. Wu et al. [66] studied a WC–Co–Cr coating deposited by HVOF onto a 1Cr18Ni9Ti stainless steel substrate to increase its cavitation erosion resistance. The microstructural analysis of the coating after the cavitation erosion tests indicated that most of the corruptions took place at the interface between the unmolten or half-melted particles and the matrix (Co–Cr), the edge of the pores in the coating, and the boundary of the twin and the grain in the stainless steel 1Cr18Ni9Ti.

Santa et al. [67] studied the slurry and cavitation erosion resistance of six thermal spray coatings and compared to that of an uncoated martensitic stainless steel. The results showed that the slurry erosion resistance of the steel could be improved by up to 16 times through the application of the thermally sprayed coatings. On the other hand, none of the coated specimens showed better cavitation resistance than the uncoated steel in the experiments. Lima et al. [68] deposited four different coatings onto an AISI 1020 steel substrate:

- WC–12 %Co
- As-sprayed (AS) 50 %(WC–12 %Co) + 50 %(NiCr)
- Post-melted (PM) 50 %(WC–12 %Co) + 50 %(NiCr)
- A duplex system comprising a WC–12 % Co top layer and a NiCrAl interlayer

The worst performance in cavitation erosion tests was observed for the WC–12 %Co coating, which showed the highest mass loss throughout the test. Conversely, the "PM" 50 % (WC–12 %Co) + 50 %(NiCr) coating exhibited the best cavitation resistance and a correlation between coating toughness and cavitation resistance could be established. Ding et al. [69] HVOF deposited conventional, submicron, and multimodal WC–12Co cermet coatings. They found that the multimodal WC–12Co coating exhibited the best cavitation erosion resistance among the three coatings tested, the erosion rate was approximately 40 % that of the conventional coating, and the cavitation erosion resistance of multimodal WC–12Co coating was enhanced by above 150 % in comparison with the conventional coating. Dense nanostructure, high microhardness, and strong cohesive strength of WC–12Co coating contributed to the increase in the cavitation erosion performance of multimodal WC–12Co coating.

18.3.1.6 Surface Fatigue Wear

It results in pits and pores that can extend to depths of several tenths of millimeters and are due to cyclic loading contacts, with stresses induced by rolling, shocks, or sliding in a lubricated regime. They depend on material properties: structure, cohesion, elastic limit, toughness, and residual stresses (see Sect. 15.9.4). If tangential stress is predominant, fatigue will start in the "skin" and if shear stress is more important, fatigue will occur essentially in the subsurface. The worst occurs when cracks propagate (see Sect. 15.9.4). The best materials to be used are hard ones with a high toughness. The surface must be smooth with no irregularities where cracks are initiated.

Stewart and Ahmed [70] made in 2002, a review of the thermal-sprayed coatings used in rolling contact fatigue (RFC). Coatings of WC–12 %Co, WC–17 %Co, and WC–10 %Co–4 %Cr, were sprayed on steel substrates using APS or HVOF; those of NiBSiCrFeC, Al_2O_3–TiO_2, Cr_2O_3–SiO_2–TiO_2, Mo were sprayed by APS; those of WC–Co and WC–Cr–Ni were sprayed by HVOF; and those of WC–12 %Co, WC–15 %Co, and Al_2O_3 were sprayed by D-gun. The HVOF-deposited coatings presented superior RCF performance, probably because of their dense microstructure and high cohesive strength combined with a minimum number of detrimental brittle phases. Cermet coatings displayed superior RCF performance followed by ceramic and metallic coating, respectively. Thermal and mechanical mismatch between the coating and the substrate influenced the RCF performance of the coating through the control the degree of compressive residual stress. Coatings thicker than 200 μm displayed superior RCF performance over thinner ones.

Ahmed and Hadfield [71] studied cermet (WC–Co) and ceramic (Al_2O_3) coatings deposited by D-Gun, HVOF, and high-velocity plasma spraying (HVPS) techniques, in a range of coating thicknesses (20–250 μm) on various steel substrates to deliver an overview of the various competing failure modes in rolling/sliding contact. Four modes of fatigue failure, competing during fatigue failure and that can be combined, were identified: abrasive, delamination, bulk deformation, and spalling. The conclusions of authors were the following:

Abrasion can be controlled by appropriate selection of contacting pair and lubrication conditions. Delamination and catastrophic failure mode, can be avoided by appropriate selection of coating thickness and fracture toughness.

Controlling the hardness of substrate and also increasing the coating thickness can avoid bulk failure. Coating failures were attributed to micro- and macrocracking of either the coating material or the coating substrate interface, which also resulted in the attenuation of compressive residual stress. Savarimuthu et al. [72] have studied the possible replacement of chromium electroplated by WC–Co-sprayed coatings for commercial aircraft applications. Decarburization, volume percent and distribution of hard particles, and porosity might more strongly influence wear behavior than residual stresses. Zhang et al. [73] addressed the fatigue behavior and failure mechanisms of plasma-sprayed CrC–NiCr cermet coatings in rolling contact. As emphasized previously, failure modes of coatings could be classified into four main categories, i.e., surface abrasion, spalling, and delamination within the coating and at the coating/substrate interface. The interfacial delamination was the main failure mode of the coatings at high contact stress. The failure mechanisms of coatings were associated with the microstructures and the bonding strengths of coatings, the depths of the orthogonal shear stress, and the maximum shear stress. Berger et al. [74] studied the dependence on substrate hardness of the rolling contact fatigue of HVOF-sprayed WC–17 %Co coatings. Such coatings are for gears and other components with high-load-bearing capacity. The durability of HVOF-sprayed WC–17 wt% Co coatings under rolling contact fatigue loading was significantly improved through the use of substrates of different hardnesses. The highest endurable Hertz pressure for a probability of survival of 50 % at 5×10^7 cycles was obtained for quenched and tempered substrates of

intermediate hardness of 400 HB. Crack formation and subsequent delamination appeared to be the main causes of failure. Bolelli et al. [52] studied the tribological performance of two coatings of Fe–Cr–Ni–Si–B–C (Colferoloy) alloy HVOF sprayed. They compared results to those obtained on Ni–Cr–Fe–Si–B–C and Cr_3C_2–NiCr layers (also HVOF sprayed), hard chromium electroplating, and bulk tool steel. Colferoloy coatings were validated as alternatives to Ni-based alloys and electroplated chromium under sliding wear conditions, but appeared unsuitable for particle abrasion resistance. The different sliding wear behaviors of HVOF-sprayed coatings could be explained by coupling micro- and nano-hardness to scratch testing, which reflected cracking resistance and plastic deformability. Ganesh Sundara Raman et al. [75] D-gun-sprayed Cu–Ni–In coatings on two substrate materials: Ti–6Al–4V and Al-alloy AA-6063. The Cu–Ni–In coating was found to be beneficial on the Ti alloy, but was deleterious on the Al-alloy substrate under both plain fatigue and fretting fatigue loading. The results were explained in terms of differences in the values of surface hardness, surface roughness, surface residual stress, and friction stress. Akebono et al. [76] investigated the factors that most strongly influenced fatigue properties of steel flame sprayed with Ni-based self-fluxing alloy and prepared three types of thermally sprayed specimens, which differed in heating time in the fusing process. The sprayed specimens fused for longer time exhibited lower fatigue strength, because segregation of the chromium compound in the coated microstructures was induced. Therefore, performing the fusion for a shorter time was effective for producing sprayed materials of enhanced fatigue properties.

18.3.1.7 Wear by Fretting and Fretting-Corrosion

Fretting occurs when the two interacting mating surfaces are subjected to an oscillatory motion of small amplitude. It can be more important when corrosion or oxidation occurs, producing for example oxides with ferrous materials (fretting corrosion). In the latter case, the extent and kinetics of phenomena are linked to the balance between the formation of products and their removal through wear. Besides the material properties, the design of the machine must eliminate the micro-movement, trap or remove debris, limit the contact with the environment. Jin et al. [77] have underlined that surface coating may protect the contact area from the fretting damage; however, specific contact condition would govern the effectiveness of the coating. They [77] proposed to classify coatings into two major types: hard and soft. Hard coatings are used in the contact conditions where fretting wear is present or dominant, while soft coatings are used to reduce the fretting fatigue induced failure since they could act as a self-lubricant and reduce the coefficient of friction resulting in improvement in fretting fatigue life. Of course fretting resistance depends on coating and substrate on the one hand and contact conditions (lubricant, pressure, and amplitude of the movement on the other). For example, Kim and Korsunsky [78] studied a pad and a substrate made of Ti–6Al–4V alloy on which was plasma sprayed a metallic interlayer of

Cu59–Ni36–In5. A dry film lubricant layer was then applied on the metallic interlayer and on the pad in the form of epoxy matrix loaded with MoS_2 particles. The coated specimen was clamped between two pads that were pressed against the specimen surface with a contact pressure of ~125 MPa, conditions simulating the geometric and loading conditions experienced in aerospace components. Each fretting test was performed at a frequency of 2.5 Hz. The durability of the coating was increased when increasing its thickness. Jin et al. [77] studied Cu–Al coating on Ti–6Al–4V substrate under fretting fatigue condition. At the low-applied stress amplitudes, the coating survived up to one million cycles. At the high-applied stress amplitudes, either the coating was separated from the substrate due to insufficient interfacial strength or the specimen fractured at locations away from the contact area. Mary et al. [79] performed fretting wear tests up to 500 °C. A representative punch (Ti17)/plane (CuNiIn plasma coating) interface was investigated under air conditions. Wear was studied by varying pressure, sliding amplitude, and temperature. A threshold mean pressure $p_{th} \approx 85$ MPa was identified for the transition from a low to a high wear regime. Temperatures in the range of 20–450 °C did not modify the respective wear processes and consequently did not affect the related wear rates. Hager et al. [80] conducted, for titanium compressor bladed disk assemblies, an in-depth wear analysis on the gross slip fretting wear of Ti6Al4V-mated surfaces as well as Ti6Al4V worn against plasma-sprayed CuNiIn, Al–bronze, Mo, and Ni. Tests were performed at room temperature and 450 °C. To eliminate the stress concentrations, the test geometry was an ellipsoid on a flat plate. They determined that all coatings caused significant damage to the mating Ti6Al4V surfaces and that the wear mechanisms were all similar to those of the uncoated baseline case. In gross slip fretting, these soft thermal spray coatings did not effectively protect the mating Ti6Al4V surfaces without solid lubrication. Koiprasert et al. [81] HVOF sprayed four types of coating (≈300–400 μm), namely, WC–17 % Co ($T < 500$ °C), Cr_3C_2–25 %NiCr ($T < 800$ °C), AlSi graphite, and CoMoCrSi ($T < 800$ °C) on stainless steel substrates. They used an in-house flat-on-flat, fretting wear tester at 500 °C. At that temperature, WC–Co did not perform well, Cr_3C_2–25 %NiCr outperformed WC–Co; but the formation of Cr_2O_3 by oxidation caused rapid wear, AlSi graphite coating did not provide additional wear resistance to the stainless steel. Only the CoMoCrSi coating, with its low porosity, moderate-to-high hardness, and good high temperature corrosion resistance, exhibited the best wear property. Hager et al. [82] plasma-sprayed nickel graphite composite coatings with 5–20 % graphite and studied mitigate fretting wear within Ti6Al4V contacts at room temperature and 450 °C. The embedded graphite particles reduced the friction of the nickel thermal-sprayed coatings during both low and high temperature fretting wear experiments. The wear reduction on the mated Ti6Al4V surfaces was due to the formation of uniform transfer films graphitic based at room temperature and NiO based at 450 °C. Carrasquero et al. [83] investigated the fretting wear performance of a Ni–Cr-based alloy, containing B and C, HVOF sprayed onto a SAE 1045 steel substrate. Tests were conducted on both the uncoated and coated substrate, under un-lubricated dry conditions, at different applied normal loads, cycles, and amplitudes. They showed

that at constant wear amplitude, the wear volume increased with the applied normal load and that at under constant load conditions, the wear volume decreased as the wear test amplitude also decreased, becoming insignificant when it was less than ~100 μm. Tian et al. [84] studied the fretting wear behavior, against a steel ball, of conventional and nanostructured Al_2O_3–13 wt% TiO_2 plasma sprayed. The improved fretting wear resistance of nanostructured coatings was attributed to the nanometer-sized grains, reduced lamellar structures, and amorphous phases. Fretting wear often occurs in hip joints that must be replaced after about 10 years use. Sathish et al. [85] reported on the sliding wear performance of the nanostructured Al_2O_3–$13TiO_2$, ZrO_2, and the bilayered (ZrO_2/Al_2O_3–$13TiO_2$) coated biomedical Ti–13Nb–13Zr alloy in simulated body fluid condition. The bilayered coating exhibited 200- and 500-fold increase in the wear resistances when compared with that of the nanostructured Al_2O_3–$13TiO_2$ and ZrO_2 coatings. This substantial improvement was attributed to the lower porosity and higher adhesion strength of the bilayered coating.

18.3.1.8 Thermal Fatigue and Thermal Shock

Thermal fatigue occurs in components subjected to high temperature gradients resulting from friction or operating environment (for example, external surface subjected to hot gases). It results in high stresses, surface fatigue, and mechanical transfer (transfer of the softer body to the harder one). Of course when thermal fatigue tests are performed in air, very often oxidation problems take an important part in coating resistance. Thermal fatigue characterization is presented in Sect. 15.9.4. Thermal shock occurs when the thermal gradient causes different parts of an object to expand by different amounts, generating stress or strain. At some point, this stress can exceed the strength of the material, causing a crack to form. If nothing stops this crack from propagating through the material, it will cause the object's structure to fail. As described in Sect. 15.8.4, the thermal shock resistance is tested by alternate high-temperature exposure and cooling cycles until failure. For thermal fatigue testing, the heat flux to the sample is applied using a flame, followed by air cooling, with or without convection. On the other hand, in thermal shock tests, the heating is achieved by a furnace (moderate thermal gradients), followed by cooling using cold water (high thermal gradients). Alternately, the heating is made with a flame on one side of the sample, while the opposite side of the sample is air cooled (high thermal gradients). The cooling step can also be achieved through the replacing the flame by an air jet (moderate thermal gradients). The heating step can also be achieved with a fluidized bed or a laser.

(a) Thermal Fatigue

As it could be expected, most studies were devoted to thermal barrier coatings (TBCs). However, the first two following examples are not related to TBCs, which

are depicted in Sect. 18.3.3. Aoh and Chen [86] investigated high temperature (700 °C) wear characteristics of Stellite 6 alloy containing Cr_3C_2 after thermal fatigue and oxidation treatment at 700 °C. The coating was deposited by plasma transferred arc (PTA) process. Thermal fatigue cracks initiated from the surface of Stellite 6 with Cr_3C_2 and propagated into the coating along carbide boundaries. No thermal fatigue crack was observed on sprayed Stellite 6 layer. The Cr_3C_2 content in the alloy enhanced the formation of the oxide layer. Surface oxidation was beneficial to the improvement of wear resistance and the coating exhibited the lowest wear loss if an oxidation treatment at 700 °C/100 h was achieved prior to the wear testing.

According to D'Ans et al. [87] the major wear mode of steel in the aluminum foundry industry is thermal fatigue especially affecting die-casting dies. Steel is also intensively corroded by molten aluminum and, sometimes, sliding wear occurs when extracting the molded parts from the die. D'Ans et al. [87] conducted thermal fatigue tests with samples of hot work tool steel, respectively, untreated, simply borided, and at last protected by a multilayer of YSZ, followed by a nickel superalloy and then a borided layer. Unfortunately the multi-layer coating resistance to thermal fatigue (heating between 500 and 800 °C), turned out to be lower than for a single-treatment solution (boriding) and for plain steel.

Eriksson et al. [88] subjected air plasma-sprayed thermal barrier coatings to isothermal and cyclic heat treatments (Thermal Cycling Fatigue TCF). Specimen subjected to TCF and isothermal oxidation gave very similar interface (Thermally Grown Oxide) TGO thickness and TGO composition. The heat treatment influences the adhesion of TBCs: isothermal oxidation up to 290 h has been shown to have a beneficial effect on adhesion compared to the as-sprayed condition, while cyclic heat treatment has been shown to decrease adhesion. Kwon et al. [89] studied a TBC with topcoat deposited by APS and bond coat by HVOF. Thermal fatigue did not affect the stress–strain curves, except for thermal fatigue for 500 h. However, the thermally grown oxide (TGO) layer thickness was dependent on the exposure time under thermal fatigue, showing a nominal thickness of approximately 4 μm after thermal fatigue for 500 h, independent of the number of thermal fatigue cycles. As the exposure time was increased in the thermal fatigue experiments, the damage to the topcoat was inhibited with less crack coalescence. The higher stiffness in the bond coat induced cracking or delamination at the interface between the bond coat and the substrate, whereas thermal fatigue increased the mechanical properties, especially the elastic modulus, of the bond coat and enhanced the damage tolerance of the TBC system.

(b) Thermal Shock

Luo et al. [90] deposited by high-velocity arc spraying cored wires FeMnCrAl/Cr_3C_2 and FeMnCrAl/Cr_3C_2–Ni9Al coatings onto low-carbon steel substrates. The specimens were placed inside a furnace at 800 °C, held for 15 min and then quenched into a water bath (25 °C). The first type of coating consisted of layered

splat of mainly Fe solid solution phases mixed with oxide phases, unmelted particles, and pores. The second type of coating exhibited higher bonding strength; Ni and Fe formed the diffusion layer that improved the thermal shock resistance. The cracks in the coatings were mainly initiated and propagated along the oxide phases during the thermal shock test. The uniformly shaped pores in the coatings helped preventing crack initiation and propagation. Pan et al. [91] studied the effect of SiC particles on thermal shock resistance of Al_2O_3–20 wt% 8YSZ coatings air plasma sprayed. The thermal shock resistance of Al_2O_3/8YSZ coatings was increased greatly from 5 to 83 cycles with addition of SiC particles at 1,000 °C. Some silicate fibers were formed on the coating surface and through thickness after thermal shock. The $Al_2O_3{\cdot}xSiO_2$ silicate fibers increased greatly the thermal shock resistance of ceramic coatings. Gu et al. [92] plasma sprayed NiCoCrAlY/8YPSZ coating on aluminum alloy (5A06). The failure after thermal shock tests (furnace heating at 400 °C for 0.5 h, then quenched with cold water, and dried by warm air) was mainly due to the stress caused by thermal expansion mismatch between the bond coat and the substrate as well as the galvanic corrosion of the aluminum alloy. Ni–P, Ni–W–P, and Ni–Cu–P as interlayers were electrolessly deposited on the substrate in order to mitigate the thermal stress. Diffusion layers mainly composed of AlNi, Al_3Ni_2, and Al_3Ni were observed between the interlayers and the substrate after thermal shock test. The oxidation of the substrate was effectively inhibited. Ni–P interlayer was superior to the other two interlayers and enhanced the thermal shock life from 38 to more than 200 cycles. Kokini et al. [93] studied plasma-sprayed yttria-stabilized zirconia–NiCoCrAlY bond coat alloy compositionally graded thermal barrier coatings onto Inconel steel subjected to a thermal shock loading. The thermal loading was applied using a continuous CO_2 laser. The results showed that for a given thermal resistance, as the compositional gradation was increased, the maximum surface temperature at which horizontal cracks initiated in the TBC increased. Liang et al. [94] deposited by APS nanostructured and conventional zirconia coatings and studied, by the water quenching method, the thermal shock resistances of as-sprayed coatings. The results showed that the nanostructured as-sprayed coating possessed better thermal shock resistance than the conventional one. The difference in microstructure and microstructural changes occurring during thermal shock cycling explained those results. Gilbert et al. [95] investigated the reduction of time-dependent deformation through the addition of mullite to YSZ based TBCs. Fracture mechanics analyses were performed for three coating architectures: monolithic YSZ, monolithic mullite, and a mullite-YSZ composite. The effect of coating architecture and surface crack morphology on interface fracture was investigated. They found that mullite and YSZ combined to influence the thermal shock behavior of the composite coatings. Composite coatings experienced a reduced driving force for interface fracture compared to monolithic YSZ coatings while having a higher thermal resistance compared to monolithic mullite coatings.

18.3.1.9 Wear by Very High Stresses

It is mostly characterized by dry sliding with a pin-on-disk test and depends on the high load applied and sliding distance, the wear response being dominated by subsurface cracking and removal of materials when sliding. Plasma with ceramics, HVOF, and D-gun with cermets are mainly used. Bolleli et al. [44] have investigated through pin-on-disk and dry sand–steel wheel tests the wear resistance of plasma-sprayed ceramic coatings (Al_2O_3, Al_2O_3–13 %TiO_2, Cr_2O_3). These ceramic coatings were the better performing ones in dry particles abrasion conditions, because they never undergone abrasive grooving but only splats detachment. In the pin-on-disk test, the ability to form a smooth and compact surface film by local plastic deformation was the key property determining coatings performance. Al_2O_3 and Al_2O_3–13 %TiO_2 did not form an adequately compact tribofilm and therefore showed unfavorable properties in terms of sample wear rate, pin wear rate, and friction coefficient. Cr_2O_3, instead, had the ability to form a compact tribofilm by splats plastic deformation; thus, its performances were comparable to HVOF-sprayed ceramics. However, its rather low deposition efficiency (below 45 %) and its propensity to possibly form Cr_6^+ by in-flight thermal alteration were disadvantages that must be considered. Bolelli et al. [44] found that Al_2O_3 coatings, manufactured by the high-velocity suspension flame spraying (HVSFS) technique using a nano-sized powder suspension resulted in few interlamellar or intralamellar cracks, inducing reduced pore interconnectivity. Such strong interlamellar cohesion favored much better dry sliding wear resistance at room temperature and at 400 °C. Ahmaniemi et al. [96] showed that the aluminum phosphate sealing treatment changed stress states of the alumina and chromia coatings toward compression. Tensile stress state of the Al_2O_3 coating decreased during the sealing treatment and was even compressive when measured with hole-drilling method. Dry abrasion resistance increased correlatively. Stress state of sealed Cr_2O_3 coating was more sensitive to sealing treatment temperature. Higher sealing treatment temperature led to higher compressive stress state and better abrasion wear resistance. Chen and Hutchings [97] plasma-sprayed coatings of tungsten carbide with 9, 12, and 17 wt% Co by both air (APS) and low-pressure (VPS) methods. VPS coatings had a lower porosity, better inter-pass bonding, and higher WC contents; these correlated with greater abrasion resistance. All coatings showed poor resistances to high-stress abrasive wear, which was associated with widespread fracture of the carbide constituents of coatings under these conditions. Under low-stress abrasion, however, all coatings showed a substantially greater wear resistance than the steel control. The presence of hard carbides was beneficial, and the VPS coatings all showed a greater wear resistance than the APS ones. Venkateswarlu et al. [98] sprayed diamond reinforced composite coatings deposited with both oxyacetylene flame and HVOF techniques. The feedstock material used for the coating consisted of tungsten carbide (WC) (average particle size: ~2 μm), bronze (average particle size: ~30 μm), and diamond (average particle size: ~25 μm)

powders. In addition to the high hardness of HVOF-sprayed coating, the uniform distribution of diamond particles in the matrix was considered important in the view of reduced matrix deformation. HVOF-sprayed specimen, owing to its lower porosity and higher bond strength between reinforced particulates and the matrix, led to substantial reduction in the deformation of matrix, which in turn facilitated higher wear resistance. To improve the resistance of HVOF sprayed cermets different means were used. For example, Stoica et al. [99] have HVOF (JP5000) sprayed functionally graded WC–NiCrBSi coatings and heat-treated them at 1,200 °C in argon environment. It was possible to achieve higher wear resistance, both in terms of coating wear, as well as the total wear of the test couples. This was attributed to the improvements in the coating microstructure during the heat treatment, which resulted in an improvement in coating's mechanical properties through the formation of hard phases, elimination of brittle W_2C and W, and the establishment of metallurgical bonding within the coating microstructure and at the interface coating–substrate. Valarezo et al. [100] tested the effective damage tolerance of a functionally graded coating (FGC) deposited by HVOF. The thick FGC (≈1.2 mm) consisted of 6 layers with a stepwise change in composition from 100 vol. % ductile AISI316 stainless steel (bottom layer) to 100 vol. % hard WC–12Co (top layer) deposited onto an AISI316 stainless steel substrate. The FGC structure showed the ability to reduce cracking with increased compliance in the top layer during static and dynamic normal contact loading, while retaining excellent sliding wear resistance (ball-on-disk tests). One of the main problems seemed to be the poor characteristics of HVOF-sprayed stainless steel. It suffered from extensive oxidation and phase alteration during spraying, which compromised its mechanical strength and probably impaired its adhesion to the substrate. Bolelli et al. [101] manufactured HVOF-sprayed functionally graded coating, consisting of two NiAl/WC–Co composite layers with increasing cermet content and a pure WC–Co topmost layer. Results showed that the WC–Co/NiAl FGC could provide good wear and corrosion protection to the substrate under very severe conditions, when very thick layers were demanded. This architecture also solved many of the problems highlighted by the previously considered WC–Co/stainless steel FGC. Stoica et al. [102] compared the sliding wear performance of as-sprayed and Hot Isostatically Pressed (HIPed) thermal spray cermet (WC–12Co) coatings. Results indicate that HIPing technique can be successfully applied to post-treat thermal spray cermet coatings for improved sliding wear performance, not only in terms of coating wear but also in terms of the total volume loss for test couples. The process induced phase transformations: elimination of secondary phase W_2C and metallic tungsten W, alteration of amorphous binder phase through recrystallization of Co leading to precipitation of the η carbides. It also developed the metallurgical bonding at the interface between the constituent lamellae of the coating, thereby increasing the coatings Young's modules after HIPing post treatment.

18.3.2 Corrosion and Oxidation Resistant Coating

Corrosion and oxidation correspond to a chemical or electrochemical reaction with the surrounding atmosphere. For details about corrosion either at room or high temperatures, see Sect. 15.10.1. As a general rule, except for sacrificial coatings, those used against corrosion must be as dense as possible and in many cases a post-treatment must be achieved (fusion of self-fluxing alloys, heat-treatment, sealing, austempering, laser glazing, . . . see Sect. 13.12).

18.3.2.1 Room Temperature Corrosion

The different corrosions at room temperature can roughly been categorized in atmospheric or marine corrosion, chemical, or parachemical corrosion.

(a) Atmospheric and Marine Corrosion

Large steel structures such as bridges, pipelines, oil tanks, towers, radio and television masts, overhead walkways, and large manufacturing facilities in the metallurgical, chemical, energy, and other industries must be protected from corrosion. It is the same, but with more difficulties, with structures exposed to moist atmospheres and seawater such as ships, offshore platforms, and seaports [103]. Sørensen et al. [104] have presented a review of anticorrosive coatings for containers, offshore constructions, wind turbines, storage tanks, bridges, rail cars, and petrochemical plants and "marine corrosion" corresponding to coatings for ballast tanks, cargo holds and cargo tanks, decks, and engine rooms on ships.

Flame and wire arc spraying meet such requirements. However, coatings obtained by these methods are relatively porous (up to 20 %). Sacrificial coatings (for example, Zn or Al on steel) are mainly used. Referring to Sect. 15.10.1 such coatings must have a cathodic behavior relatively to the ions of the metal to be protected, steels in almost all cases. As illustrated in Fig. 15.67b, the cathodic protection can be porous without any corrosion of the underneath metal. Zinc performs better than aluminum in alkaline conditions, while aluminum is better in acidic conditions. Zinc–aluminum (Zn–15 wt% Al) seems to combine advantages of both materials. Against marine biofouling, undesirable accumulation of marine organisms on artificial surfaces that are immersed in the sea, Murakami and Shimada [105] have studied flame sprayed aluminum–copper alloy powders, aluminum–copper blend powders, aluminum–zinc blend powders, and a zinc powder. Coatings were immersed in the sea and their corrosion and marine fouling behaviors were examined. The aluminum–copper coatings had poor anticorrosion and antifouling properties. The aluminum–zinc coating with high zinc content and the zinc coating possessed the anticorrosion and antifouling properties [105].

Of course other treatments are possible such as plastic deformation. For example, the initial porosities of 4–14 % (depending on spray conditions) of aluminum coatings, wire arc sprayed, was reduced to 0.16–0.83 % after being shot peened with SiC glass beads of 0.21–0.3 mm [106]. Sealers can also present antifouling properties. Chun-long et al. [107] have arc sprayed aluminum on steel panels and then sealed coatings with nano-composite epoxies especially developed for sealing them. In order to test their performance, some panels were tested in the East China Sea. Test panels were mounted respectively during 3 years, in the marine atmosphere zone, seawater splash zone, tidal zone, and full-immersion zone. Tests included marine atmospheric outdoor exposure test, seawater corrosion test, and coating adhesion test. It was found that the appearance of coating panels was as fine as original but with a little sea species adhering to panels on tidal zone and full-immersion zone. Basically no change in the morphology, bond strength, and any visible coating crack, blister, rust, and break off was observed. Schmidt et al. [108] investigated the corrosion protection performance of 17 different Zn and Al sacrificial coating system configurations during marine atmospheric exposure (20-month exposure time) at Kure Beach, NC, USA. The coating systems incorporated several conversion coating layers, primers, and organic topcoats. The sacrificial Zn coatings provided sacrificial protection at the defects. Of the two thermal spray Zn coatings, flame spray coatings were more protective than arc spray. Han et al. [109] wire arc-sprayed aluminum wire on Special Treatment Steel (STS) 304 base metal. The electrochemical experiment was performed in natural seawater. The coating with the higher thickness represented good corrosion resistance in seawater. Esfahani et al. [110] deposited aluminum coating on mild steel by arc spraying. The corrosion behavior was evaluated by electrochemical impedance spectroscopy (EIS) and polarization tests in 3.5 vol. % NaCl solution. The as-coated samples were also subjected to a 1,500-h salt spray assay. EIS measurements showed that the corrosion performance of the coating was improved during a long-time immersion and exposure to saline mist. This could be due to plugging of pores by corrosion products, which hinder further penetration of the electrolyte through the coating. The twin wire arc-sprayed aluminum coatings could reliably protect steel structures against corrosion in chloride-containing aqueous solutions. Gorlach [111] has developed wire (Zn–Al) spraying by HVAF process. Coatings showed considerably higher bond strength than those obtained by the conventional methods, an advantage in areas where the adhesion strength was critically important. The highly dense coating structure also eliminated the need for a top paint coat, usually applied on metal-sprayed coatings to extend service life. Concrete bridge structural deterioration in coastal marine environments or in areas where deicing salts are used for snow and ice removal is a problem.

To limit atmospheric or marine corrosion, if one uses an anodic protection (for example, nickel is anodic to steel and the cathodic area of steel exposed controls the rate), the coating should be as dense as possible (if necessary sealed). Cramer et al. [112], as well as Holcomb et al. [113], have proposed a cobalt-catalyzed, nonconsumable, thermal-sprayed titanium anode as an alternative to thermal-sprayed zinc anodes for impressed current cathodic protection. Ti was wire arc

sprayed [112], the atomization being performed with nitrogen to limit as much as possible the formation of γ TiO_2. The titanium anode had a porous heterogeneous structure composed of α-titanium containing interstitial oxygen and nitrogen, and a fcc (face cubic centered) phase thought to be Ti(O,N). The final titanium anode thickness was 50–150 μm. Electrochemical aging was studied using catalyzed titanium anodes thermal sprayed on concrete slabs containing a steel mesh cathode. Cobalt catalyst, applied to the anode as an aqueous cobalt nitrate–amine complex, penetrated the anode and accumulated at the anode–concrete interface and in cracks within the concrete adjacent to the interface. Anodic polarization during and after application converted the cobalt to the active catalyst, Co_3O_4. With aging, cobalt catalyst dissolved in the increasingly acid environment of the interface and dispersed into the Ca-deficient, silica-rich reaction zone to reprecipitate and form a more diffuse site for the anode reactions. Stable operation of catalyzed anodes was maintained for a period equivalent to 23 years service at Oregon DOT bridge ICCP conditions with no evidence that operation would degrade with further aging. Early results from the field experiment at the Depoe Bay Bridge suggested anodes may age more slowly at low current densities with lesser impact from acidification [112].

To improve the marine corrosion resistance of stainless steel coatings fabricated by high-velocity oxyfuel (HVOF) spraying with a gas shroud attachment, Kawakita et al. [114] increased the molybdenum (Mo) content of stainless steel with a chemical composition of Fe balance-18 wt% Cr-22 wt% Ni-2–8 wt% Mo. The corrosion rate in sulfuric acid was improved when increasing the molybdenum content. The pitting corrosion resistance in artificial seawater was shifted toward the noble direction with increases in the molybdenum content. The number of rust spots formed by crevice corrosion in artificial seawater decreased after the addition of molybdenum to the coatings.

(b) Chemical or Parachemical Corrosion

Non-sacrificial coatings will never protect the substrate if connected porosities and oxide networks exist, which is the case of most thermal-sprayed coatings. The substrate protection requires using a protective bond coat or producing dense coatings, or sealing them that is generally possible if the service temperature is below few hundreds of Celsius degrees. Austenitic stainless steels, aluminum bronze, nickel-base alloys, MCrAlY, cermets with WC, Cr_2C_3, and matrices containing chromium or nickel or both are used against corrosion, often associated with wear. A few examples will be presented below.

Moskowitz [115] pointed out that the use of vacuum chambers or post-treatments can eliminate most defects, but these methods are costly and impractical on a large scale. Thus he proposed using modified HVOF process using unique inert gas shrouding to achieve highly dense, low-oxide coatings of metallic alloys. Coatings of corrosion-resistant alloys for severe corrosion applications in petroleum industry, such as type 316L stainless steel and Hastelloy C-276, were shown to act as true

corrosion barriers. The oxide content also played a role. For example, 316L stainless steel coatings formed by HVAF and HVOF were applied on carbon steel panels and their resistance to salt spray was tested as sprayed or sealed [116]. When coatings were sealed, corrosion was less on the HVAF coatings than that on the sealed HVOF coating, and almost no corrosion was observed on the sealed coating sprayed with powder of the largest particles (highest porosity) after even 500 h of salt spray testing. While the amount of through pores dominated the corrosion resistance of as-sprayed coatings, the degree of oxidation of the coatings (much less with HVAF) determined the corrosion resistance when sealing was applied.

For applications with a severe wear in oil and gas industry, cermets are used, with however some problems for offshore installations. According to Meng [117] the choice between the wide varieties of tungsten carbides with different alloying binders is not simple. The corrosion resistance must be improved by the proper choice of binder. For example, Souza and Neville [118] have shown that WC–CrNi exhibited passive behavior, as stainless steel, and would be compatible for use as a coating/substrate system when exposed to seawater, which was not the case for WC–CrC–CoCr. As previously mentioned the coating porosity and its oxide content must be as low as possible, which implied using HVOF guns resulting in higher impact velocities (low coating porosity) and lower particle temperatures (less oxidation), for more details see Sect. 5.3.1.5. This was illustrated by the work of Ishikawa et al. [119] who used a commercial HVOF with a gas shroud attachment (GS-HVOF) to prepare WC–CrC–Ni coatings. The density of coatings improved as the velocity of sprayed particles increased. Results of corrosion test indicated that through porosity was eliminated at velocities above 770 m/s with a lower degree of WC degradation. Wear resistance and hardness of coatings prepared by GS-HVOF were superior to those prepared by the conventional HVOF. Fedrizzi et al. [120] showed that Cr_3C_2–NiCr coatings, in sodium chloride solution under sliding wear, presented good barrier properties, and substrate corrosion was never observed. Moreover, when chromium was added to the metal matrix of WC–Co-based systems, tribo-corrosion behavior was enhanced and lower tribo-corrosion rates were measured. Plasma sprayed Cr_2O_3–8 wt% TiO_2 coating was used on hydraulic cylinder piston rods and rolls, but the substrate was rapidly corroded by the diffusion of the corrosive solution through pores: the bond coating was destroyed by the aggressive solution and ceramic coating flakes dropped off. Zhang et al. [121] have sealed coatings with epoxy and silicone resins. The sealing treatment improved the corrosion resistance of coatings significantly by blocking the open pores and cracks of the coating. Sealed by silicone resin, the coating gained remarkable anticorrosion properties, as after 1,200-h salt spray test, there was still no rust on the silicone resin-sealed coating.

For chemical corrosion, the coating material must be adapted to the corrosive medium. Coatings are often used to reduce costs, especially when solutions have been found in the use of sophisticated materials, oxidation-, and corrosion-resistant at high and low temperatures with high strength such as nickel-base superalloy Inconel 625. However, coatings of these materials on cheaper metals would be cheaper than bulk super alloy. Tuominen et al. [122] have shown that Inconel

625 HVOF sprayed presented mechanical and corrosion properties typically inferior to wrought materials due to the chemical and structural inhomogeneity of the thermal-sprayed coating material. Laser remelting, with high-power continuous wave Nd:YAG laser equipped with large beam optics, resulted in homogenization of the sprayed structure. This strongly improved the performance of the laser-remelted coatings in adhesion, wet corrosion, and high-temperature oxidation testing.

A rudder is one of the essential ship components for navigation and safety and services in the complex conditions of cavitation erosion and marine corrosion [122]. Kim and Lee [123] have investigated ten different coatings arc sprayed with Al-, Zn-, Cu-, and Fe-based wire feedstock for a rudder application. In terms of marine corrosion resistance, aluminum coating was the best, while stainless steel coating presented the highest resistance against cavitation erosion. Si addition improved both the hardness and bond strength of Al-based coatings, resulting in drastic increment of cavitation erosion resistance by about 40 times when adding 12 wt% Si. With Cu- and Fe-based coatings, interfacial oxidation occurred in between the coating and steel substrate, leading to interfacial cracks and coating delamination. The same authors, also for rudders, wire arc-sprayed Al–Zn and then sealed them with F–Si sealer, spread with the brush at room temperature for several times. The corrosion rate of the sealed specimen after coating was lower and the hardness higher and they presented good cavitation resistance characteristics [123]. Dent et al. [124] studied the corrosion characteristics in 0.5 M H_2SO_4 of two Ni–Cr–Mo–B alloy powders HVOF sprayed. Both coatings exhibited comparable resistance to corrosion. Microstructural examination of samples revealed the prevalence of degradation at splat boundaries, especially those where significant oxidation of the deposit occurred. Ishikawa et al. [125] wire arc sprayed a duplex coating composed of aluminum on 80Ni–20Cr alloy undercoat. The duplex coating presented an excellent performance in a hot, near neutral aqueous environment. The role of the undercoat layer of the sprayed 80Ni–20Cr alloy was to decrease the surface area of the steel substrate to be protected and reduce the sacrificing load for the aluminum and also to increase the adhesion of the aluminum topcoat by its roughness.

Magnesium alloys present low density and excellent physical and mechanical properties. They are particularly suitable for their use in automotive and aerospace applications, where replacement of steel and aluminum components by magnesium components would contribute to energy savings and reduced environmental impact. However, their drawback is their relatively high corrosion susceptibility and low wear resistance. That is why many studies of thermal spray coatings have been performed to improve their corrosion resistance. Pardo et al. [126] wire arc sprayed aluminum/silicon carbide composite coatings on AZ31, AZ80, and AZ91D magnesium–aluminum alloys. Presences of SiC particles provide higher hardness and wear resistance but not necessarily a better corrosion resistance. Corrosion was investigated in 3.5 wt% NaCl solution at 22 °C. Al/SiC composite coatings in the as-sprayed state revealed high level of porosity with poor bonding at the Al/SiC and coating/substrate interfaces, facilitating the degradation of the magnesium

substrates by galvanic corrosion. Cold-pressing post-treatment produced more compact coatings with improved corrosion performance. Arrabal et al. [127] evaluated also the corrosion behavior of wire arc-sprayed Al/SiC coatings on AZ31, AZ80, and AZ91D Mg–Al–Zn alloys in neutral salt fog (ASTM B 117) and high relative humidity (98 % RH, 50 °C) environments. As Pardo et al. [126], they found that the application of a cold-pressing post-treatment improved the corrosion performance of the coatings. In high humidity atmosphere, corrosion signs were only visible at the Al/SiC interfaces in the outermost surface of the coatings and in salt fog environment the galvanic corrosion of the substrates was delayed. Pokhmurska et al. [128] deposited on magnesium substrates (AM20, AZ31, AZ91) by wire arc spraying Zn, ZnAl4, and ZnAl15 solid wires and cored wires in aluminum core with powder filling containing different hard particles, such as boron, silicon, and tungsten carbide or titanium oxide. Remelting of thermal spray coatings was carried out by means of continuous irradiation of CO_2 laser in nitrogen or argon atmosphere, electron beam in vacuum, and focused tungsten halogen lamp line heater in atmosphere. Electrochemical behavior of modified surface layers was mostly improved due to alloying, homogenization of element distribution, and strong decrease of as-sprayed coating porosity.

18.3.2.2 High Temperature Corrosion

Against carburization, high nickel- and chromium-containing alloys are often used.

Against nitriding, many austenitic stainless steel and nickel base alloys present a good resistance to nitriding in ammonia.

Against sulfidation, certain Hastelloy and CoCrAlY are used.

Against molten salt corrosion resulting from sodium sulfates (such as Na_2SO_4), sodium chlorides (such as NaCl), and vanadium oxides (such as V_2O_5) no protection exists. However, corrosion consists of two stages: initiation and propagation. Thus CoCrAlY is recommended, provided, it contains 10–12 wt% of Al, because it has a very long initiation period.

For oxidation–corrosion resistance, nickel- and/or cobalt-based alloyed coatings are used: high chromium-containing alloys (NiCrMo: Hastelloy or Nistelle, CoCrSiMo: Tribaloy and MCrAlYs) Against molten glass, which is among the most corrosive media, plasma-sprayed coatings of platinum or their alloys are performed, spraying being performed in inert atmosphere where the over spray can be collected. Thermal sprayed ceramics can retard the corrosion. At last Mo–Ni–Cr coatings with addition of MoS_2 are used to reduce the wear and the friction of glass when transferred to mold.

Hot corrosion occurs mainly in thermal barrier coatings (TBCs), boilers, and molds:

– As summarized by Mohan et al. [129] and Jones [130] for TBCs when cost-effective alternative fuels, containing appreciable levels of elemental impurities such as V, Na, S, P, and Ca are used, corrosive compounds such as vanadates and

sulfates might arise as combustion by-products. In addition, TBCs are also increasingly susceptible to degradation by air-ingested CMAS [131] (acronym of each oxide deposits CaO, MgO, Al_2O_3, and SiO_2), especially in aircraft engines that operate in a dust-laden environment. Mohan et al. [129] have studied, at temperatures up to 1,400 °C, the degradation by V_2O_5 and a laboratory-synthesized CMAS of freestanding (on grit-blasted graphite substrates) yttria partially stabilized zirconia and CoNiCrAlY coatings (300 μm). The molten deposits destabilized the YPSZ with the formation of YVO_4 and reacted with the thermally grown oxide with various phase transformations and reaction product formation. CMAS melt readily dissolved the YSZ and then re-precipitated ZrO_2 with a composition based on local melt chemistry that deviates in the content of the Y_2O_3 stabilizer. Extensive dissolution of the TGO α-Al_2O_3 from freestanding APS CoNiCrAlY coatings by CMAS melt was observed. Enriching CMAS composition with Al promoted the crystallization of anorthite platelets and $MgAl_2O_4$ spinel and mitigated CMAS ingression [131]. Li et al. [132] investigated, in laboratory scale, the effect of CMAS. They found that the porous nature of the thermal-sprayed TBCs made them vulnerable to CMAS attack even before discernible chemical reaction started. A denser coating had the potential to resist the CMAS attack for a longer time than a more porous coating. Habibi et al. [133] compared the hot corrosion performance of YSZ, $Gd_2Zr_2O_7$, and YSZ + $Gd_2Zr_2O_7$ composite coatings in the presence of molten mixture of Na_2SO_4 + V_2O_5 at 1,050 °C. For YPSZ results were similar to those of Mohan et al. [129]. For the second composite coating, by the formation of $GdVO_4$, the amount of YVO_4 formed was significantly reduced. Molten salt also reacted with $Gd_2Zr_2O_7$ to form $GdVO_4$, but under 1,050 °C, these coatings were more stable, both thermally and chemically, than YPSZ and exhibited a better hot corrosion resistance. $LaTi_2Al_9O_{19}$ (LTA) exhibited [134] promising potential as a new kind of TBC material, with its excellent high-temperature capability and low thermal conductivity. Xie et al. [134] demonstrated its good chemical stability in molten salt of Na_2SO_4 and NaCl at 1,000 °C. However, the molten salt infiltrated to the bond coat, dissolving the TGO and resulting in hot corrosion of the bond coat. Mei et al. [135] studied the corrosion kinetics and mechanisms of NiCoCrAlTaY cold-sprayed coating and uncoated Mar-M247 superalloy in molten Na_2SO_4 salt vapor. Mass gain and microstructures after 200 h indicated that the NiCoCrAlTaY coating provided good oxidation and corrosion resistance in this vapor at 900 °C. Sidhu et al. [136] HVOF sprayed NiCrBSi, Cr_3C_2–NiCr, Ni–20Cr, and Stellite-6 coatings on a nickel-base superalloy and tested them at 900 °C in the molten salt (Na_2SO_4–60 %V_2O_5) environment under cyclic oxidation conditions. Among them, Ni–20Cr-coated superalloy imparted maximum hot corrosion resistance, whereas Stellite-6 coated indicated minimum resistance. The hot corrosion resistance of all the coatings was attributed to the formation of oxides and spinels of nickel, chromium, or cobalt.

– Hot corrosion degradation of metals and alloys is also a serious problem for many high temperature aggressive environment applications, such as boilers, fluidized bed combustion, and industrial waste incinerators. Chatha et al. [137]

deposited by HVOF process 80Ni–20Cr and 75Cr_3C_2–25(Ni–20Cr) coatings on T91 boiler tube steel. Hot corrosion was studied on bare and HVOF-coated steel specimens after exposure to a molten salt (Na_2SO_4–60 %V_2O_5) environment at 750 °C under cyclic conditions. The 80Ni–20Cr coating was found to be more protective than the cermet coating. Tani and Harada [138] examined the corrosion resistance of Ni–50Cr alloy coating, plasma-sprayed onto the fireside of steam generating tubes in a heavy oil-fired boiler. This coating, applied on steam generating tubes at Tocalo Co. Ltd., had remained for more than 20 years (about 140,000 h) demonstrating the corrosion resistant effect. Bala et al. [139] studied the corrosion resistance of Ni–50Cr coatings cold sprayed on two boiler steels SA-213-T22 and SA 516 (Grade 70). The aggressive environment consisted of Na_2SO_4–60 %V_2O_5 under cyclic conditions at 900 °C. The Ni–50Cr coated steels showed lesser weight gains than the bare metals and the oxide scales remained intact till the end of the experiment. According to Matsubara et al. [140], nickel-based self-fluxing alloy coating extended the service life of furnace wall tubes at waste incineration plants due to its excellent corrosion resistance and heat resistance. Fusing of such coatings by induction heating offered improved efficiency and reliability of products. A successful experimental application of 11 units in a waste incinerator revealed virtually no corrosion on the exposed surfaces and showed an improved water heating efficiency over that of the original tubes. Chatha et al. [141] investigated the corrosion resistance of HVOF sprayed Cr_3C_2–NiCr coating on ASME-SA213-T91 boiler steel without and with post-treatment of the coating by sealing and heat treatment. Corrosion tests consisted of exposure to a molten salt (Na_2SO_4–60 % V_2O_5) environment at 900 °C under cyclic conditions. Post-treated coating resulted to be more effective than as-deposited coating in enhancing the corrosion resistance of T91 steel. Tao et al. [142] HVAF-sprayed conventional and nanostructured NiCrC coatings. Hot corrosion was conducted in the Na_2SO_4–30 %K_2SO_4 environment, in the temperature range of 550–750 °C for periods up to 160 h. Both types of dense coatings possessed high corrosion resistance, especially the nanostructured NiCrC coating. The enhanced grain boundary diffusion in the nanostructured coating not only promoted the formation of a denser Cr_2O_3 scale with a higher rate but also helped to mitigate the Cr depletion at the metal/scale interface. Ceramic coatings are also used against corrosion.

Jansen et al. [143] compared the performance of dicalcium silicate-based coatings plasma sprayed to that of YPSZ coatings. Coatings were exposed to a V_2O_5–15 wt% Na_2SO_4 slag at 700 and 900 °C. At 700 °C, gaseous sulfidation was stimulated by an addition of 0.5 vol. % sulfur dioxide in air. The dicalcium silicate withstood combined attack without debonding, while the YPSZ coating deteriorated and spalled. Hirata et al. [144] investigated the influence of impurities of Al_2O_3 on the hot corrosion resistance against V_2O_5–Na_2SO_4 molten salt. Thickness of damage zone in Al_2O_3 ceramics, whose purity was high, depended linearly on the holding time. On the other hand, thickness of damage zone in Al_2O_3 whose purity was relatively low depended on square root of

holding time. In the impurities, SiO_2 especially affected the corrosion rate influencing the diffusion rate of corrosive elements through grain boundaries and thus the corrosion rate.

– Two examples of mold protection are presented. For the protection of aluminum for injection mold tools, Gibbons and Hansell [145] HVOF or plasma sprayed 100 ± 20 μm thick coatings of WC–10Co–4Cr, Cr_2C_3–20(Ni20Cr), 316 Stainless Steel, or Al_2O_3–40TiO_2. Substrates were made of three grades of aluminum: 2014 (90.4–95.0Al 3.9–5.0Cu 0.5–1.2Si 0.4–1.2Mn), 5083 (92.4–95.6Al 4.0–4.9Mg 0.4–1.0Mn), and 6082 (94.7–98.8Al 0.7–1.3Si 0.4–1.0Mn 0.06–1.2Mg). HVOF, except for the alumina–titania coating only plasma sprayed, was the most suitable of the two types of thermal spray systems evaluated, since APS was unable to provide high bond strengths. Furthermore, the processing by HVOF was not found to be detrimental to the fatigue life of the aluminum substrate. Mizuno and Kitamura [146] HVOF sprayed on AISI 316L substrate MoB/CoCr, a novel cermet material, with high durability in molten alloys for aluminum die-casting parts, and for hot continuous dipping rolls in Zn and Al–Zn plating lines. This coating presented a much higher durability without dissolution in the molten Al–45 wt% Zn alloy. Using undercoat was effective to reduce the influence of large difference in thermal expansion between the MoB/CoCr topcoat and stainless steel substrate. Combinations of topcoat and undercoat thickness were optimized to obtain intrinsic performance.

18.3.2.3 Oxidation

A variety of oxides can form on the surface and the further oxidation depends on the oxide layer forming a stable and continuous film. Of course the oxidation depends on the oxygen affinity of the elements forming the alloy. In most cases Cr and Al additions to the coating's matrix are used to form the oxidation barrier. Their quantity must be important enough to provide the renewal of the oxide layer that must be tough, well adhered and self-healing. Up to 430 °C, chromium–molybdenum steel presents a good resistance to oxidation. Up to 980 °C the high chromium (16–28 wt%)-containing alloys: NiCr, Inconel (Ni–Cr alloys), stellites (Co–Cr alloys), stainless steel present a good resistance. Over that temperature superalloys with aluminum (up to 5 wt%) are used, because aluminum forms an alumina film, which is more adherent than Cr_2O_3, thin enough to be ductile, and nonvolatile at 1,000 °C and over.

Many studies were devoted to the bond coat and the Thermally Grown Oxide (TGO) layer formation. The problem is that MCrAlY coatings contain only limited aluminum content because high values can lead to brittleness and potential crack. For example, Koolloos and Houben [147] have shown that pre-oxidation of the bond coat had a beneficial effect on lifetime when the oxidation was the main cause of failure. The pre-oxidation time and temperature were chosen such that a dense alumina layer was formed and the forming of spinel-type structures avoided. Fossati et al. [148] sprayed by VPS CoNiCrAlY coatings onto CMSX-4 single

crystal nickel superalloy disk substrates. As-sprayed samples were annealed at high temperatures in low vacuum. Three kinds of finishing processes were carried out producing three types of samples: as sprayed, mechanically smoothed by grinding, ground and PVD coated by using aluminum targets in an oxygen atmosphere. Samples were tested under isothermal conditions, in air, at 1,000 °C, and up to 5,000 h. Several differences were observed: grinding operations decreased the oxidation resistance, whereas the PVD process can increase the performances over longer time with respect of the as-sprayed samples. Jiang et al. [149] designed gradient coating that could provide a balance between high Al content and high-stress bearing ability. The gradient coating showed better performance of re-healing alumina β scale due to its possession of more β phase as Al reservoir. The improved high-temperature performance of the gradient coating was due to the Al enrichment of Al in the outer layer. Yuan et al. [150] sprayed the MCrAlY bond coat by HVOF and D-gun processes. The isothermal oxidation rate at 1,100 °C of the TBC system with the HVOF bondcoat was two times lower than that of the TBC system with the detonation-sprayed bondcoat. The rough surface of the detonation-sprayed bondcoat created a large specific surface area and unfavorable oxides on the bondcoat. Pint et al. [151] investigated by furnace cycling several different oxidation-resistant substrates with dry, flowing oxygen at temperatures from 1,000 to 1,200 °C. They determined the cyclic lifetimes of YSZ topcoat plasma sprayed or EB-PVD deposited. For NiAl + Zr (0.05–0.08 at.% Zr) substrate, the testing revealed that a more adherent alumina scale may extend the lifetime of commercial EB-PVD and PS coatings. Oxide-dispersion strengthened (ODS) FeCrAl substrates with YSZ topcoat seemed promising for the metallic skin of the next generation space shuttle. Limarga et al. [152] produced Al_2O_3/ZrO_2 functionally graded (FG) thermal barrier coatings, system incorporating an oxygen barrier layer between bondcoat and topcoat. Alumina has been highlighted as a potential material as oxygen barrier to improve the oxidation resistance of the bond coat since it has very low oxygen diffusivity. The results showed that FG systems exhibited superior mechanical properties and oxidation resistance at the expense of a slightly lower thermal insulating effect. Thin interlayer was preferred in order to minimize the detrimental effect of phase transformation of γ-Al_2O_3 to α-Al_2O_3 that resulted in tensile residual stresses at the interface.

High-temperature oxidation and corrosion phenomena in boilers are the source of many problems. Both the HVAF-sprayed conventional and nanostructured NiCrC coatings possess good properties against the oxidation and hot corrosion attacks [141]. Compared with its conventional counterpart, nanostructured NiCrC coating [141] exhibited better performance, which was believed to result from the faster formation of Cr_2O_3 scale with a denser structure. Even after thermal exposure at 650 °C for over 100 h, the nanostructured coating still kept its mean grain size less than 100 nm and seemed to be stable. Consequently, a large number of grain boundaries in the nanostructured coating served as "short circuit" channels for Cr diffusion [141]. Ramesh et al. [153] HVOF sprayed Ni-based hard facing NiCrFeSiB alloy powder on three kinds of boiler tube steels. Thermo cyclic oxidation studies were performed in static air at 900 °C. NiCrFeSiB-coated steels

showed slow oxidation kinetics and considerably lower weight gains than that of uncoated steels. The superior performance was attributed to continuous and protective thin oxide scale of amorphous SiO_2 and Cr_2O_3 formed on the surface of the oxidized coatings. Kaur et al. [154] deposited with D-gun Cr_3C_2–NiCr coating on T22 boiler steel. High-temperature oxidation in air and oxidation–erosion in actual boiler environment at 700 °C under cyclic conditions were carried out. While the uncoated boiler steel suffered from a catastrophic degradation in the form of intense spalling of the scale, the Cr_3C_2–NiCr coating showed good adherence to the boiler steel during the exposures with no tendency for spallation of its oxide scale. Sidhu et al. [155] HVOF sprayed WC-NiCrFeSiB coating on Ni-based superalloy (Superni 75) and Fe-based superalloy (Superfer 800H). The coated as well as uncoated specimens were exposed to air and molten salt (Na_2SO_4–25 % NaCl) environment at 800 °C under cyclic conditions. The oxides of active elements of the coatings, formed in the surface scale as well as at the boundaries of nickel and tungsten rich splats, have contributed for the oxidation and hot corrosion resistance. These oxides acted as barriers for the diffusion/penetration of the corrosive species through the coatings.

Singh et al. [156] deposited by a shrouded plasma spray process Stellite-6 on two Ni-base superalloys, Superni 601 and Superni 718, and one Fe-base superalloy, Superfer 800H. Oxidation studies were conducted on the coated superalloys in air at 900 °C under cyclic conditions for 50 cycles. The rate of oxidation was observed to be high in the early cycles of the study for the coated superalloys, which may be attributed to the interconnected network of pores and splat boundaries present in the coating structure. The Stellite-6 coating after exposure to air oxidation showed the presence of mainly oxides in its surface scale. The phases revealed where oxides of Cr and Co and spinels containing CoCr mixed oxides were present, oxides reported to be protective in nature against the high-temperature oxidation. Bala et al. [157] have deposited by cold spray Ni–20Cr and Ni–50Cr coatings on two boiler steels. The coatings, in general, were found to follow the parabolic rate of oxidation and were successful in maintaining their surface contact with their respective substrate steels.

18.3.2.4 Corrosive Wear

Corrosive wear occurs when the effects of corrosion and wear are combined, resulting in a more rapid degradation of the material's surface. A surface that is corroded or oxidized may be mechanically weakened and more likely to wear at an increased rate. Furthermore, corrosion products including oxide particles that are dislodged from the material's surface can subsequently act as abrasive particles. Stress corrosion failure results from the combined effects of stress and corrosion. At high temperatures, reactions with oxygen, carbon, nitrogen, sulfur, or flux result in the formation of oxidized, carburized, nitrided, sulfidized, or slag layer on the surface. Temperature and time are the key factors controlling the rate and severity of high-temperature corrosive attack [5].

The effect of fluids containing solid particles is complex and depends on the surface temperature. At low temperature the main phenomenon is erosion, with

increasing temperature both erosion and oxide scale formation are similar. The loss of oxide prevails with further increase of temperature (chipping of the brittle scale). It is thus necessary to use a compatible matrix with hard reinforcing phases such as carbides and oxides. It is also necessary to limit residual stresses within coating for example by using graded layers.

The problem of erosion–corrosion of materials at elevated temperatures is that the extent of wastage in such environments is dependent on a wide variety of parameters, which include properties of the impacting particles (angularity, for example), impact angle, target material, and nature of the corrosive environment, as well as the composition of the oxide scale formed during the erosion–oxidation process.

(a) Low Temperature

Hill et al. [158] investigated HVOF-sprayed coatings of Fe–Cr–C and Fe–Cr–V–C on high-chromium high-carbon tool steels in the as-processed state and after a quenching and tempering treatment. Coatings were also achieved by super solidus liquid phase sintering (SLPS). In comparison, sintered steels were analyzed in the quenched and tempered conditions only. The performed heat treatment was able to improve the properties of both steels leading to an increase of hardness due to martensite formation (SLPS and HVOF) and also carbide precipitation (HVOF) and an assumed increase of wear. The lower corrosion resistance of the high-vanadium tool steel X420CrVMo18-16 in comparison to X190CrVMo20-4 was due to a lower concentration of dissolved chromium in the metal matrix. The HVOF coatings showed a decrease in corrosion resistance in relation to the sintered material because of smaller precipitates and formation of chromium oxides. Kembaiyan and Keshavan [159] deposited, on drill bits in mining, oil and gas drilling, 82W–15Co–3C by Super-D-gun, 8ONi–1OCr–4Fe–4Si–1.8B–.4C by spray fused and laser cladded, Fe–Cr–Ni by wire feeded and fuse welded, WC based by plasma, 36Ni–44W–6Cr–6Co–1.8Si–1.9Fe–1.35B by flame and laser cladded, all heat treated afterwards. The D-gun coating offered beneficial compressive residual stresses on the inserts and cone shell, thereby being the best coating protecting three cone drill bits from corrosion and fluid erosion. Uozato et al. [160] plasma sprayed Fe–C powders, with or without nickel added (up to 14 wt%), on a cast AA383 aluminum alloy plate. Corrosion and wear tests in engine oil with or without sulfuric acid water solutions added were performed as well. The corrosion performance was dependent upon the nickel content. Souza and Neville [118] studied the influence of microstructure on the overall material loss in erosion–corrosion environments for WC–Co–Cr coatings applied by HVOF and D-Gun processes. The work was devoted to the enhancement of erosion due to corrosion effects. HVOF coatings had a slightly lower corrosion resistance than the D-Gun coatings but higher overall erosion–corrosion resistance. The formation of different tungsten species, η phases and a higher Cr amount reduced the toughness of WC–Co–Cr coatings and the corrosion rates under erosion–corrosion. Stainless steel components coated with Inconel-625 are very common in the oil/gas industry. That is why Al-Fadhli

et al. [161] HVOF sprayed Inconel-625 on three different metallic surfaces: (a) plain stainless steel (SS), (b) spot-welded stainless steel (SW-SS), and (c) a composite surface of stainless steel and carbon steel welded together (C-SS-CS). The erosion experiment was carried out using a jet impingement rig through which natural seawater (pH 8.3) or sand slurry was circulated. The coating exhibited excellent erosion–corrosion resistance, as it was not highly affected by the type of substrate material. The coating was found to be highly sensitive to the presence of sand particles in the impinging fluid. As the period of coating exposure to the flow of slurry fluid increased, weight loss increased significantly, the increment being dependent on the type of substrate material.

Polymer coatings have received increased attention as protection against corrosion and wear for several environmental conditions mainly in the automotive, petrochemical, oil, and gas industries. Lima et al. [162] flame-sprayed (Terodyn-System2000 gun of Eutectic) Polyetherimide (PEI), poly-ether-ether-ketone (PEEK), and Polyamide 12 (PA 12) polymers onto carbon steel substrates. The obtained coatings had formed a dense and smooth deposit with good adhesion and no significant defects. The abrasive wear test showed a better performance for polyamide 12 samples, almost twice better than PEEK and 20 % better than PEI. Polyamide 12 and PEEK coatings showed no corrosive attack in a very aggressive H_2SO_4 40 vol. % solution after 2,000 h of testing. Under the experimental conditions used in their work [162], PEEK and PA 12 coatings had a better corrosion performance but PA 12 had much better abrasive wear performance. As the presence of sand and mineral particles flowing in a corrosive fluid produced a high degradation rate of the hydro-transport equipment, Flores et al. [163] studied the erosion–corrosion behavior of two tungsten carbide cermets coatings obtained by PTA process. Two variations of the CNiCrFeBSi matrix, called soft and hard, with different concentration of chromium (Cr), carbon (C), and boron (B) were evaluated with and without reinforcing hard phase. Important microstructural differences were identified between the two Metal Matrix Composites (MMCs). Elongated precipitates rich in W and Cr were identified near the WC grains and in the matrix phase of the WC-hard overlay. Needle-like precipitates with a lower concentration of W were identified in the WC-soft overlay. For both MMCs the γ-Ni phase and silicides were present in the matrix phase. The MMC with the harder matrix showed the lower mass loss and the erosive degradation was predominant in the overall erosion–corrosion process at the lower temperature. A different behavior was observed when the temperature of the testing solution was increased and a low sand concentration was used. PTA coatings are excellent, when wear and corrosion are present at low temperature, see Sect. 10.7.4 of Chap. 10.

(b) High Temperature

Sidhu and Prakash [164] evaluated the erosion–corrosion (E-C) behavior of as-sprayed plasma and laser remelted Stellite-6 coatings on boiler tube steels (3 different ones) in the actual coal fired boiler environment at 755 °C. Coating

has been found to be effective in increasing the E–C resistance of boiler steels in the coal-fired boiler environment. Among the as-coated steels the highest E–C resistance has been observed for T11 steel, probably due to the presence of a continuous chromium-rich band lying at bond coat–substrate interface. A less porous structure obtained after laser remelting was found to be effective for increasing E–C resistance to the given environment for this coated T11 steel. Wang [165] HVOF sprayed Cr_3C_2–NiCr coating and tested them in conditions simulating erosive conditions in tubular heat exchangers of fluidized bed combustor boilers. These coatings showed excellent E–C behavior as compared with 1018 steel, A213 T22 steel. Coating high E–C resistance was attributed to its high compactness, fine grain size structure, and the homogeneous distribution of the skeletal network of hard carbides within a ductile, corrosive-resistant metal binder. Uusitalo et al. [166] sprayed various coatings by HVOF, wire arc, and plasma and simulated the E–C conditions in the superheater section of a circulating fluidized bed combustor by a burner-rig type working at elevated temperature. The gas temperature was 850 °C and the specimen temperature was adjusted to 550 °C by cooling the specimen internally with pressurized air. In E–C tests in presence of chlorine, nickel-based HVOF coatings performed the best, whereas carbide containing HVOF coatings and diffusion coatings wore away. Kaur et al. [154] D-gun sprayed Cr_3C_2–NiCr coating on T22 boiler steel. Coated and not coated boiler steel were subjected to high-temperature oxidation in air and oxidation–erosion in actual boiler environment at 700 °C. The uncoated boiler steel suffered from a catastrophic degradation in the form of intense spalling of the scale in both environments. The Cr_3C_2–NiCr coating showed good adherence to the boiler steel during the exposures with no tendency for spallation of its oxide scale.

Kim and Walker [21] developed a nanostructured titania coating for ball valves destined for high-pressure acid-leach (HPAL) service. The nanostructured titania coating provided dramatically superior resistances against abrasive and erosive wear compared to titania conventional coatings. The enhanced wear performance seemed to be due to improved toughness. The nanostructured titania coating has been applied onto ball valve components in ten locations around the world and has performed very well. PTA coatings are also successful against corrosion and wear at high temperatures, see Sect. 10.7.4 of Chap. 10.

18.3.3 Thermal Protection Coatings

Thermal protection helps reducing exposure temperature of the metal, increases thermal efficiency, often limits oxidation or corrosion, and finally extends the lifetime of the component. The main problem is that good heat flux protection requires low thermal conductivity materials that are generally refractory metals (W, Mo, Ta, Nb) or oxides, the expansion coefficients of which are relatively low compared to those of protected metals or alloys. Thus a bond coat is often

mandatory both to adapt the expansion mismatch and also to protect the metal or alloy from oxidation, the low thermal conductivity oxide coatings being often rather porous.

- Refractory metals give a good protection to high heat fluxes but their resistance to oxidation is relatively poor. Thus they are used against high heat fluxes for short times (rockets for example) or in nonoxidizing environment,
- Alumina can be used up to 900 °C because over that temperature the γ phase of plasma sprayed coatings transform into α phase with an important volume change resulting in coating peeling off.
- Zirconia is the most used material, but it must be stabilized to avoid phase transformations with temperature. The problem is then the price of the stabilizer. The cheapest ones are CaO or MgO but unfortunately over about 600 °C the stabilization becomes inefficient [167] and these powders, especially CaO, are essentially used for diesel engines. For higher temperatures yttria is used either with 7–8 wt% (partially stabilized zirconia: tetragonal phase) or 12 wt% (stabilized zirconia: cubic phase). The maximum service temperature is around 1,200 °C and the thermal conductivity of plasma sprayed coatings is around 1 W/m K. One of the problems of these coatings is their sintering increasing their thermal conductivity. When using powder manufactured from chemical route (sol–gel technique with an intimate mixing of zirconia and yttria at the nanometer level) the maximum temperature reaches 1,350 °C, but the powder price is higher. Other stabilizers are used such as CeO_2, GeO_2, Nb_2O_5, To_2O_5, Sc_2O_3, however, they are more expensive than Y_2O_3 and 24 wt% of them are required for zirconia stabilization. Even if their thermal conductivities are slightly lower than that of ZrO_2–7 wt% Y_2O_3 the maximum service temperature is about the same. Researches are now about pyrochlore structures such as La_2ZrO_7, Nd_2ZrO_7 et $Gd_2Zr_2O_7$ that melt at temperatures over 2,000 K but have no phase change. Another important problem with high-temperature thermal barriers is the compatibility of their coefficient of thermal expansion with that of the substrate especially under conditions of temperature changes (stopping and starting the reactor). Unfortunately, the drawback of the high compliance obtained with the columnar structure of EB-PVD coatings is that it eases the access of high temperature air or CMAS (acronym of each oxide: CaO, MgO, Al_2O_3, and SiO_2) to the bond coat, which resistance must be improved.

18.3.3.1 Thermal Barrier Coatings for Aero Engines

As illustrated in Fig. 1.8, many parts (hundreds of components) are sprayed in an aircraft engine. If at the beginning coatings were APS and VPS sprayed, HVOF spraying has been rapidly adapted to needs and twin-arc spray process is now explored. Coatings are used against fretting wear, to reduce friction, for clearance control, for high temperature protection, as thermal barrier, as seals, to replace hard chromium in landing gear [1].

TBCs were first successfully tested in the turbine section of a research gas turbine engine in the mid-1970s. By the early 1980s they had entered revenue service on the vane platforms of aircraft gas turbine engines [167, 168], and today they are flying in revenue service on vane and blade surfaces [168]. Thermal insulation benefits provided by TBCs and the resulting impact on component creep and thermomechanical fatigue life have made them enablers of high-thrust gas turbine engines. As underlined by Pratt and Whitney, of particular importance is the EB-PVD-based TBC, presenting an excellent compliance upon thermal cycles were then anticipated to improve blade life by a factor of 3 [169]. The aging of TBC's topcoat strongly depends upon the spray conditions and powder morphologies used to spray or deposit it, conditions acting on its sintering [170, 171]. The second problem is the oxidation of bond coat with the formation of Thermally Grown Oxide (TGO) [172–177] as well as the bond coat corrosion with oxides such as CMAS [129, 130, 132, 174] or vanadium oxide [178]. Feuerstein et al. [179] have shown that the most advanced thermal barrier coating (TBC) systems for aircraft engine and power generation hot section components (combustors, blades and vanes) consist of electron beam physical vapor deposition (EBPVD) applied yttria-stabilized zirconia and platinum-modified diffusion aluminide bond coating. Thermally sprayed ceramic and MCrAlY bond coatings, however, are still used extensively for combustors and power generation blades and vanes. Feuerstein et al. [179] have reviewed and compared the state-of-the-art processes for the deposition of TBC systems: shrouded plasma and HVOF for MCrAlY bond coat, plasma for low-density YSZ, and dense vertically cracked Zircoat, platinum aluminide diffusion coatings, EBPVD TBC. They outlined and compared key features of coatings and their cost elements actually used in industry. Vaßen et al. [180, 181] have presented last developments using advanced processing: methods allowing obtaining highly segmented TBCs [182] and the important recent directions of development for TBC systems, including improved processing routes and advanced TBC materials are discussed. Numerous studies were devoted to the resistance of the bond coat [176] and the way to improve it [167, 174] by bond coat treatment, or the choice of the spray process [182, 183]. For the TBC topcoat, promising new technologies such as TF-LPPS (Thin Film-Low Pressure Plasma Spraying) [184, 185] or solution or suspension or nanometer-sized agglomerated particles plasma sprayed will probably play an increasing role in future applications [186].

(a) Conventional Plasma Spraying

The evolution of TBCs for aero engines is well summarized when comparing review papers published at the end of 1990s [187–189] with more recent ones [180, 190, 191] and also those related to coating materials [192–199]. In 1999, Miller [168] said that TBCs have evolved from the laboratory to low risk turbine section applications and then on to an integral part of engine design. Beele et al. [189] underlined that if partially stabilized zirconia became the standard

material very early on, thermal spraying and electron beam physical vapor deposition in the early 1990s were even considered as competing technologies. In 2008 Feuerstein et al. [179] emphasized that "the most advanced thermal barrier coating (TBC) systems for aircraft engine and power generation hot section components consisted of electron beam physical vapor deposition (EBPVD)-applied yttria-stabilized zirconia and platinum-modified diffusion aluminide bond coating. Thermally sprayed ceramic and MCrAlY bond coatings, however, are still used extensively for combustors and power generation blades and vanes." However, as for any industrial production, the coating cost is a key parameter. For thermal spray processes, the labor and material costs are the major ones, while for EBPVD, the equipment cost is substantial (up to 50 % of the cost is for depreciation interest [179]) and its utilization must be effective. During the last decade many works were devoted to bond coats, see [176] and Sect. 18.3.5. Zirconia partially stabilized with yttria (YPSZ) was identified as the best ceramic topcoat material and has been established as standard for the last 30 years. However, correlatively, especially the last decade, other ceramic materials have been studied:

- Zirconia stabilized with CeO_2 [193, 194]: low thermal conductivity, less phase transformation than YSZ, but increased sintering rate compared to YSZ.
- Zirconia partially stabilized with dysprosia [195, 196]: more resistant to sintering than standard YSZ coatings up to 200 h at 1,150 °C, but the thermal properties of which were significantly influenced by the operating conditions. The lowest thermal conductivity at high temperatures was reached with the HOSP 4DyPSZ coatings (0.70 W/m K at 700 °C and 0.76 W/m K at 1,000 °C).
- Pyrochlore structure ($A_2B_2O_7$) materials offer properties comparable to YSZ with a lower thermal conductivity for several zirconate pyrochlores, especially $La_2Zr_2O_7$, that have also an excellent thermal stability [191].
- Zirconia doped by different rare-earth cations with the formation of dopant clusters as in the ZrO_2–Y_2O_3–Nd_2O_3(Gd_2O_3, Sm_2O_3)–Yb_2O_3(Sc_2O_3) [190].
- Hexaaluminates such as (La,Nd)$MAl_{11}O_{19}$, where M could be Mg and Mn to Zn, Cr, and Sm, present excellent longtime sintering resistance and structural stability up to 1,800 °C. For example, Chen et al. [197] have sprayed YSZ-based composite coatings with the addition of $LaMgAl_{11}O_{19}$ (LaMA) as the secondary phase. Unfortunately composite coatings showed much shorter thermal cycling lifetime than the monolithic YSZ coating due to the presence of as-sprayed LaMA (La $MgAl_{11}O_{19}$) coating with a large amount of amorphous phase reducing the thermal insulating efficiency and accelerating the oxidation and degradation of bond coat. Chen et al. [198] also sprayed five layer functionally graded TBC based on LaMA/YSZ system. The amorphous LaMA phase underwent recrystallization processes during high temperature aging, resulting in the formations of LaMA platelet-like grains and imparting the TBC with improved thermal and mechanical properties and a higher strain tolerance. Such coatings presented a good thermal cycling lifetime at the surface testing temperature above 1,350 °C.

- Perovskites (ABO_3 crystal structure such as $BaZrO_3$ or $SrZrO_3$ or $CaZrO_3$) have also been extensively studied [191]. Jarligo et al. [199] synthesized Ba $(Mg_{1/3}Ta_{2/3})O_3$ and La$(Al_{1/4}$ $Mg_{1/2}$ $Ta_{1/4})O_3$ compositions and plasma sprayed them as ceramic topcoats of TBC either in single layer or in double-layer combination with conventional YSZ. The low value of fracture toughness for the complex perovskites and the thermally grown oxide at the topcoat–bondcoat interface of the TBCs were, however, the major factors which led to the coating failure on thermal cycling at about 1,250 °C. Similar results were obtained by Ma et al. [200]. Yu et al. [201] tested $Sm_2Zr_2O_7$ coatings that exhibited low microhardness and elastic modulus, which increased with rise in aging temperature because of the microstructure reconfiguration.
- Other ceramics were also tested. $LaTi_2Al_9O_{19}$ (LTA) was synthesized by solid-state reaction at 1,773 K by Xie et al. [202], and the mechanical properties of the LTA bulk were evaluated. A double-ceramic layer LTA/YSZ TBC structure was proposed and the TBC sprayed by plasma spraying. The LTA/YSZ TBC remained intact even after 3,000 cycles, exhibiting a promising potential as new TBC materials. Guo et al. [203] produced $BaLa_2Ti_3O_{10}$ (BLT) by solid-state reaction and plasma sprayed it. The coating contained segmentation cracks and had a porosity of around 13 %. Thermal cycling result showed that the BLT TBC had a lifetime of more than 1,100 cycles of about 200 h at 1,100 °C and the failure occurred by cracking at TGO.
- Ceramic mixtures were also proposed: Liu et al. [204] showed that the La_2O_3 addition can effectively alleviate the grain growth of YSZ coatings under high temperatures.

Of course, besides the choice of the TBC's materials, works on the process optimization were also developed. Paul et al. [205] studied the influence of the YSZ purity on the YSZ TBS. They showed that reducing the contents of alumina and silica, from 0.1–0.2 wt% down to 0.01–0.05 wt%, induced a significant reduction in the sintering rates. Mihm et al. [206] studied the spray process optimization. Tan et al. [207] showed, with process mapping strategies and spraying hollow powders, that it was feasible to produce tailored microstructures with substantially lower thermal conductivity than generally reported for YSZ TBCs. It also allowed enhancing thermostructural compliance and reducing propensity to sintering during elevated temperature exposure. Guo et al. [208] studied the segmentation cracks density of thick TBCs (1.5 mm) for thermal protection of combustor. A segmentation crack density of 3.65/mm exhibited a thermal cycling lifetime of more than 1,500 cycles at 1,250 °C for the surface/950 °C for the bond coat, indicating an excellent thermal shock resistance. Zhu et al. [209] tested conventional TBCs (APS sprayed ZrO_2–8 wt% Y_2O_3 with a NiCrAlY VPS bond coat) sprayed onto 25.4-mm diameter and 3.2-mm thick nickel base superalloy specimens. A high-power CO_2 laser was used to test the TBC specimens under high temperature (1,287 °C) and high-thermal gradient cyclic conditions. If the initial average cracks propagation rates were in the range of 3–8 μm/cycle, the crack propagation rates increased to 30–40 μm/cycle at later stages of testing and the critical spalling crack size ranged

from 3 to 5 mm. According to Shin et al. [210] the failure of TBC is directly connected to the failure of the blades because the spallation of the ceramic layer accelerates the local corrosion and oxidation. They performed thermal fatigue tests at 1,100 °C and 1,151 °C for coin-type specimens. Delamination cracks occurred at the edge of a specimen first and then the area of the edge delamination gradually increased toward the center. A thermally grown oxide (TGO) was formed and grew at the interface between the topcoat and the bond coat. The crack propagated with increase of cycle number, growth resulting from the TGO formation, and the high normal stress at the edge. Kim et al. [211] also investigated the failure mechanisms of coin-shaped plasma-sprayed TBCs for gas turbine blades due to cyclic thermal fatigue. Hernandez et al. [174] quantified, through finite element analyses, the thermomechanical response of the bond coat (NiCoCrAlY) and the thermally grown oxide (TGO) for a YPSZ. The models they developed include nonlinear and time-dependent behavior such as creep, TGO growth stress, and thermomechanical cyclic loading. Eriksson et al. [87] for the same type of TBCs studied the effect of three different heat treatments: isothermal oxidation, thermal cycling fatigue (TCF), and burner rig test (BRT) using a thermal shock rig (TSR). The specimens subjected to BRT gave much thinner interface TGO due to their shorter exposure time to high temperature, and the TGO consisted almost exclusively of Al_2O_3. TCF-subjected specimens had areas of cracked interface TGO, while the thin interface TGO in the BRT-subjected specimens did not contain any cracks. Jang et al. [212] studied TBCs bond coats (0.08, 0.14, and 0.28 mm) HVOF sprayed. The TGO layer with the thickness of 2.8–3 μm was formed after thermal fatigue tests, showing the same effects in both the temperature and the dwell time. The bond coat thickness did not affect the formation of the TGO layer. As the thickness of the bond coat increased, the damage zone in the substrate decreased, the bond coat acting as a buffer layer under applied loads. Re-sintering of the top coating during the thermal fatigue tests was evident from the fatigue damage and the observed increase in the hardness values. Li et al. [213] examined through thermal cyclic test TBCs behavior with the NiCoCrAlTaY bond coats deposited by cold spraying and low-pressure plasma spraying. The surface of the cold-sprayed bond coat presented a smoother configuration than that of the LPPS-sprayed bond coat. Ni/Cr oxides easily formed on the LPPS bond coat during oxidation. In contrast, TGO on the cold-sprayed bond coat was uniform in both thickness and composition. The uniform protective TGO enhanced the thermal cyclic behavior of the TBCs. These results suggested that cold spraying is a promising process to deposit MCrAlY bond coat for high performance of TBCs.

(b) New Spray Processes

Plasma spray-physical vapor deposition (PS-PVD), recently developed by Sulzer Metco [214], is a low-pressure plasma spray technology to deposit coatings out of the vapor phase. PS-PVD is a part of the family of new hybrid processes. It is then possible to deposit a coating by vaporizing the injected material. Coatings show a

unique columnar microstructure, so far only known from other vapor phase deposition processes like EB-PVD.

But economical evaluations for columnar coatings on turbine components under production conditions show a clear saving potential when using the PS-PVD process. Hospach et al. [184] showed that quasi vapor deposition from clusters resulted in columnar coatings with high porosity and growth rate. The low working pressure (about 100 Pa) increased the size of the plasma plume and enabled homogeneous coatings, which made this process interesting in particular for large-scale applications.

New developments in suspension or solution plasma spraying seem also very promising (see Chap. 14). Vaßen et al. [180] pointed out that suspension spraying offers the manufacture of strain-tolerant, segmented TBCs with low thermal conductivity. In addition, highly reflective coatings, which reduce the thermal load of the parts from radiation, can be produced. Gell et al. [215] showed that solution sprayed TBCs have a microstructure characterized by: strain relieving through thickness vertical cracks, fine, dispersed porosity ultra-fine splats with enhanced splat-to-splat bonding. First tests showed that such coatings have equal or greater durability, lower thermal conductivity, higher in-plane toughness and bond strength, and costs comparable to APS. However, to our best knowledge such coatings have not yet been tested in industry

(c) Coatings Against Fretting

In the lower and higher temperature sections of engines, carbide cermets are the common materials used against fretting. Below 540 °C WC in cobalt matrices (6–12 wt%) with chromium addition (4–12 wt%) are used and at higher temperatures CrC carbides in NiCr matrices are used [1]. HVOF spraying is often used to limit carbides decomposition. CuNiIn is one of the oldest coatings used against fretting [1, 78].

18.3.3.2 Thermal Barrier Coatings for Land-Based Turbines

Coating life for land-based turbines (time to refurbish aircraft turbines), should be approximately 24,000 h, with a majority of all service time at maximum conditions, against 8,000 h for aircraft turbines with only 5–15 % is at maximum conditions. Thus problems of bond coat oxidation, interdiffusion of bond coat and substrate, coating densification, and changes in thermal or mechanical properties of the coating are more important. Accessibility for inspection, repair, and refurbishment is also more difficult for power generation machines than for aircraft engines. Components size is also more important (a factor of 10 for turbine blades), thus requiring adapted spray processes. At last the quality of the combustible is far from that used in aircraft engines [216–220].

Compared to aero engines land-based turbines work in different conditions: the external environment might range from cold (−40 °C) to high temperature (55–60 °C) and corrosive and erosive contaminants due to the environment and fuel are present. Coatings are applied onto bearing journals, bearing seals, sub-shaft journal, labyrinth seals, blades, tip seals, inlet and exhausts, and housing [1]. A detailed description of the different land-based turbines can be found in the paper of Lebedev and Kostennikov [221]. Pomeroy [222] gives a good description of coatings for gas turbine materials and long-term stability issues. Due to the demand to increase turbine inlet temperatures and thus cycle efficiencies, ceramic insulating coatings can be applied to decrease the temperature of the hottest parts of the turbine components by up to 170 °C. A review of the next generation of TBCs for gas turbines is presented by Curry et al. [223].

Turbines are also exposed to excessive amounts of moisture and chlorides and also two types of hot corrosion and oxidation occur:

– Type II hot corrosion occurring at temperatures in the range 500–800 °C and involving the formation of base metal (nickel or cobalt) sulfates which require a certain partial pressure of sulfur trioxide for their stabilization,
– Type I hot corrosion, observed in the range 750–950 °C, involving the transport of sulfur from a sulfatic deposit (generally Na_2SO_4) across a preformed oxide into the metallic material with the formation of the most stable sulfides. Once stable sulfide formers (e.g., Cr) are fully reacted with the sulfur moving across the scale, then base metal sulfides can form with catastrophic consequences as they are molten at the temperatures at which Type I hot corrosion occurs.

At last oxidation starts at temperatures over 1,000 °C.

Sprayed materials with a good corrosion and oxidation resistance are nickel- and/or cobalt-based alloyed coatings [1], such as NiCrMo (Hastelloy or Nistelle), CoCrSiMo (Triballoy), and MCrAlYs plasma or HVOF sprayed. Oxidation- and corrosion-resistant coatings are applied on air inlets, combustor liners, injectors, turbine tip shoes, nozzles, and exhausts [1]. On blades and vanes MCrAlY coatings are used as bond coats and for corrosion–oxidation protection.

For thermal barrier coatings mainly ZrO_2–Y_2O_3 (6–8 wt%), ceria or dysprosia-stabilized zirconia are used [220] and also ceria and yttria-stabilized zirconia or for certain applications calcium titanate [1]. It is worth underlying that for abradable and seals in the low-temperature areas, where moisture is important, porous aluminum-base coatings containing polyester, polyimide or BN, as well as nickel–graphite coatings are used. For higher temperatures (over 450 °C), abradables are made of MCrAlY with BN or polyester [1, 222]. Ceramic abradables have also been introduced but the expansion mismatch with the metal substrate must be accounted for with the cooling of the superalloy.

18.3.3.3 Thermal Barrier Coatings for Diesels

TBC for diesel engines either thick [224], or eventually phosphate sealed [225], or thin [226] are used to:

- Increase the piston head temperature and improve the fuel combustion [227]
- Reduce NO_x emissions [227]
- Reduce the heat rejection [228]
- Improve the usability of vegetable oils as a fuel [229]

18.3.3.4 Other Applications

- Ultrahigh temperature ceramics (UHTC) coatings deposited by plasma spraying are studied, such as ZrB_2–SiC(30 vol. %)–$MoSi_2$ (10 vol. %) [230]. Advanced coating systems based on monazite (two-phase mixture of $LaPO_4$ and Al_2O_3), a weak interphase for oxide composites, have been investigated as a means to increase the service temperatures of thermal protection blankets for re-entry space craft [231].
- Thermal barriers of zirconia stabilized by 8 wt% yttria (8YPSZ) for rare earth magnesium alloy were fabricated by atmospheric plasma spraying [232]. The thermal resistance of coating is obvious. The thermal insulation tests indicated that the coating with a topcoat thickness of 108 μm reduces the substrate temperature for about 80 °C and the coating surface could sustain a temperature of 534 °C. The coating also largely improves hardness, wear, and corrosion resistances of Mg alloy.
- Thermal barrier coatings were fabricated on polyimide matrix composites via air plasma spray process [233]. They consisted of Al (30 μm) as the bond coating and YSZ (130 μm) as the top ceramic. When thermal ablation test was at about 815 °C, the weight loss of the sample decreased from 7.05 % to 1.90 %, while the corresponding mass ablation rate reduced from 0.48 to 0.21 mg/s.
- Other ceramics were studied for TBCs. For example, Limarga et al. [152] studied Al_2O_3/ZrO_2 functionally graded (FG) thermal barrier coatings. The proposed FG system exhibited superior mechanical properties and oxidation resistance at the expense of a slightly lower thermal insulating effect. Thin interlayer was preferred in order to minimize the detrimental effect of phase transformation of γ-Al_2O_3 to α-Al_2O_3 that resulted in tensile residual stresses at the interface. Cojocaru et al. [234] plasma sprayed two different types of mullite powders (spray dried and freeze granulated) and a mullite-YSZ 75/25 vol.% mixture spray-dried powders. They showed that mechanical properties of coatings produced from particles with different morphologies (e.g., spray dried and fused and crushed) could be matched and tailored if the deposition conditions were carefully controlled to produce coatings with similar microstructural features. Suzuki et al. [235] studied plasma-sprayed zircon ($ZrSiO_4$) for an environmental barrier coating (EBC) application and reported that substrate temperature was one of the most important factors to obtain crack-free and

highly adhesive coating. Four different amount of yttria addition: 3, 5, 10, and 20 mol. % of $YO_{1.5}$ into $ZrSiO_4$ were tested. YSZ, zircon, and yttrium silicate were formed in the yttria-added coatings. More amount of yttria addition decreased the zircon formation. This resulted in less porosity in the coating even after the heat treatment at 1,400 °C, thereby improving the coating stability and adhesion.

18.3.4 Clearance Control Coatings

In compressors, gas turbines, and turbochargers, dimensional changes take place between the rotor and stator components because of thermal and mechanical effects during operation. These dimensional changes affect sealing and clearance control systems, consisting of a sacrificial element and a cutting component, are used. Thermal spray coatings, called abradables, and honeycomb seals form effective sacrificial systems. Abradable coatings are machined in situ and consist of a soft metal with polymer particles in cold sections and Ni–graphite or MCrAlY with polyester or BN particles in hot areas [1, 236, 237]. Additives provide the necessary friability, as well as aid in dry lubrication. Other thermal sprayed coatings can also be used on the "cutting" side of the clearance control system, and when the dynamic member of the system is too soft to cut without a coating.

Abradable materials have a strong impact on the turbine efficiency and fuel consumption [238]. At rotating speeds of the order of 10,000 rpm, rotating blade tip may rub against the stationary casing, due to either thermal expansion or misalignment or rotation, inducing strains [239]. Abradable seals act as sacrificial layers between the blades and the casing and are soft enough to avoid significant wear to blade tips, thus allowing much smaller clearances. They also offer a wear protection to the shroud material and rubbing blades. High-temperature abradable seals are used in high-pressure gas turbine of jet engines [238].

Abradable materials are rather complex because they must be abradable with a good resistance and strength as well with a good resistance to oxidation and corrosion. Their porosity also plays a key role and is often achieved by spraying also polymers, which size and volume percentage are critical for optimizing both the "abradability" and erosion-resistance performance. The polymer is then removed by heating the sprayed coating. At last the coating composition must be such that particle debris, released from the coating into the engine, are kept to a minimum. Their composition must also be adapted to the blade materials: titanium or nickel or steel. They are classified in low- and mid- (<540 °C) and high-temperature (540–980 °C) abradables. Low-temperature abradables are aluminum based with graphite or polyester or polyimide or boron nitride, or nickel based with graphite or calcinated bentonite clay [238, 239]. In the cold compressor section aluminum base is preferred due to the high risk of moisture. At high temperature one uses super alloys (MCrAlY with M=Ni or Co or both) with polyester and/or boron nitride or bentonite or graphite. Recently, ceramic mixed

with softer material (BN and polyester) abradable coatings have been developed to reduce slightly the alloy surface temperature. Other seals, which do not interact with the blades, are coatings composed of Babbit (tin–copper–lead), bronze, and AlSi-polyimide. They are used against labyrinth seals along the engine shafts in the compressor and turbine, sealing either gas or oil paths [1].

A few examples are presented below. For high temperature Bardi et al. [240] have tested, for the first stage of industrial gas turbines, the behavior of composite coatings: plasma-sprayed CoNiCrAlY/Al_2O_3 and laser-cladded CoNiCrAlY/graphite coatings. After 1,000 h at 1,100 °C both coatings did not show relevant microstructural modifications. Steinke et al. [241] showed that the hardness could be used as an indication for the abradability. It should be in the range of 500 $HV_{0.5N}$. A hardness of approximately 600 $HV_{0.5N}$ seemed to be the upper end at which a good cut-in was no longer reliably reproducible. Sporer et al. [242] performed abradability tests of YSZ abradables with the Sulzer Innotec test rig that can operate up to 1,200 °C with blade tip speeds up to 410 m/s. At intermediate temperatures (<450–480 °C), AlSi-hexagonal BN or NiCrAl–bentonite are popular [237, 243–246]. For example, the AlSi–hBN coating was characterized by a proportion of about 40 % of hBN "lubricant" particles trapped in the metallic matrix [244]. The amount of porosity was about 5 %. The NiCrAl–bentonite coating contained about 25 % of relatively spherical bentonite particles together with about 30 % porosity constituted mainly of large pores [244]. Comparatively to the hBN particles, the majority of the large bentonite particles and pores in this coating are distributed without significant preferred orientation [244]. Johnston [237] studied the net thermal spraying residual stress (NTSRS) and showed that it was most sensitive to changes in substrate thickness, abradable deposit thickness, and deposit modulus. Such results could be used for the creation of new abradable materials with optimum stress profiles and greater mechanical integrity. Stringer and Marshall [243] studied the wear at high speed: impact velocities between 100 and 200 m/s and incursion rates between 3.4 and 2,000 μm/s. They suggested that the adhesion of abradable material was due to plucking out of complete phases from the abradable coating, rather than a conventional cutting mechanism. Ma and Matthews [239] suggested using "Progressive abradability hardness" (also called "specific grooving energy"), abbreviated as "PAH," to measure abradability in the scratch test. At low temperature Dowson et al. [247] studied, for abradable seals to centrifugal compressors and steam turbines, the development of a new abradable silicon rubber adhesively bonded to a metal substrate. Lima and Marple [20] showed that a material that was generally considered as being hard and stiff, as YSZ, could be engineered to produce a nanostructured 100 % ceramic coating with a friable structure possessing attributes required for an abradable coating. In order to engineer a friable ceramic coating, the molten part of a semi-molten agglomerate particle must not fully infiltrate into the capillaries of its non-molten core during thermal spraying. The porous nano-zones spread throughout the coating microstructure acted as weak links, thereby making the coating friable. Abrasive wear resistant coatings are applied to blade tips and labyrinth seal teeth. They are often made of alumina, alumina–titania, nickel–aluminum cermet, Ni–Cr–Cr_3C_2 cermet.

18.3.5 Bonding Coatings

Bond coats are very important to:

- Improve the coating adhesion by forming an anchoring subcoat or adhering to clean and smooth surfaces that cannot be grit blasted properly (too thin or too hard or with a configuration making roughening difficult)
- Form a layer with an expansion coefficient between that of substrate and topcoat
- Provide an oxidation or corrosion resistant barrier to the substrate

According to the oxidation or corrosion barrier, and the working temperature of the coated part, the bond coat must be properly chosen.

For example, Mo can be used up to 315 °C [2]. NiAl bond coats are oxidation resistant up to 650 °C with Ni–Al (20 wt%) and 800 °C with Ni–Al (5 wt%), but they can also be used against corrosion. For example, Lekatou et al. [248] have investigated the corrosion behavior of an HVOF Ni–5Al/WC–17Co coating on Al-7075 in 0.5 M H_2SO_4. In the temperature range of 25–45 °C, the coating exhibited pseudo-passivity that effectively protected from localized corrosion. In case of surface film disruption, the bond coat successfully hindered corrosion propagation into the Al alloy. Yılmaz [249] has shown that the application of NiAl (5 wt%) bond coat layer in the plasma spraying of Al_2O_3 and Al_2O_3–13 wt% TiO_2 on pure titanium substrate has increased the hardness and bonding strength of coatings. Ni–Cr (20 wt%) bond coats can be used up to 980 °C and are designed to resist oxidation and corrosive gases. Cho et al. [250] coated micron-sized WC-Co powder onto a 420J2 steel substrate and bond coats of Ni, NiCr, and Ni/NiCr using HVOF spraying. The fracture locations were at interfaces with top coatings of WC–Co and NiCr indicating that adhesion between metal/similar metal is much stronger than between metal/cermet (WC–Co) because of the easy diffusion between similar metal atoms. Bond coats for TBCs have been extensively studied. They are of the MCrAlY type with M = Ni, Co, ... that can be doped with Pt, Hf, ... and can support temperatures of 1,100–1,200 °C. A few examples are presented below. Schulz et al. have studied [251] NiPtAl bond coats as well as NiCoCrAlY (X) deposited by LPPS and EB-PVD underneath conventional EB-PVD yttria-stabilized zirconia top coats on three different substrate alloys. The longest lifetimes were achieved on a novel Hf-doped EB-PVD NiCoCrAlY bond coat owing to a differing TGO formation and failure mechanism. Zhao et al. [252] investigated the effect of the Pt content on the durability of thermal barrier coatings (TBCs) with a Pt-enriched $\gamma + \gamma'$ bond coat. During oxidation, impurities such as S, C, and refractory elements segregating to the interface would degrade the TGO adherence to the bond coat. However, a higher content of Pt can inhibit this segregation and thus improve the TBCs life. Tang and Schoenung [253] observed multilayered accumulation of thermally grown oxide (TGO) locally on the tops of the roughness protrusions of the bond coat in thermal barrier coatings. Chen et al. [254] have compared TGO growth and cracking behaviors in TBC systems with APS-, HVOF-, and CGDS-CoNiCrAlY bond coats during thermal exposure.

Results pointed the potential advantage of using CGDS technique to produce TBC bond coats, for its significantly improved durability over the commercial air plasma spray bond coat, as well as its fast deposition rate and low deposition temperature. The TBCs with HVOF bond coats had an extended durability, compared to that obtained by APS but lower than that by CGDS. Other materials than superalloy were tested for TBC bond coat, such as glass–ceramics [255]. The TBC with YSZ top coat, glass–ceramic bond coat, and nickel base superalloy substrate was subjected to static oxidation test at 1,200 °C for 500 h in air. No TGO layer was found between the bond coat and the top coat in the case of glass–ceramic bonded TBC system, while the conventional TBC system exhibited a TGO layer of about 16 μm thickness at the bond coat–top coat interface region.

Bond coats are also used for other applications, as presented below:

- Lu et al. [256] plasma-sprayed two-layer hydroxyapatite (HA)/HA + TiO_2 bond coat composite coating (HTH coating) on titanium. The HA + TiO_2 bond coat (HTBC) consisted of 50 vol. % HA and 50 vol. % TiO_2 (HT). The positive effect of the HTBC on the decrease of residual stress in HA top coating (HAT coating) was evidenced through the observation on the surface cracking. The toughening and strengthening of HTBC was thought to be mainly due to TiO_2. Goller [257] plasma sprayed bioglass, known as 45S5 (45 % SiO_2, 6 % P_2O_5, 24.5 % CaO, and 24.5 % Na_2O all in weight percent) onto a titanium substrate with and without Amdry 6250 (60 % Al_2O_3–40 % TiO_2) as bond coating layer. The adhesive bonding observed at the bioglass metal interface turned into cohesive bonding by application of the bond coating layer.
- Guanhong et al. [258] have deposited on PMCs (carbon fiber reinforced unsaturated polyester) the Al bond coat and Al_2O_3 top coating by APS. The highest shear adhesion strength of the bond coating was 5.21 MPa and the hardness of the surface was much improved by the alumina coating. Liu et al. [259] arc-sprayed Al, Zn, and plasma-sprayed Al, Zn, Ni_3Al, and Cu on carbon-fiber reinforced polyimide substrate as bond coats for erosion and thermal-resistant coating. Ni_3Al or Cu damaged the substrate. Arc-sprayed and plasma-sprayed Al and Zn could be used as bond coat materials. For Zn as bond coat material, depositing method had little influence on shear adhesion strength. For Al as bond coat material, plasma spray was superior to arc spray, preheating improving shear adhesion strength.

18.3.6 Electrical and Electronic Coatings

One of the main problems of electrically conductive thermal sprayed materials, except those cold sprayed or plasma sprayed in soft vacuum VPS (generally VPS is too expensive), is that oxidation during the process increases the electrical resistance of the coating. The anisotropic structure of sprayed coatings also results in strong anisotropy between in-plane and through thickness electrical properties.

Some thermal-sprayed coatings are used to produce heater panel resistance. However, the choice of the resistance material must be such that the variation of its electrical resistance with temperature is as low as possible because otherwise electronic devices must be used to adapt the voltage to the resistance variation.

18.3.6.1 Dielectrics

Alumina is probably the most used material. The α and γ phases present different dielectric constants and loss tangent at high frequency. The γ phase resulting from the spray process can be avoided either by keeping the substrate at 1,000 °C, which is not easy to do with most substrates and requires a careful temperature control during cooling to avoid cracks, or by stabilizing it with elements such as MgO or Cr_2O_3. If the γ phase is not the phase suitable for high-frequency applications, as the α phase, the voltage breakdown is close for both phases. The dielectric properties of alumina coatings depend strongly upon their microstructure and spray conditions [6, 260]. One of the drawbacks is that the alumina coating electrical resistivity is strongly dependent on the air humidity due to the increase in water adsorption in the porous coating, generating ionic conductivity. Toma et al. [261] made the comparative study of the electrical properties and characteristics of thermally sprayed alumina and magnesium spinel coatings sprayed by HVOF and plasma. At low humidity levels, the electrical resistivity of alumina and spinel coatings was comparable (on order of magnitude of 10^{11} Ω m). At a very high humidity level (95 % RH: Relative air Humidity), a dramatic decrease in resistivity of about five orders of magnitude for alumina coatings, and about four orders of magnitude for spinel coatings was observed, water adsorption generating ionic conductivity. HVOF spinel coatings presented the best dielectric strength values ($E_d > 30$ kV/mm against 20 kV/mm for sprayed alumina) and were less sensitive to moisture. Thus, these coatings can be considered as potential candidates for use in insulating applications. Toma et al. [262] studied microstructural characteristics and electrical insulating properties of thermally sprayed alumina coatings produced by suspension HVOF (S-HVOF) and conventional HVOF spray processes. The better electrical resistance stability of the suspension-sprayed Al_2O_3 coatings could be explained by their specific microstructure and retention of a higher content of α-Al_2O_3. Kim et al. [263] studied, for plasma-sprayed Al_2O_3–13 % TiO_2 coatings, the effect of two commercial sealants based on polymers on the electrical insulation properties before and after the impregnation treatment. Cipri et al. [23] studied the interesting electromagnetic properties (complex permittivity) of Al_2O_3–SiO_2 compounds plasma sprayed. For microwave and nuclear fusion applications, BeO is sprayed by inert plasma spraying process but its toxicity requires very stringent spray conditions.

18.3.6.2 Resistors and Conductors

Prudenziati et al. [264–266] have studied Ni, Ni20Cr, or Ni5Al coatings plasma sprayed onto alumina films deposited onto steel plates. They compared electrical properties of resistors prepared with Ni and Ni–20Cr powders by thermal spray processes (APS and HVOF). The resistivity of Ni resistors decreased after annealing at temperatures in the range 200–400 °C may be due to healing of structural defects. On the contrary, the observed increase of resistivity of Ni–20Cr-based resistors was possibly due to ordering of the atoms. The temperature dependence of resistance for Ni-based resistors was invariably the same as for Ni bulk, regardless of sample origin. On the other hand, a large spread in temperature coefficient of resistance (TCR) values of Ni–20Cr-based resistors was observed. Ni-based resistors had an excellent reproducibility of the resistance versus the temperature curves, making them excellent candidates for temperature sensors and self-controlled high temperature heaters.

To limit oxidation in flight, cold spray can be used. In spite of the low flattening degree of cold-sprayed (CS) coatings, the anisotropy does not disappear even after annealing [7]. However, when compared to thermal-sprayed coatings, the electrical resistivity of cold-sprayed ones is lower (3–5 times) [267–269].

18.3.6.3 Electronic Devices

For electronics, the following applications and development areas of cold spray process can be indicated [267]: (1) deposition of electric screening coatings on plastics, (2) generation of conducting structures on nonmetals, and (3) deposition of brazing and soldering alloys.

For example, Gui et al. [270] plasma sprayed, onto a graphite substrate, Al matrix composites with high-SiC volume fraction. Al-55SiC and Al-75SiC powders were milled by stainless steel and ZrO_2 balls in a conventional rotating ball mill for 1–10 h. The SiC particles exhibited a reasonably uniform distribution in the composites sprayed from the milled powders. The Fe contamination occurred to the milled powders when stainless steel balls were used. Waveguide devices for microwave applications were achieved by spraying ferrites and dielectrics.

Yamakawa et al. [271] have studied ceramic trays (a type of kiln furniture) used for firing multilayer ceramic chip capacitors (MLCC) that are used in a large number of electronic appliances. They are being required in more compact sizes, larger capacities, and reduced costs year by year. High-thermal shock resistance and reaction resistance are desired properties for these ceramic trays. They showed that the application of plasma-sprayed ZrO_2 topcoat and an Al_2O_3-sintered basecoat made it possible to enhance longevity and reduce cost.

18.3.6.4 Electromagnetic Shielding

Thermal spray coatings cannot compete with PVD techniques to manufacture electronic devices, but wire arc sprayed coatings are used as shielding material to eliminate electromagnetic and radio frequency interference and dissipate static discharge sparks. Zn and Al are currently used to protect computers, electronic office equipment, medical monitoring devices, housing constructed of temperature-sensitive plastic, rooms containing military computers. Donner et al. [272] have cold-sprayed copper coatings onto previously thermally sprayed Al_2O_3 coatings. They either applied a bondcoat on the ceramic layer or used heated substrates during the cold spray process. By both alternatives, dense copper layers were produced. The electrical conductivity reached 98% of international annealed copper standard (IACS) in the as-sprayed condition on heated substrates, or 90 % of the IACS value after spraying on cold substrates with aluminum bondcoat and additional heat treatment, thus meeting the requirements for electronic applications. Lin et al. [273] plasma sprayed surfaces of copper plates with a thick alumina layer to fabricate a composite with a dielectric performance suitable as substrate in electronic devices with high thermal dissipation. They concluded that an alumina layer thickness of 20 μm provided low surface roughness, low thermal resistance, and highly reliable breakdown voltage (38 V/μm). Most telecommunication systems and wireless networks operate at radio and microwave frequencies. However, due to the ever-increasing exploitation of these frequencies, both electromagnetic (EM) pollution and interference occur [274]. Various plastic- and foam-layered instruments and computer equipment cases require shielding. That can be achieved by wire arc spraying zinc coating on the case. Zinc because of its low melting temperature and wire arc because of the low heat flux of the process. Of course it is better using nitrogen atomization to keep the electrical conductivity of the coating as low as possible with as less as possible oxide within coating. For military applications, the whole room can be shielded with a zinc or aluminum film wire arc sprayed outside of it.

Broadband electromagnetic wave absorbers usually correspond to spinel ferrites and hexa-ferrites operating at 45–75 GHz. Unfortunately these materials are usually decomposed when sprayed. Lisjak et al. [275] found a solution by plasma spraying atomized particles of hexa-ferrite and polymer. The hexa-ferrite crystalline structure was preserved during the spraying, while the polyester partly melted and resolidified during cooling. The coupling of the hexa-ferrite magnetic and dielectric losses with the polyester dielectric losses resulted in the superior properties of the composite coating with respect to the pure single-phase coating of the constituent phases.

18.3.6.5 Magnetic Materials

Nd–Fe–B permanent magnets have been sprayed by vacuum plasma spraying [276]. The review of Sampath [277] presents a few ferrites and soft magnetic materials plasma and HVOF sprayed that could be interesting for industrial applications.

18.3.6.6 Sensor Applications

According to the review paper of Sampath [277], interesting prospective seems to be the innovative Direct Write Thermal Spray (DWTS), which is a new and exciting manufacturing technology capable of depositing a large number of electronic materials on a wide range of substrates, enabling direct write fabrication of multilayer thick film electronic devices. One of the exciting prospects of this technology is the fabrication of integrated, embedded sensors directly onto thermal spray-coated components. Sampath [277] also presents the past, present, and future of thermal spray applications in electronics and sensors. The different dielectrics that are used or that have been used are presented: alumina, beryllia, $MgO–3Al_2O_3$ spinel, alumina–titania, cordierite ($2MgO–2Al_2O_3–5SiO_2$), and forsterite ($MgO–SiO_2$), perovskite-based dielectric systems including lead zirconate titanate (PZT), $BaTiO_3$, and strontium-doped $BaTiO_3$, ... deposited by plasma or HVOF.

18.3.6.7 Other Applications

Cold-sprayed nickel or further ferromagnetic metals and alloys are used as induction heating coats on cooking appliances or cooking pots [268]. Superficial metallization on polymer improves the corrosion-resistant and antiaging property but also achieves some special features such as electrical conductivity, thermal conductivity, electromagnetic shielding, and radial protection [269].

Electrically conductive and flexible aluminum coatings (flame sprayed with powder or wire) were deposited onto diverse polyester textiles for wearable electronics, lighting, or communication in medical techniques [278]. Coatings produced using wire as raw material had much better morphologies than those produced using powder as starting material. Successful preliminary test results for Al–polyester composites used as current collectors showed that application-specific electrically conductive composites with adjustable specific surface conductivity values and microstructures can be produced without inducing any thermal or chemical damages to the fabric material [278].

18.3.7 Freestanding Spray-Formed Parts

The freestanding bodies are produced by plasma spraying for refractory or ceramic materials [279–285] and by HVOF spraying for thin alloys or cermets [286] and also by cold spray [287]. Of course rotationally symmetrical shapes are preferred: the core is easy to produce, the stress in the sprayed material is low and evenly distributed, and at last separating the core from the coating is easier. In most cases the core is made of smooth graphite or other material coated by atomization of a

product preventing the substrate–coating adhesion. It is also possible to achieve very complex shapes, such as manifolds of racecar engines, by spraying on special materials that can be afterwards dissolved. It becomes then possible to coat externally the sprayed ceramic thermal barrier by an alloy to achieve the hot gases tightness. This technique, having a high cost, is hardly suitable for large-scale production, but it offers advantages as far as cost and fast delivery are concerned. For example, sprayed ceramic bodies offer good mechanical strength at high temperatures, excellent electrical insulation at temperatures where glass insulators give-up and chemical resistance against corrosive gases or liquids. For example, in rocketry nozzle inserts are achieved that way. Ceramic tubing is used in furnace construction as well as in chemistry. The production of crucibles for the melting of materials is also an important application. Such crucibles are made of partially (YPSZ) or totally (YSZ) stabilized zirconia, strontium zirconate, alumina, tungsten, and molybdenum. A relatively new application of PTA deposition is the fabrication of freestanding shapes, or solid free form fabrication, see Sect. 10.7.6 of Chap. 10.

A few examples of freestanding coatings are presented below:

- Chen et al. [288] vacuum plasma-sprayed dense, oxide-free and pore-free freestanding forms of NiAl and NiAl-B. The deposits retained the same phase structure as the starting powders. The as-sprayed freestanding deposits exhibited a large grain size due to self-annealing during vacuum plasma spray processing. The hardness of NiA1-B was about 10 % higher than that of NiAI.
- Saeidi et al. [289] produced freestanding VPS and HVOF-sprayed CoNiCrAlY coatings. The as-sprayed HVOF coating retained the γ/β microstructure of the feedstock powder, and the VPS coating consisted of a single γ phase. A 3 h, 1,100 °C heat treatment in vacuum converted the single-phase VPS coating to a two-phase γ/β microstructure and coarsened the γ/β microstructure of the HVOF coating. Oxidation of the freestanding as-sprayed coatings produced a dual-layer oxide consisting of an inner layer of α-Al_2O_3 and an outer spinel layer.
- Fan and Ishigaki [290] used induction plasma spraying to produce free-standing parts of Mo_5Si_3-B composite and $MoSi_2$ materials. The oxidation resistance, up to 1,210 °C, of the former composite was compared with that of the latter, known to be resistant to high-temperature oxidation. At boron contents greater than 1 wt %, composites demonstrated encouraging oxidation resistance and with 2 wt% boron it was comparable to $MoSi_2$ [290].
- Waki et al. [291] sprayed freestanding circular tube specimen of CoNiCrAlY by VPS, HVOF, and APS. They studied the effect of post-spray thermal treatments, in vacuum and in air, on the mechanical properties in the 400–1,100 °C temperature range. High-temperature thermal treatment in air was effective in increasing the bending strength and Young's module. It was especially effective on the APS coatings, which were produced using powders with average size of 60 μm, and on HVOF coatings, those bending strengths increased by approximately three times [291].
- Plasma-sprayed freestanding zircon pipes (inside diameter 83 mm, wall thickness 1.5–2 mm, lengths up to 2,000 mm) are used in furnaces as shields

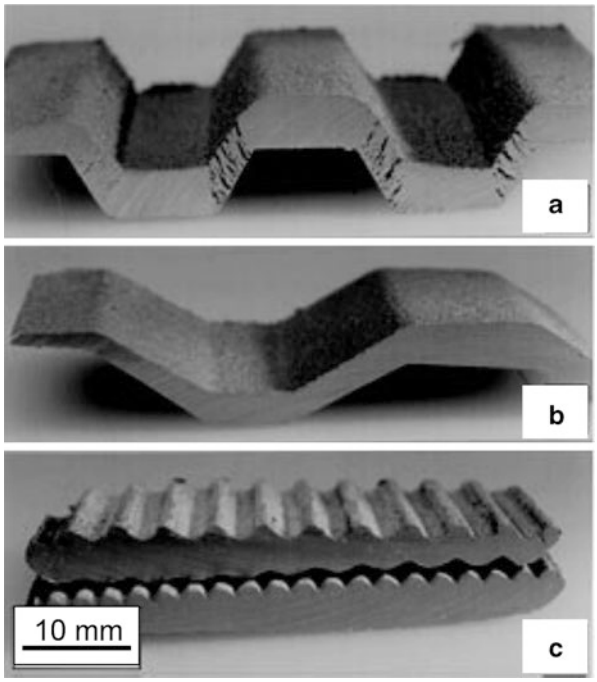

Fig. 18.1 Radio frequency plasma-deposited freestanding parts of bipolar plate material. (**a**) Made with a geometrically extended contour of the substrate (removed), incidence angle at the flanks of 30° (with respect to the direction of the jet). (**b**) Like (**a**), but with an incidence angle of 60°. (**c**) Made with a finer substrate contour. Reprinted with kind permission from Springer Science Business Media [294], copyright © ASM International

for heating elements [292]. The plasma deposits contained glassy silica and various modifications of zirconia in addition to a small amount of the amorphous phase. This combination of zirconia and silica exhibited properties such as a high -thermal shock resistance, good corrosion resistance, and low wettability [292].

– Chen et al. [293] obtained by plasma spraying freestanding $La_2Zr_2O_7$ coatings, using an amorphous La–O–Zr precursor as the feedstock. During thermal spraying, the amorphous powder crystallized, and fine grains were formed, while with crystallized feedstock powder the average grain size was 750 nm. The thermal conductivity of the as-sprayed coating with the amorphous feedstock powder was approximately 0.42 W/m K and its average coefficient of thermal expansion was 11.1×10^{-6}/K, value similar to that of metallic bond coatings [293].
– Henne et al. [294] processed by induction plasma spraying the material of metallic bipolar plates for solid oxide fuel cells, a chromium alloy with the composition 94 % Cr, 5 % Fe, and 1 % Y_2O_3. Freestanding parts had a density above 95 % of the theoretical density of the material. From the deposits obtained, it was positively concluded that, as long as the deposit thickness did not exceed about half the characteristic substrate dimension, the contour of the free side of the deposit sufficiently followed the contour of the substrate [294]. Figure 18.1 presents radio frequency plasma-deposited freestanding parts of bipolar plate material.

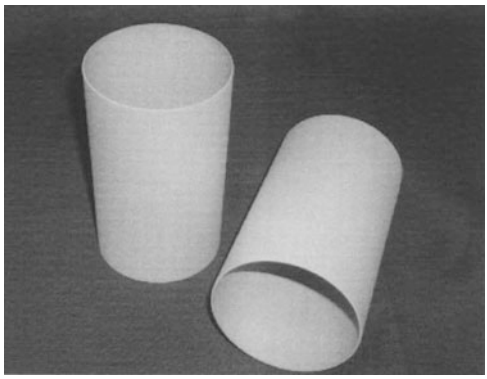

Fig. 18.2 Plasma spray-formed nanostructured aluminum oxide shells with a wall thickness of 0.4–0.6 mm. Reprinted with kind permission from Springer Science Business Media [295], copyright © ASM International

- Agarwal et al. [295] plasma sprayed a mixture of commercially available aluminum oxide powder (99.8 % pure), in the 15–45 μm particle size range, with nanosized aluminum oxide powder (99.9 % pure) thoroughly mixed in a rotating ball (alumina ones) mill for 24 h. Coatings were sprayed on conical mandrels. Spray parameters were controlled with an innovative proprietary cooling technique to retain a large fraction of nanosize Al_2O_3 powder particles in the spray deposit. Nanosize particles were partially melted and trapped between the fully melted coarser (micrometer size) Al_2O_3 grains [295]. Figure 18.2 presents the spray-formed nanostructured alumina-tapered cylindrical cones.
- Laha et al. [296] plasma sprayed freestanding structures hollow conoid (100 mm taper-length, 62 mm diameter, 2 mm thickness) of Al-based nanostructured composite with carbon nanotubes as second phase. Carbon nanotubes (CNT) were successfully retained in the spray-formed composite structure. The CNTs were observed largely between the consecutive Al–Si splats with dangling structure.
- Hussain et al. [297] cold sprayed titanium freestanding coatings, some of them being vacuum heat treated to further decrease porosity levels. Cold spraying using N_2 as a process gas heated to 800 °C deposited titanium with less interconnected porosity than N_2 gas at 600 °C due to a higher degree of particle deformation on impact. Pores above 1 μm were reduced to 0.2 vol. % and the total interconnected porosity to 1.8 vol. % after heat treatment of deposits produced at a process gas temperature of 800 °C.
- Herman et al. [298] sprayed by the VPS process dense deposits of unreinforced and composite matrices of Ni_3A1 alloy and $MoSi_2$. Geibel et al. [279] showed that plasma spray deposition was a suitable technique to produce freestanding, near-net-shaped components of the difficult-to-shape NiAl intermetallic compound.
- Weiss et al. [299] described a new spray-forming process based on thermal spray shape deposition. Shape deposition processes build three-dimensional shapes by incremental material buildup of thin, planar cross-sectional layers.

These processes did not require preformed mandrels and can be used to directly build three-dimensional structures of arbitrary geometrical complexity. The basis for the thermal spray approach was to spray each layer using a disposable mask that had the shape of the current cross section. Masks could be produced from paper rolls, for example, with a CO_2 laser.

18.3.8 Medical Applications

Orthopedic and dental market is developing very fast with either bioinert coatings (Ti–6Al–4V, Ti–6Al–7Nb, Ti–13Nb–13Zr, . . .) or bioactive ones (hydroxyapatite (HA), tricalcium phosphate) [300, 301]. Two types of coatings are used [1]:

Bioinert ones with no activity between them and the bone or soft tissues, the most used materials being Ti and Ti–6Al–4V. These coatings must be porous (at least 30 %).

Bioactive coatings, interacting with bone to promote bonding interfaces, are ceramic coatings with material compositions similar to that of bone tissue (calcium phosphate). The most used ceramic is hydroxyapatite (HA) Ca_{10} $(PO_4)_6$ $(OH)_2$ exhibiting a strong activity to join the bone. Examination of four retrieved HA coated orthopedic prostheses by Gross et al. [302] has indicated bone attachment, along with coating removal, from a range of areas on the prosthesis surface. Coating removal occurred by dissolution provided the higher bone-remodeling rate accompanied by the release of calcium and phosphate. Coatings dissolved faster on elevated areas or those subjected to a higher level of loading. Coatings located in less loaded areas provided a higher longevity. In fact very different methods have been tested to spray HA [303].

RF induction plasma sprayed [304] where the HA coatings, prepared with supersonic plasma nozzle, was highly crystalline in nature with insignificant phase decomposition. Both the crystallinity and purity of HA decreased when sprayed with normal plasma nozzle.

Air plasma-sprayed coatings and HA and HVOF-sprayed nano-titania coatings on Ti–6Al–4V and fiber-reinforced polymer composite substrates [305] were compared. The surface cell coverage after 7 days of incubation was more complete on nano-TiO_2 than HA. Preliminary results indicated that osteoblast activity after 15 days of incubation on nano-TiO_2 was equivalent to or greater than that observed on HA. Chang et al. [306] studied hydroxyapatite coatings sprayed with a vacuum plasma spray system at different power levels. They showed that the spray power greatly affected the crystallinity, chemical composition, and microstructure of as-sprayed hydroxyapatite coatings, which were linked to the melting state of hydroxyapatite powder. Prevéy [307], to overcome the complexities of characterizing plasma-sprayed HA coatings, has developed an external standard method of XRD quantitative analysis that can be applied nondestructively. Khor et al. [308] have studied the formation of a composite made of HA and Ti–6Al–4V, APS or HVOF sprayed, to enhance the poor mechanical properties of hydroxyapatite (HA).

The composite presented excellent bond strength due to the superior interfacial bond between the Ti–6Al–4V rich splats and the substrate. Wang et al. [309] have studied the preparation of a functionally graded bio-ceramic coating composed of essentially calcium phosphate compounds.

HVOF-sprayed HA: compared to plasma-sprayed one, the HVOF system has proven to be a novel method for HA deposition with maximum crystallinity and purity values of 93.81 and 99.84 %, respectively. With FDA-approved plasma spray technique, values of only 87.6 and 99.4 % crystallinity and purity, respectively, were found [310].

HVOF-sprayed nanostructured titania (n-TiO_2) and 10 wt% hydroxyapatite (HA) (n-TiO_2–10 wt% HA) powders have been engineered by Lima et al. [311] as possible future alternatives to HA coatings deposited via air plasma spray (APS).

The n-TiO_2–10 wt% HA coatings exhibited bond strength levels higher than 77 MPa, i.e., at least twice those of APS HA coatings deposited on Ti–6Al–4V substrates. In addition, due to the high stability of TiO_2 in the human body, longevity related concerns of HA coatings, such as dissolution and osteolysis, were unlikely to occur. HA coatings with a high content of both crystalline HA and nanostructures were preferred for cell proliferation [20].

Coatings resulting from agglomerated nanostructure coatings: It was demonstrated by using an osteoblast cell culture (in vitro) that the type of HA coating phase is more important than the nanostructure character of the coating, however, HA coatings with a high content of both crystalline HA and nanostructures were preferred for cell proliferation [20, 311, 312]. Based on cell culture (in vitro) results observed for bulk nanostructured ceramics, the nanostructure zones being found on the TiO_2 coating surface may have played an important role in producing good biocompatibility results. However, up to this point there is no experimental evidence to prove this [20].

ZrO_2/SiO_2 composite coatings have high-abrasive wear resistance compared with pure HA and HA/ZrO_2 coatings because they exhibit high hardness and dense structure. The in vitro test of the composite coatings in simulated body fluid showed a growth of nanometer-sized particles apatite after the immersion of the coatings for 20 days [313].

Well-adherent, flawless, glass–ceramic (SiO_2–CaO–K_2O) coatings on alumina and Ti6Al4V substrates were realized [314, 315]. The obtained results were reproducible and the applied techniques were low cost and not complex. When tested in vitro, the coatings showed an extensive precipitation of a thick HA layer, well adherent to the coatings.

SiO_2–CaO–P_2O_5-based bioactive glasses and glass–ceramics are attractive materials for biomedical applications, because of the excellent levels of bioactivity, which can be achieved by formulating and selecting appropriate compositions [316]. Preliminary results with high-velocity suspension flame spraying bioactive glasses seemed to be promising.

The sprayed coatings can be heat treated:

HA coatings deposited by HVOF spraying showed similar advantages as coatings obtained by APS, but with higher crystallinity. Heat treatment of the coating allowed crystallization of the amorphous calcium phosphate (ACP) present in the coatings [317]. XRD analysis confirmed that the ACP transforms directly to HA and not to other calcium phosphate phases. Similarly functionally graded calcium phosphate coatings were produced on Ti–6Al–4V substrates by plasma spraying [317]. The microstructure of the coating was dense with the typical lamellar structure. The top layer of the coating was mainly composed of a-(Tricalcium Phosphate) TCP, which suggested high bio-resorbability. After post-spray heat treatment, the TCP phase, from either the decomposition of HA or the TCP feedstock, and the tetracalcium phosphate (TTCP) phase were no longer detected by XRD, but the CaO phase remained.

Yu et al. [318] plasma-sprayed HA coatings and post-spray treated them by the spark plasma-sintering (SPS) technique at 500 °C, 600 °C, and 700 °C for duration of 5 and 30 min. The HA coatings treated in SPS for 5 min revealed rapid surface morphological changes during in vitro incubation (up to 12 days), indicating that the surface activity is enhanced by the SPS treatment.

Bellucci et al. [319] coated titanium plates by high-velocity suspension flame spraying (HVSFS) technique using a novel bioactive glass composition based on the K_2O–CaO–P_2O_5–SiO_2 composition ("Bio-K"). On half of the samples, an atmospheric plasma-sprayed (APS) TiO_2 bond coat was preliminarily deposited; suspensions of attrition milled micron-sized glass powders, dispersed in a water and isopropanol mixture, were then sprayed onto both bare and bond-coated plates using five different process parameter sets. All coatings exhibited analogous behavior when soaked in a simulated body fluid (SBF) solution. Their interaction with the SBF involved ion release from the glass, conversion of its surface into an amorphous and hydrated silica layer followed by nucleation, and growth of a carbonated hydroxyapatite film on top of the latter. This interaction seemed particularly fast, as the hydroxyapatite film started to appear after 3 days of soaking.

Other materials were tested for their potential application in biomedicine: Liang et al. [320] plasma sprayed three kinds of powders composed of Ca_2SiO_4, ZrO_2, and $CaZrO_3$ with different Ca_2SiO_4. Results showed that the chemical stability of the coatings was significantly improved compared with pure calcium silicate coatings and increased with the increase of Zr contents. Results indicated that plasma-sprayed coating with 40 wt% of Ca_2SiO_4 had medium dissolution rate and good biological properties, suggesting its potential use as bone implants.

At last bactericidal effects of coatings were also studied.

Preliminary results showed that thermal-sprayed nanostructure TiO_2 coatings exhibited photocatalytic bactericidal activity with *Pseudomonas aeruginosa* [321].

The antibacterial behavior of HA–Ag (silver-doped hydroxyapatite) nanometer-sized powder and their composite coatings were investigated against *Escherichia coli* (DH5a). HA–Ag nanometer-sized powder and PEEK (poly-ether-ether-ketone)-based HA–Ag composite powders were synthesized using in-house powder processing techniques. These nanometer-sized composite powders were

cold sprayed. The results indicated that the antibacterial activity increased with increasing HA–Ag nanometer-sized powder concentration in the composite powder feedstock and cold-sprayed coating [322].

The antibacterial behavior of CS–Cu (chitosan–copper complex) powder and their composite coatings were investigated against *E. coli* (DH5a). The cold-sprayed coatings retained the antibacterial properties of the original feedstock powders [323].

18.3.9 Replacement of Hard Chromium

Electrolytic hard chromium plating is extensively used against wear and sometimes corrosion. However, the chromium plating baths contain chromic acid, in which the chromium is in hexavalent state, known carcinogen. Thus this technology presents harmful effects on the environment and the public health and it has also some intrinsic technical limitations. That is why research efforts on its replacement by sprayed coatings, especially cermet coatings HVOF sprayed, are numerous since the beginning of the 1990s.

Few other examples are presented below:

Sahraoui et al. [324] investigated and compared microstructural properties, wear resistance, and potentials of HVOF-sprayed Tribaloy©-400 (T-400), Cr_3C_2–25 wt% NiCr, and WC–12 wt% Co coatings for a possible replacement of hard chromium plating in gas turbine shafts repair. HVOF carbide-based coatings exhibited higher hardnesses and superior performances in wear resistance than hard chromium coatings. In the case of shafts repair, hard chromium plating process proved to be time consuming and to involve high costs.

Heydarzadeh and Ghadami [325] plasma deposited APS onto steel substrates WC–12 wt% Co powders. Heat treatment of the coatings in an inert atmosphere above 900 °C promoted the formation of Z-carbides from the amorphous phase. Microhardness of coatings for different heat-treating conditions was relatively higher than that of the conventional hard chromium electro deposit.

Ishikawa et al. [119] used a commercial HVOF and a gas shroud attachment HVOF to prepare WC/CrC/Ni cermet coatings under various combustion conditions. The density of coatings improved as the velocity of sprayed particles increased. With the gas-shrouded HVOF, high density was achieved with a lower degree of WC degradation. Such coatings could be alternative candidates of hard chrome plating.

Bolelli et al. [326] studied mechanical properties and tribological behavior (abrasion and un-lubricated sliding wear resistance) of various kinds of electrolytic hard chrome (EHC) coatings and of metallic and cermet HVOF-sprayed coatings (WC–17Co, WC–10Co–4Cr, Co–28Mo–17Cr–3Si). HVOF-sprayed cermet coatings were harder but less tough than EHC ones. Therefore, they undergone a comparable or even higher mass loss when subjected to three-body abrasion conditions. However, their two-body sliding resistance definitely overcame that

of EHC coatings, because they form a tough and uniform surface film protecting them from further damage [326].

Savarimuthu et al. [72] studied sliding wear characteristics of WC thermal spray coatings HVOF sprayed and electroplated chrome tested against Al–Ni–Bz blocks, Cu–Be blocks, and against themselves. The fatigue resistance of WC coatings increased when compressive residual stresses existed.

Deng et al. [327] used high-velocity oxygen/air fuel (HVO/AF) to spray WC-17Co and WC-10Co4Cr on 300M ultrahigh-strength steel. WC-17Co coating exhibited higher fracture toughness than that of WC-10Co4Cr coating. WC-17Co coating demonstrated better impingement resistance than WC-10Co4Cr, and the impingement resistance of chrome electroplating felled between that of WC-17Co and WC-10Co4Cr coatings.

Guilemany et al. [328] compared wear and corrosion properties of Cr_3C_2–NiCr (CC-TS) HVOF sprayed and hard chromium (HC) coatings obtained on a steel substrate. Three orders of magnitude lower volume loss were found for CC-TS (HVOF) after friction tests compared with HC. The best corrosion resistance was also obtained for the CC-TS by HVOF.

Picas et al. [329] compared the mechanical and tribological properties of HVOF CrC75–(NiCr20)25 coatings sprayed from three different agglomerated feedstock powders with various powder size distributions and compared results with conventional hard chromium plating. The CrC–NiCr coating, obtained with the lowest feedstock powder size, presented the best wear resistance under all studied conditions and demonstrated superior performance to hard chrome with regard to mechanical and tribological properties [329].

Staia et al. [330] investigated the tribological behavior of a VPS sprayed Cr_2C_3–25 wt% NiCr chromium carbide coating both in the as-deposited and heat-treated conditions. The samples were subsequently annealed for 2 h at 600 °C, 800 °C, and 900 °C in Ar. The wear values indicated a satisfactory behavior from the tribological point of view. However, the heat treatment had no important consequences on the tribological performance of these coatings. The only problem is that VPS coating is about 4 times more expensive than HVOF ones [330].

Lu et al. [331] compared the microstructure and corrosion behavior of hard chromium coating HCC and plasma-sprayed Fe-based alloy coatings (FAC) on low carbon steel, using the salt-spray test and electrochemical corrosion test. After 60 days of salt-spray test, the weight loss of the FAC was only about 10 % of HCC. After sealing treatment, the defects of pores and micro-cracks existing in FAC disappeared. The sealing treatment further decreased the weight loss of FAC to be about 4 % of HCC [331].

Abdi and Lebaili [332] flame sprayed NiCrBSiCFe coatings for a possible replacement of hard chromium plating in mechanical parts repair. Coatings presented a high hardness after cyclic heat treatment, an excellent resistance to wear and friction, a good corrosion resistance, and an excellent adhesion to steel. Tests have been also positive for the replacement of hard chromium in landing gear by HVOF sprayed WC–CoCr coatings [1, 333, 334].

18.3.10 Applications Under Developments

18.3.10.1 Solid Oxide Fuel Cells

A solid oxide fuel cell (SOFC) is an electrochemical conversion device that produces electricity directly from oxidizing fuel. They are made of four layers comprising three ceramic layers, which are not electrically and ionically active below about 600 °C. Such high operating temperatures result in mechanical and chemical compatibility issues. To achieve an affordable manufacturing cost, the whole SOFCs have been manufactured by plasma spraying: cathode, electrolyte, and anode. One of the disadvantages of the process is the thickness of the electrolyte that must be below a few tens of micrometers and impervious. However, it seems that thin and impervious electrolyte (around 10 μm) can be achieved by suspension plasma spraying. Henne [335] presented in 2007 an excellent overview of thermal-sprayed coatings to make SOFC components and also entire cells. Among the numerous studies, essentially with plasma spraying, published before that year, "only few have proven their potential for a reliable and efficient production of relevant layers and components and promised the status for a technical breakthrough for mass production where a continuous operation with high throughput and yield producing the desired quality is required" [335]. Henne recommends for further developments to improve plasma sources, increase deposition efficiency, work on less costly materials, and combine synthesis and deposition of cell materials based on low-cost precursors. He also evokes the possibility of the recycling of "plasma gas" and overspray [335]. A few examples are given below.

- Takenoiri et al. [336] developed a seal-less planar SOFC consisting of a cell supported with a porous metallic substrate and a metallic separator. The anode and electrolyte were fabricated using flame spraying and APS, respectively, and APS was also used to form a protective coating of the separator. It was shown that the electrical resistance of the separator could be kept lower than $25 \times 10^{-3}\ \Omega\ cm^2$ for at least 3,000 h by the application of $(LaSr)MnO_3$ protective coatings.
- Barthel et al. [337] deposited by thermal spray processes (VPS and flame spraying) porous composite cathodes of $(La_{0.8}\ Sr_{0.2})_{0.98}MnO_3$ (LSM) and ZrO_2–12 % Y_2O_3 (YSZ). The electrochemical performance of the cathodes, evaluated by impedance spectroscopy, indicated significant improvements, especially for the bilayer technique, whereas the concentration profiles of the multilayer gradients still must be optimized. Flame spraying seemed promising.
- $La_{10}\ Mg_{0.2}\ Si_{5.8}\ O_{26.8}$ was prepared by solid-phase sintering and also plasma sprayed by Sun et al. [338]. The amorphous transformation of lanthanum silicates happened during APS process. The heat treatment effectively ameliorated phase composition of as-sprayed coatings, complete recrystallization being achieved after 1,000 °C for 4 h. However, it decreased the permeability of coatings.

- Puranen et al. [339] plasma sprayed Mn–Co–Fe spinel coating on the thin metallic interconnectors in SOFCs. They optimized spray conditions to produce coatings with low thickness and low amount of porosity. The original spinel structure decomposed because of the fast transformation of solid–liquid–solid states but was partially restored by using post-annealing treatment.
- Harris et al. [340] manufactured by axial-injection APS (Mettech Axial torch) single phase and composite cathodes based on LSCF ($La_{0.6}$ $Sr_{0.4}$ $Co_{0.2}$ $Fe_{0.8}$ $O_{32-\delta}$) and SSC ($Sm_{0.5}$ $Sr_{0.5}$ Co O_3). An average surface temperature of approximately 2,200 °C was needed for adequate melting of LSCF particles and approximately 2,100 °C to melt SSC. But too much particle heating resulted in coarser and denser microstructures.
- Suspension plasma spraying [186] seems to be promising for the SOFC cathode deposition, as coatings with high porosity levels in combination with fine pore size can be produced. Shen et al. [341], using induction plasma technology and solution plasma spraying, achieved a homogeneously mixed nano-sized composite GDC/LSCF powder without using a prolonged period of mechanical mixing. The nano-powders exhibited a perovskite structure and a fluorite structure as well as separated GDC ($Ce_{0.8}$ $Gd_{0.2}$ $O_{1.9}$) and LSCF phases. The coatings were homogeneous and porous (51 % porosity) with cauliflower structures. Wang et al. [342] successfully deposited with Axial III Mettech torch Ni–YSZ anode and YSZ electrolyte half-cells on porous Hastelloy X substrates by SPS. The thickness of the anode and electrolyte layers was ~40 μm and 10–20 μm, respectively. The density of YSZ electrolyte coatings increased as plasma torch input power increased. The anodes of the deposited half-cells were porous and electrolytes dense, with no interconnected pores. Michaux et al. [343] prepared and characterized porous anode layers with homogeneous nickel distribution and nanometer sized microstructure for SOFC application. They investigated the effects of some spray parameters on the layer architecture and composition.

18.3.10.2 Other Sensors

For oxygen permeation membranes Zotov et al. [344] prepared $La_{1-x}Sr_xFe_{1-y}$ $Co_yO_{3-\delta}$ (LSFC) coatings by low-pressure plasma spraying thin film processes using different plasma spray parameters. The microstructures of the investigated LSFC coatings depended sensitively on the oxygen partial pressure, the substrate temperature, the plasma jet velocities, and the deposition rate. Coatings deposited with Ar-rich plasma and higher plasma jet velocities were most promising.

Oxygen sensors based on ionic conduction of plasma-sprayed ZrO_2 (measurement of the small electrical current caused by oxygen ions diffusing through the layer) are now extensively used in catalytic car exhaust pipes [345].

18.3.10.3 Decorative Coatings

Thermal spraying is not widely adapted to decorative coatings, and the main efforts were achieved on relatively large structures such as bridges, water tower, chimneys, . . . that were sprayed with zinc or aluminum for corrosion protection. They can be left as-sprayed or sealed with plain or colored sealers. The liquid flame spraying process has been developed to uniformly color hot glass objects [346]. Thermal spraying of concrete or bricks have been performed with glazing materials. Arcondéguy et al. [347, 348] manufactured glaze layers by flame spraying onto substrates that decomposed when heated and for which the traditional glazing process was not appropriate. Adjusting the chemical composition permitted to adjust the transition temperature of the materials. Adjusting their morphology by post-treatment permitted to increase the deposition efficiency and reduce the pore content of the coatings. Of course the decorative value of such coatings is important for the aesthetic but it has a cost.

18.3.10.4 Spent Nuclear Fuel

Many works are now devoted to the containment of spent nuclear fuel that poses a challenge from the perspective of materials science. These applications require to safely provide neutron absorption and corrosion resistance at reasonable costs for very long periods. Identifying a single material that can meet all these requirements has been quasi-impossible and the introduction of coatings seems promising. Alternate coating materials such as amorphous metals and ceramics have been developed and studied to better resist corrosion. Amorphous coatings with boron or other neutron-absorbing element have demonstrated promising results against corrosion [349–353]. The absence of long-range structure (grain boundaries, dislocations, and segregations), in corrosion-resistant materials, further enhances the corrosion resistance of amorphous alloys. One of the most promising formulations was found to be $Fe_{49.7}Cr_{17.7}Mn_{1.9}Mo_{7.4}W_{1.6}B_{15.2}C_{3.8}Si_{2.4}$ (SAM2X5), which included chromium (Cr), molybdenum (Mo), and tungsten (W) for enhanced corrosion resistance, and boron (B) to enable glass formation and neutron absorption [353]. The parent alloy for this series of amorphous alloys, which is known as SAM40 and represented by the formula $Fe_{52.3}Cr_{19}Mn_2Mo_{2.5}W_{1.7}B_{16}C_4Si_{2.5}$, has less molybdenum than SAM2X5 and was originally developed by Branagan [353]. Coatings, HVOF sprayed, have demonstrated phase stability well above 500–600 °C and at high neutron dose (equivalent to 4,000 years inside the container) [351].

Alumina plasma-sprayed coatings manufactured with graded alumina–titania coatings, and phosphate-sealed alumina coatings were investigated to improve the properties of metallic substrates operating in extreme environments of spent nuclear fuel. The effects of particle sizes distribution, phosphate sealant, and graded titania additions on the dielectric strength of the as-sprayed, thermally cycled, and

thermally aged coatings were investigated [354]. Spinel ($MgAl_2O_4$) coatings were also investigated [355]. All studies demonstrated the necessity to have impervious coatings.

18.3.10.5 Combined Cycle Power Plant Combinations

Hardwicke and Lau [356] emphasized that recent power generation company announcements centered on integrating renewable resources onto the power grid for cleaner, more efficient energy generation. They think that these technical breakthroughs can certainly utilize the new developments in the thermal spray industry.

18.3.10.6 Future Nuclear Fusion Reactor

At last thermonuclear fusion is a potential source of cleaner and safer energy for the future. Its technological realization depends on the development of materials able to survive and function in extreme conditions. According to the review of Matejicek et al. [357], materials to be applied in a fusion reactor will be subjected to extreme and complex loading conditions and have to fulfill very complex and sometimes contradicting requirements. A number of the demands on fusion materials can be fulfilled by the application of coatings. Thermal spraying is just one of the available coating technologies. Thermal spray (especially plasma spray) coatings were developed and tested for a variety of applications in fusion environments, including plasma facing components, tritium permeation barriers, and electrical insulation.

18.4 Thermal-Sprayed Coatings by Industry

In his paper [358], published in 1992, Longo had already identified 34 industrial sectors where thermal spray and other coatings were used. The broad base of end-user activity with thermal spray coatings for 12 industrial sectors was profiled in three tables. The main activities he has considered were gas turbine and aircraft, gas turbine and industry, turbine and steam, engines and automotive, engines and diesel, transportation, oil and gas exploration, chemical processing, paper and pulp, defense and aerospace, medical and dental, electric and electronic.

Longo [358] estimated that "the total market was projected to reach 1.8 to 2.0 billion dollars (1990 dollars) by the end of the decade (2000) on the strength of a growing and expanding powder business, a strong demand for standard equipment systems and vacuum plasma systems, and a growing demand for contract coating services."

Twenty-one years later Dorfman and Sharma [359] estimated that the thermal spray industry is worth approximately a $6.5 billion with the majority of revenue generation in coating services, thus underlying the growth of thermal processes.

The last ASM Handbook, Volume 5A: Thermal Spray Technology [360] is a replacement for the Handbook of Thermal Spray Technology [1]. In this book are developed more recent selection of applications, including electronics and semiconductors, automotive, energy, and biomedical. Emergent thermal spray market sectors such as aerospace and industrial gas turbines and important areas of growth such as advanced thermal barrier materials, wear coatings, clearance control coatings, and oxidation/hot corrosion resistant alloys also are reviewed.

18.4.1 Aerospace

Aero engines are probably those where thermal sprayed coatings, especially APS or HVOF sprayed, were extensively developed since the 1970s–1980s. The fan, compressor, combustion chamber, and turbine must be protected with coatings against oxidation, hot gas corrosion, erosion, and wear. Hundreds of components are now sprayed (see Fig. 1.8) in an aero engines used both for military and industrial turbine engine units worldwide. Their main role is to reduce wear, corrosion, and thermal flux, improve the engine efficiency, and promote life extension... In aero engines almost all types of sprayed materials are used (carbides, iron and steel, nickel alloys, cobalt alloys superalloys, nonferrous metals) except the self-fluxing alloys. The following list, far to be exhaustive, presents the different parts where coatings are used [1, 361]:

Against fretting wear, occurring in both lower- and higher temperature sections of engines, carbides, and refractory metals are used, and for clearance control CuNiIn, Nickel–Aluminum-base coatings, for more details (see Sect. 18.3.1.7).

Where rotating parts need some sealing to reduce by-pass of hot combustion or cold compressor gases (through spaces between blade tips and stationary housing) abradable seals are used. For example, in cold sections they are made of polymers and soft metals, while in the hot ones nickel–graphite, superalloy–polyester or boron carbide, YPSZ with polyester or boron carbide, NiCrAl, and bentonite (for more details see Sect. 18.3.4). Seal coatings are also used in the labyrinth seal knife-edges.

For the high-temperature sections, coatings are used on the one hand for protection against corrosion and high-temperature metal fatigue and on the other to reduce the temperature of the metallic substrate to improve components durability and increase fuel efficiency by higher turbine inlet temperatures: thermal barrier coatings. Besides the fuel consumption reduction, emissions of nitrogen oxide, hydrocarbon gases, and smoke are reduced, which is important to have environmental-friendly engines. For example, Airbus A380 and Boeing 787 cope with the limits set by International Civil Aviation Organization (ICAO).

Against corrosion, materials of the family MCrAlYs are used with M being nickel, cobalt, molybdenum, iron, or alloys of these elements (NiCo, CoNi, ...).

Fig. 18.3 Coated gas turbine vanes (courtesy of Sulzer-Metco)

Fig. 18.4 Coated combustion chamber (courtesy of Sulzer-Metco)

These alloys are VPS, HVOF and for some of them cold sprayed. It is important for these materials to reduce or suppress oxidation during spraying and achieve excellent adhesion. The latter is obtained by spraying on substrates cleaned from oxide layer and kept at high temperature to achieve diffusion between coating and substrate, which requires VPS spraying.

Thermal barrier coating systems (TBCs) are widely used in modern gas turbine engines to lower the metal surface temperature in combustor and turbine section hardware. The engine components exposed to the most extreme temperatures are the combustor and the initial rotor blades and nozzle guide vanes of the high-pressure turbine. Metal temperature reductions of up to 165 °C are possible when TBCs are used in conjunction with external film cooling and internal component air cooling [179]; for more details see Sect. 18.3.3.1. TBCs are applied on vane bases, burner cans, after burners, and also other small engine components. An example of coated gas turbine vane is presented in Fig. 18.3 and that of a combustion chamber in Fig. 18.4.

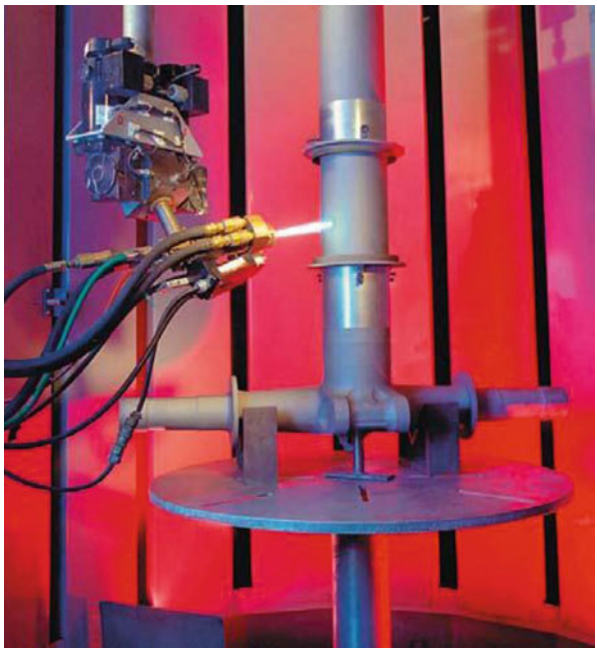

Fig. 18.5 Robot coating a landing gear (courtesy of Sulzer-Metco)

As developed in Sect. 18.3.4, rotating vane assemblies in aircraft engines require limiting the bypass flow of either hot combustion gases or cold compressor gases through the spaces between the blade tips and the stationary housing. These seals can improve drastically the engine efficiency. As developed in Sect. 18.3.4, two types of seals are used: abradable ones that are machined in situ by the rotating components (blades, for example) and labyrinth ones to match stator and rotor components with an intermeshing saw tooth geometry

Against wear, chrome plating has been intensively used because of its durability, ease of application, and low cost. Of course it suffers from pitting, spalling, and other failures under stress. For airlines the replacement of traditional industrial chromium plating process, used in landing gear, is time intensive and the aircraft is out of service for long periods, which is expensive.

Moreover chrome plating has some environmental and health problem with hexavalent chromium emissions. That is why alternatives have been searched to replace it: hard trivalent chrome coating and HVOF or plasma-sprayed coatings. Both present difficulties such as limited coating thickness for trivalent chrome and only line-of-sight geometries for thermal-sprayed coatings [361]. Coatings of tungsten carbides especially developed for landing gears and HVOF sprayed have considerably increased the service life of exposed cylinders and seals used in landing gears. Figure 18.5 presents a robot coating a landing gear.

Tests were also made to prevent corrosion of exhaust silencer segments with aluminum coatings arc sprayed.

18.4.2 Land-Based Turbines

Compared to aero engines the working conditions are tougher according to the longer life time expected (about 3 times longer), the larger size (for example, a ratio of 10 for turbine blades), the poor quality of the fuels used, and the working conditions with external temperatures varying from −40 to 60 °C. For more details see Sects. 18.3.3.2 and 18.3.4. Coatings are applied on bearing journals, bearing seals, stub shaft journals, labyrinth seals, blades nozzles, tip seals, inlets and exhausts, and housings [1, 360]. The overview of Rajendran [238] presents the different coatings used, methods of application and characterization, degradation mechanisms and indicates future directions, which are of use to a practicing industrial engineer. Coatings are applied to the compressor blades and vanes for enhanced erosion resistance. Anti-fretting coating protects the contact area of the dovetail part of the compressor blade root from fretting fatigue failure. Abradable coatings offer close clearance control thereby increasing the engine efficiency. Wear-resistant coatings give extended life of the parts that undergo rotary and reciprocating rubbing motion. Oxidation and corrosion resistant coatings are applied through either diffusion or overlay process. YPSZ (7 wt%) thermal barrier coatings offer increased component life with a decrease in operating temperature of the metal. Hardwicke and Lau [356] in their review paper about advances in thermal spray coatings for gas turbines and energy generation describe functional coatings widely used in energy generation equipment in industries such as renewables, oil and gas propulsion engines, and gas turbines. They present the current status of materials, equipment, processing, and properties' aspects for key coatings in the energy industry, especially the developments in large-scale gas turbines. In addition to the most recent industrial advances in thermal spray technologies, future technical needs are also highlighted. For more details see Sect. 18.3.3.2.

18.4.3 Automotive

Figure 18.6 from Vetter et al. [362] show a variety of car parts treated by different surface technologies (from sprayed coatings to PVD or PECVD). The different coating applications are related to [1, 362–365] the power train components, thermal barriers protecting certain components from overheating, brake discs, cylinder bore in diesel engines, aluminum alloy cylinder bore, exhaust valves, crankshaft, transmission and rear end gear clusters, body and chassis, synchronizer rings, shifter forks, valve seats, and connecting rods.

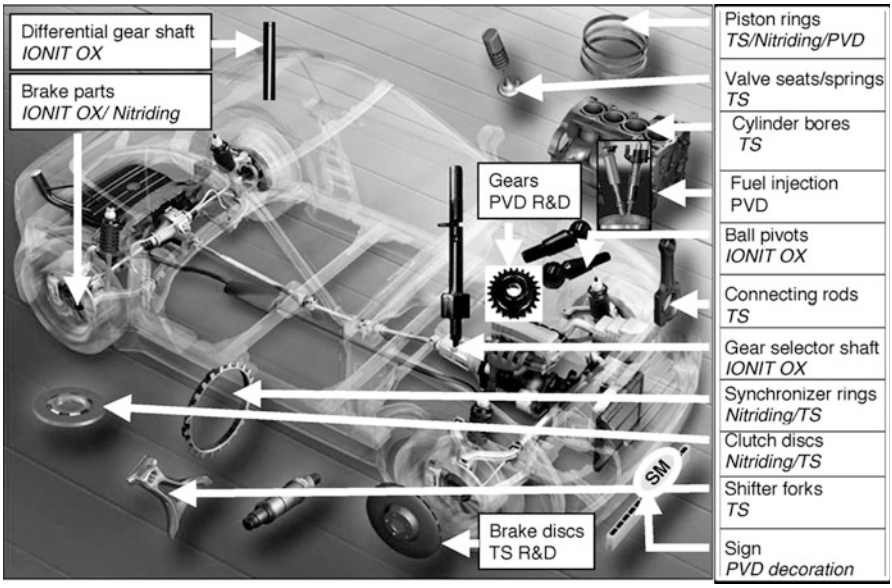

Fig. 18.6 Selected parts to be treated by surface technologies in cars. Reprinted with the kind permission of Elsevier [362]

18.4.3.1 Power Train Components

1. Against hot corrosion: Exhaust systems components (exhaust headers, exhaust pipes) are protected from hot corrosion by aluminum coatings wire arc sprayed.
2. Against wear: piston rings are commonly coated with molybdenum and molybdenum-bearing compounds using the plasma spray process in general. The HVOF spray process is used in the case of high performance piston rings for diesel engines. Molybdenum coatings are also used on aluminum piston skirts to prevent galling. Some aluminum piston tops are coated with molybdenum to limit erosion due to the impingement of fuel from injectors. Cylinder bore in diesel engines are coated with molybdenum plasma sprayed or WC–Co and WC–Co–Cr HVOF sprayed. Such coatings, slightly porous, retain oil and improve friction. Coated transmission parts such as synchronizing rings and shift forks are widely coated using wire flame spraying with molybdenum to provide a constant coefficient of friction and prevent scuffing.

In order to reduce the weight and size of the engine, iron cylinder blocks are replaced by aluminum ones, usually equipped with cast-iron cylinder linings. Instead of them, Sulzer-Metco has been the first to propose aluminum cylinder bores coated with a special iron alloy, to replace the cast-iron cylinder lining. This plasma coating acts as a direct running surface for the similarly coated piston rings, which reduces diesel or gasoline consumption and the amount of oil needed.

Fig. 18.7 Photo of the Rotaplasma process of Sulzer Metco (courtesy of Sultzer Metco)

The process called Rota-plasma developed by Sulzer-Metco was introduced in 2000 for automobile production. It allows coating aluminum alloy (cast aluminum–silicon) cylinder bores to provide a good wear resistance. Coating materials can be: carbon steel with its own oxides wustite and magnetite as solid lubricant, composite of carbon tool steel and molybdenum, corrosion-resistant steel (Cr and Mo alloyed), and metal matrix composite with ceramic particles. The process is entirely automated and lasts about one minute for a bore of conventional car engine (see Fig. 18.7).

The process advantages are the following:

- The pitch distance between the cylinders can be reduced allowing a further reduction of the engine block weight
- The friction between the piston rings and the liner surface can be significantly reduced (more than 30 % in gasoline engines)
- Considering that the majority of the energy losses in the engine is due to thermodynamic cycle efficiency, the potential fuel savings is limited to 4 to 5 %
- Very low surface wear rate (about 5 nm/h of service)

Transmission and rear end gear clusters receive often Mo thin coatings plasma sprayed to lessen the friction and produce smoother movement.

18.4.3.2 Rebuilding and Dimensional Restoration

It concerns crankshafts, clutches, and transmission shafts.

18.4.3.3 Thermal Barrier Coatings (See Sect. 18.3.3.3)

TBCs have been used on piston heads and valves and exhaust ports of high-performance engines. Thick TBCs (0.5–1 mm) on piston heads are attractive for the gains in engine performance and lifetime and the pollution reduction (hydrocarbons and NO_x). TBCs on brake pads insulate the hydraulics and avoid the risk of its boiling, especially on race cars.

They can also be applied externally on manifolds and other exhaust systems when the air cooling becomes insufficient. They increase the efficiency of turbochargers.

18.4.3.4 Other Applications

Metal matrix composites are used in brake discs to tailor the mechanical resistance and the thermal conductivity. The wire arc spray provides low-cost filler for weld seam and is also used for dimensional restoration. Ceramic overlay are sprayed for oxygen sensor protection, the sensor itself using zirconia-sprayed coating.

18.4.4 Electrical and Electronic Industries

First of all thermal spray coatings that allow achieving thick coatings cannot compete with the thin film technology (CVD, PECVD, sputtering, ion plating, . . .) used in electronic devices. However, they can be very useful in capacitors, insulators, resistors, and inductors. Coatings of oxide ceramics (alumina, titanate, beryllia) are used as dielectrics, while metals, and alloys are used for current carrying and bonding to ceramic substrates, metals for electromagnetic shielding, . . . [1, 360]. A few examples are presented below.

Alumina plasma-sprayed coatings are currently used in ozonizers. Standard ozonizer tubes consist of a borosilicate glass tube serving as dielectric with a metal coating applied to the inner surface of the tube serving as the HV-electrode. In order to increase the ozone production efficiency, a material with a higher permittivity is needed. Alumina coatings with a thickness up to 1,000 μm and serving as dielectric is deposited together with the metal electrode on top of the glass tube in ozonizers. Alumina is also used for high-temperature strain gages and insulation of induction heating coils.

Multilayer ceramic chip capacitors (MLCC) are used in a large number of electronic appliances. According to Yamakawa et al. [271] they are being required in more compact sizes, larger capacities, and reduced costs year-by-year and ceramic trays (a type of kiln furniture) are used for firing them. Normally, this ceramic tray consists of an Al_2O_3–SiO_2 body, an Y_2O_3-stabilized ZrO_2 topcoat and Al_2O_3 basecoat. The application of plasma-sprayed ZrO_2 topcoat and an Al_2O_3-sintered basecoat makes it possible to enhance longevity and reduce cost.

Pure beryllia (BeO) present excellent thermal and dielectric properties and is used in many high-performance semiconductor parts for applications such as radio equipment. Some power semiconductor devices use beryllia between the silicon chip and the metal mounting base of the package in order to achieve a lower value of thermal resistance than the alumina currently used. It is also used as a structural ceramic for high-performance microwave devices, vacuum tubes, magnetrons, and gas lasers. Vacuum plasma-sprayed beryllia coatings present excellent properties. Unfortunately their handling, especially that of fine powders, is highly toxic resulting in very stringent safety conditions such as keeping the rooms where spraying is achieved at pressure lower than atmospheric one. These conditions are often economically prohibitive and such coatings are essentially used for army and nuclear applications [1, 360].

According to Smyth and Anderson [366], for electrical heaters, arc-sprayed coatings are used, masking permitting to define the geometry. The choice of the material (NiCr, NiAl, . . .) depends on its resistance variation with temperature that must be as low as possible because the electricity source is a constant voltage one. The resistance depends on the coating oxide content that can also modify the alloy composition, chromium being preferentially oxidized compared to nickel, for example. Most sprayed resistors are used at relatively low temperatures (<250 °C). The resistance value can also be increased when adding alumina particles. Coatings can be sprayed on ceramic material, even polished ones, with a very good adhesion, when eutectics are formed or diffusion occurs. It requires heating the substrate to temperatures close to the sprayed alloy or metal temperature.

Cold-sprayed copper coatings are used to improve the heat conductivity between electronic devices, an underlying copper plate, and a soldered copper-coated heat sink, which is fabricated out of aluminum [267]. Cold spray also permits the generation of solderable surfaces on materials with poor wettability (for example, heat sinks, such as copper on aluminum) [268]. Similarly PTA allows spraying very thick (up to 1 cm or more) copper coatings that are used in powerful computer systems to improve their cooling. These copper layers, Fig. 2.8, achieve a good heat distribution and remove the heat more easily.

Alumina films plasma sprayed are more and more used as insulators in electronic devices. Plasma-sprayed alumina is used for electronic package mount in automotive industry.

Wire arc-sprayed coatings are used as shielding material to eliminate electromagnetic and radio frequency interference and dissipate static discharge sparks. Zn and Al are currently used to protect computers, electronic office equipment,

medical monitoring devices, housing constructed of temperature-sensitive plastic, and rooms containing military computers.

The review paper of Sampath [277] points out the industrial success of the lambda sensor for exhaust gas oxygen measurement for engine fuel control. This sensor uses a porous plasma-sprayed zirconia membrane coating between electrodes. When subjected to a differential partial pressure of oxygen, a rapid variation in electric resistance related to the oxygen partial pressure can be monitored through an electrical circuit [277].

Aluminum coatings, wire arc sprayed, are used in the production of electrolytic condensers. A thin film of copper is sprayed on carbon and ceramic resistors and carbon brushes to provide the electrical connection of high electrical conductivity. Thermal sprayed coatings are also used to produce thick films electrical circuits that can carry higher current than printed ones. The most used materials for these applications are Cu, Al, Zn, and Ag.

18.4.5 Corrosion Applications for Land-Based and Marine Applications

When metal coatings are needed to enhance the properties of a given surface wire combustion spray systems or wire arc spray systems are very good solutions to spray protective coatings, especially sacrificial ones. The investment is rather low and coating adherence is generally good (over 20 MPa), with almost no heating of the substrate. However coatings obtained by these methods are relatively porous (up to 20 %), which is not a problem for sacrificial ones. These coatings are extensively used throughout the maritime, paper/pulp/printing, manufacturing, steel, aerospace, automotive, and railroad industries.

18.4.5.1 Sacrificial Coatings

The corrosion protection of large steel structures such as bridges, pipelines, oil tanks, towers, radio and television masts, overhead walkways, and large manufacturing facilities in the metallurgical, chemical, energy, and other industries is a key issue. The protection of structures exposed to moist atmospheres and seawater such as ships, offshore platforms, seaports, is even more difficult [103, 104], see also Sect. 18.3.2.1. In most cases the surface to be protected is thousands and even tens of thousands of square meters, requiring that coating costs is competitive with those of traditional painting methods. The coating rate must be equal or higher than 10 m^2/h and if possible deposited in one unique pass. The equipment must be mobile and autonomous for operation in field conditions and must work under manual control, automation being generally difficult for large-scale operations, and at last, the spray gun can be up to 30 m from its power supply and control center [103, 104]. Flame wire arc spraying meet such requirements.

Fig. 18.8 Iron bridge arc sprayed with zinc and then painted. Reproduced with kind permission of Dr. M. Ducos [367]

Sacrificial coatings (cathodic behavior relatively to ions, for example, Zn or Al on steel) are mainly used: the thicker they will be the longer will be the protection. Typical thicknesses vary from 50 to 500 μm; the most frequent ones being around 230 μm. Referring to Sect. 15.10.1, such coatings must have a cathodic behavior relatively to the ions of the metal to be protected, in almost all cases steels. Metals used are then zinc, aluminum, and zinc–aluminum. Zinc performs better than aluminum in alkaline conditions, while aluminum is in acidic conditions. Zinc and aluminum replace more and more painting and galvanizing because their lifetime is predictable, they have good erosion resistance and require one application with no drying problems. Sluice gates and canal lock gates of the St. Denis Canal in France, that have been zinc coated in the early 1930s, have remained in perfect condition with virtually no maintenance for decades. According to [1] the lifetime of a 255 μm thick zinc or zinc aluminum coating is about 25 years and it can be extended 15 years by sealing it with vinyl paint. Painting is not the only sealer used; impregnation with special compositions (epoxy resin, silicon resin, . . .) being also intensively used. As soon as sealing is considered, the porosity of these coatings becomes an advantage for the adhesion of the sealer. Figure 18.8 represents an iron bridge arc sprayed with zinc and then painted.

Zinc–aluminum (Zn–15 wt%Al) seems to combine advantages of both materials. If resistance to wear must be improved, aluminum coatings can be sprayed with alumina particles, for example, using cored wires.

In case of the protection of steel reinforcement in concrete, zinc is generally used, but titanium has also been used in spite of the fact it is an anodic protection. In that case the coating is applied directly on the concrete substrate [1, 360]. Aluminum must be avoided where thermite sparkling may occur. That is due to the reaction of rusted steel and aluminum smears when this combustible mix is

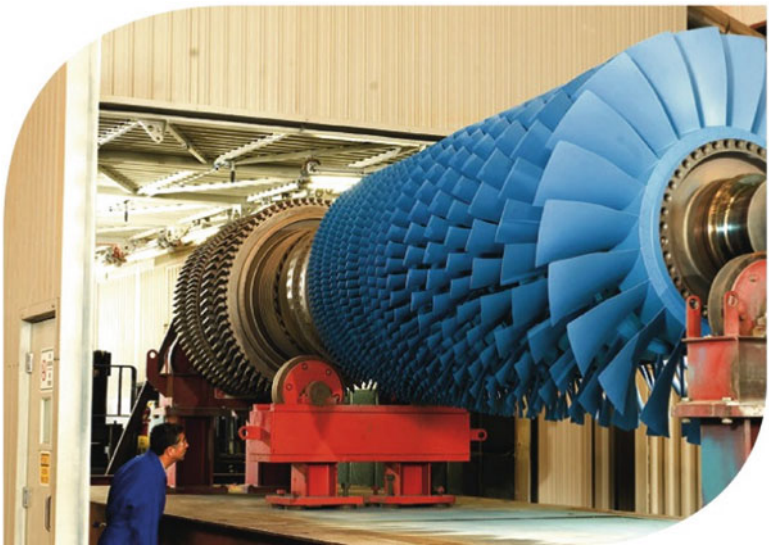

Fig. 18.9 Coated blades of the compressor airfoil of an industrial gas turbine compressor (courtesy of Sulzer-Metco Turbo)

ignited by an impact [1, 360]. Another interest of such coatings is their antifouling properties. Marine biofouling is the undesirable accumulation of marine organisms on artificial surfaces that are immersed in the sea. For example, when marine biofouling occurs on ship hulls, it leads to an increase in weight of the ship and friction to sail.

In the protection from corrosion and/or erosion of industrial gas turbine compressor airfoils, a sacrificial aluminum-filled metallic coating has been recently developed by Sulzer-Metco. The aluminum-filled metallic coating is made conductive via mechanical abrasive finishing. The thickness of these coatings is typically between 25 and 75 μm and the maximum operating temperature 870 °C. Figure 18.9 presents the coated blades of the compressor airfoil.

18.4.5.2 No-Sacrificial Coatings

Austenitic stainless steels, aluminum bronze, nickel-base alloys, MCrAlY, cermets with WC, Cr_2C_3, and matrices containing chromium or nickel or both are used against corrosion, often associated with wear. However such coatings, presenting no galvanic protection, will never protect the substrate if connected porosities and oxide networks exist, which is the case of most thermal sprayed coatings. The substrate protection requires using a protective bond coat or producing dense coatings, or sealing them that is not always possible if the service temperature is over a few hundreds of Celsius degrees.

Coatings of corrosion-resistant alloys for severe petroleum industry corrosion applications, such as type 316L stainless steel and Hastelloy C-276, were shown to act as true corrosion barriers. The oxide content also plays a role (see section "(b) Chemical or Parachemical Corrosion").

For applications with a severe wear in oil and gas industry, cermets are used, with however some problems for offshore installations. According to Meng [117] the corrosion resistance is improved by the proper choice of binder between the wide varieties of tungsten carbides.

18.4.6 Medical Applications

Orthopedic and dental market is developing very fast with either bioinert coatings (Ti–6Al–4V, Ti–6Al–7Nb, Ti–13Nb–13Zr, . . .) or bioactive ones (hydroxyapatite (HA), tricalcium phosphate). Both orthopedic and dental implants receive coatings designed to aid fixation in bone tissues, see Sect. 18.3.8. For example according to [300, 301], the report published in *Implant Dentistry*, estimated that 910,000 dental implant procedures were performed in 2000, and the numbers grew at an annual rate of 18.6 % through 2005. By 2005, annual sales exceeded half a billion dollars. The implant success is dependent on quality bone formation, optimization of the local surface structure, chemistry, morphology, and use of bioactive factors that are equally important [301]. Coated implants are now currently used for tooth, hip, knee, elbow, and shoulder. Two types of coatings are used [1, 360]:

- Bioinert ones with no activity between them and the bone or soft tissues, the most used materials being Ti and Ti–6Al–4V. These coatings must be porous (at least 30 %). Plasma spraying allows preparing porous-graded coatings with dense coating close to substrate to achieve a strong adhesion with substrate and very porous outermost layer (with pore sizes over 100 up to 400 μm). To achieve that, the plasma power was gradually reduced and the particle sizes increased while regulating the degree of powder melting layers to achieve porous graded coatings [300, 301, 360].
- Bioactive coatings, interacting with bone to promote bonding interfaces, are ceramic coatings with material compositions similar to that of bone tissue (calcium phosphate). The most used ceramic is hydroxyapatite (HA) $Ca_{10}(PO_4)_6(OH)_2$ exhibiting a strong activity to join the bone. The provision of a high-calcium and phosphorus-rich environment promotes rapid bone formation within the vicinity of the implant. Unfortunately when HA is plasma sprayed in air, calcium oxide (CaO) is usually formed, thereby affecting the integrity of plasma-sprayed HA coatings. Plasma-sprayed HA coatings also contain other bioresorbable phases, such as tricalcium phosphate (TCP) α or β forms, tetra-calcium phosphate (TTCP), and amorphous calcium phosphate (ACP) [307]. Gross et al. [302] investigated four HA-coated hip components recovered from patients during revision surgery. Analysis of the coating surface indicated

dissolution, osteoclastic resorption, and carbonate apatite precipitation identical to observations from previous in vitro studies. The coating microstructure differed between three coatings that remained on the prosthesis surface, ranging from completely crystalline coatings made by vacuum plasma spraying to less crystalline coatings manufactured by air plasma spraying. Increasing the amorphous and TCP concentration predisposes the coatings to higher dissolution rates [302]. Nelson et al. [368] have deposited by flame spraying powders of titanium alloy (Ti–6Al–4V) and bioactive glass (45S5) to fabricate composite porous coatings for potential use in bone fixation implants. Bioactive glass and titanium alloy powder were blended and deposited in various weight fractions and with two sets of spray conditions, which produced different levels of porosity. The HA formation on the alloy–bioactive glass composite coating suggested that the addition of bioactive glass to the blend may greatly increase the bioactivity of the coating through enhanced surface mineralization. Drnovšek et al. [369] studied the ability of nanoparticle bioactive glass (BAG) to infiltrate into the porous titanium (Ti) layer on Ti-based implants to promote osseointegration. Juhasz and Best [370] reviewed bioactive implants, coatings, and scaffolds made of ceramics, glasses, glass–ceramics, and composites that were able to form a chemical interfacial bond with tissue and can be resorbable or non-resorbable.

The ratio of HA to TCP has been reported to be crucial for bone regeneration. The dissolution rate of HA coating is dependent on the biochemical calcium phosphate phase of the coating as well as coating crystallinity. With adapted spray conditions it is possible to achieve up to 75 % crystallinity for APS, 80 % for HVOF spraying, and 95 % for VPS [302, 303, 306, 311, 312]. The result also depends on powder preparation, best results being obtained with dense HA particles. In Fig. 2.13 is presented the vacuum plasma spraying of (VPS) of HA coating on a knee prosthesis and in Fig. 18.10 a biocompatible coating on the lower part of hip joints.

18.4.7 Ceramic and Glass Manufacturing

For the production of a variety of glasses, platinum is currently used thanks to its high melting point, strength, and resistance to corrosion that allows withstanding the abrasive action of molten glass. Rhodium is often alloyed with platinum to increase the strength of the alloy and extend the life of the equipment. According to the prices of these metals, instead of using them as plates or sheets, they are often plasma sprayed in inert atmosphere chambers where over-sprayed powder can be collected. A ceramic coating, that is reapplied regularly according to its wear [1, 360], can protect these precious metal coatings. The electric glass melting for homogenizing, feeding, and shaping was developed with molybdenum electrode materials, since stirrers, mixing paddles, and some mold surfaces are plasma coated with molybdenum and its alloys [1, 360].

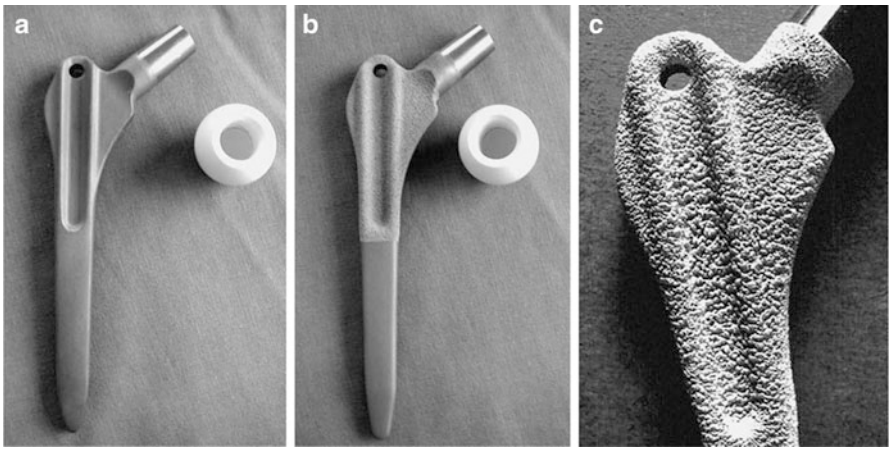

Fig. 18.10 (**a**) Femoral stem Walter, without coating, (**b**) Femoral stem with titanium alloy/hydroxyapatite coating, (**c**) Magnified view of the coating at the proximal end of the porous coated femoral stem [371]

Mold glass material must have sufficient strength, hardness, and accuracy (no deforming process) at high temperature and pressure. Of course, its oxidation resistance must be good, its thermal expansion low, and its thermal conductivity high. Therefore, the mold material choice depends critically on the transition temperature of the glass material. For low temperature-transition-glasses, steel molds with a nickel alloy coating can be used. For example, self-fluxing alloy NiCrBSi flame sprayed and refused. For higher transition temperatures NiCr–Cr_2C_3 or TiC cermets are used.

Hamashima [372] has developed a new boride cermet coating consisting of Mo-system ternary boride and iron-group metal alloys. MoCoB–Co/Cr cermets have a very low friction coefficient with glass at high temperature. The cermet coating has been applied to the lower mold on an industrial scale and the results were very satisfactory. In particular, the production efficiency of the forming process was improved substantially.

18.4.8 Printing Industry

According to Döering et al. [373] "the printing processes need all an ink transferring unit, a print form, and an impression cylinder. They differ in the process of transferring the print image to the substrate, leading to additional cylinders for generating the inverted image—in case of offset printing the so called offset cylinder—or even a shortcut from the ink transferring roller to the print form and directly to the substrate if gravure printing is regarded. Additionally, dampening

Fig. 18.11 SUME™CAL coating after super-finishing on calendar roll (Courtesy of Sulzer-Metco)

units require other surface energy than ink leading rollers. Moreover, the precision of shape and surface roughness of these core components is rather high. Therefore not only the requirements for an appropriate coating in terms of the function but also the requirements for the grinding and finishing step after the coating process are rather high." This will be illustrated with few examples:

- The ink transporting systems in offset printing machines consists of several different rollers, providing a homogenous film of ink for the print form. For example, the duct-roller elevates the ink from the ink box to the ink conditioning system. Its surface roughness R_z must be better than 2 µm and tolerances must be better than 2/1,000 mm in concentricity. Such conditions are achieved with chromia-rich coating consisting of a bond coat (Ni, NiCr, NiAl) and the ceramic topcoat [374].
- Rollers in the paper industry are subject various operating environments resulting in wear, chemical attack from dyes, thermal stress on heated rollers, and mechanical stress from doctor blades. They also must exhibit a high surface finish lasting as long as possible. Figure 18.11 presents a calendar roll coated with the so-called Sulzer-Metco SUME^{TM}CAL developed to meet these requirements.
- In contrast to common offset inking units, the anilox unit consists of a laser-engraved roller, taking the ink from a chamber doctor blade system [373]. The gravure procedure is performed after finishing the roller surface. Producing pure chromia coatings implies using carefully adapted plasma spray conditions and adapted powders, for more details see the works of Pawlowski [6, 374].

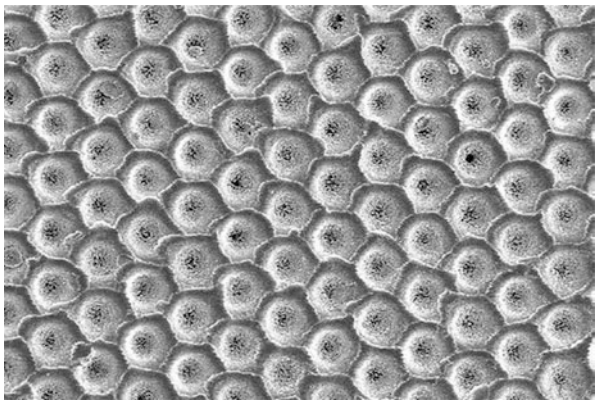

Fig. 18.12 Anilox printing roll with a laser engraved chromium oxide coating (Courtesy of Sulzer-Metco)

– Many other rolls are used in printing machines [374], where different oxides [chromia, alumina–titania (3 or 13 wt%)] are plasma sprayed. Lima and Marple [375] have proposed to replace the alumina–titania conventionally plasma sprayed by HVOF-sprayed nanostructured titania coating exhibiting a very dense (nearly pore free) and uniform isotropic microstructure with an excellent wear and corrosion resistance. Plasma-sprayed chrome oxide coatings for inking rollers exhibit very fine microstructures, which can then be laser engraved with a very small and tight pattern (Fig. 18.12).
– Other rolls such as blanket cylinders are coated with Hastelloy C by either APS or HVOF and at last draw rolls are coated with nickel–chromium [1, 362].

18.4.9 Pulp and Paper

Machines producing paper and cardboard comprise many parts that can be rather important (for example, rolls over one meter in diameter and ten meters in length) with high wear and corrosion problems. Coatings are used in several types of rolls and cylinders, including for instance, center press rolls, dryer cylinders, calender rolls, traction rolls, and Yankee cylinders [376]. Coating materials used are iron- and nickel-base alloys, nickel–chromium self-fluxing alloy, carbides, oxide ceramics, and various multilayers, again depending on the application. For example, rolls are coated by NiCrBSi coatings flame sprayed and others by WC–Co coatings HVOF sprayed. Figure 1.11 presents calendar roll of a paper machine protected by thermal spraying.

Functionally graded (FG) coatings are considered as an option to increase compatibility between ceramic coatings and metallic substrates. In this concept material properties such as CTE (Coefficient of Thermal Expansion) and elastic modulus are designed to gradually change in order to reduce the thermal stresses within the coating. Post-treatments, such as coating with fluoropolymers or sealing

Fig. 18.13 Paper machine center press-roll with a thermally sprayed ceramic coating (Metso Paper Inc.). Reproduced with kind permission of ASM [376]

coatings against corrosive process environments, are also used. A few examples are presented below:

- Press rolls are used to remove as much water from the sheet using mechanical forces. First they were made of granite rock and were very expensive with limited rotation velocity. Now one uses cast iron or steel roll bodies with coatings that are application specific and tailored to perform optimally in various different types of paper production conditions. Factors such as wear and corrosion resistances, and the functionality of the roll surface in the paper manufacturing process, are key properties in these applications [376]. In most cases alumina–titania and chromia coatings are used with HVOF-deposited bond coat [1, 360]. According to the size of the coated cylinders, high-power plasma torches, such as Plazjet, are used for deposition.
- Dryer cylinders of paper machines and large Yankee drying cylinders of tissue paper machines are HVOF thermal spray coated with cermets containing various carbides. According to their weight and size, these components are commonly coated on-site (surface preparation, coating, surface finish) in the paper factory. Ceramic-coated center press rolls are, nowadays, used to replace conventional granite rolls [376]. Ceramic coatings are based on aluminum and chromium oxides with an underlying bond coat and corrosion barrier. They are application specific and tailored to perform optimally in various different types of paper production conditions. According to the size of the components, Metso Paper is the world's leading manufacturer, both in Finland and elsewhere Fig. 18.13 represents a ceramic center press roll of a paper machine after finishing.

Sprayed coatings can also be top-coated with a fluoropolymer layer to improve the release properties of the roll surfaces [376]. Steels with high molybdenum contents (better corrosion resistance and thermal conductivity) HVOF sprayed are also used [1, 360].

- Machine knives (slitters, guillotine, blades) are coated with HVOF sprayed WC–Co coatings and then sharpened [1, 360].
- Carbon Fiber-Reinforced Plastics rolls (CFRP roll), exhibiting excellent characteristics including lightweight, high stiffness, and low flexure, have been increasingly employed in manufacturing industrial fields. Compared to conventional metal rolls, CFRP roll is lighter and stiffer and exhibits lower inertia moment [377]. Unfortunately carbide-cermet coatings failed because of their poor thermal shock resistance on CFPR rolls. Ni-base composite porous coating including ceramics particles developed by Nagai et al. [378] showed high-thermal shock resistance. Five coated rolls were installed in the actual papermaking line. They achieved successful results with 10 % improvement of the line speed, whereby outstanding performance and maintenance-free has been confirmed even after 4 years of use. Yoshiya et al. [377] have developed a 5.4-m long thermal sprayed carbon roller, installed in a paper slitter/winder, that is moving stably at ultrahigh speed, 2,300 m/min, with no abrasive wear. The roller is a formed three-layer structure: a tungsten carbide cermet layer on grooved metal sleeve, which covers the CFRP substrate roller shell. The thermal spray process is the finishing process because no after grinding is performed.
- Blow tanks, that are storage bins, are also on-site HVOF sprayed with WC–Co coatings to improve their wear resistance.

18.4.10 Metal Processing Industries

Many parts in metal working industries are submitted to severe wear and corrosion, which consequences can be reduced by thermal-sprayed coatings. The main parts that can be sprayed are [1, 362, 379] components of electric arc furnace (EAF) and basic oxygen furnace (BOF), molds, casting dies, casting salvage, molten metal containment and delivery, steel mill rolls working in both wet and dry mill environment: entrance and exit rolls of steel processing line, rolls for galvanized and aluminized steel sheets, …. PTA coatings are also used in processing industries, see Sect. 10.7.4 of Chap. 10.

18.4.10.1 Components of Furnaces or Boilers

Boilers are large and expensive installations which suffer enormously from wear caused by corrosion and erosion, aggravated by very high temperatures. The exact type of wear experienced varies from one part of a boiler to another and is

Table 18.1 Different parts of the boiler that can be affected with the corresponding wear phenomena [380]. Reproduced with the kind permission of Castolin, copyright © Castolin Eutectic

	Part of boiler affected	Principal wear phenomena
1	Combustion chamber waterwalls	Corrosion/abrasion/erosion
2	Secondary superheater	Corrosion/oxidation/erosion (ash)
3	Economiser	Erosion (ash)/corrosion
4	Primary superheater	Erosion (ash)/corrosion
5	Reheater	Corrosion/oxidation/erosion (ash)
6	Superheater soot blowers	Erosion (steam)
7	Combustion chamber soot blowers	Erosion (steam)

Fig. 18.14 Flame fusing of flame sprayed self-fluxing alloy on boiler tubes (Courtesy of Castolin)

influenced by the overall design of the boiler and the type of combustible fuel. For example, Table 18.1 from Castolin [380] presents the different parts of the boiler that can be affected with the corresponding wear phenomena.

A wide variety of components associated with electric arc furnace (EAF) and basic oxygen furnace (BOF) are under severe attack from heat, particulate, and acidic gases. Water-cooled components, in the off-gas duct systems such as pans, roofs, boxes, and panels, are subjected to high-velocity combustion gases that contain a number of corrosives chemicals that condense and attack the heat transfer surfaces [381]. Coatings used are those developed for high-temperature wear and corrosion resistance see for example [379, 381–388]. For example, Fig. 18.14 presents the deposition of spray and fuse coating on boiler tubes.

18.4.10.2 Molds

In continuous casting the cast shell in the lower half of the mold abrades and wears the bottom of the mold. Diffusion of the copper substrate from the mold into the surface of the cast product leads to a quality defect called "star cracking" [379]. Chrome- and nickel-based coatings protect copper molds from wear and also enhances caster product quality by greatly reducing cast product contamination and star cracking problems [379]. Thermal barrier coatings are also used to control the heat flow and retard rapid chilling [1, 360, 387]. For very corrosive melts, pure yttria is used instead of zirconia partially stabilized with yttria. Of course bond coats are necessary, and sometimes multilayer coatings, to achieve a good compliance between the expansion coefficients of mold and topcoat. Sanz [387] has studied different coatings to protect the mold wall. Casting salvage is also achieved by filling the voids, after grinding of porosity or wear zones, with plasma or wire arc coatings that are then remachined [1, 360]. Gross and Kovalevskis [388] have shown that metallic molds from iron, nickel, Ni–Al, and Ni–Cr–B–Si can be produced by air plasma spraying onto steel and chrome-plated steel models. The main processing criterion was the mold temperature that must be heated above 400 °C to avoid coating warpage and fragmentation. Heating to 600–700 °C is required to remove coating porosity and reduce coating pullout. Weiss et al. [389] have demonstrated the feasibility of making sprayed steel-faced tooling. Kim and Kweon [390] investigated various flame- and plasma-sprayed coatings to extend the life of these molds. Coating materials studied include plasma-sprayed ceramic coatings with bond coats as well as flame for casting pig iron ingots. Cyclic furnace tests from room temperature to 1,100 °C in air, simulating the thermal cycle in casting, indicated that failure occurred along the interface between the bond coat and the gray iron substrate because of iron oxidation, and not at the interface between the ceramic top coating and the bond coating. The field test results indicated that plasma-sprayed alumina coatings with 200 μm top coating thickness are the most promising materials for pig iron casting.

18.4.10.3 Die Casting

Gibbons and Hansell [391] have shown that two thermal spray materials, one Cr_2C_3–25(Ni–20Cr) and one WC–10Co–4Cr, deposited using JP5000 HVOF hardware, offered properties that could enable low-cost, low-volume production aluminum injection mold tooling to be upgraded to higher volume production tooling. Hot dipping rolls: MoB/CoCr, a novel cermet material for thermal spraying, with high durability in molten alloys has been developed to utilize for aluminum die-casting parts, and for hot continuous dipping rolls in Zn and Al–Zn plating lines [146]. The tests revealed that the MoB/CoCr coating had much higher durability without dissolution in the molten Al–45 wt%Zn alloy. Using undercoat was effective to reduce the influence of large difference in thermal expansion

between the MoB/CoCr topcoat and substrate of stainless steel of AISI 316L, widely used for the hot continuous dipping [146]. MoB-based cermet feedstock powders (MoB/NiCr and MoB/CoCr) were deposited on SKD61 (AISI H-13) substrates used as a preferred die (mold) material [392]. The durability of these coatings on cylindrical specimens against soldering also has been investigated by immersing in molten aluminum alloy (ADC-12) for 25 h at 670 °C and subsequently, compared with that of NiCr and CoMoCr coatings. Both types of MoB-based cermet coatings have shown high soldering resistance as negligible intermetallic formation occurred during the immersion test [392]. Weiss et al. [389] have used arc-sprayed steel-faced tooling to create matched die sets for injection molding applications.

18.4.10.4 Entrance and Exit Rolls of Steel Processing Line

When coating bridle and accumulator rolls in entrance and exit ends of a steel processing line with tungsten carbide coating surface damage on the roll is eliminated and proper grip provided and slippage prevented. The surface coating is properly textured to provide the required characteristics or profile on the strip surface [379]. Multi-component white cast iron is a new alloy that belongs to system Fe–C–Cr–W–Mo–V, HVOF sprayed seems to be promising for rolls [392].

18.4.10.5 Galvanized and Aluminized Steel Sheets

They require very high surface quality, particularly in exposed panels. In continuous galvanizing and aluminizing, the steel strip is dipped in the molten bath through a series of rolls, which control the speed and tension of the strip and guide the steel strip through the molten metal bath. The rolls operating in the molten Zn–Al alloy are subjected to severe corrosive environment and require frequent change and repair [1]. Seonga et al. [394] have shown that WC–Co coatings were not very good with molten Zn–Al. By coating the sink and stabilizer rolls with molybdenum boride, tungsten carbide, and other materials, the rolls remained smoother and produced an improved strip surface.

18.4.11 Petroleum and Chemical Industries

The main problem is to prevent corrosion and wear, all forms of wear, especially those linked to corrosion arising at low, intermediate, and high temperatures. As previously pointed out, against corrosion dense (no-sacrificial) coatings (no pores or cracks and very low oxide level) of the appropriate material are mandatory. For porous coatings, especially ceramic ones, a dense bond coat with a good resistance to the corrosive media is mandatory. Porous coatings can be sealed but

Fig. 18.15 Typical coating against corrosion sprayed on-site onto refinery pipe (Courtesy of Sulzer-Metco)

the seal must be adapted to the service temperature. Moreover many components have sizes that require on-site spraying. Usually dense coatings are obtained with vacuum plasma spraying or D-gun or HVOF, but soft vacuum plasma and D-gun spraying are not adapted to big parts. Thus HVOF spraying, that can be used on-site, is extensively used against corrosion and abrasive and erosive wear mainly with carbide-based cermets [1, 116, 118, 119, 166, 294, 379, 381–384, 397–399]. Of course for the protection of external steel structures, pipes, tanks, ... Al, Zn, or Zn–Al wire arc or flame sprayed are used [1, 103–109], as well as polymers sprayed by flame, HVOF, plasma according to the polymer melting temperature [402]. For example, Fig. 18.15 present an aluminum protection flame sprayed on a refinery pipe.

Coatings in chemical industry are used for pressure and storage vessels with Hastelloy B or C, Inconel 600, for heat-affected zones where solutions found in gas turbines are often used. In some chemical reactors, submitted to strong acids in combination with organic solvents, glass lining are used that are repaired by APS-spraying tantalum, bonding well to the glass, and followed by an overlay of chromium oxide [1, 360]. For example, Moskowitz [115] have tested HVOF process using unique inert gas shrouding to produce highly dense, low-oxide coatings of metallic alloys, which were tested in laboratory and plant, with exposures as long as 5 years. Coatings of corrosion-resistant alloys, such as type 316L stainless steel and Hastelloy C-276, were shown to act as true corrosion barriers.

For the oil, gas, and petrochemical industries, the following components are coated using thermal spray technologies: mud drill rotors, pump impellers, plunger, turbine, rotor shaft of centrifugal compressor/pump, pump shafts, boiler tube, thermo-well, mixing screw, mandrels, actuator shafts and housings, housings and valves, valve gates and seats, ball valve with large diameter, progressive cavity mud motor rotors, rock drill bits, riser tensioner rods, impeller/blade drilling and production risers, sub-sea piping, wellhead connectors, fasteners, compressor rods, mechanical seals, pump impellers, tank linings, external pipe coatings, structural

Fig. 18.16 General view of practical spraying of ball valve by the MET-JET III system. Reprinted with kind permission of ASM [395]

Fig. 18.17 Wear band on drilling pipe PTA coated (courtesy of Castolin)

steel coating, . . . [1, 360]. It also seems that wear-coating applications have started to replace hard chrome [361].

Two examples of coatings used in oil, gas, and petrochemical industries are presented below. Stainless steel ball valves must be wear resistant, have a low friction coefficient, a good erosion and heat resistance, good fatigue strength and seal performances, etc., are significantly improved by applying HVOF coatings [395]. loping trend of these ball valves for highly harsh working conditions. Figure 18.16 shows the practical spraying of a ball valve having a diameter of over 500 mm. Wear bands on drilling pipes, as shown in Fig. 18.17, are PTA coated, for more details see Sects. 10.7.3 and 10.7.4 of Chap. 10.

18.4.12 Electrical Utilities

Coatings against corrosion and wear (C–W) are used in fluidized-bed combustor (FBC) and conventional coal-fired boilers.

18.4.12.1 For Fluidized Bed Combustor Boilers

The problem is linked to the finely divided mixtures of coal and limestone particles eroding and corroding steam pipes and boiler walls, as well as the high sulfur content of coals or low grade combustibles resulting in corrosion at high temperature. Different coatings are used:

- Cr_2O_3 (20 wt%)–Al_2O_3 on NiCrAlY bond coat (against corrosion through the porous ceramic coating) [1, 360], the addition of approximately 20 wt% chromia resulting in the formation of one solid solution of $(Al–Cr)_2O_3$ in the α-modification (working temperatures can reach 1,000 °C and the transformation of γ phase starts around 900 °C).
- HVOF sprayed Cr_3C_2–NiCr coatings with high compactness and fine grain size [165], the wear resistance being due to hard carbides particles homogeneously distributed within coating, the ductile matrix being corrosive-resistant.

18.4.12.2 For Coal-Fired Boilers

Plasma sprayed stellite-6 coating has been found to be effective in increasing the erosion–corrosion resistance of boiler steels in the coal-fired boiler environment. A less porous structure obtained after laser remelting was found to be effective for increasing erosion–corrosion resistance [164]. Inconel systems or high-chromium alloys or chromium–nickel alloys coatings, presenting a good resistance to sulfur, have also been used, sprayed with plasma, wire arc, or HVOF [1, 360]. Notomi and Sakakibara [403] have proposed low cost and high hardness plasma-sprayed coatings, developed by addition of carbon and hardening elements to high chromium cast iron (C–Si–Mn–Cr–Mo–V–other–Fe) used for wear-resistant material. Nitrogen gas atomization was applied to manufacture the powder in order to prevent oxidation of particles. These coatings showed the same or more erosion resistance than Cr_3C_2–NiCr cermet coating and had higher reliability for long period operation and higher practicality.

18.4.13 Textile and Plastic Industries

The abrasive qualities of man-made fibers, particularly nylon and polyester, and the corrosive characteristics of additives, such as fiber finishes and lubricants, combine to deteriorate yarn contact surfaces. High rotation speed of grooved rollers results in considerable abrasion wear. Due to the very high rotational speed, the roller has to be made from aluminum, and therefore, the reduction in wear can only be achieved by the deposition of a coating that also must be as light as possible. For years, thermal spray coatings have been used against wear and corrosion on textile machinery: steel thread guiders, thread breaks, stretch roll, grooved roll, separator roll, oiling roll, draw roll, feed roll, conditioning rollers, snick pins, collets, disk grip, cutter base, feed drum, rotor for open-end, extruder dies, knives, heating bars, heater/hot plate, . . . [1, 360]. The high-velocity rotating parts are often coated with alumina or alumina–titania coatings. TiO_2 addition lowers significantly the microhardness of the alumina coating but increases its toughness [404]. Parts such as knives and extruder dies are coated by HVOF-sprayed tungsten carbides, while textile rolls are plasma sprayed with alumina–titania (13 wt%) as illustrated in Fig. 1.12. A printing roll with laser engraved chromium oxide coating is shown in Fig. 18.12.

Lima and Marple [375] showed that nanostructured titania feedstock HVOF-sprayed exhibited a superior abrasion wear resistance (27 % lower volume loss) when compared with an air plasma-sprayed conventional alumina–titania coating, in spite of the fact that the latter is 33 % harder than the HVOF sprayed titania. The higher wear resistance of the HVOF-sprayed nanostructured titania was provided by the nanostructured zones embedded in the dense and uniform coating microstructure acting as crack arrester. They are probably worth to be tested in textile industry.

18.4.14 Polymers

Thermal spraying polymers [1, 360, 402, 405–417] is one-coat process that acts as both the primer and the sealer, with no additional cure times processes. Polymer thermal spraying is ideally suited for large structures that otherwise could not be dipped in a polymer suspension. Moreover it seems that functionalized polyethylene polymers such as ethylene methacrylic acid copolymer (EMAA) and ethylene acrylic acid (EAA) can be applied in high humidity. Of course the use of polymer coatings depends strongly on its service conditions. Especially it must be kept in mind that melting temperatures vary from 40 to 60 °C for ethylene methacrylic acid copolymer (EMAA) to 300 °C for polyimide. They are deposited onto metals, ceramics, cermets, and composites. . . As they present a high chemical resistance, a high impact, and abrasion resistance at low temperature, they are used in many industries, especially in food industry.

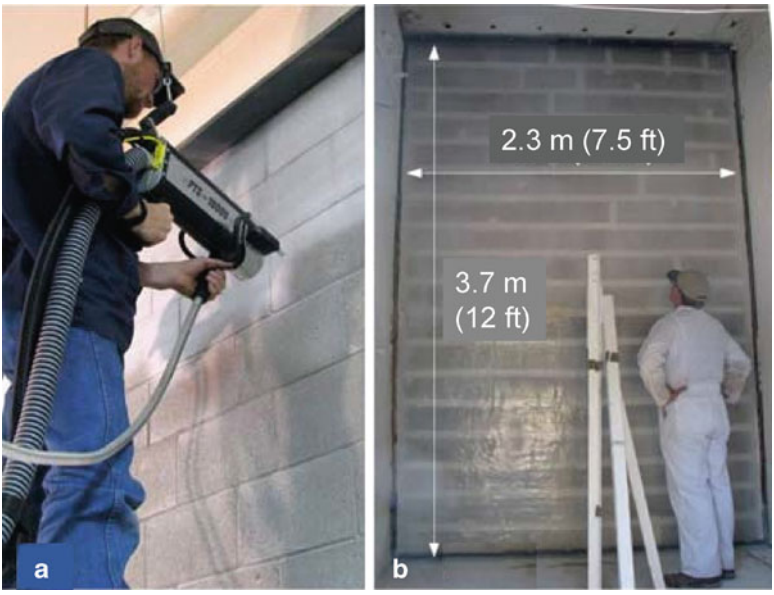

Fig. 18.18 (**a**) thermal spraying of blast mitigation polymer membrane to the internal side of test walls; (**b**) wall dimensions and appearance of a completed membrane. Reprinted with kind permission of ASM [417]

In food industry polymer coatings replace paints on the wall because they have a much better resistance to the chemical products used for cleaning (about 1 week for paint against about a quarter for the polymer coating). They are even used on the floors where polymer coatings doped with alumina particles provide an excellent anti-slip lining, the alumina particles rippling out when people walk on it.

A novel coating process (Polymer Thermal Spray PTS), has been developed by Isocevic et al. [417]. It utilizes an electro-resistive heating element for rigorous temperature control and for heating the main process gas that could be air, nitrogen, inert, or other gases. They have deposited advanced polymer coatings and structures such as (1) blast mitigation coatings for protecting civil structures against external explosions and (2) thermal spray forming of syntactic foams based on polyimide micro-balloons. For blast mitigation, Fig. 18.18 shows thermally sprayed polymer (thermoplastic elastomer) membranes applied to the internal side of the test walls 3.7 × 2.3 m. Figure 18.19 presents the test setup for evaluation of thermally sprayed blast mitigation treatments. The explosion impulse reached 215 kPa and lasted about 50 ms. Both walls successfully passed the test and remained standing. The total wall deflection toward the inside of the test room was 8 in. with no visible damage to the membrane and no flying debris or wall segments penetrated the room.

Spraying syntactic foams based on polyimide micro-balloons was developed [417] in the frame of a research project funded by NASA Langley Research Center.

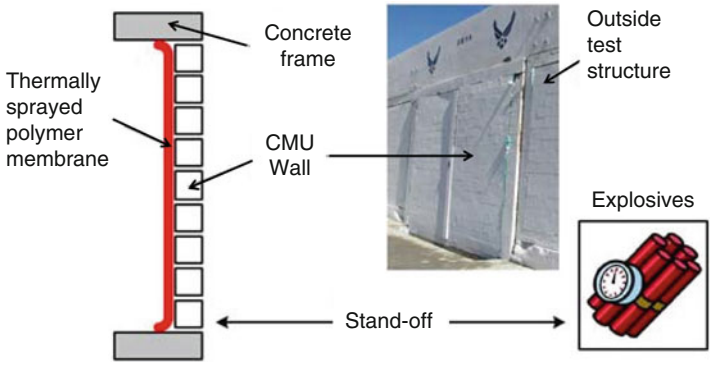

Fig. 18.19 Test setup for evaluation of thermally sprayed blast mitigation treatments. Reprinted with kind permission of ASM [417]

The coating was supposed to be used as high temperature insulation (up to 325 °C) and also satisfy strict flammability regulations relating to the aerospace industry. The polyimide syntactic foam, see Fig. 18.20a, consisted of two NASA Langley-licensed materials, polyimide microspheres (PerFoma-H® from GFT Corporation), and a binder. Polyimide microspheres had a bulk density of 0.043 g/cm^{-3}, a size range 400–800 µm and service temperature between −253 °C and 315 °C. The binding powder and microspheres were thermally co-sprayed using the PTS coating system. The thermally sprayed foam did not support a flame and formed a stable isolative char without smoke at higher temperatures. The foam deposited over various complex shapes is shown in Fig. 18.20b–d and seemed to be interesting for thermal insulation in airspace applications [417].

18.4.15 Reclamation

The effects of wear and corrosion can only be retarded, but not be stopped forever and wear parts must be replaced or resurfaced. It is the same for undersize parts due to manufacturing error. The ability to apply coatings by thermal spraying with a broad spectrum of thickness, finish and composition requirements makes the different thermal spray processes ideal solutions to re-surface components, avoiding their costly replacement. Restoration is performed either with the same material as the base metal or with a more corrosion- and/or wear-resistant material. However, it is better to choose coatings that can be machined. In a wide range of industrial applications, thermal coatings are used to renew components by restoring their specified dimensions and matching and sometimes improving their original performance. Very often it is possible to design a coating that meets the functional requirements of the component, and moreover offers better resistance to corrosion, oxidation, and mechanical wear than the original product. Of course the cost of the

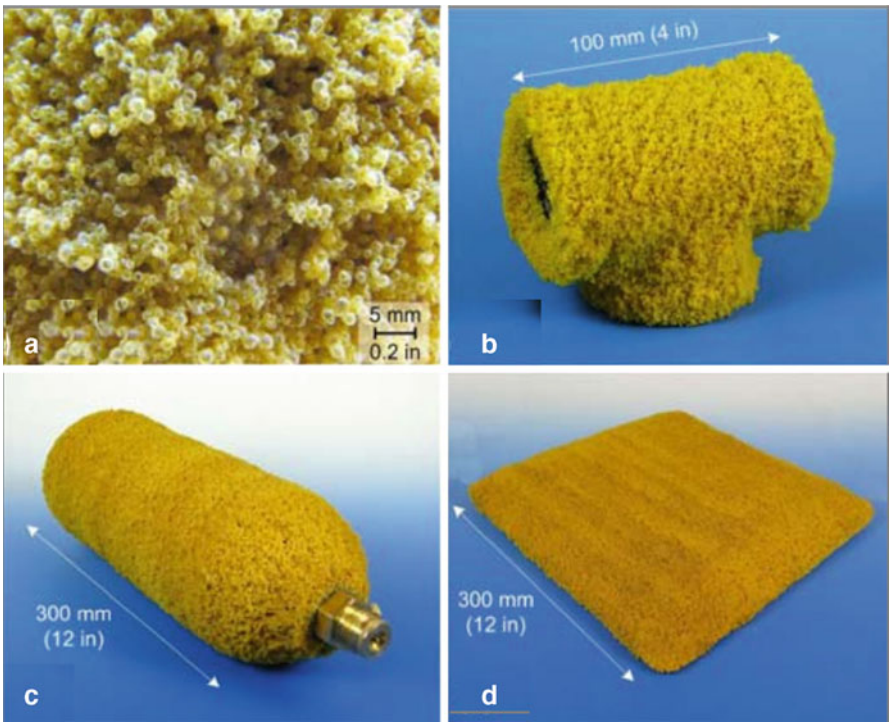

Fig. 18.20 Thermally sprayed syntactic foam based on polyimide micro-balloons; (**a**) foam microstructure; (**b**) thermally sprayed on pipe T joint; (**c**) on a gas cylinder; (**d**) on a flat aluminum plate. Reprinted with kind permission of ASM [417]

resurfacing must be lower than that of a new part (a fraction of it). For example, this technique is particularly used for roller faces and journals, dryer drums for paper-making, pump seals (shafts and sleeves), pump housings, compressor rods, rotary airlocks and feeders, conveyer screws, ... [1, 360]. PTA also are used for refurbishing components, even with a complex shape as turbine, see Sect. 10.7.6 of Chap. 10.

A few examples are given below to illustrate the use of sprayed coatings in re-surfacing components:

- The use of aluminum alloy for injection mold tools, especially for the automotive industry, is not new and has been utilized as bridge tooling to support the manufacture of typically up to 10,000 components. Two thermal spray materials, one Cr_2C_3–25(Ni–20Cr) and one WC–10Co–4Cr, deposited using JP5000 HVOF hardware, have been shown to offer properties that could enable low-cost, low-volume production aluminum injection mold tooling to be upgraded to higher volume production tooling [389].
- The thermal-sprayed Tribaloy T-800 coatings deposited by the HVOF process exhibited lower cavitation wear rates than the stainless steel bulk material [63].

- Massive turbines and the valves used to regulate water flow at hydroelectric dams are often exposed to the wearing effects of high-velocity water containing abrasive particulate. As mentioned by Sulzer-Metco, coatings can replace lost material and, at the same time, provide a more wear-resistant surface, increasing useful life by up to 20 times over the original.
- Hard chromium plating is usually used to restore to original dimensions the worn surfaces of gas turbine shafts. In the case of shafts repair, hard chromium plating process proved to be time consuming and to involve high costs. High hardness and good wear resistance performances of WC–12 %Co HVOF sprayed coatings support their candidature for the replacement of hard chromium plating in this field [326].
- Song et al. [418] have studied the effect of repair of NiCrAlYSi coating after longtime use on the coherence of coating to substrate and mechanical properties of Ni_3Al base alloy IC6. For secondary coating repair, the room temperature tensile properties of base alloy had no obvious change, while stress rupture lives decreased, but still were rather long, compared to the alloy with first repair coating. Therefore, they deduced that NiCrAlYSi coating repair is feasible to prolong the service lives of IC6 turbine vanes.
- Ducos [419] has presented a few industries where PTA is used for resurfacing: extruder screw, vanes, turbine blades, engine valves (especially big diesel engines), and rail train car wheels.
- Isakaev et al. [420] have shown that plasma-sprayed coating of railway frogs, working under contact fatigue and wear-out provides a good solution for repairing them.
- The surfaces of printing press cylinders wear quickly. Coatings of nickel/chrome alloy, Cr_2O_3, and others, have supplanted chrome plating as the preferred method of reclaiming worn cylinders because thermal spray processing is far faster.
- It has been shown that cold spray is a promising cost-effective and environmentally acceptable technology to impart surface protection and restore dimensional tolerances to aluminum alloy [421] or magnesium alloy components on helicopters and fixed-wing aircraft [425]. Kashirin et al. [426] have shown that using a portable cold spray system working with air at pressures below 0.8 MPa, made possible to restore on site aluminum alloy molds for plastics, corrosion defects on car aluminum engines, casting defects for various aluminum alloys, antique art objects such as copper sculptures of Isaac Cathedral in Saint-Petersburg, . . .

18.4.16 Other Applications

As previously described, thermal spray coatings provide superior wear (abrasive, erosive, fretting, . . .) resistance and corrosion protection with coatings having low porosity, high hardness, good toughness for cermets, and great flexibility of composition [1, 360]. Thus they are also used in the following:

- *Mining industry* where good abrasive and/or adhesive resistance is very important. For example, HVOF, PTA (alloys doped with ceramic particles), and wire arc-sprayed cored wire coatings are used on conveyor belt idlers, steel oscillating tub, fan components such as removable leading edges, bolt-covers, blades, deflectors and large inlet entrance cone ducts, scraper or excavator teeth as illustrated in Fig. 2.18.
- *Nuclear industry* where the use of cobalt-based alloys (stellites or cermets matrix) is limited, thus coatings against wear and corrosion rely on nickel alloy-based coatings (NiCr–WC or Cr_3C_2). Cermets with hafnium carbide have been developed that present a large neutron cross section. However sprayed coatings are essentially used in pumps, turbines, heat exchangers, vanes, etc.

  In numerous applications developed at CEA-DEN, French Atomic Agency, Atomic Energy Department, particularly those encountered in the processing of nuclear wastes, metallic components are subjected to extreme environments in service, in terms, for example, of aging at moderated temperature (several months at about 300 °C) coupled to thermal shocks (numerous cycles up to 850 °C for a few seconds and a few ones up to 1,500 °C) under a reactive environment made of a complex mixture of acid vapors in the presence of an electric field of a few hundred volts and a radioactive activity. Berard et al. [354] have tested alumina plasma-sprayed coatings manufactured with feedstock of different particle size distributions, graded alumina–titania coatings, and phosphate-sealed alumina coatings to improve the properties of metallic substrates operating in such extreme environments. The effects of particle size distribution, phosphate sealant, and graded titania additions on the dielectric strength of the as-sprayed, thermally cycled, and thermally aged coatings were investigated. Thermal aging test was realized in furnace at 350 °C for 400 h and thermal shocks tests resulted from cycling the coating between 850 and 150 °C using oxyacetylene flame and compressed air cooling. Aluminum phosphate impregnation appeared to be an efficient post-treatment to fill connected porosity of these coatings. Alumina as-sprayed coatings manufactured with +22–45 μm and +5–20 μm particle size distributions exhibited good dielectric strengths after thermal solicitations compared to those manufactured with larger size distributions or to graded titania coatings.
- *Cement industry*: Again the main role of sprayed coatings is against wear and corrosion in mechanical seal, sleeve, burner tip, boiler tube, thermo-well, kiln support roll, pinion shaft, coating for cement preheat tower, impeller blade, calender roll, cone crusher, and hydraulic rams with acid-resistant coatings.
- *Drawing Machine*: Guide roller and ceramic disc, rod breakdown drawing machine, fine drawing machine, and other accessories.
- *Waste treatment*: Steel tubes oxidation causes an important problem in Municipal Solid Waste Incinerator (MSWI) plants due to burned wastes containing high concentrations of chemically active compounds of alkali, sulfur, phosphorus, and chlorine. Ni-based HVOF coatings are a promising alternative to the MSWI conventional protection against chlorine environments [424].

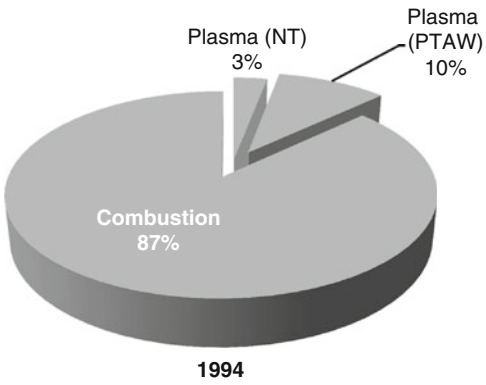

Fig. 18.21 Percentages of the different spray processes in industry in 1994, after M. L. Thorpe, Oral presentation ITSC

– *Sheet metal forming dies*: Conventionally mold and dies are manufactured by machining from bulk metallic materials. Tooling by using arc spray process to spray metal directly onto a 3D master pattern is an alternative method to manufacture mold and dies for plastic injection molding and other applications [1, 360].

18.4.17 Thermal-Sprayed Coatings in the Different Countries

Up to the 1980s thermal spraying was more an art than a science with a reputation of high complexity (up to 60 parameters to be adjusted to achieve coatings with specific service properties) and rather low reproducibility and reliability. Thus it is not surprising that the firsts industries where coatings (except metallization) were successful were those used to rather sophisticate production techniques such as aeronautics and nuclear ones. This is illustrated in Fig. 18.21 from TAFA Co. representing the percentages of the different spray techniques in industry in 1994. It shows that the majority of processes are flame spraying (87 %) with 10 % PTA and 3 % of plasma spraying. Of course such figures give only trends because some spray activities performed in companies, and which activity is not directly linked to spray process, are often ignored.

In the 1980s, thermal spraying has dramatically evolved from an art to a science [428] with many research developments in laboratories and also new spray techniques such as HVOF, HVAF, and arc spraying. This is illustrated in Fig. 18.22, again from TAFA, and representing percentages of the different spray techniques in 2000. Of course flame spraying is now reduced to 50 % and the rest of the market comprises all other techniques except of course cold spray that had not yet diffused in industry at that period. This trend is confirmed by the repartition of the different spray processes in industry in Europe in 1998 [426] presented in Fig. 18.23, where the developments of HVOF and D-gun as well as wire arc are no more negligible.

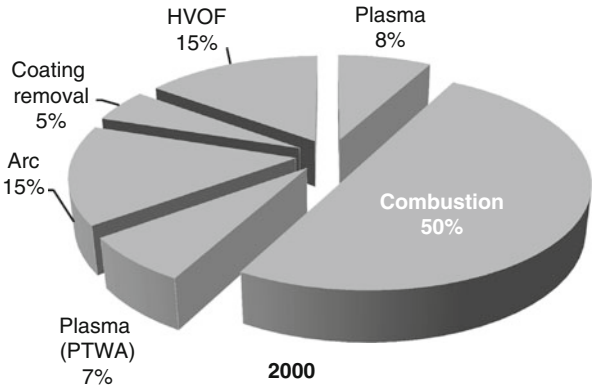

Fig. 18.22 Percentages of the different spray processes in industry in 2000, after M. L. Thorpe, Oral presentation ITSC

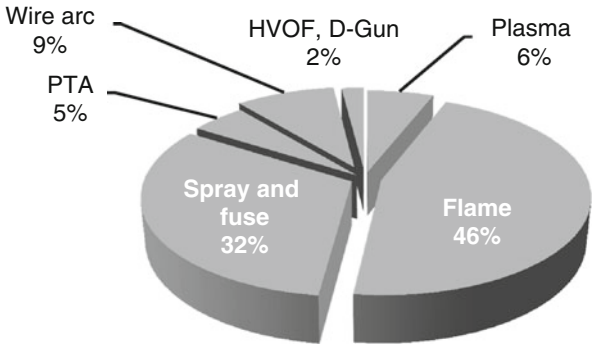

Fig. 18.23 Percentages of the different spray processes in European industry in 1998 after Ducos and Durand. Reprinted with the kind permission of ASM [426]

The distribution of the 615 M€ coating activities in Europe across end-use sectors is presented in Fig. 18.23 from Ducos and Durand [426] (source: MAGETEX study [427]). It can be seen that at the "low end" are mechanical repair and metallic coatings for heavy wear or corrosion protection (including pipes and gas bottles). At the "high end," high value coatings used in aircraft, industrial gas turbines, printing rolls, or medical and dental. In between can be found process industries (primary metals, polymer processing and food, glass, pulp and paper, chemical, oil and gas, textile, . . .), the automotive industry or other OEMs [427] (Fig. 18.24).

Besides new marketing issues of the thermal spray market, the development is linked to a better reproducibility and reliability of substrate surface preparation, spraying, and post-treatment of coatings. Particularly consistent effort has been made in the following areas:

- Better control of surface preparation with a grit residue level as low as possible and a roughness adapted to sprayed particles and a desired grit blasting residual stress level (see Chap. 12).
- Better control of the spray process parameters thanks to computerized control panels (see Chap. 16).

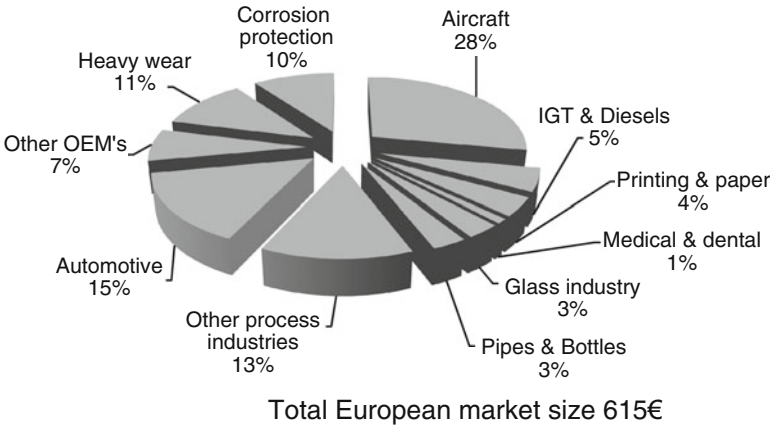

Fig. 18.24 Repartition of the 615 M€ coating activities across end-use sectors in Europe in 1998. Reprinted with the kind permission of ASM [426]

- Development of robust sensors to follow the key parameters of coating manufacturing, i.e., trajectories distribution of hot particles linked to their injection conditions, particle impact velocities and temperatures, coating and substrate temperature, and coating thickness during spraying. For coating and substrate temperature, rather cheap IR and small pyrometers are now available (see Chap. 16).
- More researches about reliable correlations between coating properties and particle impact parameters as well as coating and substrate temperature during spraying, pass thickness, etc., in order to establish feedback control. It is now possible to establish empirical correlations for given spraying conditions and particle parameters at impact, which could be used to keep, with the help of sensors previously described (see Chap. 16), the measured parameters in a "window," resulting in an acceptable coating property.
- Better control of the dust, especially that resulting from the condensation of vaporized material, in the booth and close to the sprayed part.
- Standardization of coating characterization methods that has been started [428].
- Finally, education at all levels that are slowly developed and expert systems need to be created that can help operators and designers.

According to Dorfman and Sharma [359] it is estimated that the TS industry is worth approximately a $6.5 billion with the majority of revenue generation in coating services, see Fig. 18.25a. In terms of market segmentation, approximately 60 % of the total TS market belongs to the turbine industry, 15 % to automotive, and the remaining 25 % is distributed over a large number of other industries, as shown in Fig. 18.25b [359].

Approximately two-thirds of this market is split evenly between North America, Europe, and the Middle East. The balance is from the rest of the world [359]. It is unfortunately difficult to follow the evolution of the industrial spray equipment in

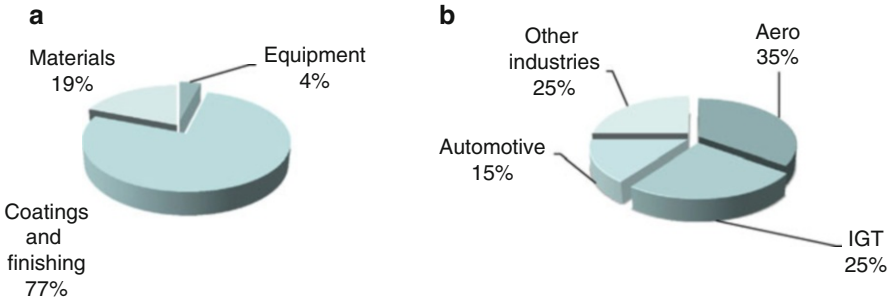

Fig. 18.25 (**a**) Distribution of revenue generation in coating services, (**b**) market segmentation in thermal spray industry. Reprinted with kind permission from Springer Science Business Media [359], copyright © ASM International

the world because few data are published in this field. In connection with the thermal spray conference in 2009 data have been published about thermal spraying in Korea [429], Nordic region of Europe [375], India [430], Japan [431, 432], and also in Asia [433], all these data giving trends about last developments.

Thermal spraying is used widely in many industrial sectors in the Nordic Countries [375]. Important areas where thermal spraying is used are in the manufacture of products for the petroleum, paper, metals, transport, defense, and high-tech machinery industries. In Finland thermal spray technology has wide areas of application in the pulp and paper industries. In Sweden, thermal spray technology is of great importance in the manufacture of aero engines and in industrial gas turbine applications. In Norway thermal spraying is widely used in various offshore applications, including sub-sea oil drilling enterprises. Unfortunately, if the paper indicates that all of the major spray processes are currently used (from flame and arc spraying, to plasma, HVOF and HVAF), depending on the application and type of coating applied, no precision is given about their distribution.

In Japan [431, 432], the growth rate from 2004 to 2006 for the thermal spray industry is estimated to be more than 5 %. Thermal spraying output for fiscal 2004 for the three sectors of the Japanese market were contract job shop productions just under 40 billion Yen, in-house production by large enterprises about 45 billion Yen, and consumables and spray equipment manufacturing 10–15 billion Yen. Figure 18.26 represents the repartition of coating services by job shops in 2004 (total amount of 45 billion Yen) [432]. It is worth noting that the growth rate in the semiconductor/LCD field is very high. Figure 18.27 shows the corresponding distribution among spray processes with the important contribution of APS, HVOF, and the reduction, compared to 2000, of flame-sprayed coatings.

The previous examples were related to countries (Europe, Japan), where research centers and industries have worked on sprayed coatings since the 1970s and 1980s. For countries, which came more recently in the field, the development is also spectacular.

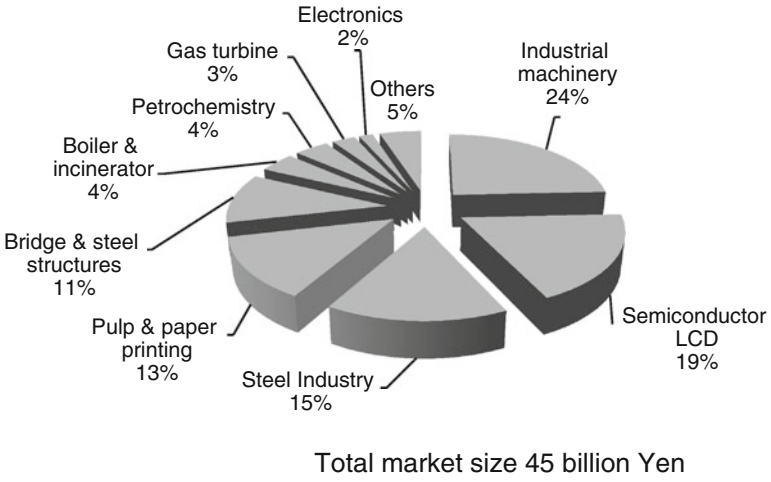

Fig. 18.26 Coating services by job shops in Japan in 2004. Reprinted with kind permission from Springer Science Business Media [432], copyright © ASM International

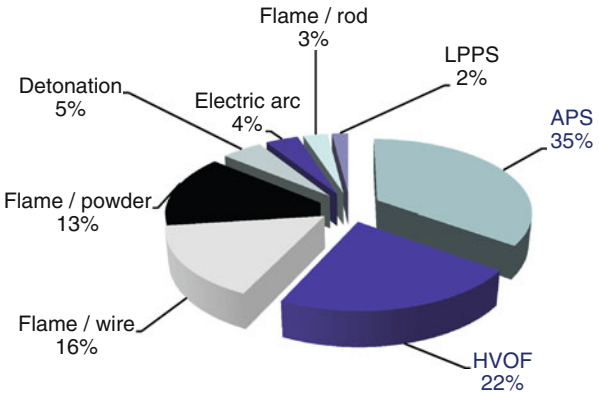

Fig. 18.27 Segmentation of spray process/turnover of contract job shops in fiscal 2004 in Japan. Reprinted with kind permission from Springer Science Business Media [432]. copyright © ASM International

Statistical data [433] show that Chinese applications of plasma spraying are only about 10 % of the total thermal spray market compared with about 50 % in developed countries. According to Li in the paper of Fukumoto [430], the total output of the thermal spray industry in China increased from about US$0.14 billion in 2002 to US$0.24 billion in 2005, representing an annual growth rate of about 20 %. Spray technology has been applied to different industrial fields including steelmaking, textiles, paper and pulp, energy, petroleum and chemicals, aeronautics, and others (Fig. 18.28). The application of thermal spray coatings in the steel industry has been the fastest growing field in the last several years. The energy industry mainly includes coatings for coal-fired power plants and hydro-electric power plants. Applications of thermal spray technology to the aeronautics

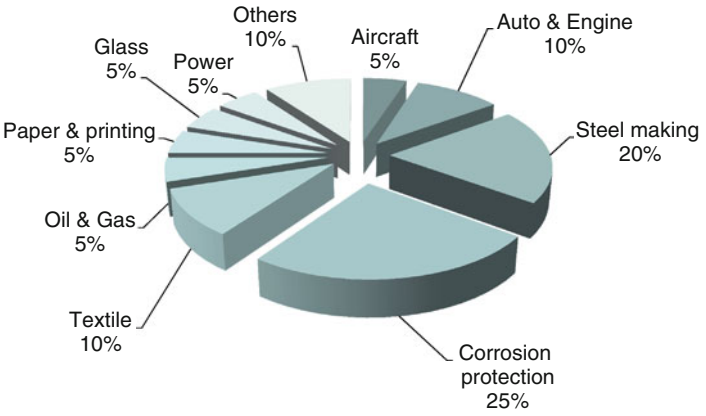

Fig. 18.28 Estimated share of different thermal spray application fields in China. Reprinted with kind permission from Springer Science Business Media [433], copyright © ASM International

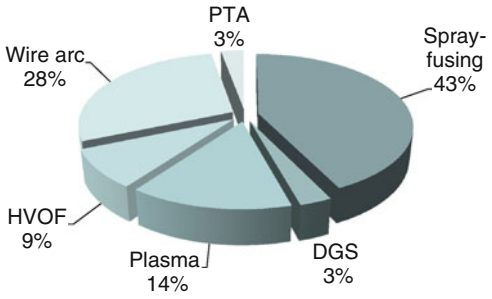

Fig. 18.29 Estimated share of different spray processes in Korea. Reprinted with kind permission of ASM International [429]

industry in China are mainly performed in five large job shops that share 5 % of the total thermal spray output in China. The national program to develop different types of aircraft will promote further fast expansion of R&D and thermal spraying applications in this field. Figure 18.29 shows the distribution among the different spray processes. The plasma spray is about 5 times less than that in other industrial countries. The HVOF market share is probably over the 6 % of Fig. 18.29. Li in the paper of Fukumoto [433] underlines that this figure, compared with those of developed countries, implies the potential for growth in the thermal spray industry in China in the coming decade.

Another country where sprayed coatings are developing is Korea. For example, Fig. 18.30 from Lee [429] gives an idea of estimated share of different spray processes in Korea for the year 2008. As presented in Fig. 18.31 [429], chemical and power plants clearly dominate the market share. Semiconductor and shipbuilding industries also have significant share of the pie. In terms of revenue, semiconductor/LCD, steel making, and power plant industries are the dominant sectors, based on the current fiscal reports, seen in Fig. 18.32.

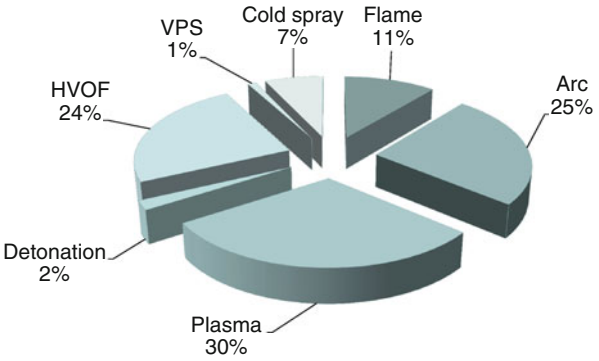

Fig. 18.30 Estimated share of different spray application fields in Korea. Reprinted with kind permission of ASM International [429]

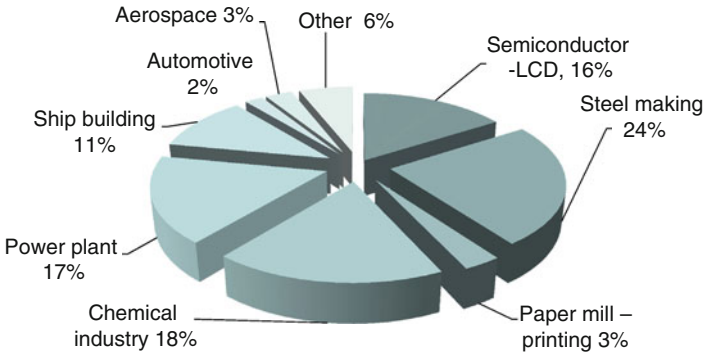

Fig. 18.31 Estimated annual sales of different spray application fields in Korea. Reprinted with kind permission of ASM International [429]

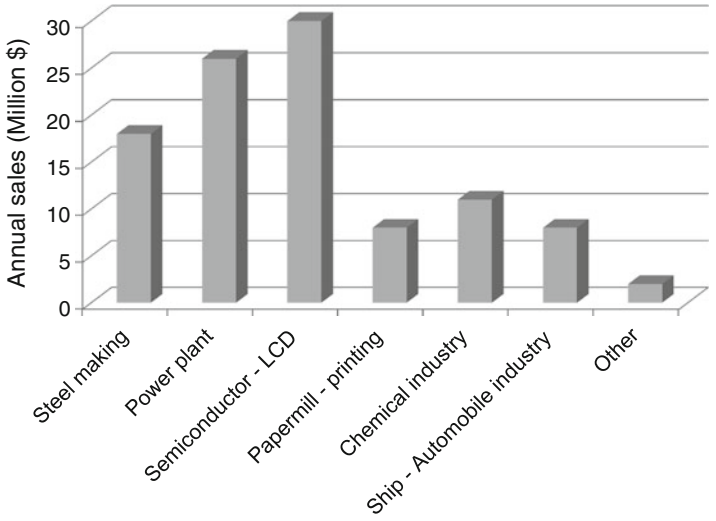

Fig. 18.32 Estimated annual sales of different spray application fields in Korea. Reprinted with kind permission of ASM International [429]

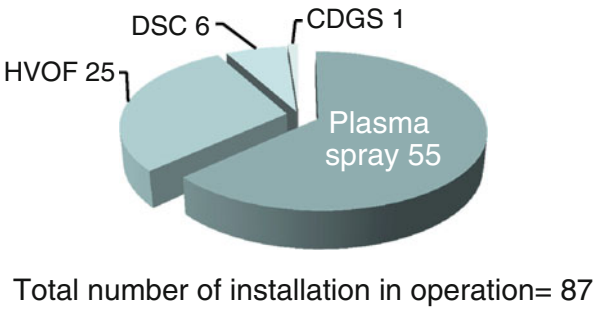

Fig. 18.33 Total number of installations in India by thermal spray variant (excludes flame, arc, and wire spray systems). Reprinted with kind permission of ASM International [430]

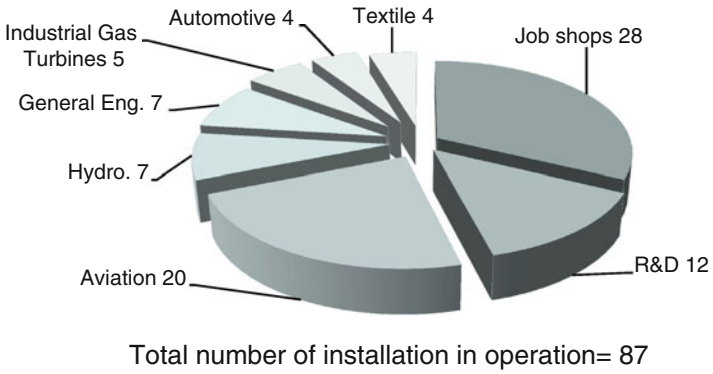

Fig. 18.34 Total number of installations in India by user segment (excludes flame, arc, and wire spray systems). Reprinted with kind permission of ASM International [430]

In India the perceptible change occurred in the 1990s and a good indicator of the success in industry is the growth in sale of spray-grade powder [430] that has been multiplied by a factor 3 between 2000 and 2008. The number of systems, as shown in Fig. 18.33 is still low for country of India's size but it is an important change compared to that prevailed not so long ago. The distribution of the country's thermal spray systems installations among the various segments is presented in Fig. 18.34. The data clearly reveal that the highest number of thermal spray units operate as "job-shops." They play a crucial role both in addressing the needs of a vast majority of industrial users as well as running a crusade to demonstrate "new" applications to the industry and facilitating further growth [430].

To conclude, the coating market is still wide open to (1) protect parts from wear, corrosion, and high heat fluxes; (2) produce parts and manufacture forms and volumes that are difficult or even impossible to obtain using conventional processes; and (3) manufacture parts with complex shapes and material gradients, with associated protection against wear, heat, and other advances challenging operating conditions; and (4) replace hard chrome plating. For example, the automotive industry reveals a wide market with more automated, more reproducible, and less expensive coatings.

18.5 Economic Analysis of the Different Spray Processes

18.5.1 Different Cost Contribution Factors

In spite of its fundamental importance toward the acceptance of a new technology, few papers have been devoted to the economic analysis of thermal spray processes [2, 179, 367, 425–427, 429–436]. This is due to the generally confidential nature of the relevant information in an industrially competitive environment. Moreover, in our rapidly evolving global economy, process economics changes rapidly with time and location. In the context of this book, it is more important to focus on the methodology of carrying out a detailed economic analysis, rather than on the absolute values. These can and will change with time. Emphasis is placed on understanding of the relative importance of the different cost factors in the overall process economics and means of controlling them. Typical examples are provided at the end of this section for the illustration of the methodology and a comparative analysis of the different thermal spray technologies. For a more precise economic analysis, it is best to work with your local provider of thermal spray equipment and materials supplier.

The first step in an overall cost analysis is to identify the different steps of the operation, which can involve a single or multiple process technologies. A typical coating process often involves all or most of the following process steps:

1. Substrate preparation
   - Machining
   - Masking
   - Degreasing
   - Grit blasting
   - Ultrasonic cleaning
2. Coating
   - Part setting up
   - Preheating
   - Coating
   - Online post-treatment (Whenever necessary)
   - Part removal
3. Post-coating operations
   - Off-line post-treatment, annealing, austempering, laser glazing, hot isostatic pressing (whenever necessary)
   - Surface machining, grinding, and polishing
   - De-masking
   - Cleaning
   - Quality control
   - Packing and labeling

The overall cost for the coating for a given part, constitutes essentially of two broad categories of cost contributing factors:

Direct costs (S_{di}); which includes all cost items directly related to each of the different process steps. These depend directly on the complexity of the technology used, the number, size, shape, and complexity of the parts to be coated, and the nature of the coating material. Direct costs are usually calculated on a per hour basis of the operation. Their conversion to cost per part depends on the number of parts that could be produced in 1 h. The principal factors that contribute to the direct cost of a coating operation are

- The cost of material to be sprayed (powder, wires, rods, etc.)
- The cost of gases, electricity, and consumables supplies for the operation
- Direct labor cost for each of the different stages of the operation
- Quality control, packing, and labeling

Indirect costs (S_{in}); often referred to as *fixed cost* or *overhead costs*, include all other expenses, which are related to the investment needed and general running cost of the coating site. The indirect costs factors are usually calculated on a yearly basis of the operation. Their conversion to a per hour basis depends on the number of hours of operation of the coating center per year (N_{hy}). They include, though not limited to, the following:

- Equipment acquisition and amortization of the capital investment
- Building, ancillary equipment, and necessary infrastructure
- Maintenance workshop
- Quality control laboratory
- General administrative and services
- Marketing and financial expenses

The total cost of the coating of a single part is the sum of all direct S_{di}, and indirect S_{in} cost factors, on a per hour basis, multiplied by the number of hours needed per part (N_{hp}).

$$\text{Total cost per part}\,(/\text{part}) = \left[S_{di}(/\text{h}) + S_{in}(/\text{y})/N_{hy}(\text{h/y})\right] \times N_{hp}(\text{h/part}) \tag{18.1}$$

18.5.2 Direct Cost Factors

18.5.2.1 The Cost of Materials

This is often the most important single cost item of the coating operation. It varies widely depending on the nature of the coating material, its purity, and its form. As presented in Chap. 11, coating material are available as powders, wires, cords, or rods depending on the coating technology used. By far the most common form of materials used in coating operations is powders with particle size ranging from 5 to 10 μm up to a few hundred microns in diameter or more. Generally the cost of a powder increases rapidly with the following parameters:

- *The purity level of the material*. For example, a 5N Si powder would cost almost one order of magnitude higher than a 3N Si.
- *Oxygen level*. For example, a grade 1 Titanium powder with an oxygen level lower than 1,200 ppm will cost considerably more than a grade 2 powder of the same particle size but with an oxygen level in the 2,500 ppm or grade 4 with an oxygen level of 4,000 ppm.
- *Particle size distribution*. The narrower the particle size distribution of the powder, the higher will be the cost of the powder on a $/kg basis.
- *Powder morphology*. Generally, spherical, free-flowing dense powders will have a higher cost than a standard spray dried or fused and crushed powder.
- *Specialty alloys* When custom made, with tightly controlled specification of its elemental analysis, the powder will cost considerably more that standard materials.

It is important to underline that these parameters are also interactive between them. For example, a Titanium powder with a particle size $\leq$45 μm and an oxygen content of less than 1,300 ppm (grade 1), will be more difficult to obtain, and would be significantly more expensive, than a Titanium powder with the same oxygen level (grade 1), but a coarser particle size range (45–106 μm). Delivery time and volume of annual consumption can also have a significant influence on the cost of powders. The same reasoning equally applies for other materials in the form of cords, wires, or rods.

The key parameters that influences the quantity of material needed to spray a part are:

- The surface to be coated, A_c, taking into account its shape complexity, its holes distribution that must be protected, and the sprayed material lost at edges.
- The average thickness of the coating, δ_c, (including the mean thickness that has to be removed from the as-sprayed part to achieve the final specified dimensions, sprayed coatings dimensional precision being in the range of tenths of millimeters).

These two quantities, together with the feed stock specific mass, ρ_p, (kg/m^3),

and the deposition efficiency, η_c (%), (which depends strongly on the spray process and the geometry of the part to be coated), allow calculating the powder quantity necessary for each part, m_p (kg),

$$m_p = \frac{\delta_c \cdot A_c \cdot \rho_p}{\eta_c} \tag{18.2}$$

It is important to underline the very important impact of the deposition efficiency on the overall cost of materials in the coating process. This is because overspray powders, which do not end up in the coating, are collected from the exhaust gases or ambient air strictly for environmental reasons, and are never recycled in the coating operation because of the risk of introducing major defects in the coating.

Table 18.2 Investment costs of equipment for spray processes in 2006. Reprinted with the kind permission of Dr. M. Ducos [367]

	Value in Euro (€)	Value in US$
Manual powder or wire flame	About 5,000	About 6,500
Automated powder or wire flame	5,000–10,000	6,500–13,000
HVOF–HVAF	50,000–100,000	65,000–130,000
Arc–spray	9,000–22,500	11,700–29,250
APS	75,000–185,000	97,500–240,500
VPS–CAPS	600,000 to >2 M	780,000 to >2.6M
PTA	50,000–75,000	65,000–97,500

One way of reducing powder waist, and accordingly reduce powder consumption in the spray process, is through automation. For example, if a multi-axis robot handles the arc spray gun, the operation of powder feeder can be synchronized with the robot to stop spraying during substrate transfer or repositioning, thus reducing feed stock losses and coating costs.

18.5.2.2 The Cost of Gases, Electricity, and Consumables

The cost of gases can represent an important component of the cost of the coating operation. This depends significantly on the nature of the gases used, their purity level, and overall volume flow rates required for the coating operation. The unit cost of gases ($/m^3) also depends on the overall size of the operation and the associated gas consumption. For example, the cost for industrial purity argon gas in North America can be more than 5 times higher when in the form of compressed gas cylinders compared to cryogenic form in industrial scale Dewar's. A compilation of typical cost of gases used in thermal spray and cold spray coating operations in North America and Europe is given in Table 18.2. These values are based on 2013 prices and should be adjusted for inflation and price changes in subsequent years. It is important to note that the decision on which size of gas packaging to use is essentially based on the volume of the operation. For example, the use of cryogenic gases, while generally less expensive per m^3 of gas used, can be completely offset by the constant loss factor which has to be bleed to the atmosphere from cryogenic containers for any prolonged period of time in which the gas is not in use. Compressed gas cylinders, or bulk packs, required manual handling and rental fee for the cylinders, which in large volume operation can be important especially if the operation requires a wide range of different specialty gases. Generally, the cost of the gas varies drastically with its consumption and on-site storage linked to the corresponding delivery mode [435] (from cylinder, vehicles delivering liquid gases with different storage volumes and pressures, trailer for He, bulk vehicle).

With cold spray process the gas consumption rate, as illustrated in Fig. 18.35, depends on the process variables, the type of gas, operating pressure and temperature and finally of nozzle internal diameter [435]. The use of Helium in cold spray

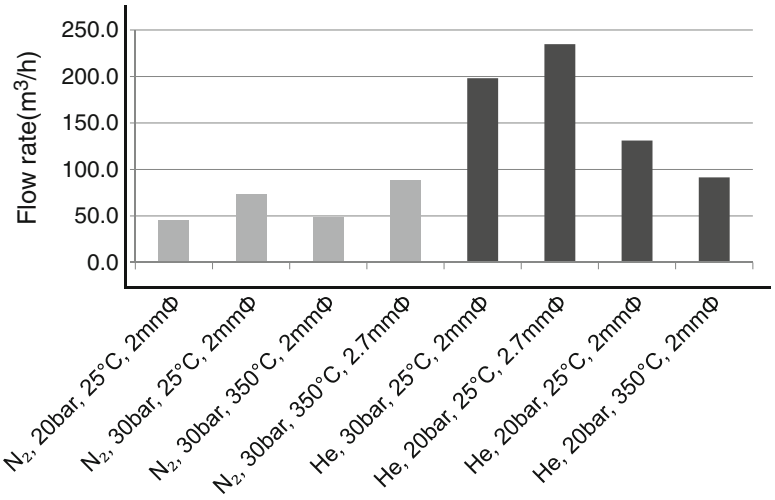

Fig. 18.35 Gas consumption rates for different cold spray systems configurations [435]

requires flow rates that are 4.2 times higher than those for N_2, due to the large difference in sonic velocity. Increasing the gas temperature, on the other hand, allows for the decrease of the gas consumption.

Gas recycling and on-site gas generation are two of the common means of reducing the cost of gases in the coating operation. Gas recycling is generally limited to operation in a closed environment such as in vacuum plasma spraying, whether d.c. or r.f. induction plasma. More recently, gas recycling has been increasingly introduced in cold spray operations, which requires often the use of Helium at relatively large volume flow rates with a significant financial burden on the operation. Gas recycling in this case has to be associated with a gas cleaning and recompression operation. On-site gas generation on the other hand is only used in large volume operation, which justifies the capital investment whether for the generation of oxygen or nitrogen on side through cryogenic distillation or hydrogen through water electrolysis.

The cost of energy, whether in the form of fuels in combustion spraying, or electrical, in plasma spray operations, varies considerably with type of technology used and the scale of operation. A comparison of the power requirement by different spray technologies is given in Fig. 18.36. This shows that HVOF and high-velocity liquid fuel (HVLF) technologies are among the largest energy consumers. This is supplied in this case in the form of liquid or gaseous fuels. Comparative data on the efficiency of different spray processes and the associated specific energy requirement (SER) of different spray processes is given in Figs. 18.37 and 18.38, respectively.

Molz and Hawley [436] have pointed out that the comparison of the effective performance of each process, in relation to each other, is hampered and difficult to compare on an equal basis. Thus they proposed a more generic and global method,

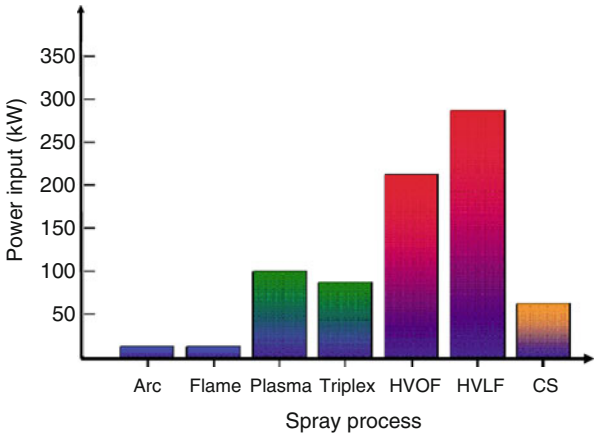

Fig. 18.36 Total power consumption by spray process. Reprinted with kind permission of ASM International [436]

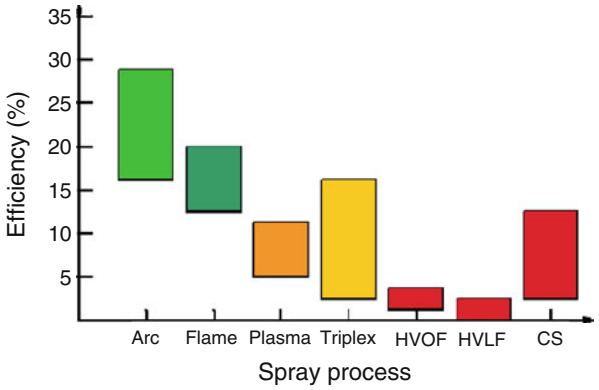

Fig. 18.37 Spray process efficiencies. Reprinted with kind permission of ASM International [436]

based on deriving a unified process efficiency formula that takes into account all energy inputs and energy outputs of a process in the same energy units. They made a direct comparison of process efficiency for each process and specific coating conditions. For example, the energy input to the "system" could either be already included in the supply to the thermal spray gun or created (as in combustion guns) within the gun itself. Two sources exist, one for the gas itself being used (in raw form prior to any reaction) and one for the material input into the system. This illustrated in Fig. 18.36 from Molz and Hawley [436] representing the total energy required (input) for a process. As for each process the total range of input energy is large, they have plotted the range of energies instead of the maximum amount of energy consumed. As it could have been expected, flame and wire arc spraying exhibit the lowest energy consumptions. Figure 18.37 from Molz and Hawley [436] represents the process efficiency for each thermal spray process based on the measured power output in terms of particle temperatures and velocities. The drawback of these calculations is that they are based on the particle temperature measured assuming that it is representative of the total thermal energy

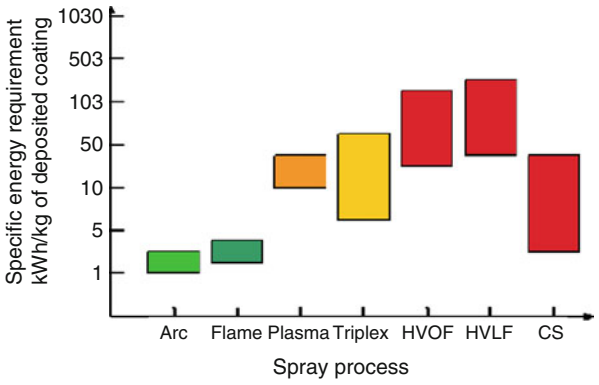

Fig. 18.38 Energy ranges to deposit 1 kg of coating for different spray processes. Reprinted with kind permission of ASM International [436]

state of the particle. However, Fig. 18.37 shows that arc has the highest efficiency, but still barely manages to achieve 30 % efficiency at the best operating parameters. The difference between arc and combustion is the lower efficiency derived from using a combustion process. HVOF processes have the lowest efficiency (in the 2 % range). The third figure (Fig. 18.38) of Molz and Hawley [436] represents the energy consumed per kg of coating deposited. The scaling in Fig. 18.38 is now logarithmic in order to fit the entire range of values in. The typical high velocity coatings such as carbides, with lower deposit efficiency and higher energy input, require considerably more energy to deposit per unit mass, almost one order of magnitude higher than that to spray pure ceramics or metals.

Electric energy-based technologies such as plasma and arcs, uses typically industrial electricity rates which are composed of two components:

- *Power* (*kW*), which is set by an annual agreement with the electric energy utilities reflecting the overall size of the operation and its peak energy demand.
- *Energy* (*kWh*) is the electrical energy consumption by the operation for running the plasma system as well as all of the ancillary equipment.

Electricity cost for building illumination, heating, and other operations is not included under direct cost of the operation. These constitute part of the indirect costs. Electricity rates vary widely between locations and period of operation over the range $0.09–0.15/kWh.

The cost of consumables and spare parts also varies widely with the nature of the spray process and the complexity of the part. For example, in d.c. plasma spraying operation whether atmospheric or under vacuum, a close monitoring of the state of the electrodes is essential for insuring a consistent quality of the coating. Generally, the allowed life of the electrodes is based on the recommendations of the equipment manufacturer and/or the operator experience. It is generally accepted practice to replace consumable parts in a setup after a well-defined lifetime, rather than wait for a disruption of the operation and a failure of the quality of the coating. It has to be recognized that the cost of a failed coating is not limited to the loss of the coating martial and associated labor and expenses, but also the damage caused to the part

being coated, which can be order of magnitude higher than that of the coating operation itself. The cost of consumables is not limited to torch components; it can also include certain important components of the plasma generating equipment. In induction plasma spraying, for example, the r.f. power supply has a triode tube which need to be replaced depending on its projected lifetime, which can be in the 10,000–20,000 h. The triode life also depends on the mode of operation and the number of starts and stops per hour of unit. In a 100 kW installation, the cost of such a components can be in the US$15,000–20,000 range.

The cost of consumables also includes the cost of masking tapes used to protect the surface which should not be exposed to sand blasting or coating, the cost of the grit, used in the sand blasting operation prior to coating, and cost of grinding and polishing materials and supplies used for surface finishing of the part.

18.5.2.3 Direct Labor Cost

In thermal spray operations, direct labor cost is inversely proportional to the degree of automation of the operation. The higher is the level of automation and the larger is the scale of the operation; the lower will be the direct cost of labor per part. In a typical coating operation direct labor is needed for:

- Preparation of the part to be coated, including its, masking, sandblasting, and cleaning
- Setting up of the part in the coating booth. Starting of the operation, preheating, and coating, followed by removal of the part from the rig
- Cleaning of the part, surface machining, grinding, and polishing
- De-masking and cleaning
- Quality control
- Packing and labeling

The total cost of labor for the coating operation is also relatively sensitive to the overall management of the facility and the efficient definition of the operation steps and the definition of responsibilities.

18.5.2.4 Direct Cost for Quality Control, Packing, and Labeling

This depends on the maturity of the technology used for the coating operation and on the nature of the parts to be coated. The most stringent quality control rules are generally applied for medical and aerospace applications, where very rigorous quality control (QC) procedures are needed and have to be strictly in forced. Other applications, with generally lower value items, such as in automobile industry, quality control on individual parts would be too expensive. The industry has to rely in this case on well-developed, mature, and reliable technologies.

The overall cost of quality control includes direct and indirect cost factors. Basic investment in QC in instrumentation and laboratory equipment will go under

indirect cost, while the labor cost associated with the QC procedures will go under *direct cost* and will depend on whether it is applied on all of the coated parts or on randomly selected parts. For obvious reasons, QC procedures tend to use nondestructive testing as much as possible in order to avoid sacrificing the part being tested. In the development stage of a new part, both nondestructive and destructive testing procedures are generally needed.

18.5.3 Indirect or Fixed Cost Factors

18.5.3.1 Capital Investments

This covers the total investment needed for the setting up of the operation. It includes

- Cost of land, building, and building permits including environmental studies necessary for the setting up of the operation
- Ancillary equipments and infrastructure including spray booth, dust collection and disposal, air cleaners, sound control, operator safety equipment
- Production equipment including spray system and associated operations, instrumentation, and data acquisition
- Equipments for post-treatment and finishing including heat treatment furnaces, laser glazing, hot isostatic pressing, machining, grinding and polishing equipments
- Maintenance workshop
- Quality control laboratory
- Storage space for materials, supplies, spare parts, and finished part
- Office space

Direct investment for the acquisition of the coating production equipments rarely exceeds 15–20 % of the total investment needed for the setting up of a new production facility. The investment structure needed for the expansion of an existing facility can be different with a considerably higher percentage needed for the acquisition of the production equipment.

Capital investment contributes to indirect production cost through the amortization of the investment made. It is important to note that the amortization rules vary from country to country as well as between the different types of investments. For example, investments for the building and infrastructure is generally depreciated over a 25-year period, production equipment, over a 5–7-year period, while computer and automation equipments may need to be amortized over a 3–5-year period due to the rapid evolution of the technology. The simplest method of calculating amortization cost per hour of operation, S_{ih}, is based on a linear amortization over the number of year over which the equipment is depreciated, N_y, divided by the number of operating hours per year, N_{hy}, as follows:

Table 18.3 Investment costs of ancillary equipments in 2006. Reprinted with the kind permission of Dr. M. Ducos [367]

	Value in Euro (€)	Value in US$
Grit blasting	10,000–40,000	13,000–52,000
Linear movements	35,000–75,000	45,500–97,5000
Robot	75,000–150,000	97,500–195,000
Spray booth	12,000–25,000	15,600–32,500
Ventilation and filtering	30,000–45,000	39,000–58,500
Machining and grinding	200,000–1M	260,000–1.3M
Quality control	75,000–200,000	97,500–260,000

$$S_{\mathrm{ih}} = \frac{P_{\mathrm{e}}}{N_{\mathrm{y}} \times N_{\mathrm{hy}}}, \tag{18.3}$$

where P_{e} is the cost of the equipment. For more information on investment cost calculation, the interested reader can see the paper of de Munter et al. [431]. Typical investment costs estimates for coating equipments and ancillary equipments are given in Tables 18.3 and 18.4, respectively, based on a study by Magetex [427] and presented by Ducos [367]. These were compiled in 2006.

18.5.3.2 Other Indirect or Fixed Costs

These include essentially the cost of general administration and services, insurances, marketing, and financial services. These are strongly dependent on the scale of the operation and its location.

18.5.4 Few Examples

18.5.4.1 Cost of d.c. Plasma Spraying of Partially Yttria-Stabilized Zirconia

To illustrate the relative importance of each of these cost factors, de Botton [425] in his master of science, calculated the costs for d.c. plasma spraying of partially yttria-stabilized zirconia (PYSZ) coatings on a flat 1 m^2 surface. The coating thickness was 300 μm. The spray rate was 3 kg/h, with a deposition efficiency of 60 % and a coating density of 0.9. Losses at holes and edges were assumed to be of 10 %.

For the costs calculation he assumed 5 years to recover investment, a capital cost of 10 %, a maintenance cost of 4 %, 250 production days, and a total productive time per year of 4,000 h. Results are summarized in Figs. 18.39 and 18.40 which represent the different factor of prices per sprayed part. It is obvious from this figure

Table 18.4 Evaluation of the NiCrAlY coating cost for Plazjet and arc spray processes. Reprinted with kind permission from Springer Science Business Media, copyright © ASM International [437]

	Plazjet	Arc Jet 9000 (N2)	Arc Jet 9000 (Air)
System cost (US$)	198,000	3,800	23,800
Amortization time (years)	5	5	5
Material feed rate (kg/h)	12	12	12
Spraying time per year (h)	278	278	278
Amortization (US$/kg of coating)	19.83	2.38	2.38
NiCrAlY powder and wire (US$/kg)	90	63	63
Powder cost (US$/kg of coating)	1.26	0.11	0.11
Electric power (kW)	115	10	10
Electric energy cost per (US$/100 kWh)	7.90	7.90	7.90
Energy cost US$/kg of coating	1.26	0.11	0.11
Plasma and atomization gas flow rates (m^3/h)	9.6	105	65
Gas cost (US$/100 m^3)	3.40	3.40	0.50
Gas consumption (m^3/year)	2,670	29,200	18,000
Electrodes and tips costs (US$)	635	6	6
Electrodes and tips lifetime (h)	12	6	6
Consumable cost US$/kg of coating	7.39	0.63	0.18
Production cost US$/kg of coating	162.10	154.80	107.30
Labor cost US$/kg of coating	8.45	8.45	8.45
Production cost without amortization US$/kg	158.65	105.74	105.29
Total production cost US$/kg of coating	178.48	108.12	107.67

[a]The production cost was calculated per kilogram of coating at a deposition rate of 12 kg/h and a deposition efficiency of 60 %. The total production was set to 2 tons per year. Coatings were sprayed without substrate cooling

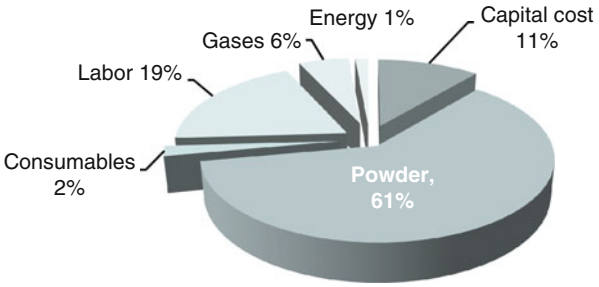

Fig. 18.39 Spray costs distribution of YPSZ coatings. Reprinted with the kind permission of MIT [425]

that the most important one is the powder, followed by labor (automation can reduce it notably) and capital cost. Figure 18.40 shows that after the coating cost (81.9 %), the grinding process is the most important (11.5 %) followed by the surface preparation (4.4 %). The quality control and storage represent only 2.1 %.

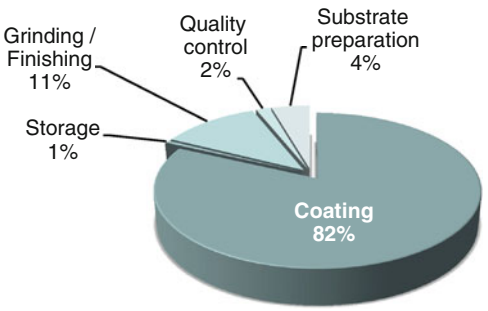

Fig. 18.40 Total costs distribution of YPSZ coatings. Reprinted with the kind permission of MIT [425]

Table 18.5 Different costs for manually wire arc-spraying zinc on 1 m^2 of steel. Reprinted with kind permission of Dr. M. Ducos [367]

Thickness	120 µm
Labor	40 €/h
Zn wire	2 €/h
Amortizing	3 y and 1.200 h/y
Surface preparation	7.3 €
Spraying (air atomization)	6.9 €
Amortizing	1.0 €
Total	15.2 €/m^2

18.5.4.2 MCrAlY Coatings Sprayed by Arc Spray and High-Power Plasma Spraying

In the work of Sacriste et al. [437] the bond coat of TBCs was deposited on large-sized substrates and used under given working conditions: vacuum and corrosion by hot liquids but with no thermal cycling. As the thickness of the topcoat was limited to 200 µm for this application, the roughness of the bond coat must also be low (*Ra* must be less than 10 µm). The substrate was a nickel-based super alloy, with a surface area of 100 × 50 mm^2 and a thickness of 2 mm. For deposition, the following setups were used to deposit the bond coat:

- The TAFA PlazJet gun model 7070 equipped with a 120-mm long anode and working with a mixture of nitrogen and hydrogen, the powder being injected at feed rates up to 12 kg/h.
- The twin-wire arc spray system used in this study was a TAFA model Arc Jet 9000. Wires were fed with the push–pull system capable to work with wires and cored wires 7.50 m in length. The NiCrAlY material was available as cored wire with a NiCr envelope containing particles of Al, Cr, and Y. Air and nitrogen were used as atomization gases with different air caps. After optimization of the spray conditions, Table 18.5 summarizes the different costs of the three coatings.

According to Sacriste et al. [437], coatings obtained by arc spraying exhibited a higher surface roughness due to a relatively low particle velocity compared to that obtained with the Plazjet process. The deposition efficiency was the same as that obtained with the Plazjet gun, for both air and nitrogen atomizing gas. The

Table 18.6 Spray conditions and costs of APS- and WA-Sprayed NiAl (5 wt%) 1.8 mm thick coatings for aeronautic application. Reprinted with kind permission of Dr. M. Ducos [367]

	Air plasma sprayed	Wire arc sprayed
Deposition rate (kg/h)	2.5	11.2
Deposition efficiency (%)	60	70
Material costs (€/kg)	35 (powder)	45 (wire)
Spray time (h)	2.93	0.56
Material used (kg)	7.33	6.29
Replacement parts (€)	13.49	0.45
Gases and electricity (€)	30.26	1.4

use of nitrogen atomization resulted in a 10 wt% reduction of the oxygen content, but no changes were observed in the bond strength (higher than 40 MPa). The composition of the arc-sprayed NiCrAlY coatings was very heterogeneous, which was attributed to the wire manufacturing method.

Considering only the costs of these coatings [437], Table 18.5 shows that the arc spray process, using air or nitrogen atomization, is about 40 % less expensive than the Plazjet process. As with the majority of spraying systems, the material feed stock is the most expensive parameter for both systems. In this study, it represents about 84 % of the total coating price for Plazjet and 97 % for arc spraying, while, since the deposition rate is high, the labor cost represents less than 5 % for Plazjet and of the order of 7 % for arc spraying. The major cost point of the Plazjet system is its purchasing cost. It represents 11 % of total production cost, whereas it is about 2 % for the arc spray system. The difference in the electric power shows that arc spraying is more thermally efficient than plasma spraying, as it requires a power of 10 kW to spray 12 kg of NiCrAlY material per hour, whereas Plazjet needs, at least, 110 kW.

18.5.4.3 Manual Wire Flame Zn Coating per Square Meter

According to Ducos [367] and calculations of MAGETEX [427] the different costs for manually wire arc-spraying zinc on 1 m^2 of steel are summarized in Table 18.6.

With this spray process, which is the cheapest, the surface preparation becomes slightly more important than the spray cost. According also to the low investment cost, amortizing is rather low as already emphasized in Table 18.6 for wire arc spraying.

18.5.4.4 Cost Comparison Between APS and Wire Arc for NiAl (Aeronautic)

Ducos [367] has evaluated the cost of a NiAl coating 1.8 mm thick for aeronautic application plasma (APS) and wire arc (WA) sprayed. Coatings are performed with robotized setups according to conditions and costs summarized in Table 18.7.

Table 18.7 Thermal processes used by various industrial segments. Reprinted with the kind permission of SPRAYTIME a publication of the International Thermal Spray Association, a standing committee of the American Welding Society [439]

Industry	Oxy-fuel	Spray/fuse	HVOF	D-gun	Air Plasma	Vac-plasma	Shroud Plasma
Aero gas turbine	✓		✓	✓	✓	✓	✓
Stationary gas turbine	✓		✓	✓	✓	✓	
Hydro-steam turbine	✓		✓	✓	✓	✓	✓
Automotive engines	✓		✓		✓		
Diesel engines	✓		✓		✓		
Transportation non-engine	✓			✓	✓		
Agriculture implementations	✓	✓			✓		
Railroad	✓		✓		✓		
Iron and steel manufacture	✓	✓			✓		
Steel rolling mills	✓	✓	✓		✓		
Iron and steel casting			✓		✓		
Forging	✓		✓				
Copper and brass mills	✓						
Ship and boat manufacture and repair	✓						
Oil and gas exploration	✓	✓	✓	✓	✓		
Mining, construction, and dredging	✓	✓	✓		✓		
Rock products	✓	✓	✓		✓		
Screening							
Cement and structural clay	✓	✓	✓				
Chemical processing	✓	✓	✓	✓	✓		
Rubber and plastic manufacture	✓	✓	✓		✓		
Textile	✓		✓	✓	✓		
Food processing	✓	✓	✓	✓	✓		
Electrical utilities			✓		✓		
Pulp and paper	✓		✓		✓		
Printing equipment			✓	✓	✓		
Defense and aerospace	✓		✓	✓	✓	✓	
Nuclear			✓	✓	✓		
Medical			✓	✓	✓	✓	✓
Business equipment			✓	✓	✓		
Electrical and electronic			✓	✓	✓	✓	
Architectural	✓	✓			✓		
Glass manufacture		✓		✓	✓		

Figure 18.41 presents the costs distribution of the different items of the spray process for APS. It can be seen, as for YPSZ coatings (see Sect. 18.5.4.1), the most important cost factor is the powder (51 %) followed by the investment amortization (22 %) and labor (18 %). Gases electricity and replacement parts represent only 9 %. The distribution of other costs (surface preparation, grit blasting and cleaning,

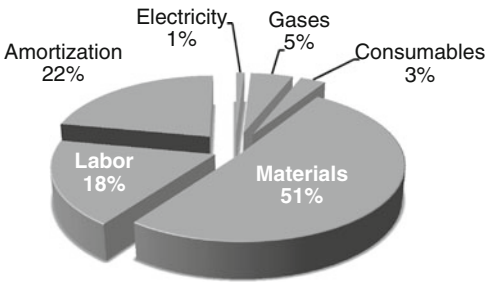

Fig. 18.41 Distribution of spray costs for a 1.8 mm thick NiAl (5 wt%) coating plasma sprayed in air. Reprinted with kind permission of Dr. M. Ducos [367]

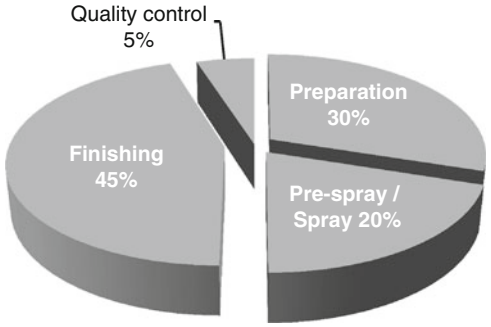

Fig. 18.42 Distribution of pre- and post-spray costs for a 1.8 mm thick NiAl (5 wt%) coating plasma sprayed in air. Reprinted with kind permission of Dr. M. Ducos [367]

finishing, and quality control) is presented in Fig. 18.42. It can represent 50–80 % of the spray costs.

Finally Fig. 18.43 represents the cost distribution per sprayed hour for the APS and WA coatings. The WA coating cost per hour is about 60 % of that of the APS coating that is mainly due to the investment and labor costs.

18.5.4.5 Cost Comparison for Hard Chromium Replacement on a Jack

Based on same principles, Ducos [426] calculated the costs per m^2 of Al_2O_3–TiO_2 (13 wt%) APS sprayed, WC–Co HVOF sprayed, and NiCrBSi HVOF sprayed to replace electrolytic hard chromium. Results are presented in Fig. 18.44. They show that the cheapest coating is that of NiCrBSi HVOF sprayed, but its cost (21.6 €) is higher than that of hard chromium (18 €), followed by the ceramic coating plasma sprayed in air, but to which the cost of the bond coat must be added (46.6 + 20 = 66.6 €) and then by the WC–Co HVOF-sprayed coating (122.5 €), which is essentially due to the powder cost.

Coating price is linked to many parameters and in any application it must be compared to the money saved by reducing wear, corrosion, . . . and improving the lifetime of the part. Its competitiveness is generally very good when used to repair. Anyhow, as shown in the examples presented, besides the main cost that is that of

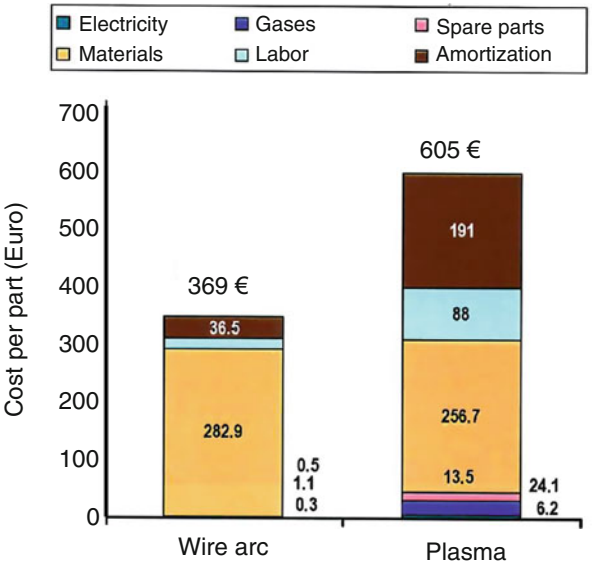

Fig. 18.43 Comparison of the cost per part of 1.8 mm thick NiAl (5 wt%) coatings plasma sprayed in air or wire arc sprayed. Reprinted with kind permission of Dr. M. Ducos [367]

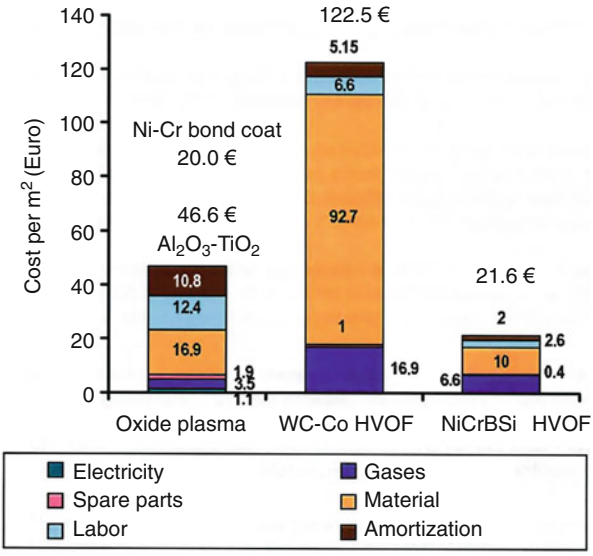

Fig. 18.44 Comparison of the costs per m^2 of Al_2O_3–TiO_2 (13 wt%) APS sprayed, WC–Co HVOF sprayed, NiCrBSi HVOF sprayed to replace hard chromium. Reprinted with kind permission of ASM International [426]

powder or wire or rod or cord, the amortization of the spray process can become very important when comparing flame or wire arc spraying to other processes (plasma, HVOF, ...) and, of course, when considering VPS this item becomes drastically important (see Table 18.3).

18.6 Summary and Conclusions

Moign et al. [438] have tried evaluating the comparison of life cycle assessment (LCA) of electroplating and various thermal spray processes (plasma, twin-wire arc, HVOF, and cold spraying) for the formation of nickel coatings. According to the number of parameters that can affect the final result, it is not an easy task. Comparing damages to human health and resources is that thermal spraying processes have a similar impact, while electroplating exhibits a lower impact when alumina for grit blasting is recycled two times. These results show that the nickel production process and also the alumina production for grit blasting have the largest impact, in comparison to energy production and other processes used during the coating step itself. The electroplating process can also be highly pollutant in countries that do not apply stringent environmental regulations on air and water emissions. Moreover, to be more realistic, the environmental impact of nickel electroplating processes should incorporate the environmental impacts of the production of the chemicals used in this process.

Thermal-sprayed coatings, including cold spray are more and more used in industry because of the following advantages:

- They provide specific properties onto substrates which properties are very different from those of the sprayed coating.
- They can be applied with rather low or no heat input to substrates (allowing for example spraying ceramics onto polymer substrates).
- Virtually any material that melts without decomposing or vaporizing can be sprayed. Moreover when preparing powders or wires for spraying it is possible to achieve cermets, very complex metal or ceramic mixtures, opening new possibilities to obtain very sophisticated coatings that can be tailored to the wished service property.
- Sprayed coatings can be stripped off and the worn or damaged coatings can be recoated without changing part properties and dimensions.
- Some spray processes can be moved on site, allowing spraying rapidly big parts, which displacement would otherwise be rather long and expensive.

Of course these coatings have also drawbacks such as:

- They are a line of sight technology, for example, making impossible coating small and deep cavities.
- Most of them have lamellar structures with contacts between layered splats that, depending on spray conditions, represent between 15 and 60 % of the splat surfaces.
- They have pores, cracks, ... that can be connected, depending on the spray process chosen and spray conditions, and that must be sealed for certain applications.

Of course the choice of a spray process, in connection with the sprayed material, depends on the specific properties expected from the coating on the one hand and on the cost of the coating also linked to the process and to the sprayed material. For example, spraying platinum or nickel alloy with the same process makes a huge difference in the coating cost for the same surface and thickness.

Finally the following tables prepared by the International Thermal Spray Association [436] summarize the different processes used in industry (Table 18.8), the coating application according to industry served (Table 18.9), and materials sprayed in industry. Unfortunately, these tables give no information about the industrial use of cold spray coatings, which is probably due to the fact that this process has been introduced at the end of the 1980s. Even in the recent book about cold spray [7] published in 2007 very few information is given about the industrial use.

Appendix: Use of the Different Spray Materials

In this appendix only basic information about the main sprayed materials and the most frequently sprayed materials are presented. For more detailed information the reader must consult the different powder and wire suppliers. It must also be kept in mind that the coating resulting from the spray process has properties (thermal and electrical conductivities for example) different from those of powder or wire properties. Such differences result from the increase of the oxide content, the pores generated during spraying, the real contacts between layered splats, ... Properties also depend on the way the sprayed material has been manufactured. In the following X-20Y-10Z means 20 wt% of Y, 10 wt% of Z, the balance being X.

A.1 Metals

Aluminum Al (99 wt%) $T_m = 660$ °C:

- Good corrosion resistance in industrial atmospheric conditions
- Good electrical and thermal conductivity
- Soft and ductile → repair Al alloys
- Non-magnetic (electromagnetic shielding)
- Sprayed by flame (powder or wire), wire arc, plasma, and cold spray

Aluminum base Al–Si (95/5 or 12 wt%)

- Salvage of parts made of Al, Mg, and their alloys: excellent finish
- Sprayed by flame (powder or wire), wire arc, plasma, and cold spray

Table 18.8 Thermal spray processes used by various industrial segments. Reprinted with the kind permission of SPRAYTIME a publication of the International Thermal Spray Association, a standing committee of the American Welding Society [439]

Industry	Wear							Clearance Control			Corross/	Electrical	
	Abrasive	Adhesive	Fretting	Erosion	Cavitation	Impact	TBC	Abradable	Abrasive	Restoration	Oxidat	Resistance	Conduct
Aero gas turbine	✓	✓	✓	✓			✓	✓	✓	✓	✓		
Stationary gas turbine	✓	✓	✓	✓			✓	✓	✓	✓	✓		
Hydro-steam turbine	✓	✓	✓	✓	✓					✓	✓		
Automotive engines	✓	✓		✓		✓	✓	✓	✓	✓	✓	✓	
Diesel engines	✓	✓		✓		✓	✓			✓	✓		
Transportation non-engine	✓	✓					✓			✓	✓	✓	
Agriculture implementations	✓			✓		✓				✓			
Railroad	✓	✓				✓				✓	✓		✓
Iron and steel manufacture	✓			✓		✓				✓	✓		
Steel rolling mills	✓	✓				✓				✓	✓		
Iron and steel casting	✓			✓		✓				✓	✓		
Forging	✓	✓				✓				✓	✓		
Copper and brass mills	✓									✓	✓		
Ship and boat manufacture/repair	✓			✓						✓	✓		
Oil and gas exploration	✓	✓		✓		✓				✓	✓		

(continued)

Table 18.8 (continued)

Industry	Wear							Clearance Control			Corross/	Electrical	
	Abrasive	Adhesive	Fretting	Erosion	Cavitation	Impact	TBC	Abradable	Abrasive	Restoration	Oxidat	Resistance	Conduct
Mining, construction, and dredging	✓			✓	✓	✓				✓	✓		
Rock products	✓					✓				✓	✓		
Screening	✓					✓				✓	✓		
Cement and structural clay	✓					✓				✓	✓		
Chemical processing	✓			✓						✓	✓		
Rubber and plastic manufacture	✓			✓		✓				✓	✓		
Textile	✓									✓			
Food processing	✓									✓			
Electrical utilities	✓	✓		✓	✓	✓				✓	✓		
Pulp and paper	✓				✓	✓				✓	✓		
Printing equipment	✓	✓								✓			
Defense and aerospace	✓	✓	✓	✓	✓	✓	✓			✓			
Nuclear											✓		
Medical	✓		✓								✓		
Business equipment	✓	✓	✓										
Electrical and electronic										✓	✓		
Architectural	✓					✓							
Glass manufacture	✓	✓								✓	✓		

Table 18.9 Thermal spray-coating applications according to industry served. Reprinted with the kind permission of SPRAYTIME a publication of the International Thermal Spray Association, a standing committee of the American Welding Society [439]

Industry	Chrome carbide	Self-fluxing	Iron and Steel	Nickel alloys	Superalloys	MCrAlY	Cobalt alloys	Non-ferrous
Aero gas turbine	✓		✓	✓	✓	✓	✓	✓
Stationary gas turbine	✓		✓	✓	✓	✓	✓	✓
Hydro-steam turbine	✓	✓	✓	✓	✓		✓	✓
Automotive engines	✓			✓	✓	✓	✓	
Diesel engines	✓		✓	✓	✓	✓	✓	
Transportation non-Engine			✓	✓				✓
Agriculture implementations		✓	✓	✓				✓
Railroad		✓	✓	✓				✓
Iron and steel manufacture		✓	✓	✓	✓		✓	✓
Steel rolling mills		✓	✓	✓	✓		✓	✓
Iron and steel casting		✓	✓					✓
Forging		✓	✓	✓	✓		✓	
Copper and brass mills							✓	
Ship and boat manufacture/repair			✓	✓				✓
Oil and gas exploration		✓	✓	✓			✓	✓
Mining, construction, and dredging		✓	✓					✓
Rock products		✓	✓					✓
Screaming			✓					
Cement and structural clay		✓	✓					✓
Chemical processing			✓	✓	✓		✓	
Rubber and plastic manufacture		✓	✓	✓			✓	
Textile			✓					
Food processing		✓	✓					
Electrical utilities		✓	✓	✓			✓	✓
Pulp and paper		✓	✓	✓				✓

(continued)

Table 18.9 (continued)

Industry	Chrome carbide	Self-fluxing	Iron and Steel	Nickel alloys	Superalloys	MCrAlY	Cobalt alloys	Non-ferrous
Printing equipment								✓
Defense and aerospace	✓	✓	✓	✓	✓	✓	✓	✓
Nuclear								
Medical								✓
Business equipment								✓
Electrical and electronic								✓
Architectural	✓							✓
Glass manufacture	✓	✓	✓					

Cobalt based powders (Pure cobalt $T_m = 1{,}495$ °C):

- Stellite® (Co–xCr–yW–zC)
- Against galling, cavitation
- For metal friction, high angle erosion, high temperature hardness, good resistance to abrasion, rather good wettability
- Very good oxidation resistance
- Replace WC in high temperature applications
- Repair of Cobalt-based parts
- Sprayed by HVOF, flame, PTA, Plasma

Triballoy® (Co–xCr–yMo–zSi) or (Co–xCr–yMo–zSi–tNi)

- Against galling for metal to metal friction
- High temperature hardness
- Good resistance to corrosion and oxidation
- Very good wear properties from room temperature to 860 °C
- Sprayed by HVOF, flame, PTA, Plasma

Co–25.5Cr–10.5Ni–7.5W–0.5C

- High abrasive, sliding fretting and cavitation wear resistance up to 800–850 °C
- Good oxidation resistance
- Behave well between 540 and 840 °C
- Sprayed by HVOF, flame, PTA, plasma

Co–28Mo–8Cr–2Si

- Up to 760 °C low coefficient of friction
- Good corrosion resistance
- Sprayed by HVOF, flame, PTA, plasma

Co–28Mo–17Cr–3Si

- Excellent sliding wears resistance
- Good hot corrosion resistance and moderate oxidation resistance up to 800 °C
- Sprayed by HVOF, flame, PTA, plasma

Copper Cu (99 wt%) ($T_m = 1{,}084$ °C)

- Very good electrical and thermal conductivities
- Good resistance to inks (paper and printing)
- Used to repair Cu base alloys
- Non-magnetic (electromagnetic shielding)
- Sprayed by flame (powder or wire), wire arc, plasma, HVOF, and cold spray

Copper-based powder: Cu–36Ni–5In ($T_m = 1{,}150\ ^\circ C$):

- Very dense coatings with good resistance to galling and fretting
- Sprayed by flame (powder or wire), wire arc, plasma, HVOF, and cold spray

Aluminum Bronze Cu–9.5Al–1Fe:

- For pumps (against cavitation)
- Piston guides (soft bearing surfaces)
- Shifter forks and compressor air seals (friction)
- Strength and hardness twice that of other bronzes
- Sprayed by flame (powder or wire), wire arc, plasma, HVOF, and cold spray

Supra bronze: Cu–40Zn–0.8Sn–0.75Fe–0.24Mn

- For metallizing work
- Sprayed by flame (powder or wire), wire arc, plasma, HVOF, and cold spray

Iron-based powders (Pure iron $T_m = 1{,}538\ ^\circ C$)

Low carbon steels (C $<$ 0.25 wt%):

- An inexpensive low carbon steel powder
- Corrosion resistant $\rightarrow$ repair + good wear resistance in lubricated service
- May contain martensitic phases
- Produces machinable coatings
- Sprayed by flame, wire arc, plasma, HVOF, and cold spray

High carbon steels (C $>$ 0.8 wt%)

- Reclamation
- Wear and erosion resistance
- Sprayed by flame, wire arc, plasma, HVOF

Stainless steels (SS) Fe-13 or 14Cr–1Ni:

- Good resistance to wear and corrosion
- Best all purpose (SS)
- Sprayed by flame, wire arc, plasma, HVOF

Stainless steels (SS) Fe–18Cr–8Mg–5Ni:

- Reclamation
- Corrosion protection
- Low shrinkage and good machinability
- Sprayed by flame, wire arc, plasma, HVOF

Stainless steels (SS) Fe–17Cr–12NI–2.5Mo–1Si–0.1C (ASI 316):

- Corrosion protection
- Dimensional restoration

– Cavitation and low temperature erosion resistance
– Sprayed by wire or powder flame, wire arc, HVOF

Cored Wires (wire arc sprayed):

– Some of them (Fe–Cr–P–C–. . .) form amorphous phases upon spraying
– Rather good resistance to corrosion (for example, with H_2SO_4)
– Good resistance to abrasion

Molybdenum Mo (Pure molybdenum $T_m = 2{,}623\ ^\circ C$)

– Self bonding to most metallic surfaces, especially steels
– Natural lubricity and high hardness: good wear properties
– Maximum service temperature 316 °C
– Salvage and build-up of Ni base alloy components
– High density coatings
– Fretting resistant
– Used for pump parts, diesel engine fuel, injectors, piston rings, synchronized ring, press fits, valves, gears, cam followers, . . .
– Sprayed by HVOF, flame (powder or wire), wire arc, plasma

Self-fluxing alloys: Mo+25 (Ni–Cr–B–Si–Fe)

– High wear resistance, low friction coefficient
– Against steel, good scuff resistance
– Can be used for hard facing, hard bearing surfaces
– Against abrasion

Nickel Ni (99.5 wt%) (Pure nickel $T_m = 1{,}455\ ^\circ C$)

– Good bonding to steel
– Good corrosion and oxidation resistance up to 980 °C
– Resist heat and prevent scaling of carbon and low alloy steels in hot atmospheres
– Salvage and build-up of Ni base alloys
– Easily machined
– Sprayed by HVOF, flame (powder or wire), wire arc, plasma

Ni–20Cr:

– Good surface appearance
– Good machinability
– Protective coatings against oxidizing gases at high temperature (up to 980 °C)
– Electrical conductors
– Surfacing

– Other different types of NiCr (Cr 10–17 wt%) but also addition of Fe, Mo with specific applications (see suppliers guides); for example:

Ni–16Cr–8Fe

– Machinable "stainless" coatings for salvage and build-up applications on corrosion resistant steels
– Sprayed by HVOF, flame (powder or wire), wire arc, plasma

Ni–18Cr–6Al (composite or clad):

– Good oxidation resistance
– Good machinability
– Bonding and surfacing layers
– Self-bonds to most metallic surfaces
– Sprayed by HVOF, flame (powder or wire), wire arc, plasma

Ni–20Cr–10W–9Mo–4Cu–1C–1B–1Fe:

– Wear and corrosion protection
– Coatings contain some amounts of glassy phases (due to addition of refractory metals and metalloids)
– Sprayed by HVOF, flame (powder or wire), wire arc, plasma

Ni–5Al (clad):

– Good hardness and refractoriness (formation of nickel aluminide)
– Oxidation and abrasion resistant
– Adhere very well to smooth substrates
– Bond coat
– Resizing of over machined parts or of worn-out parts
– Possible: Al 20 wt% (clad) → self-bonds to most metal surfaces
– Sprayed by HVOF, flame (powder or wire), wire arc, plasma

Nickel-based self-fluxing alloys

– Ni–10Cr–2.5B–2.5Fe–2.5Si–0.15C
– The only one producing machinable-fused coating
– Resistance to abrasive wear, fretting, cavitation, and erosion up to 840 °C
– Ni–17Cr–4Fe–4Si–3.5B–1C
– Dense coating good corrosion resistance
– Ni–17Cr–4Fe–4Si–3.5B–1C
– Dense, hard, oxide free coating
– Piston rings, cylinder liners, utility exhaust fan

Superalloys: M.Cr.Al.Y with M = Ni, Co, Fe, Ni–Co

- Composition optimized: for substrate compatibility and environmental resistance
- Protection against corrosion and oxidation in high temperature applications:
- Aero gas turbines
- Marine turbines
- Stationary gas turbines
- Design criteria—Avoid phase transformation during engine start up and shut down, Avoid brittle phases (ex μ, σ, αCr)
- Limit brittleness increasing with oxide content
- Form a stable and adherent oxide scale of Al_2O_3 (addition of active elements: 0.5 % wt Y)
- Increase corrosion resistance (by increasing Cr content)
- Control thermal expansion coefficient: increasing with Cr and decreasing with Al
- Keep ductile coatings (ductile to brittle temperature influenced by Cr and Al contents)
- Many compositions exist
- Sprayed by HVOF, plasma (if possible under soft-vacuum to limit oxidation)

A.2 Ceramics (Oxides)

For most oxides the thermal expansion coefficient is low compared to that of most metals and it has to be taken into account because they are often used at high temperature.

Alumina Al_2O_3 (T_m = 2,050 °C)

- Main problem: Starting from α phase, melting and fast cooling (spraying) result in γ phase. Unfortunately around 1,000 °C γ phase transforms into α phase with a volume increase of about 4 % resulting in coating peeling off. Thus coatings should be used below 900 °C
- They are not too sensitive to oxygen losses
- They have a good resistance to abrasive, sliding and friction wear up to approximately 800 °C
- Poor resistance to shock or impact loading
- High dielectric strength, good electrical insulating coatings
- Reactive with molten salts
- Porous coatings
- Sprayed mainly by plasma, sometimes by HVOF (particles below 22 μm in diameter) and also by flame (rods or cords)

Titanium dioxide TiO_2 (T_m = 1,843 °C)

- Very sensitive to oxygen losses resulting in strong modifications of coating properties: color from white to black and especially electrical properties
- Loss and gain of oxygen reversible
- Very good wettability
- Excellent surface finish
- Excellent adhesion
- Rather low porosity
- Sprayed by plasma, HVOF, and also by flame (rods or cords)

Alumina–Titanium dioxide Al_2O_3–xTiO_2

- TiO_2 in the range 2–50 wt% (most common: 3–13–40 wt%):

  Lowers Al_2O_3 coatings porosity.

Al_2O_3–3TiO_2

- Can be used with most acids and alkalis
- Good for abrasion, erosion, and sliding wear
- Maximum service temperature 840 °C
- Less brittle but lower dielectric strength than pure Al_2O_3 coatings
- Sprayed by plasma

Al_2O_3–13TiO_2

- Applications similar to those of Al_2O_3–3TiO_2 but lower hardness and dielectric strength and less resistance to chemical attack
- Maximum service temperature 540 °C
- Sprayed by plasma

Al_2O_3–40TiO_2

- Formation of Al_2TiO_5
- Softer and less resistant to chemicals
- Excellent finishing properties
- Sprayed by plasma
- Other compositions are used, for example, with SiO_2 below 2 wt%

Chromium Oxide Cr_2O_3 (T_m = 2,435 °C)

- Its stoichiometry depends strongly upon spray conditions (high oxygen pressure needed), and sub-stoichiometric coatings have a metallic behavior with a poor corrosion resistance
- Coatings have high hardness (1900–2000 HV_{5N})
- Excellent wear resistance
- Low porosity

- Excellent finish
- Used on sliding surfaces
- Good wear resistance
- Insoluble in acids, alkalis, and alcohol
- Maximum service temperature 540 °C
- Excellent engraving properties
- Sprayed by plasma, HVOF, and also by flame (rods or cords)

Cr_2O_3–$3TiO_2$–$5SiO_2$

- TiO_2 limits oxygen losses
- Resist better than Cr_2O_3 to impacts
- High wear and corrosion resistance

Hydroxyapatite $Ca_5\ (PO_4)_3\ OH$

- For coating medical and dental implants
- Biocompatible and bioactive (main constituent of bones)
- Sprayed by plasma

Zirconia, ZrO_2

- Interesting mechanical properties
- Good wear resistance
- Low thermal conductivity (1–5 W/m K)
- Three phases: monoclinic (m), tetragonal (t), and cubic (c). Upon cooling around 1,000 °C, cubic or tetragonal phases transform into monoclinic with volume increase of about 10 % and coating peeling off. Thus only totally (c phase) or partially (t′ non-transformable t phase) stabilized zirconia can be sprayed.

  Most used stabilizers are CaO, MgO, Y_2O_3, CeO_2. CaO and MgO are rather cheap but the maximum service temperature is about 500 °C. Very good results are obtained with Y_2O_3; with about 8 wt% t′ phase is obtained, while with13 wt% c phase is obtained, as with 24–25 wt% CeO_2. The maximum service temperature (about 1,350 °C at the best) depends not only on the phase (best results with c phase) but also on the way the powder is manufactured (see Sect. 11.1.2.9) best results being obtained when zirconia and stabilizer particles are very small and uniformly distributed.
- Coatings have excellent thermal shock resistance and good oxidation and corrosion resistance.
- They are mainly used as thermal barriers.
- Sprayed by plasma and also by flame (rods or cords)

Zircon $ZrSiO_4$ (infusible)

- Dissociated during spraying (65 % ZrO_2, 35 % SiO_2)
- Not wetted by liquid metals: used for casting
- Good resistance to liquid glass.
- Good resistance to combustion gases

A.3 Cermets

They are made of a metal matrix, to achieve a good toughness, where are imbedded ceramic particles either of oxides or carbides for the hardness and wear resistance. Here again the manufacturing process plays a key role, for example, sintered particles behaving very differently than blended ones.

With oxides. In most cases they are blends. For example

$$Al_2O_3–30(Ni–20Al)$$

- Denser coatings than pure ceramic, more abrasion, and shock resistant, hard, and smooth
- Addition of alumina particles modifies the electrical resistance of the metal matrix

MCrAlY + Al_2O_3 (<3 μm)

- Hardness increases with Al_2O_3 content
- Electrical resistance decreases with Al_2O_3 %

With carbides (the most used)
Most used ones are:
WC, Cr_3C_2, and also sometimes TiC

- If all of them have melting temperatures over 1,900 °C (for example, T_m = 2,870 °C for WC) they are relatively sensitive to oxidation
- WC oxidation starts at 500–600 °C and oxidation produces W_2C decomposing into W over 1300 °C

Cr_3C_2

- Is not the only chromium carbide: Cr_7C_3 (T_m = 1,782 °C), $Cr_{23}C_6$ (T_m = 1,518 °C). Cr_3C_2 is mostly used in spraying and its oxidation starts at 800–900 °C, however, $Cr_{23}C_6$ has an excellent wear resistance.

TiC

- Has a unique cubic phase (T_m = 3,170 °C), which oxidation starts at 800–900 °C.
- At last carbides dissolve more or less in the liquid metal or alloy matrix, the dissolution increasing with temperature over the matrix melting temperature. The metal matrix lowers the wear resistance of carbides but increases resistance to mechanical or thermal shock. Phase changes of metal matrix must be avoided during the service (for example, that of Co occurs at about 480 °C). To conclude chemical changes occur during spraying especially in air atmosphere: oxidation, decomposition, and dilution. Thus microstructural properties of sprayed cermets

depend strongly on spray conditions (VPS, IPS, APS, HVOF, HVAF, ...), particle morphology and manufacturing process, and ceramic mean grain size. Only a few examples are given below:

WC–8Co

- Dense, hard wear-resistant coating
- Sprayed by plasma, HVOF, HVAF

WC–12Co

- Excellent low-temperature wear resistance
- Sprayed by plasma, HVOF, HVAF

WC–17Co

- Higher Co level improves toughness and fretting resistance
- Cannot be used in corrosive media

Cr_3C_2–25(Ni–20Cr)

- Oxidation resistant up to 900 °C
- Good corrosion resistance
- Excellent for high-temperature cavitation, abrasion, and sliding wear

Cr_3C_2–7(Ni–20Cr)

- Very good resistance to high temperature fretting and wear (higher carbide content increases hardness)

A.4 Abradables

They are designed to wear preferentially upon contact with mating part in order to automatically establish clearance. They comprise a metal matrix and non-metallic filler such as graphite, polyester, polymide, boron nitride, and friable material, the role of filler being to weaken the matrix integrity. The metal matrix is made of Ni, Al, Cu, Co bases, and superalloys.

The main difference of the base material is related to service temperature.

- Al–Si with C: up to 315–425 °C
- Al–Si with polyester: up to 350 °C
- The filler content can be varied
- Both are used for the compressor section of jet engines
- Co–polyester–BN
- They are used up to 700 °C
- Cu: Aluminum bronze alloy–polyester or Cu–14polyester–8Al–1Fe–5Binder

- Maximum service temperature: 650 °C
- Ni–graphite
- They are used up to 480 °C
- Also self-lubricating
- MCrAlY–polyester and/or BN
- Temperatures up to 1,200–1,300 °C

Nomenclature

Latin Alphabet

Ah	Amount to be amortized per hour of equipment work (€/h or USD/h)
Ap	Amortization cost per kilogram of powder used (€/kg or USD/kg)
Fr	Process gas flow rate per hour (m^3/h)
Nh	The number of hours devoted per year to spray the specific coating
Ny	Number of years of the amortization period
p	Pressure (Pa)
Pc	Deposited powder cost per kilogram (€/kg or USD/kg)
Pcc	Cost of each component (electrodes, nozzle, O-ring, . . .) (€ or USD)
Pcp	Deposited powder cost per hour (€/h or USD/h)
Pe	Cost of the equipment (€ or USD)
Pee	Cost of 100 kW (€ or USD)
Pen	Energy cost per deposited powder kilogram (€/kg or USD/kg)
Pep	Cost of components related to the deposition of powder kilogram (€/kg or USD/kg)
Pg	Gas price per 100 m^3 (€ or USD)
Pgp	Gas price per kilogram deposited (€/kg or USD/kg)
Pp	Energy cost per deposited powder kilogram (€/kg or USD/kg)
Pt	Plasma torch power (kW)
qp	Powder quantity necessary for each part (kg)
Qp	Quantity of powder sprayed per hour (kg/h)
Sc	Surface to be coated (m^2)
tc	Mean life time of each component (electrodes, nozzle, O-ring, . . .) (h)
tp	Time necessary to spray the part (h)
v	Velocity (m/s)
wc	Thickness of the coating including the overspray before machining (mm)

Greek Alphabet

η_e	Percentage corresponding to effective spray due to loss at holes and edges (%)
η_p	Powder or wire deposition efficiency
ρ_p	Feed stock specific mass (kg/m^3)

References

1. Davis JR (ed) (2004) Handbook of thermal spray technology. Sections introduction to applications for thermal spray processing and selected applications. ASM International, Materials Park, OH
2. American Welding Society (1985) Thermal spraying, practice, theory and application. American Welding Society, Miami, FL
3. Cartier M (2003) Handbook of surface treatments and coatings. ASME Press, New York, 412 p
4. Zhum Gahr KH (1987) Microstructure and wear of materials. Elsevier, Amsterdam
5. Chattopadhyay R (2001) Surface wear: analysis, treatment, and prevention. ASM International, Materials Park, OH, 307 p
6. Pawlowski L (1995) The science and engineering of thermal spray coatings. Wiley, New York
7. Champagne VK (2007) The cold spray materials deposition process; fundamental and applications. Woodhead, Cambridge, 362 p
8. Sobolev VV, Guilemany JM, Nutting J (2004) High velocity oxy-fuel spraying. Maney for the Institute of Materials, Minerals and Mining, London
9. Bolelli G, Lusvarghi L (2006) Heat treatment effects on the tribological performance of HVOF sprayed Co-Mo-Cr-Si coatings. J Therm Spray Technol 15(4):802–810
10. Kulu P, Hailing J (1998) Recycled hard metal-base wear-resistant composite coatings. J Therm Spray Technol 7(2):173–178
11. Sakata K, Nakano K, Miyahara H, Matsubara Y, Ogi K (2007) Microstructure control of thermally sprayed Co-based self-fluxing alloy coatings by diffusion treatment. J Therm Spray Technol 16(5–6):991–997
12. Otsubo F, Era H, Kishitake K (2000) Structure and phases in nickel-base self-fluxing alloy coating containing high chromium and boron. J Therm Spray Technol 9(1):107–113
13. Kulu P, Pihl T (2002) Selection criteria for wear resistant powder coatings under extreme erosive wear conditions. J Therm Spray Technol 11(4):517–522
14. Miranda JC, Ramalho A (2001) Abrasion resistance of thermal sprayed composite coatings with a nickel alloy matrix and a WC hard phase. Effect of deposition technique and re-melting. Tribol Lett 11(1):37–48
15. Schwetzke R, Kreye H (1999) Microstructure and properties of tungsten carbide coatings sprayed with various high-velocity oxygen fuel spray systems. J Therm Spray Technol 8 (3):433–439
16. Kasparova M, Zahalka F, Houdkova S (2011) WC-Co and Cr_3C_2-NiCr coatings in low- and high-stress abrasive conditions. J Therm Spray Technol 20(3):412–424
17. Houdkova S, Kasparova M, Zahalka F (2010) The influence of spraying angle on properties of HVOF sprayed hardmetal coatings. J Therm Spray Technol 19(5):893–901
18. Tillmann W, Vogli E, Baumann I, Kopp G, Weihs C (2010) Desirability-based multi-criteria optimization of HVOF spray experiments to manufacture fine structured wear-resistant $75Cr_3C_2$-25(NiCr20) coatings. J Therm Spray Technol 19(1–2):393–408
19. Skandan G, Yao R, Sadangi R, Kear BH, Qiao Y, Liu L, Fischer TE (2000) Multimodal coatings: a new concept in thermal spraying. J Therm Spray Technol 9(3):329–331
20. Lima RS, Marple BR (2007) Thermal spray coatings engineered from nanostructured ceramic agglomerated powders for structural, thermal barrier and biomedical applications: a review. J Therm Spray Technol 16(1):40–63
21. Kim GE, Walker J (2007) Successful application of nanostructured titanium dioxide coating for high-pressure acid-leach application. J Therm Spray Technol 16(1):34–39
22. Gawne DT, Qiu Z, Bao Y, Zhang T, Zhang K (2001) Abrasive wear resistance of plasma-sprayed glass-composite coatings. J Therm Spray Technol 10(4):599–603

23. Cipri F, Bartuli C, Valente T, Casadei F (2007) Electromagnetic and mechanical properties of silica-aluminosilicates plasma sprayed composite coatings. J Therm Spray Technol 16(5–6):831–838
24. Kang AS, Grewal JS, Jain D, Kang S (2012) Wear behavior of thermal spray coatings on rotavator blades. J Therm Spray Technol 21(2):355–359
25. Kim HJ, Kweon YG, Chang RW (1994) Wear and erosion behavior of plasma-sprayed WC-Co coatings. J Therm Spray Technol 3(2):169–178
26. Wang BQ, Luer K (1994) The erosion-oxidation behavior of HVOF Cr_3C_2-NiCr cermet coating. Wear 174:177–185
27. Kenichi S, Nakahama S, Hattori S, Nakano K (2005) Slurry wear and cavitation erosion of thermal-sprayed cermets. Wear 258:768–775
28. Hawthorne HM, Arsenault B, Immarigeon JP, Legoux JG, Parameswaran VR (1999) Comparison of slurry and dry erosion behavior of some HVOF thermal sprayed coatings. Wear 225–229:825–834
29. Ji G-C, Li C-J, Wang Y-Y, Li W-Y (2007) Erosion performance of HVOF-sprayed Cr3C2-NiCr coatings. J Therm Spray Technol 16(4):557–565
30. Yang G-J, Li C-J, Zhang S-J, Li C-X (2008) High-temperature erosion of HVOF sprayed Cr_3C_2-NiCr coating and mild steel for boiler tubes. J Therm Spray Technol 17(5–6):782–787
31. Osawa S, Itsukaichi T, Ahmed R (2005) Influence of substrate properties on the impact resistance of WC cermet coatings. J Therm Spray Technol 14(4):495–501
32. Kulu P, Hussainova L, Veinthal R (2005) Solid particle erosion of thermal sprayed coatings. Wear 258:488–496
33. Ramesha CS, Devaraja DS, Keshavamurthya R, Sridharb BR (2011) Slurry erosive wear behavior of thermally sprayed Inconel-718 coatings by APS process. Wear 271:1365–1371
34. Higuera HV, Belzunce Varela J, Carriles Menéndez A, Poveda Martiınez S (2001) High temperature erosion wear of flame and plasma-sprayed nickel–chromium coatings under simulated coal-fired boiler atmospheres. Wear 247:214–222
35. Krishnamurthy N, Murali MS, Venkataraman B, Mukunda PG (2012) Characterization and solid particle erosion behavior of plasma sprayed alumina and calcia-stabilized zirconia coatings on Al-6061 substrate. Wear 274–275:15–27
36. Branagan DJ, Breitsameter M, Meacham BE, Belashchenko V (2005) High-performance nanoscale composite coatings for boiler applications. J Therm Spray Technol 14(2):196–204
37. Pantelis DI, Psyllaki P, Alexopoulos N (2000) Tribological behavior of plasma-sprayed Al_2O_3 coatings under severe wear conditions. Wear 237:197–204
38. Sanchez E, Bannier E, Cantavella V, Salvador MD, Klyatskina E, Morgiel J, Grzonka J, Boccaccini AR (2008) Deposition of Al_2O_3-TiO_2 nanostructured powders by atmospheric plasma spraying. J Therm Spray Technol 17(3):329–337
39. Darut G, Ageorges H, Denoirjean A, Montavon G, Fauchias P (2008) Effect of the structural scale of plasma-sprayed alumina coatings on their friction coefficients. J Therm Spray Technol 17(5–6):788–797
40. Bolelli G, Rauch J, Cannillo V, Killinger A, Lusvarghi L, Gadow R (2009) Microstructural and tribological investigation of high-velocity suspension flame sprayed (HVSFS) Al_2O_3 coatings. J Therm Spray Technol 18(1):35–48
41. Ahn H-S, Kwon O-K (1999) Tribological behaviour of plasma-sprayed chromium oxide coating. Wear 225–229:814–824
42. Pratap Singh V, Sil A, Jayaganthan R (2011) Tribological behavior of plasma sprayed Cr_2O_3–3%TiO_2 coatings. Wear 272:149–158
43. Tao S, Yin Z, Zhou X, Ding C (2010) Sliding wear characteristics of plasma-sprayed Al_2O_3 and Cr_2O_3 coatings against copper alloy under severe conditions. Tribol Int 43:69–75
44. Bolelli G, Cannillo V, Lusvarghi L, Manfredini T (2006) Wear behaviour of thermally sprayed ceramic oxide coatings. Wear 261:1298–1315

45. Ramachandran CS, Balasubramanian V, Ananthapadmanabhan PV, Viswabaskaran V (2012) Understanding the dry sliding wear behaviour of atmospheric plasma-sprayed rare earth oxide coatings. Mater Design 39:234–252
46. Dallaire S (2001) Hard arc-sprayed coating with enhanced erosion and abrasion wear resistance. J Therm Spray Technol 10(3):511–519
47. Yang Q, Senda T, Hirose A (2006) Sliding wear behavior of WC–12% Co coatings at elevated temperatures. Surf Coat Technol 200:4208–4212
48. Yandouzi M, Bu H, Brochu M, Jodoin B (2012) Nanostructured Al-based metal matrix composite coating production by pulsed gas dynamic spraying process. J Therm Spray Technol 21(3–4):609–619
49. Li W-Y, Zhang G, Zhang C, Elkedim O, Liao H, Coddet C (2008) Effect of ball milling of feedstock powder on microstructure and properties of TiN particle-reinforced Al alloy-based composites fabricated by cold spraying. J Therm Spray Technol 17(3):316–322
50. Qiao Y, Liu Y-R, Fischer TE (2001) Sliding and abrasive wear resistance of thermal-sprayed WC-CO coatings. J Therm Spray Technol 10(1):118–125
51. Jacobs L, Hyland MM, De Bonte M (1999) Study of the influence of microstructural properties on the sliding-wear behavior of HVOF and HVAF sprayed WC-cermet coatings. J Therm Spray Technol 8(1):125–132
52. Bolelli G, Bonferroni B, Laurila J, Lusvarghi L, Milantia A, Niemi K, Vuoristo P (2012) Micromechanical properties and sliding wear behaviour of HVOF-sprayed Fe-based alloy coatings. Wear 276–277:29–47
53. Alam S, Sasaki S, Shimura H (2001) Friction and wear characteristics of aluminum bronze coatings on steel substrates sprayed by a low pressure plasma technique. Wear 248:75–81
54. Ouyang JH, Sasaki S, Umeda K (2001) Microstructure and tribological properties of low-pressure plasma-sprayed ZrO_2–CaF_2–Ag_2O composite coating at elevated temperature. Wear 249:440–451
55. Ahn J, Hwang B, Lee S (2005) Improvement of wear resistance of plasma-sprayed molybdenum blend coatings. J Therm Spray Technol 14(2):251–257
56. Rodriguez J, Martin A, Fernández R, Fernández JE (2003) An experimental study of the wear performance of NiCrBSi thermal spray coatings. Wear 255:950–955
57. Niebuhr D, Scholl M (2005) Synthesis and performance of plasma-sprayed polymer/steel coating system. J Therm Spray Technol 14(4):487–494
58. Li J, Liao H, Coddet C (2002) Friction and wear behavior of flame-sprayed PEEK coatings. Wear 252:824–831
59. Li Y, Ma Y, Xie B, Cao S, Wu Z (2007) Dry friction and wear behavior of flame-sprayed polyamide1010/n-SiO_2 composite coatings. Wear 262:1232–1238
60. Żórawski W, Kozerski S (2008) Scuffing resistance of plasma and HVOF sprayed WC-12Co and Cr_3C_2-25(Ni20Cr) coatings. Surf Coat Technol 202:4453–4457
61. Edrisy A, Perry T, Alpas AT (2005) Investigation of scuffing damage in aluminum engines with thermal spray coatings. Wear 259:1056–1062
62. Kim J-H, Lee M-H (2010) A study on cavitation erosion and corrosion behavior of Al-, Zn-, Cu-, and Fe-based coatings prepared by arc spraying. J Therm Spray Technol 19 (6):1224–1230
63. Hahn M, Fischer A (2010) Characterization of thermal spray coatings for cylinder running surfaces of diesel engines. J Therm Spray Technol 19(5):866–872
64. Kumar A, Boy J, Zatorski R, Stephenson LD (2005) Thermal spray and weld repair alloys for the repair of cavitation damage in turbines and pumps: a technical note. J Therm Spray Technol 14(2):177–182
65. Factor M, Roman I (2002) Use of microhardness as a simple means of estimating relative wear resistance of carbide thermal spray coatings: Part 2. Wear resistance of cemented carbide coatings. J Therm Spray Technol 11(4):482–495

66. Wu Y, Hong S, Zhang J, He Z, Guo W, Wang Q, Li G (2012) Microstructure and cavitation erosion behavior of WC–Co–Cr coating on 1Cr18Ni9Ti stainless steel by HVOF thermal spraying. Int J Refract Metals Hard Mater 32:21–26
67. Santa JF, Espitia LA, Blanco JA, Romo SA, Toro A (2009) Slurry and cavitation erosion resistance of thermal spray coatings. Wear 267:160–167
68. Lima MM, Godoy C, Modenesi PJ, Avelar-Batista JC, Davison A, Matthews A (2004) Coating fracture toughness determined by Vickers indentation: an important parameter in cavitation erosion resistance of WC–Co thermally sprayed coatings. Surf Coat Technol 177–178:489–496
69. Ding Z-X, Chen W, Wang Q (2011) Resistance of cavitation erosion of multimodal WC-12Co coatings sprayed by HVOF. Trans Nonferrous Met Soc China 21:2231–2236
70. Stewart S, Ahmed R (2002) Rolling contact fatigue of surface coatings—a review. Wear 253:1132–1144
71. Ahmed R, Hadfield M (2002) Mechanisms of fatigue failure in thermal spray coatings. J Therm Spray Technol 11(3):333–349
72. Savarimuthu AC, Taber HF, Megat I, Shadley JR, Rybicki EF, Cornell WC, Emery WA, Somerville DA, Nuse JD (2001) Sliding wear behavior of tungsten carbide thermal spray coatings for replacement of chromium electroplate in aircraft applications. J Therm Spray Technol 10(3):502–510
73. Zhang XC, Xu BS, Xuan FZ, Tu ST, Wang HD, Wu YX (2008) Rolling contact fatigue behavior of plasma-sprayed CrC–NiCr cermet coatings. Wear 265:1875–1883
74. Berger L-M, Lipp K, Spatzier J, Bretschneider J (2011) Dependence of the rolling contact fatigue of HVOF-sprayed WC–17%Co hardmetal coatings on substrate hardness. Wear 271:2080–2088
75. Ganesh Sundara Raman S, Rajasekaran B, Joshi SV, Sundararajan G (2007) Influence of substrate material on plain fatigue and fretting fatigue behavior of detonation gun sprayed Cu-Ni-In coating. J Therm Spray Technol 16(4):571–579
76. Akebono H, Komotori J, Shimizu M (2008) Effect of coating microstructure on the fatigue properties of steel thermally sprayed with Ni-based self-fluxing alloy. Int J Fatigue 30:814–821
77. Jin O, Mall S, Sanders JH, Sharma SK (2006) Durability of Cu–Al coating on Ti–6Al–4V substrate under fretting fatigue. Surf Coat Technol 201:1704–1710
78. Kim K, Korsunsky AM (2011) Effects of imposed displacement and initial coating thickness on fretting behaviour of a thermally sprayed coating. Wear 271(7–8):1080–1085
79. Mary C, Fouvry S, Martin JM, Bonnet B (2011) Pressure and temperature effects on Fretting Wear damage of a Cu–Ni–In plasma coating versus Ti17 titanium alloy contact. Wear 272:18–37
80. Hager CH Jr, Sanders JH, Sharma S (2008) Un-lubricated gross slip fretting wear of metallic plasma-sprayed coatings for Ti6Al4V surfaces. Wear 265:439–451
81. Koiprasert H, Dumrongrattana S, Niranatlumpong P (2004) Thermally sprayed coatings for protection of fretting wear in land-based gas-turbine engine. Wear 257:1–7
82. Hager CH Jr, Sanders J, Sharma S, Voevodin AA (2009) The use of nickel graphite composite coatings for the mitigation of gross slip fretting wear on Ti6Al4V interfaces. Wear 267:1470–1481
83. Carrasquero EJ, Lesage J, Puchi-Cabrera ES, Staia MH (2008) Fretting wear of HVOF Ni–Cr based alloy deposited on SAE 1045 steel. Surf Coat Technol 202:4544–4551
84. Tian W, Wang Y, Yang Y (2008) Fretting wear behavior of conventional and nanostructured Al2O3–13 wt%TiO2 coatings fabricated by plasma spray. Wear 265:1700–1707
85. Sathish S, Geetha M, Aruna ST, Balaji N, Rajam KS, Asokamani R (2011) Sliding wear behavior of plasma sprayed nanoceramic coatings for biomedical applications. Wear 271:934–941
86. Aoh J-N, Chen J-C (2001) On the wear characteristics of cobalt-based hardfacing layer after thermal fatigue and oxidation. Wear 250:611–620

87. D'Ans P, Dille J, Degrez M (2011) Thermal fatigue resistance of plasma sprayed yttria-stabilised zirconia onto borided hot work tool steel, bonded with a NiCrAlY coating: experiments and modeling. Surf Coat Technol 205:3378–3386
88. Eriksson R, Brodin H, Johansson S, Östergren L, Li X-H (2011) Influence of isothermal and cyclic heat treatments on the adhesion of plasma sprayed thermal barrier coatings. Surf Coat Technol 205:5422–5429
89. Kwon J-Y, Lee J-H, Kim H-C, Jung Y-G, Paik U, Lee K-S (2006) Effect of thermal fatigue on mechanical characteristics and contact damage of zirconia-based thermal barrier coatings with HVOF-sprayed bond coat. Mater Sci Eng A 429:173–180
90. Luo L, Liu S, Li J, Wu Y (2011) Thermal shock resistance of FeMnCrAl/Cr3C2–Ni9Al coatings deposited by high velocity arc spraying. Surf Coat Technol 205:3467–3471
91. Pan ZY, Wang Y, Wang CH, Sun XG, Wang L (2012) The effect of SiC particles on thermal shock behavior of Al2O3/8YSZ coatings fabricated by atmospheric plasma spraying. Surf Coat Technol 206:2484–2498
92. Gu L, Chen X, Fan X, Liu Y, Zou B, Wang Y, Cao X (2011) Improvement of thermal shock resistance for thermal barrier coating on aluminum alloy with various electroless interlayers. Surf Coat Technol 206:29–36
93. Kokini K, DeJonge J, Rangaraj S, Beardsley B (2002) Thermal shock of functionally graded thermal barrier coatings with similar thermal resistance. Surf Coat Technol 154:223–231
94. Liang B, Ding C (2005) Thermal shock resistances of nanostructured and conventional zirconia coatings deposited by atmospheric plasma spraying. Surf Coat Technol 197:185–192
95. Gilbert A, Kokini K, Sankarasubramanian S (2008) Thermal fracture of zirconia–mullite composite thermal barrier coatings under thermal shock: a numerical study. Surf Coat Technol 203:91–98
96. Ahmaniemi S, Vippola M, Vuoristo P, Mäntylä T, Buchmann M, Gadow R (2002) Residual stresses in aluminum phosphate sealed plasma sprayed oxide coatings and their effect on abrasive wear. Wear 252:614–623
97. Chen H, Hutchings IM (1998) Abrasive wear resistance of plasma-sprayed tungsten carbide–cobalt coatings. Surf Coat Technol 107:106–114
98. Venkateswarlu K, Rajinikanth V, Naveen T, Dhiraj Prasad Sinha (2009) Abrasive wear behavior of thermally sprayed diamond reinforced composite coating deposited with both oxy-acetylene and HVOF techniques. Wear 266:995–1002
99. Stoica V, Ahmed R, Itsukaichi T (2005) Influence of heat-treatment on the sliding wear of thermal spray cermet coatings. Surf Coat Technol 199:7–21
100. Valarezo A, Bolelli G, Choi WB, Sampath S, Cannillo V, Lusvarghi L, Rosa R (2010) Damage tolerant functionally graded WC–Co/stainless steel HVOF coatings. Surf Coat Technol 205:2197–2208
101. Bolelli, Cannillo V, Lusvarghi L, Rosa R, Valarezo A, Choi WB, Dey R, Weyant C, Sampath S (2012) Functionally graded WC–Co/NiAl HVOF coatings for damage tolerance, wear and corrosion protection. Surf Coat Technol 206:2585–2601
102. Stoica V, Ahmed R, Golshan M, Tobe S (2004) Sliding wear evaluation of hot isostatically pressed thermal spray cermet coatings. J Therm Spray Technol 13(1):93–107
103. Evdokimenko Yu I, Kisel' VM, Kadyrov VK, Korol' AA, Get'man OI (2001) High-velocity flame spraying of powder aluminum protective coatings. Powder Metallurgy Metal Ceram 40 (3–4):121–126
104. Sørensen PA, Kiil S, Dam-Johansen K, Weinell CE (2009) Anticorrosive coatings: a review. J Coat Technol Res 6(2):135–176
105. Murakami K, Shimada M (2009) Development of thermal spray coatings with corrosion protection and antifouling properties. In: Marple BR, Hyland MM, Lau Y-C, Li C-J, Lima RS, Montavon G (eds) Thermal spray 2009: Proceedings of the international thermal spray conference. ASM International, Materials Park, OH, pp 1041–1044
106. Pacheo da Silva C et al (1991) 2nd Plasma Technik Symposium 1. Plasma Technik, Wohlen, pp 363–373

107. Chun-long Y, Yun-qi A, Ya-tan S (2009) Three years corrosion tests of nanocomposite epoxy sealer for metalized coatings on the East China Sea. In: Marple BR, Hyland MM, Lau Y-C, Li C-J, Lima RS, Montavon G (eds) Thermal spray 2009: Proceedings of the international thermal spray conference. ASM International, Materials Park, OH, pp 1090–1093
108. Schmidt DP, Shaw BA, Sikora E, Shaw WW, Laliberte LH (2006) Corrosion protection assessment of sacrificial coating systems as a function of exposure time in a marine environment. Prog Org Coat 57:352–364
109. Han M-S, Woo Y-B, Ko S-C, Jeong Y-J, Jang S-K, Kim S-J (2009) Effects of thickness of Al thermal spray coating for STS 304. Trans Nonferrous Met Soc China 19:925–929
110. Esfahani EA, Salimijazi H, Golozar MA, Mostaghimi J, Pershin L (2012) Study of corrosion behavior of arc sprayed aluminum coating on mild steel. J Therm Spray Technol. doi:10.1007/s11666-012-9810-x
111. Gorlach IA (2009) A new method for thermal spraying of Zn–Al coatings. Thin Solid Films 517:5270–5273
112. Cramer SD, Covino BS Jr, Holcomb GR, Bullard SJ, Collins WK, Govier RD, Wilson RD, Laylor HM (1999) Thermal sprayed titanium anode for cathodic protection of reinforced concrete bridges. J Therm Spray Technol 8(1):133–145
113. Holcomb GR, Cramer SD, Bullard SJ, Covino Jr BS, Collins WK, Govier RD, McGill GE (1997) Characterization of thermal-sprayed titanium anodes for cathodic protection. In: Berndt CC (ed) Thermal spray: a united forum for scientific and technological advances. ASM International, Materials Park, OH, pp 141–150
114. Kawakita J, Kuroda S, Fukushima T, Kodama T (2005) Improvement of corrosion resistance of high-velocity oxyfuel-sprayed stainless steel coatings by addition of molybdenum. J Therm Spray Technol 14(2):225–230
115. Moskowitz LN (1993) Application of HVOF thermal spraying to solve corrosion problems in the petroleum industry—an industrial note. J Therm Spray Technol 2(1):21–29
116. Zeng Z, Sakoda N, Tajiri T, Kuroda S (2008) Structure and corrosion behavior of 316L stainless steel coatings formed by HVAF spraying with and without sealing. Surf Coat Technol 203:284–290
117. Meng H (2010) The performance of different WC-based cermet coatings in oil and gas applications–a comparison. In: ITSC 2010 Thermal spray: global solutions, future applications. DVS, Düsseldorf, e-Proc
118. Souza VAD, Neville A (2007) Aspects of microstructure on the synergy and overall material loss of thermal spray coatings in erosion–corrosion environments. Wear 263:339–346
119. Ishikawa Y, Kawakita J, Osawa S, Itsukaichi T, Sakamoto Y, Takaya M, Kuroda S (2005) Evaluation of corrosion and wear resistance of hard cermet coatings sprayed by using an improved HVOF process. J Therm Spray Technol 14(3):384–390
120. Fedrizzi L, Valentinelli L, Rossi S, Segna S (2007) Tribocorrosion behaviour of HVOF cermet coatings. Corros Sci 49:2781–2799
121. Zhang J, Wang Z, Lin P, Lu W, Zhou Z, Jiang S (2011) Effect of sealing treatment on corrosion resistance of plasma-sprayed NiCrAl/Cr_2O_3-8 wt.%TiO_2 coating. J Therm Spray Technol 20(3):508–513
122. Tuominen J, Vuoristo P, Mäntylä T, Kylmälahti M, Vihinen J et al (2000) Improving corrosion properties of high-velocity oxy-fuel sprayed inconel 625 by using a high-power continuous wave neodymium-doped yttrium aluminum garnet laser. J Therm Spray Technol 9(4):513–519
123. Kim S-J, Lee S-J (2011) Effects of F−Si sealer on electrochemical characteristics of 15% Al−85%Zn alloy thermal spray coating. Trans Nonferrous Met Soc China 21:2798–2804
124. Dent AH, Horlock AJ, McCartney DG, Harris SJ (1999) The corrosion behavior and microstructure of high-velocity oxy-fuel sprayed nickel-base amorphous/nanocrystalline coatings. J Therm Spray Technol 8(3):399–404

125. Ishikawa K, Suzuki T, Tobe S, Kitamura Y (2001) Resistance of thermal-sprayed duplex coating composed of aluminum and 80Ni-20Cr alloy against aqueous corrosion. J Therm Spray Technol 10(3):520–525
126. Pardo A, Merino MC, Mohedano M, Casajús P, Coy AE, Arrabal R (2009) Corrosion behaviour of Mg/Al alloys with composite coatings. Surf Coat Technol 203:1252–1263
127. Arrabal R, Pardo A, Merino MC, Mohedano M, Casajús P, Merino S (2010) Al/SiC thermal spray coatings for corrosion protection of Mg–Al alloys in humid and saline environments. Surf Coat Technol 204:2767–2774
128. Pokhmurska H, Wielage B, Lampke T, Grund T, Student M, Chervinska N (2008) Post-treatment of thermal spray coatings on magnesium. Surf Coat Technol 202:4515–4524
129. Mohan P, Patterson T, Yao B, Sohn Y (2010) Degradation of thermal barrier coatings by fuel impurities and CMAS: thermochemical interactions and mitigation approaches. J Therm Spray Technol 19(1–2):156–167
130. Jones RL (1997) Some aspects of the hot corrosion of thermal barrier coatings. J Therm Spray Technol 6(1):77–84
131. Hitchman LN, Knapp J (2010) Failure of thermal barrier coatings subjected to CMAS attack. J Therm Spray Technol 19(1–2):148–155
132. Li L, Hitchman N, Knapp J (2010) Failure of thermal barrier coatings subjected to CMAS attack. J Therm Spray Technol 19(1–2):148–155
133. Habibi MH, Li Wang, Guo SM (2012) Evolution of hot corrosion resistance of YSZ, $Gd_2Zr_2O_7$, and $Gd_2Zr_2O_7$ + YSZ composite thermal barrier coatings in Na_2SO_4 + V_2O_5 at 1050 °C. J Eur Ceram Soc 32:1635–1642
134. Xie X, Guo H, Gong S, Xu H (2012) Hot corrosion behavior of double-ceramic-layer $LaTi_2Al_9O_{19}$/YSZ thermal barrier coatings. Chin J Aeronautics 25:137–142
135. Mei H, Liu Y, Cheng L, Zhang L (2012) Corrosion mechanism of a NiCoCrAlTaY coated Mar-M247 superalloy in molten salt vapor. Corros Sci 55:201–204
136. Sidhu TS, Prakash S, Agrawal RD (2006) Hot corrosion resistance of high-velocity oxyfuel sprayed coatings on a nickel-base superalloy in molten salt environment. J Therm Spray Technol 15(3):387–399
137. Chatha SS, Sidhu HS, Sidhu BS (2012) High temperature hot corrosion behaviour of NiCr and Cr_3C_2–NiCr coatings on T91 boiler steel in an aggressive environment at 750 °C. Surf Coat Technol 206:3839–3850
138. Tani K, Harada Y (2007) Enhancement of service life of steam generating tubes in oil-fired boiler for power generation employing plasma spray technology. J Therm Spray Technol 16 (1):111–117
139. Bala N, Singh H, Prakash S (2010) Accelerated hot corrosion studies of cold spray Ni–50Cr coating on boiler steels. Mater Design 31:244–253
140. Matsubara Y, Sochi Y, Tanabe M, Takeya A (2007) Advanced coatings on furnace wall tubes. J Therm Spray Technol 16(2):195–201
141. Chatha SS, Sidhu HS, Sidhu BS (2012) The effects of post-treatment on the hot corrosion behavior of the HVOF-sprayed Cr_3C_2–NiCr coating. Surf Coat Technol 206:4212–4224
142. Tao K, Zhou X-L, Cui H, Zhang J-S (2009) Oxidation and hot corrosion behaviors of HVAF-sprayed conventional and nanostructured NiCrC coatings. Trans Nonferrous Met Soc China 19:1151–1160
143. Jansen F, Xi W, Dorfman MR, Peters JA, Nagy DR (2002) Performance of di-calcium silicate coatings in hot-corrosive environment. Surf Coat Technol 149:57–61
144. Hirata T, Ota S, Morimoto T (2003) Influence of impurities in Al_2O_3 ceramics on hot corrosion resistance against molten salt. J Eur Ceram Soc 23:91–97
145. Gibbons GJ, Hansell RG (2008) Thermal-sprayed coatings on aluminium for mould tool protection and upgrade. J Mater Process Technol 204:184–191
146. Mizuno H, Kitamura J (2007) MoB/CoCr cermet coatings by HVOF spraying against erosion by molten Al-Zn alloy. J Therm Spray Technol 16(3):404–413

147. Koolloos MFJ, Houben JM (2000) Behavior of plasma-sprayed thermal barrier coatings during thermal cycling and the effect of a preoxidized NiCrAlY bond coat. J Therm Spray Technol 9(1):49–58
148. Fossati A, DiFerdinando M, Bardi U, Scrivani A, Giolli C (2012) Influence of surface finishing on the oxidation behaviour of VPS MCrAlY coatings. J Therm Spray Technol 21(2):314–324
149. Jiang SM, Li HQ, Ma J, Xu CZ, Gong J, Sun C (2010) High temperature corrosion behavior of a gradient NiCoCrAlYSi coating II: oxidation and hot corrosion. Corros Sci 52:2316–2322
150. Yuan FH, Chen ZX, Huang ZW, Wang ZG, Zhu SJ (2008) Oxidation behavior of thermal barrier coatings with HVOF and detonation-sprayed NiCrAlY bond coats. Corros Sci 50:1608–1617
151. Pint BA, Wright IG, Brindley WJ (2000) Evaluation of thermal barrier coating systems on novel substrates. J Therm Spray Technol 9(2):198–203
152. Limarga AM, Widjaja S, Yip TH (2005) Mechanical properties and oxidation resistance of plasma-sprayed multilayered Al_2O_3/ZrO_2 thermal barrier coatings. Surf Coat Technol 197:93–102
153. Ramesh MR, Prakash S, Nath SK, Pawan Kumar Sapra, Krishnamurthy N (2011) Evaluation of thermocyclic oxidation behavior of HVOF-sprayed NiCrFeSiB coatings on boiler tube steels. J Therm Spray Technol 20(5):992–1000
154. Kaur M, Singh H, Prakash S (2011) Surface engineering analysis of detonation-gun sprayed Cr3C2–NiCr coating under high-temperature oxidation and oxidation–erosion environments. Surf Coat Technol 206:530–541
155. Sidhu TS, Malik A, Prakash S, Agrawal RD (2007) Oxidation and hot corrosion resistance of HVOF WC-NiCrFeSiB coating on Ni- and Fe-based superalloys at 800 °C. J Therm Spray Technol 16(5–6):844–849
156. Singh H, Puri D, Prakash S, Rama Rao VV (2006) On the high-temperature oxidation protection behavior of plasma-sprayed stellite-6 coatings. Metallurgical Mater Trans A 37A:3048–3056
157. Bala N, Singh H, Prakash S (2011) Characterization and high-temperature oxidation behavior of cold-sprayed Ni-20Cr and Ni-50Cr coatings on boiler steels. Metallurgical Mater Trans A 42A:3399–3416
158. Hill H, Weber S, Raab U, Theisen W, Wagner L (2012) Influence of processing and heat treatment on corrosion resistance and properties of high alloyed steel coatings. J Therm Spray Technol 21(5):987–994
159. Kembaiyan KT, Keshavan K (1995) Combating severe fluid erosion and corrosion of drill bits using thermal spray coatings. Wear 186–187:487–492
160. Uozato S, Nakata K, Ushio M (2003) Corrosion and wear behaviors of ferrous powder thermal spray coatings on aluminum alloy. Surf Coat Technol 169–170:691–694
161. Al-Fadhli HY, Stokes J, Hashmi MSJ, Yilbas BS (2006) The erosion–corrosion behaviour of high velocity oxy-fuel (HVOF) thermally sprayed inconel-625 coatings on different metallic surfaces. Surf Coat Technol 200:5782–5788
162. Lima CRC, de Souza NFC, Camargo F (2012) Study of wear and corrosion performance of thermal sprayed engineering polymers. Surf Coat Technol 220:140–143
163. Flores JF, Neville A, Kapur N, Gnanavelu A (2009) An experimental study of the erosion–corrosion behavior of plasma transferred arc MMCs. Wear 267:213–222
164. Sidhu BS, Prakash S (2006) Erosion-corrosion of plasma as sprayed and laser remelted Stellite-6 coatings in a coal fired boiler. Wear 260:1035–1044
165. Wang B (1996) Erosion-corrosion of thermal sprayed coatings in FBC boilers. Wear 199:24–32
166. Uusitalo MA, Vuoristo PMJ, Mäntylä TA (2002) Elevated temperature erosion–corrosion coatings in chlorine containing environments of thermal sprayed. Wear 252:586–594

167. Billah BM, Ahmad Khalid F, Nusair Khan A (2012) Behavior of calcia-stabilized zirconia coating at high temperature, deposited by air plasma spraying system. J Therm Spray Technol 21(1):121–131
168. Miller RA (1997) Thermal barrier coatings for aircraft engines: history and directions. J Therm Spray Technol 6(1):35–42
169. Schulz U, Bernardi O, Ebach-Stahl A, Vaßen R, Sebold D (2008) Improvement of EB-PVD thermal barrier coatings by treatments of a vacuum plasma-sprayed bond coat. Surf Coat Technol 203:160–170
170. Bose S, de Masi-Marcin J (1997) Thermal barrier coating experience in gas turbine engines at Pratt & Whitney. J Therm Spray Technol 6(1):99–104
171. Cipitria A, Golosnoy IO, Clyne TW (2009) A sintering model for plasma-sprayed zirconia TBCs. Part I: Free-standing coatings. Acta Mater 57:980–992
172. Markocsan N, Nylén P, Wigren J, Li X-H, Tricoire A (2009) Effect of thermal aging on microstructure and functional properties of zirconia-base thermal barrier coatings. J Therm Spray Technol 18(2):201–208
173. Golosnoy IO, Cipitria A, Clyne TW (2009) Heat transfer through plasma-sprayed thermal barrier coatings in gas turbines: a review of recent work. J Therm Spray Technol 18 (5–6):809–821
174. Hernandez MT, Karlsson AM, Bartsch M (2009) On TGO creep and the initiation of a class of fatigue cracks in thermal barrier coatings. Surf Coat Technol 203:3549–3558
175. Vaßen R, Giesen S, Stöver D (2009) Lifetime of plasma-sprayed thermal barrier coatings: comparison of numerical and experimental results. J Therm Spray Technol 18(5–6):835–845
176. Toscano J, Vaβen R, Gil A, Subanovic M, Naumenko D, Singheiser L, Quadakkers WJ (2006) Parameters affecting TGO growth and adherence on MCrAlY-bond coats for TBC's. Surf Coat Technol 201:3906–3910
177. Pint BA, Haynes JA, Zhang Y (2010) Effect of superalloy substrate and bond coating on TBC lifetime. Surf Coat Technol 205:1236–1240
178. Chen Z, Mabon J, Wen J-G, Trice R (2009) Degradation of plasma-sprayed yttria-stabilized zirconia coatings via ingress of vanadium oxide. J Eur Ceram Soc 29:1647–1656
179. Feuerstein A, Knapp J, Taylor T, Ashary A, Bolcavage A, Hitchman N (2008) Technical and economical aspects of current thermal barrier coating systems for gas turbine engines by thermal spray and EBPVD: a review. J Therm Spray Technol 17(2):199–213
180. Vaßen R, Jarligo MO, Steinke T, Mack DE, Stöver D (2010) Overview on advanced thermal barrier coatings. Surf Coat Technol 205:938–942
181. Vaßen R, Stuke A, Stöver D (2009) Recent developments in the field of thermal barrier coatings. J Therm Spray Technol 18(2):181–186
182. Richer P, Yandouzi M, Beauvais L, Jodoin B (2010) Oxidation behaviour of CoNiCrAlY bond coats produced by plasma, HVOF and cold gas dynamic spraying. Surf Coat Technol 204:3962–3974
183. Karger M, Vaßen R, Stöver D (2011) Atmospheric plasma sprayed thermal barrier coatings with high segmentation crack densities: spraying process, microstructure and thermal cycling behaviour. Surf Coat Technol 206:16–23
184. Hospach A, Mauer G, Vaßen R, Stöver D (2012) Characteristics of ceramic coatings made by thin film low pressure plasma spraying (LPPS-TF). J Therm Spray Technol 21(3–4):435–440
185. Muehlberger E, Meyer P (2009) LPPS – thin film processes: overview of origin and future possibilities. In: Marple BR, Hyland MM, Lau Y-C, Li C-J, Lima RS, Montavon G (eds) Thermal spray 2009: Proceedings of the international thermal spray conference. ASM International, Materials Park, OH, pp 737–740
186. Fauchais P, Montavon G, Lima RS, Marple BR (2011) Engineering a new class of thermal spray nano-based microstructures from agglomerated nanostructured particles, suspensions and solutions: an invited review. J Phys D Appl Phys 44:093001

187. Musil J, Alaya M, Oberacker R (1997) Plasma-sprayed duplex and graded partially stabilized zirconia thermal barrier coatings: deposition process and properties. J Therm Spray Technol 6 (4):449–455
188. Soechting FO (1999) A design perspective on thermal barrier coatings. J Therm Spray Technol 8(4):505–511
189. Beele W, Marijnissen G, van Lieshout A (1999) The evolution of thermal barrier coatings—status and upcoming solutions for today's key issues. Surf Coat Technol 120–121:61–67
190. Gupta M, Curry N, Nylén P, Markocsan N, Vaßen R (2012) Design of next generation thermal barrier coatings — experiments and modeling. Surf Coat Technol 220:20–26
191. Cao XQ, Vaßen R, Stöver D (2004) Ceramic materials for thermal barrier coatings. J Eur Ceram Soc 24:1–10
192. Haynes JA, Ferber MK, Porter WD (2000) Thermal cycling behavior of plasma-sprayed thermal barrier coatings with various MCrAIX bond coats. J Therm Spray Technol 9 (1):38–48
193. Hamacha R, Fauchais P, Nardou E (1996) Influence of dopant on the behaviour under thermal cycling of two plasma sprayed zirconia coatings, Part 1: Relationship between powder characteristics and coating properties. J Therm Spray Technol 5(4):431–438
194. Ma B, Li Y, Su K (2009) Characterization of ceria–yttria stabilized zirconia plasma-sprayed coatings. Appl Surf Sci 255:7234–7237
195. Markocsan N, Nylén P, Wigren J, Li X-H (2007) Low thermal conductivity coatings for gas turbine applications. J Therm Spray Technol 16(4):498–505
196. Curry N, Donoghue J (2012) Evolution of thermal conductivity of dysprosia stabilised thermal barrier coating systems during heat treatment. Surf Coat Technol 209:38–43
197. Chen X, Zou B, Wang Y, Ma H, Cao X (2011) Microstructure and thermal cycling behavior of air plasma-sprayed YSZ/LaMgAl11O19 composite coatings. J Therm Spray Technol 20 (6):1328–1338
198. Chen X, Gu L, Zou B, Wang Y, Cao X (2012) New functionally graded thermal barrier coating system based on LaMgAl11O19/YSZ prepared by air plasma spraying. Surf Coat Technol 206:2265–2274
199. Jarligo MO, Mack DE, Vaßen R, Stöver D (2009) Application of plasma-sprayed complex perovskites as thermal barrier coatings. J Therm Spray Technol 18(2):187–193
200. Ma W, Jarligo MO, Mack DE, Pitzer D, Malzbender J, Vaßen R, Stöver D (2008) New generation perovskite thermal barrier coating materials. J Therm Spray Technol 17 (5–6):831–837
201. Yu J, Zhao H, Zhou X, Tao S, Ding C (2011) Effect of thermal aging on microstructure and mechanical properties of plasma-sprayed samarium zirconate coatings. J Therm Spray Technol 20(5):1056–1062
202. Xie XY, Guo HB, Gong SK (2010) Mechanical properties of $LaTi_2Al_9O_{19}$ and thermal cycling behaviors of plasma-sprayed $LaTi_2Al_9O_{19}$/YSZ thermal barrier coatings. J Therm Spray Technol 19(6):1179–1185
203. Guo H, Zhang H, Ma G, Gong S (2009) Thermo-physical and thermal cycling properties of plasma-sprayed $BaLa_2Ti_3O_{10}$ coating as potential thermal barrier materials. Surf Coat Technol 204:691–696
204. Liu Y, Gao YF, Tao SY, Zhou XM, Li WD, Luo HJ, Ding CX (2008) Microstructure of plasma sprayed La_2O_3-modified YSZ coatings. J Therm Spray Technol 17(5–6):603–607
205. Paul S, Cipitria A, Golosnoy IO, Xie L, Dorfman MR, Clyne TW (2007) Effects of impurity content on the sintering characteristics of plasma-sprayed zirconia. J Therm Spray Technol 16(5–6):798–803
206. Mihm S, Duda T, Gruner H, Thomas G, Dzur B (2012) Method and process development of advanced atmospheric plasma spraying for thermal barrier coatings. J Therm Spray Technol 21(3–4):400–408

207. Tan Y, Srinivasan V, Nakamura T, Sampath S, Bertrand P, Bertrand G (2012) TBC optimizing compliance and thermal conductivity of plasma sprayed thermal barrier coatings via controlled powders and processing strategies. J Therm Spray Technol 21(5):950–962
208. Guo HB, Vaßen R, Stöver D (2004) Atmospheric plasma sprayed thick thermal barrier coatings with high segmentation crack density. Surf Coat Technol 186:353–363
209. Zhu D, Choi SR, Miller RA (2004) Development and thermal fatigue testing of ceramic thermal barrier coatings. Surf Coat Technol 188–189:146–152
210. Shin I-H, Koo J-M, Seok C-S, Yang S-H, Lee T-W, Kim B-S (2011) Estimation of spallation life of thermal barrier coating of gas turbine blade by thermal fatigue test. Surf Coat Technol 205:S157–S160
211. Kim D-J, Shin I-H, Koo J-M, Seok C-S, Lee T-W (2010) Failure mechanisms of coin-type plasma-sprayed thermal barrier coatings with thermal fatigue. Surf Coat Technol 205: S451–S458
212. Jang H-J, Park D-H, Junga Y-G, Jang J-C, Choi S-C, Pai U (2006) Mechanical characterization and thermal behavior of HVOF-sprayed bond coat in thermal barrier coatings (TBCs). Surf Coat Technol 200:4355–4362
213. Li Y, Li C-J, Yang G-J, Xing L-K (2010) Thermal fatigue behavior of thermal barrier coatings with the MCrAlY bond coats by cold spraying and low-pressure plasma spraying. Surf Coat Technol 205:2225–2233
214. von Niessen K, Gindrat M, Refke A (2010) Vapor phase deposition using plasma spray-PVD™. J Therm Spray Technol 19(1–2):502–509
215. Gell M, Jordan EH, Teicholz M, Cetegen BM, Padture N, Xie L, Chen D, Ma X, Roth J (2008) Thermal barrier coatings made by the solution precursor plasma spray process. J Therm Spray Technol 17(1):124–135
216. Mutasim Z, Brentnall W (1997) Thermal barrier coatings for industrial gas turbine applications: an industrial note. J Therm Spray Technol 6(1):105–108
217. Nelson WA, Orenstein RM (1997) Land based gas turbines TBC experience in land-based gas turbines. J Therm Spray Technol 6(2):176–180
218. Parks WP, Hoffman EE, Lee WY, Wright IG (1997) Thermal barrier coatings issues in advanced land-based gas turbines. J Therm Spray Technol 6(2):187–192
219. Tamura M, Takahashi M, Ishii J, Suzuki K, Sato M, Shimomur K (1999) Multilayered thermal barrier coating for land-based gas turbines. J Therm Spray Technol 8(1):68–72
220. Wright IG, Gibbons TB (2007) Recent developments in gas turbine materials and technology and their implications for syngas firing. Int J Hydrogen Energy 32:3610–3621
221. Lebedev AS, Kostennikov SV (2008) Trends in increasing gas-turbine units efficiency. Therm Eng 55(6):461–468
222. Pomeroy MJ (2005) Coatings for gas turbine materials and long-term stability issues. Mater Design 26:223–231
223. Curry N, Markocsan N, Li X-H, Tricoire A, Dorfman M (2011) Next generation thermal barrier coatings for the gas turbine industry. J Therm Spray Technol 20(1–2):108–115
224. Beardsley MB (1997) Thick thermal barrier coatings for diesel engines. J Therm Spray Technol 6(2):181–186
225. Ahmaniemi S, Tuominen J, Vuoristo P, Mäntylä T (2002) Sealing procedures for thick thermal barrier coatings. J Therm Spray Technol 11(3):320–332
226. Hejwowski T, Weronski A (2002) The effect of thermal barrier coatings on diesel engine performance. Vacuum 65:427–432
227. Buyukkaya E, Cerit M (2007) Thermal analysis of a ceramic coating diesel engine piston using 3-D finite element method. Surf Coat Technol 202:398–402
228. Parlak A, Yasar H, Eldogan O (2005) The effect of thermal barrier coating on a turbo-charged diesel engine performance and exergy potential of the exhaust gas. Energy Convers Manag 46:489–499
229. İşcan B, Aydın H (2012) Improving the usability of vegetable oils as a fuel in a low heat rejection diesel engine. Fuel Process Technol 98:59–64

230. Pulci G, Tului M, Tirillo J, Marra F, Lionetti S, Valente T (2011) High temperature mechanical behavior of UHTC coatings for thermal protection of re-entry vehicles. J Therm Spray Technol 20(1–2):139–144
231. Davis JB, Marshall DB, Oka KS, Housley RM, Morgan PED (1999) Ceramic composites for thermal protection systems. Composites A 30:483–488
232. Fan X, Liu Y, Xu Z, Wang Y, Zou B, Gu L, Wang C, Chen X, Khan ZS, Yang D, Cao X (2011) Preparation and characterization of 8YSZ thermal barrier coatings on rare earth-magnesium alloy. J Therm Spray Technol 20(4):948–957
233. Huang W, Fan X, Zhao Y, Zhou X, Meng X, Wang Y, Zou B, Cao X, Wang Z (2012) Fabrication of thermal barrier coatings onto polyimide matrix composites via air plasma spray process. Surf Coat Technol 207:421–429
234. Cojocaru CV, Wang Y, Moreau C, Lima RS, Mesquita-Guimarães J, Garcia E, Miranzo P, Osendi MI (2011) Mechanical behavior of air plasma-sprayed YSZ functionally graded mullite coatings investigated via instrumented indentation. J Therm Spray Technol 20 (1–2):101–107
235. Suzuki M, Sodeoka S, Inoue T (2008) Zircon-based ceramics composite coating for zircon-based ceramics composite. J Therm Spray Technol 17(3):404–409
236. Ma X, Matthews A (2009) Evaluation of abradable seal coating mechanical properties. Wear 267:1501–1510
237. Johnston RE (2011) Mechanical characterization of AlSi-hBN, NiCrAl-Bentonite, and NiCrAl-Bentonite-hBN freestanding abradable coatings. Surf Coat Technol 205:3268–3273
238. Rajendran R (2012) Gas turbine coatings – an overview. Eng Fail Anal 26:355–369
239. Ma X, Matthews A (2007) Investigation of abradable seal coating performance using scratch testing. Surf Coat Technol 202:1214–1220
240. Bardi U, Giolli C, Scrivani A, Rizzi G, Borgioli F, Fossati A, Partes K, Seefeld T, Sporer D, Refke A (2008) Development and investigation on new composite and ceramic coatings as possible abradable seals. J Therm Spray Technol 17(5–6):805–811
241. Steinke T, Mauer G, Vaßen R, Stöver D, Roth-Fagaraseanu D, Hancock M (2010) Process design and monitoring for plasma sprayed abradable coatings. J Therm Spray Technol 19 (4):756–764
242. Sporer D, Dorfman M, Xie L, Refke A, Giovannetti I, Giannozzi M (2007) Processing and properties of advanced ceramic abradable coatings. In: Marple MR, Hyland MM, Lau Y-C, Li C-J, Lima RS, Montavon G (eds) Thermal spray 2007: global coating solutions. ASM International, Materials Park, OH, pp 495–500
243. Stringer J, Marshall MB (2012) High speed wear testing of an abradable coating. Wear 294–295:257–263
244. Faraoun HI, Grosdidier T, Seichepine J-L, Goran D, Aourag H, Coddet C, Zwick J, Hopkins N (2006) Improvement of thermally sprayed abradable coating by microstructure control. Surf Coat Technol 201:2303–2312
245. Johnston RE (2009) The sensitivity of abradable coating residual stresses to varying material properties. J Therm Spray Technol 101318(5–6):1004–1013
246. Bounazef M, Guessasmaa S, Ait Saadi B (2004) The wear, deterioration and transformation phenomena of abradable coating BN–SiAl–bounding organic element, caused by the friction between the blades and the turbine casing. Mater Lett 58:3375–3380
247. Dowson P, Walker MS, Watson AP (2004) Development of abradable and rub-tolerant seal materials for application in centrifugal compressors and steam turbines. Seal Technol Dec:5–10
248. Lekatou A, Regoutas E, Karantzalis AE (2008) Corrosion behaviour of cermet-based coatings with a bond coat in 0.5 M H_2SO_4. Corros Sci 50:3389–3400
249. Yılmaz S (2009) An evaluation of plasma-sprayed coatings based on Al_2O_3 and Al_2O_3–13 wt. % TiO_2 with bond coat on pure titanium substrate. Ceram Int 35:2017–2022
250. Cho TY, Hong Yoon J, Young Cho J, Kon Joo Y, Ho Kang J, Zhang S, Gon Chun H, Young Hwang S, Chol Kwon S (2009) Surface properties and tensile bond strength of HVOF thermal

spray coatings of WC-Co powder onto the surface of 420J2 steel and the bond coats of Ni, NiCr, and Ni/NiCr. Surf Coat Technol 203:3250–3253
251. Schulz U, Fritscher K, Ebach-Stahl A (2008) Cyclic behavior of EB-PVD thermal barrier coating systems with modified bond coats. Surf Coat Technol 203:449–455
252. Zhao X, Xiao P (2008) Effect of platinum on the durability of thermal barrier systems with a $\gamma+\gamma'$ bond coat. Thin Solid Films 517:828–834
253. Tang F, Schoenung JM (2005) Local accumulation of thermally grown oxide in plasma-sprayed thermal barrier coatings with rough top-coat/bond-coat interfaces. Scr Mater 52:905–909
254. Chen WR, Irissou E, Wu X, Legoux J-G, Marple BR (2011) The oxidation behavior of TBC with cold spray CoNiCrAlY bond coat. J Therm Spray Technol 20(1–2):132–138
255. Das S, Datta S, Basu D, Das GC (2009) Glass–ceramics as oxidation resistant bond coat in thermal barrier coating system. Ceram Int 35:1403–1406
256. Lu Y-P, Li M-S, Li S-T, Wang Z-G, Zhu R-F (2004) Plasma-sprayed hydroxyapatite-titania composite bond coat for hydroxyapatite coating on titanium substrate. Biomaterials 25:4393–4403
257. Goller G (2004) The effect of bond coat on mechanical properties of plasma sprayed bioglass-titanium coatings. Ceram Int 30:351–355
258. Guanhong S, Xiaodong H, Jiuxing J, Yue S (2011) Parametric study of Al and Al_2O_3 ceramic coatings deposited by air plasma spray onto polymer substrate. Appl Surf Sci 257:7864–7870
259. Liu A, Guo M, Gao J, Zhao M (2006) Influence of bond coat on shear adhesion strength of erosion and thermal resistant coating for carbon fiber reinforced thermosetting polyimide. Surf Coat Technol 201:2696–2700
260. Beauvais S, Guipont V, Jeandin M, Juve D, Treheux D, Robisson A, Saenger R (2005) Influence of defect orientation on electrical insulating properties of plasma-sprayed alumina coatings. J Electroceram 15:65–74
261. Toma F-L, Scheitz S, Berger L-M, Sauchuk V, Kusnezoff M, Thiele S (2011) Comparative study of the electrical properties and characteristics of thermally sprayed alumina and spinel coatings. J Therm Spray Technol 20(1–2):195–204
262. Toma F-L, Berger L-M, Scheitz S, Langner S, Rödel C, Potthoff A, Sauchuk V, Kusnezoff M (2012) Comparison of the microstructural characteristics and electrical properties of thermally sprayed Al_2O_3 coatings from aqueous suspensions and feedstock powders. J Therm Spray Technol 21(3–4):480–488
263. Kim H-J, Odoul S, Lee C-H, Kweon Y-G (2001) The electrical insulation behavior and sealing effects of plasma-sprayed alumina-titania coatings. Surf Coat Technol 140:293–301
264. Prudenziati M, Gualtieri ML (2008) Electrical properties of thermally sprayed Ni- and Ni20Cr-based resistors. J Therm Spray Technol 17(3):385–394
265. Prudenziati M, Cirri G, Dal Bo P (2006) Novel high-temperature reliable heaters in plasma spray technology. J Therm Spray Technol 15(3):329–331
266. Prudenziati M (2008) Development and the implementation of high-temperature reliable heaters in plasma spray technology. J Therm Spray Technol 17(2):234–243
267. Gärtner F, Stoltenhoff T, Schmidt T, Kreye H (2006) The cold spray process and its potential for industrial applications. J Therm Spray Technol 15(2):223–232
268. Marx S, Paul A, Köhler A, Hüttl G (2006) Cold spraying: innovative layers for new applications. J Therm Spray Technol 15(2):177–183
269. Wu X-K, Zhang J-S, Zhou X-L, Cui H, Liu J-C (2012) Advanced cold spray technology: deposition characteristics and potential applications. Sci China Technol Sci 55(2):357–368
270. Gui M, Kang SB, Euh K (2004) Al-SiC powder preparation for electronic packaging aluminum composites by plasma spray processing. J Therm Spray Technol 13(2):214–222
271. Yamakawa O, Nihonmatsu H, Morisasa M, Hotta H (2009) Plasma sprayed ceramic tray members for firing ceramic capacitor. In: Marple BR, Hyland MM, Lau Y-C, Li C-J, Lima RS, Montavon G (eds) Thermal spray 2009: Proceedings of the international thermal spray conference. ASM International, Materials Park, OH, pp 624–627

272. Donner K-R, Gärtner F, Klassen T (2011) Metallization of thin Al_2O_3 layers in power electronics using cold gas spraying. J Therm Spray Technol 20(1–2):299–306
273. Lin KH, Xu ZH, Lin ST (2011) A study on microstructure and dielectric performances of alumina/copper composites by plasma spray coating. J Mater Eng Perform 20(2):231–237
274. Osbond P (1992) Plasma sprayed anti-reflection coatings for micro-wave optical components. Adv Mater 4:807–809
275. Lisjak D, Bégard M, Bruehl M, Bobzin K, Hujanen A, Lintunen P, Bolelli G, Lusvarghi L, Ovtar S, Drofenik M (2011) Hexaferrite/polyester composite coatings for electromagnetic-wave absorbers. J Therm Spray Technol 20(3):638–644
276. Rieger G, Wecker J, Rodewald W, Sattler W, Bach FW, Duda T, Unterberg W (2000) Nd-Fe-B permanent magnets (thick films) produced by a vacuum-plasma-spraying process. J Appl Phys 87(9):5329–5331
277. Sampath S (2010) Thermal spray applications in electronics and sensors: past, present, and future. J Therm Spray Technol 19(5):921–949
278. Voyer J, Schulz P, Schreiber M (2008) Electrically conductive flame sprayed aluminum coatings on textile substrates. J Therm Spray Technol 17(5–6):818–823
279. Geibel A, Froyen L, Delaey L, Leuven KU (1996) Plasma spray forming: an alternate route for manufacturing free-standing components. J Therm Spray Technol 5(4):419–430
280. Devasenapathi A, Ng HW, Yu SCM, Indra AB (2002) Forming near net shape free-standing components by plasma spraying. Mater Lett 57:882–886
281. Chráska P, Neufuss K, Herman H (1997) Plasma spraying of zircon. J Therm Spray Technol 6 (4):445–448
282. Neufuss K, Chráska P, Kolman B, Sampath S, Trávnícek Z (1997) Properties of plasma-sprayed freestanding ceramic parts. J Therm Spray Technol 6(4):434–438
283. Shi S, Hwang J-Y (2003) Plasma spray fabrication of near-net-shape ceramic objects. J Miner Mater Charact Eng 2(2):145–150
284. Patel RR, Keshri AK, Dulikravich GS, Agarwal A (2010) An experimental and computational methodology for near net shape fabrication of thin walled ceramic structures by plasma spray forming. J Mater Process Technol 210:1260–1269
285. Brožek V, Ctibor P, Cheong DI, Yang S-H (2009) Plasma spraying of zirconium carbide-hafnium carbide-tungsten cermets. Powder Metallurgy Prog 9:1–49
286. Helali M, Hashmi MSJ (1996) Production of free-standing objects by high velocity oxy-fuel (HVOF) thermal spraying process. J Mater Process Technol 56:431–438
287. Pattison J, Celotto S, Morgan R, Bray M, O'Neill W (2007) Cold gas dynamic manufacturing: a non-thermal approach to freeform fabrication. Int J Machine Tools Manuf 47:627–634
288. Chen JZ, Herman H, Safai S (1993) Evaluation of NiAI and NiAI-B deposited by vacuum plasma spray. J Therm Spray Technol 2(4):357–361
289. Saeidi S, Voisey KT, McCartney DG (2009) The effect of heat treatment on the oxidation behavior of HVOF and VPS CoNiCrAlY coatings. J Therm Spray Technol 18(2):209–216
290. Fan X, Ishigaki T (2001) Mo_5Si_3-B and $MoSi_2$ deposits fabricated by radio frequency induction plasma spraying. J Therm Spray Technol 10(4):611–617
291. Waki H, Kitamura T, Kobayashi A (2009) Effect of thermal treatment on high-temperature mechanical properties enhancement in LPPS, HVOF, and APS CoNiCrAlY coatings. J Therm Spray Technol 18(4):500–509
292. Chraska P, Neufuss K, Herman H (1997) Plasma spraying of zircon. J Therm Spray Technol 6 (4):445–448
293. Chen H, Gao Y, Luo H, Tao S (2011) Preparation and thermophysical properties of $La_2Zr_2O_7$ coatings by thermal spraying of an amorphous precursor. J Therm Spray Technol 20 (6):1201–1208
294. Henne R, Müller M, Proß E, Schiller G, Gitzhofer F, Boulos M (1999) Near-net-shape forming of metallic bipolar plates for planar solid oxide fuel cells by induction plasma spraying. J Therm Spray Technol 8(1):110–116

295. Agarwal A, McKechnie T, Seal S (2003) Net shape nanostructured aluminum oxide structures fabricated by plasma spray forming. J Therm Spray Technol 12(3):350–359
296. Laha T, Agarwal A, McKechnie T, Seal S (2004) Synthesis and characterization of plasma spray formed carbon nanotube reinforced aluminum composite. Mater Sci Eng A 381:249–258
297. Hussain T, McCartney DG, Shipway PH, Marrocco T (2011) Corrosion behavior of cold sprayed titanium coatings and free standing deposits. J Therm Spray Technol 20 (1–2):260–274
298. Herman H, Sampath S, Tiwari R, Neiser R (1994) Plasma spray forming of intermetallics and their composites. J Therm Spray Technol 3(3):295–296
299. Weiss LE, Prinz FB, Adams DA, Siewiorek DP (1992) Thermal spray shape deposition. J Therm Spray Technol 1(3):231–237
300. Yang Y, Oh N, Liu Y, Chen W, Oh S, Appleford M, Kim S, Kim K, Park S, Bumgardner J, Haggard W, Ong J (2006) Enhancing osseo-integration using surface-modified titanium implants. JOM 58:71–76
301. Ong JL, Appleford M, Oh S, Yang Y, Chen W-H et al (2006) The characterization and development of bioactive hydroxyapatite coatings. JOM 58(7):67–69
302. Gross KA, Walsh W, Swarts E (2004) Analysis of retrieved hydroxyapatite-coated hip prostheses. J Therm Spray Technol 13(2):190–199
303. Khor KA, Cheang P, Wang Y (1997) The thermal spray processing of HA powders and coatings. JOM Feb:51–57
304. Roy M, Bandyopadhyay A, Bose S (2011) Induction plasma sprayed nano hydroxyapatite coatings on titanium for orthopaedic and dental implants. Surf Coat Technol 205:2785–2792
305. Legoux J-G, Chellat F, Lima RS, Marple BR, Bureau MN, Shen H, Candeliere GA (2006) Development of osteoblast colonies on new bioactive coatings. J Therm Spray Technol 15 (4):628–633
306. Chang C, Shi J, Huang J, Hu Z, Ding C (1998) Effects of power level on characteristics of vacuum plasma sprayed hydroxyapatite coating. J Therm Spray Technol 7(4):484–488
307. Prevéy PS (2000) X-ray diffraction characterization of crystallinity and phase composition in plasma-sprayed hydroxyapatite coatings. J Therm Spray Technol 9(3):369–376
308. Khor KA, Yip CS, Cheang P (1997) Ti-6AI-4 hydroxyapatite composite coatings prepared by thermal spray techniques. J Therm Spray Technol 6(1):109–115
309. Wang Y, Khor KA, Cheang P (1998) Thermal spraying of functionally graded calcium phosphate coatings for biomedical implants. J Therm Spray Technol 7(1):50–57
310. Hasan S, Stokes J (2011) Design of experiment analysis of the Sulzer Metco DJ high velocity oxy-fuel coating of hydroxyapatite for orthopedic applications. J Therm Spray Technol 20 (1–2):186–194
311. Lima RS, Dimitrievska S, Bureau MN, Marple BR, Petit A, Mwale F, Antoniou J (2010) HVOF-sprayed Nano TiO_2-HA coatings exhibiting enhanced biocompatibility. J Therm Spray Technol 19(1–2):336–343
312. Lima RS, Li H, Khor KA, Marple BR (2006) Biocompatible nanostructured high-velocity oxyfuel sprayed titania coating: deposition, characterization, and mechanical properties. J Therm Spray Technol 15(4):623–627
313. Morks MF, Kobayashi A (2008) Development of ZrO_2/SiO_2 bioinert ceramic coatings for biomedical application. J Mech Behav Biomed Mater 1:165–171
314. Vitale-Brovarone C, Verné E (2005) SiO_2-CaO-K_2O coatings on alumina and Ti6Al4V substrates for biomedical applications. J Mater Sci Mater Med 16:863–871
315. Xie Y, Zheng X, Ding C, Zhai W, Chang J, Ji H (2009) Preparation and characterization of CaO-ZrO_2-SiO_2 coating for potential application in biomedicine. J Therm Spray Technol 18(4):678–685
316. Bolelli G, Cannillo V, Gadow R, Killinger A, Lusvarghi L, Rauch J (2009) Microstructural and in vitro characterisation of high-velocity suspension flame sprayed (HVSFS) bioactive glass coatings. J Eur Ceram Soc 29:2249–2257

317. Fernandez J, Gaona M, Guilemany JM (2007) Effect of heat treatments on HVOF hydroxyapatite coatings. J Therm Spray Technol 16(2):220–228
318. Yu L-G, Khor KA, Li H, Cheang P (2003) Effect of spark plasma sintering on the microstructure and in vitro behavior of plasma sprayed HA coatings. Biomaterials 24:2695–2705
319. Bellucci D, Bolelli G, Cannillo V, Gadow R, Killinger A, Lusvarghi L, Sola A, Stiegler N (2012) High velocity suspension flame sprayed (HVSFS) potassium-based bioactive glass coatings with and without TiO_2 bond coat. Surf Coat Technol 206:3857–3868
320. Liang Y, Xie Y, Ji H, Huang L, Zheng X (2010) Chemical stability and biological properties of plasma-sprayed CaO-SiO_2-ZrO_2 coatings. J Therm Spray Technol 19(6):1171–1178
321. Jeffery B, Peppler M, Lima RS, McDonald A (2010) Bactericidal effects of HVOF-sprayed nanostructured TiO_2 on Pseudomonas aeruginosa. J Therm Spray Technol 19(1–2):344–349
322. Sanpo N, Lu Tan M, Cheang P, Khor KA (2009) Antibacterial property of cold-sprayed HA-Ag/PEEK coating. J Therm Spray Technol 18(1):10–15
323. Sanpo N, Ming Ang S, Cheang P, Khor KA (2009) Antibacterial property of cold sprayed chitosan-Cu/Al coating. J Therm Spray Technol 18(4):600–608
324. Sahraoui T, Fenineche N-E, Montavon G, Coddet C (2004) Alternative to chromium: characteristics and wear behavior of HVOF coatings for gas turbine shafts repair (heavy-duty). J Mater Process Technol 152:43–55
325. Heydarzadeh SM, Ghadami F (2010) Comparative tribological study of air plasma sprayed WC–12% coating versus conventional hard chromium electro deposit. Tribol Int 43:882–886
326. Bolelli G, Cannillo V, Lusvarghi L, Ricco S (2006) Mechanical and tribological properties of electrolytic hard chrome and HVOF-sprayed coatings. Surf Coat Technol 200:2995–3009
327. Deng C, Liu M, Wu C, Zhou K, Song J (2007) Impingement resistance of HVAF WC-based coatings. J Therm Spray Technol 16(5–6):604–609
328. Guilemany JM, Espallargas N, Suegama PH, Benedetti AV, Fernández J (2005) High-velocity oxyfuel Cr_3C_2-NiCr replacing hard chromium coatings. J Therm Spray Technol 14 (3):335–341
329. Picas JA, Forna A, Matthäus G (2006) HVOF coatings as an alternative to hard chrome for pistons and valves. Wear 261:477–484
330. Staia MH, Suárez M, Chicot D, Lesage J, Iost A, Puchi-Cabrera ES (2012) Cr_2C_3–NiCr VPS thermal spray coatings as candidate for chromium replacement. Surf Coat Technol 220:225–231
331. Lu W, Wu Y, Zhang J, Hong S, Zhang J, Li G (2011) Microstructure and corrosion resistance of plasma sprayed Fe-based alloy coating as an alternative to hard chromium. J Therm Spray Technol 20(5):1063–1070
332. Abdi S, Lebaili S (2008) Alternative to chromium, a hard alloy powder NiCrBCSi (Fe) coatings thermally sprayed on 60CrMn4 steel. Phase and comportements. Phys Proc 2:1005–1014
333. Matthäus G, Henry J, Ackermann D (2009) Further developments in internal diameter HVOF application of WC-CoCr for hard chrome replacement in critical applications such as landing gear. In: Marple BR, Hyland MM, Lau Y-C, Li C-J, Lima RS, Montavon G (eds) Thermal spray 2009: Proceedings of the international thermal spray conference. ASM International, Materials Park, OH, pp 722–724
334. Krishnan N, Vardelle A, Legoux JG (2008) A life cycle comparison of hard chrome and thermal sprayed coatings: a case example of aircraft landing gears. In: Lugscheider E (ed) Thermal spray conference: Crossing the border. DVS, Dûsseldorf, e-Proc
335. Henne R (2007) Solid oxide fuel cells: a challenge for plasma deposition processes. J Therm Spray Technol 16(3):381–403
336. Takenoiri S, Kadokawa N, Koseki K (2000) Development of metallic substrate supported planar solid oxide fuel cells fabricated by atmospheric plasma spraying. J Therm Spray Technol 3639(3):360–363

337. Barthel K, Rambert S, Barthel S, Rambert S, Siegmann S (2000) Microstructure and polarization resistance of thermally sprayed composite cathodes for solid oxide fuel cell use. J Therm Spray Technol 9(3):343–347
338. Sun F, Zhang N, Liao H, Li J (2012) Effect of heat treatment temperature on performance of plasma-sprayed apatite-lanthanum silicate coatings as electrolytes for IT-SOFC. J Therm Spray Technol 21(6):1257–1267
339. Puranen J, Lagerbom J, Hyvärinen L, Kylmälahti M, Himanen O, Pihlatie M, Kiviaho J, Vuoristo P (2011) The structure and properties of plasma sprayed iron oxide doped manganese cobalt oxide spinel coatings for SOFC metallic interconnectors. J Therm Spray Technol 20(1–2):154–159
340. Harris J, Qureshi M, Kesler O (2012) Deposition of composite LSCF-SDC and SSC-SDC cathodes by axial-injection plasma spraying. J Therm Spray Technol 21(3–4):461–468
341. Shen Y, Alexandra V, Almeida B, François Gitzhofer (2011) Preparation of nanocomposite GDC/LSCF cathode material for IT-SOFC by induction plasma spraying. J Therm Spray Technol 20(1–2):145–153
342. Wang Y, Legoux J-G, Neagu R, Hui S, Marple BR (2012) Suspension plasma spray and performance characterization of half cells with NiO/YSZ anode and YSZ electrolyte. J Therm Spray Technol 21(1):7–15
343. Michaux P, Montavon G, Grimaud A, Denoirjean A, Fauchais P (2010) Elaboration of porous NiO/8YSZ layers by several SPS and SPPS routes. J Therm Spray Technol 19(1–2):317–327
344. Zotov N, Hospach A, Mauer G, Sebold D, Vaßen R (2012) Deposition of La12xSrxFe12yCoyO32d coatings with different phase compositions and microstructures by low-pressure plasma spraying-thin film (LPPS-TF) processes. J Therm Spray Technol 21 (3–4):441–447
345. Fedtke P, Wienecke M, Bunescu M-C, Barfels T, Deistung K, Pietrzak M (2004) Yttria-stabilized zirconia films deposited by plasma spraying and sputtering. J Solid State Electrochem 8:626–632
346. Gross KA, Tikkanen J, Keskinen J, Pitkänen V, Eerola M, Siikamaki R, Rajala M (1999) Liquid flame spraying for glass coloring. J Therm Spray Technol 8(4):583–589
347. Arcondéguy A, Grimaud A, Denoirjean A, Gasgnier G, Huguet C, Pateyron B, Montavon G (2007) Flame-sprayed glaze coatings: effects of operating parameters and feedstock characteristics onto coating structures. J Therm Spray Technol 16(5–6):978–990
348. Arcondéguy A, Gasgnier G, Montavon G, Pateyron B, Denoirjean A, Grimaud A, Huguet C (2008) Effects of spraying parameters onto flame-sprayed glaze coating structures. Surf Coat Technol 202:4444–4448
349. Blink J, Farmer J, Choi J, Saw C (2009) Applications in the nuclear industry for thermal spray amorphous metal and ceramic coatings. Metallurgical Mater Trans A 40A:1344–1354
350. Farmer JC, Choi J-S (2007) Criticality-control applications in the nuclear industry for thermal spray amorphous metal and ceramic coatings, UCRL-TR-234171. Lawrence Livermore National Laboratory, Aug 31, pp 1–7
351. Blink J, Choi J, Farmer J (2007) Applications in the nuclear industry for thermal spray amorphous metal and ceramic coatings, UCRL-CONF-232603. Lawrence Livermore National Laboratory, July 9, pp 1–14
352. Farmer J, Choi J, Saw C, Haslam J, Day D, Hailey P, Lian T, Rebak R, Perepezko J, Payer J, Branagan D, Beardsley B, D'Amato A, Aprigliano L (2009) Iron-based amorphous metals: high-performance corrosion-resistant material development. Metallurgical Mater Trans A 40A:1289–1305
353. Branagan D (2004) Properties of amorphous/partially crystalline coatings. US Patent 20040253381
354. Berard G, Brun P, Lacombe J, Montavon G, Denoirjean A, Antou G (2008) Influence of a sealing treatment on the behavior of plasma-sprayed alumina coatings operating in extreme environments. J Therm Spray Technol 17(3):410–419

355. Haslam JJ, Farmer JC, Hopper RW, Wilfinger KR (2005) Ceramic coatings for a corrosion-resistant nuclear waste container evaluated in simulated ground water at 90 °C. Metallurgical Mater Trans A 36A:1085–1095
356. Hardwicke CU, Lau Y-C (2013) Advances in thermal spray coatings for gas turbines and energy generation: a review. J Therm Spray Technol 22(5):564–576
357. Matejıcek J, Chraska P, Linke J (2007) Thermal spray coatings for fusion applications—review. J Therm Spray Technol 16(1):64–83
358. Longo FN (1992) Industrial guide–markets, materials, and applications for thermal-sprayed coatings. J Therm Spray Technol 1(2):143–145
359. Dorfman M, Sharma A (2013) Commentary challenges and strategies for growth of thermal spray markets: the six-pillar plan. J Therm Spray Technol Comment 22(5):559–563
360. Tucker RC (ed) (2013) ASM handbook, vol 5A: Thermal spray technology. ASM International, Materials Park, OH
361. Thintri Inc. (2013) Thermal spray wear coatings find growing markets and greater competition. Spraytime 20(1):1–36
362. Vetter J, Barbezat G, Crummenauer J, Avissar J (2005) Surface treatment selections for automotive applications. Surf Coat Technol 200:1962–1968
363. Barbezat G (2006) Application of thermal spraying in the automobile industry. Surf Coat Technol 201:2028–2031
364. Barbezat G (2005) Advanced thermal spray technology and coating for lightweight engine blocks for the automotive industry. Surf Coat Technol 200:1990–1993
365. Barbezat G (2003) Low-cost high-performance coatings produced by internal plasma spraying for the production of high efficiency engines. In: Moreau C, Marple B (eds) International thermal spray conference 2003. ASM International, Materials Park, OH, pp 139–142
366. Smyth RT, Anderson JC (1975) Production of resistors by arc plasma spraying. Electrocompon Sci Technol 2:135–145
367. Ducos M (2006) Evaluating the costs of thermal spraying, ALIDERTE course. ALIDERTE, Limoges (in French)
368. Nelson GM, Nychka JA, McDonald AG (2011) Flame spray deposition of titanium alloy-bioactive glass composite coatings. J Therm Spray Technol 20(6):1339–1351
369. Drnovšek N, Novak S, Dragin U, Čeh M, Gorenšek M, Gradišar M (2012) Bioactive glass enhances bone ingrowth into the porous titanium coating on orthopaedic implants. Int Orthop 36:1739–1745
370. Juhasz JA, Best SM (2012) Bioactive ceramics: processing, structures and properties. J Mater Sci 47:610–624
371. Landor I, Vavrik P, Sosna A, Jahoda D, Hahn H, Daniel M (2007) Hydroxyapatite porous coating and the osteointegration of the total hip replacement. Arch Orthop Trauma Surg 127 (2):81–89
372. Hamashima K (2007) Application of new boride cermet coating to forming of glass sheets. J Therm Spray Technol 16(1):32–33
373. Döring J-E, Hoebener F, Langer G (2008) Review of applications of thermal spraying in the printing industry in respect to OEMs. In: Lugscheider E (ed) Thermal spray conference: Crossing the border. DVS, Düsseldorf, e-Proc
374. Pawlowski L (1996) Technology of thermally sprayed anilox rolls: state of art, problems, and perspectives. J Therm Spray Technol 5(3):317–334
375. Lima RS, Marple BR (2005) Superior performance of high-velocity oxyfuel-sprayed nanostructured TiO_2 in comparison to air plasma-sprayed conventional Al_2O_3-13TiO_2. J Therm Spray Technol 14(3):397–404
376. Vuoristo P, Nylén P (2009) Industrial and research activities in thermal spray technology in the Nordic region of Europe. In: Marple BR, Hyland MM, Lau Y-C, Li C-J, Lima RS, Montavon G (eds) Thermal spray 2009: Proceedings of the international thermal spray conference. ASM International, Materials Park, OH, pp 517–522, e-Proc

377. Yoshiya A, Shigemura S, Nagai M, Yamanaka M (2009) Advances of thermal sprayed carbon roller in paper industry. In: Marple BR, Hyland MM, Lau Y-C, Li C-J, Lima RS, Montavon G (eds) Thermal spray 2009: Proceedings of the international thermal spray conference. ASM International, Materials Park, OH, pp 601–606
378. Nagai M, Shigemura S, Yoshiya A (2009) Thermal-sprayed CFRP roll with resistant to thermal shock and wear - for papermaking machine. In: Marple BR, Hyland MM, Lau Y-C, Li C-J, Lima RS, Montavon G (eds) Thermal spray 2009: Proceedings of the international thermal spray conference. ASM International, Materials Park, OH, pp 607–611
379. Iyengar RK (2009) Thermal spray coating for steel processing. Technovations International, Littleton, MA
380. Process Industries: Power, http://www.castolin.com
381. Kaushal G, Singh H, Prakash S (2011) High-temperature erosion-corrosion performance of high-velocity oxy-fuel sprayed Ni-20Cr coating in actual boiler environment. Metallurgical Mater Trans A 42(7):1836–1846
382. Espallargas N, Berget J, Guilemany JM, Benedetti AV, Suegama PH (2008) Cr_3C_2–NiCr and WC–Ni thermal spray coatings as alternatives to hard chromium for erosion–corrosion resistance. Surf Coat Technol 202:1405–1417
383. Wang B-Q, Verstak A (1999) Elevated temperature erosion of HVOF Cr_3C_2/TiC– NiCrMo cermet coating. Wear 233–235:342–351
384. Higuera HV, Belzunce Varela FJ, Carriles Menéndez A, Poveda Martinez S (2001) A comparative study of high-temperature erosion wear of plasma-sprayed NiCrBSiFe and WC–NiCrBSiFe coatings under simulated coal-fired boiler conditions. Tribol Int 34:161–169
385. Sidhu TS, Prakash S, Agrawal RD (2005) Studies on the properties of high-velocity oxy-fuel thermal spray coatings for higher temperature applications. Mater Sci 41(6):805–823
386. Sidhu HS, Sidhu BS, Prakash S (2006) Comparative characteristic and erosion behavior of NiCr coatings deposited by various high-velocity oxyfuel spray processes. J Mater Eng Perform 5(6):699–704
387. Sanz A (2001) Tribological behavior of coatings for continuous casting of steel. Surf Coat Technol 146–147:55–64
388. Gross KA, Kovalevskis A (1996) Mold manufacture with plasma spraying. J Therm Spray Technol 5(4):469–475
389. Weiss LE, Thuel DG, Schultz L, Prinz FB (1994) Arc-sprayed steel-faced tooling. J Therm Spray Technol 3(3):275–281
390. Kim H-J, Kweon Y-G (1996) The application of thermal sprayed coatings for pig iron ingot molds. J Therm Spray Technol 5(4):463–468
391. Gibbons GJ, Hansell RG (2006) Down-selection and optimization of thermal-sprayed coatings for aluminum mould tool protection and upgrade. J Therm Spray Technol 15(3):340–347
392. Khan FF, Bae G, Kang K, Na H, Kim J, Jeong T, Lee C (2011) Evaluation of die-soldering and erosion resistance of high velocity oxy-fuel sprayed MoB-based cermet coatings. J Therm Spray Technol 20(5):1022–1034
393. Maranho O, Rodrigues D, Boccalini M, Sinatora A (2009) Bond strength of multicomponent white cast iron coatings applied by HVOF thermal spray process. J Therm Spray Technol 18 (4):708–713
394. Seonga BG, Hwanga SY, Kima MC, Kimb KY (2001) Reaction of WC-Co coating with molten zinc in a zinc pot of a continuous galvanizing line. Surf Coat Technol 138:101–110
395. Huang XO, Wang RJ, Zhang TJ, Luo HJ, Lü YF (2007) Several application cases of thermal spraying technology on industrial components and its considerations. In: Marple BR, Hyland MM, Lau Y-C, Li C-J, Lima RS, Montavon G (eds) Thermal spray 2007: Global coating solutions. ASM International, Materials Park, OH, e-Proc
396. Vicenzi J, Marques CM, Bergmann CP (2008) Hot and cold erosive wear of thermal sprayed NiCr-based coatings: influence of porosity and oxidation. Surf Coat Technol 202:3688–3697
397. Bolelli G, Lusvarghi L, Giovanardi R (2008) A comparison between the corrosion resistances of some HVOF-sprayed metal alloy coatings. Surf Coat Technol 202:4793–4809

398. Godoya C, Lima MM, Castro MMR, Avelar-Batista JC (2004) Structural changes in high-velocity oxy-fuel thermally sprayed WC–Co coatings for improved corrosion resistance. Surf Coat Technol 188–189:1–6
399. Choa JE, Hwang SY, Kim KY (2006) Corrosion behavior of thermal sprayed WC cermet coatings having various metallic binders in strong acidic environment. Surf Coat Technol 200:2653–2662
400. Bolelli G, Giovnardi R, Lusvarghi L, Manfredini T (2006) Corrosion resistance of HVOF-sprayed coatings for hard chrome replacement. Corros Sci 48:3375–3397
401. Perry JM, Neville A, Wilson VA, Hodgkiess T (2001) Assessment of the corrosion rates and mechanisms of a WC-Co-Cr HVOF coating in static and liquid-solid impingement saline environments. Surf Coat Technol 137:43–51
402. Petrovicova E, Schadler LS (2002) Thermal spraying of polymers. Int Mater Rev 47 (4):169–190
403. Notomi A, Sakakibara N (2009) Recent application of thermal spray to thermal power plants. In: Marple BR, Hyland MM, Lau Y-C, Li C-J, Lima RS, Montavon G (eds) Thermal spray 2009: Proceedings of the international thermal spray conference. ASM International, Materials Park, OH, pp 1106–1111
404. Yilmaz R, Kurt AO, Demir A, Tatli Z (2007) Effects of TiO_2 on the mechanical properties of the Al_2O_3–TiO_2 plasma sprayed coating. J Eur Ceram Soc 27:1319–1323
405. Lathabai S, Ottmuller M, Fernandez I (1998) Solid particle erosion behaviour of thermal sprayed ceramic, metallic and polymer coatings. Wear 221:93–108
406. Lins VFC, Branco JRT, Diniz FRC, Brogan JC, Berndt CC (2007) Erosion behavior of thermal sprayed, recycled polymer and ethylene–methacrylic acid composite coatings. Wear 262:274–281
407. Berndt CC, Brogan JA, Montavon G, Claudon A, Coddet C (1998) Mechanical properties of metal- and ceramic-polymer composites formed via thermal spray consolidation. J Therm Spray Technol 7(3):337–339
408. Leivo E, Wilenius T, Kinos T, Vuoristo P, Mäntylä T (2004) Properties of thermally sprayed fluoropolymer PVDF, ECTFE, PFA and FEP coatings. Prog Org Coat 49:69–73
409. Zhang T, Gawne DT, Bao Y (1997) The influence of process parameters on the degradation of thermally sprayed polymer coatings. Surf Coat Technol 96:337–344
410. Chen H, Zhao H, Qu J, Shao H (1999) Erosion-corrosion of thermal-sprayed nylon coatings. Wear 233–235:431–435
411. Zhang G, Liao H, Cherigui M, Paulo Davim J, Coddet C (2007) Effect of crystalline structure on the hardness and interfacial adherence of flame sprayed (poly-ether–ether–ketone) coatings. Eur Polym J 43:1077–1082
412. Zhang G, Liao H, Yu H, Ji V, Huang W, Mhaisalkar SG, Coddet C (2006) Correlation of crystallization behavior and mechanical properties of thermal sprayed PEEK coating. Surf Coat Technol 200:6690–6695
413. Zhang C, Zhang G, Ji V, Liao H, Costil S, Coddet C (2009) Microstructure and mechanical properties of flame-sprayed PEEK coating remelted by laser process. Prog Org Coat 66:248–253
414. Sweet GK (1993) Applying thermoplastic/thermoset powder with a modified plasma system. In: Berndt CC, Bernicki F (eds) Proceedings of the 1993 national thermal spray conference. ASM International, Materials Park, OH, pp 381–384
415. Brogan JA, Margolies S, Sampath H, Herman CC, Berndt SD (1995) Adhesion of combustion-sprayed polymer coatings. In: Berndt CC, Sampath S (eds) Thermal spray science and technology. ASM International, Materials Park, OH, pp 521–526
416. Henne RH, Schitter C (1995) Plasma spraying of high performance thermoplastics. In: Berndt CC, Sampath S (eds) Thermal spray science and technology. ASM International, Materials Park, OH, pp 527–532
417. Ivosevic M, Coguill SL, Galbraith SL (2009) Polymer thermal spraying: a novel coating process. In: Marple BR, Hyland MM, Lau Y-C, Li C-J, Lima RS, Montavon G (eds) Thermal

spray 2009: Proceedings of the international thermal spray conference. ASM International, Materials Park, OH, pp 1078–1083
418. Song JX, Han YF, Li SS, Xiao CB (2005) Repair of NiCrAlYSi overlay coating on Ni3Al base alloy IC6. Intermetallics 13:351–355
419. Ducos M (1988) Plasma transferred arc reclamation. In: Laroche G, Orfeuil M (eds) Plasmas in industry. Dopee Diffusion, France, pp 251–262 (in French)
420. Isakaev E, Yablonsky A, Kogan A, Katarzhis V, Kutnov V, Ivanov P (1999) The repair of railway frogs using plasma sprayed coatings, heat and mass transfer under plasma conditions. Ann NY Acad Sci 891:231–235
421. Tapphorn R, Henness J, Gabel H (2009) Kinetic metallization-a repair process for damaged IVD-Al coatings, Mg, and Al alloy components. In: Marple BR, Hyland MM, Lau Y-C, Li C-J, Lima RS, Montavon G (eds) Thermal spray 2009: Proceedings of the international thermal spray conference. ASM International, Materials Park, OH, pp 261–266
422. Champagne VK (2008) The repair of magnesium rotorcraft components by cold spray. J Fail Anal Prevent 8:164–175
423. Kashirin A, Klyuev O, Buzdygar T, Shkodkin A (2007) DYMET technology evolution and application. In: Marple BR, Hyland MM, Lau Y-C, Li C-J, Lima RS, Montavon G (eds) Thermal spray 2007: Global coating solutions. ASM International, Materials Park, OH, pp 141–145
424. Guilemany JM, Torrell M, Miguel JR (2007) Properties of HVOF coating of Ni based alloy for MSWI boilers protection. In: Marple BR, Hyland MM, Lau Y-C, Li C-J, Lima RS, Montavon G (eds) Thermal spray 2007: Global coating solutions. ASM International, Materials Park, OH, pp 1115–1119, e-Proc
425. de Botton O (1988) Master of Science in Technology and Policy. MIT, Cambridge, MA
426. Ducos M, Durand JP (2001) Thermal coatings in Europe, a business perspective. In: Berndt CC, Khor KH, Lugscheider E (eds) Thermal spray 2001. ASM International, Materials Park, OH, pp 1267–1276
427. MAGETEX (n.d.) Thermal coatings in Europe: a business prospective. MAGETEX, Les bureaux de Sèvres, 2 rue Troyon, 92316 Sèvres
428. Wigren J, Kristina Täng (2007) Quality considerations for the evaluation of thermal spray coatings. J Therm Spray Technol 16(4):533–540
429. Lee C (2009) Market direction and application opportunities for T/S growth in Korea. In: Marple BR, Hyland MM, Lau Y-C, Li C-J, Lima RS, Montavon G (eds) Thermal spray 2009: Proceedings of the international thermal spray conference. ASM International, Materials Park, OH, pp 505–510, e-Proc
430. Sundararajan G, Mahajan YR, Joshi SV (2009) Thermal spraying in India: status and prospects. In: Marple BR, Hyland MM, Lau Y-C, Li C-J, Lima RS, Montavon G (eds) Thermal spray 2009: Proceedings of the international thermal spray conference. ASM International, Materials Park, OH, pp 511–516
431. Tani K, Nakahira H (1992) Status of thermal spray technology in Japan. J Therm Spray Technol 1(4):333–339
432. Nakahira A (2009) Current status and future prospect of thermal spray coating applications and coating service market of job shops in Japan. In: Marple BR, Hyland MM, Lau Y-C, Li C-J, Lima RS, Montavon G (eds) Thermal spray 2009: Proceedings of the international thermal spray conference. ASM International, Materials Park, OH, pp 499–504, e-Proc
433. Fukumoto M (2008) The current status of thermal spraying in Asia; Hwang SY Status of thermal spraying in Korea; Li C-J The current state of thermal spray activities in China; Tani K, Nakahira A The current status of thermal spray in Japan; Khor MKA Thermal spray activities in Singapore. J Therm Spray Technol 17(1): 5–13
434. de Munter AJ, Bult A, de Jong JA (2002) On the economical and environmental aspects of TSA coatings. In: Lugscheider E (ed) International thermal spray conference 2002. DVS, Düsseldorf, e-Proc

435. Celotto S, Pattison J, Ho JS, Johnson AN, O'Neill W (2007) The economics of the cold spray process. In: Champagne V (ed) Cold spray materials deposition process - fundamentals and applications. Woodhead, Sawston
436. Molz R, Hawley D (2007) A method of evaluating thermal spray process performance. In: Marple BR, Hyland MM, Lau Y-C, Li C-J, Lima RS, Montavon G (eds) Thermal spray 2007: Global coating solutions. ASM International, Materials Park, OH, e-Proc
437. Sacriste D, Goubot N, Dhers J, Ducos M, Vardelle A (2001) An evaluation of the electric arc spray and (HPPS) processes for the manufacturing of high power plasma spraying MCrAlY coatings. J Therm Spray Technol 10(2):352–358
438. Moign A, Vardelle A, Legoux JG, Themelis NJ (2009) LCA Comparison of electroplating and other thermal spray processes. In: Marple BR, Hyland MM, Lau Y-C, Li C-J, Lima RS, Montavon G (eds) Thermal spray 2009: Proceedings of the international thermal spray conference. ASM International, Materials Park, OH, pp 1207–1212, e-Proc
439. International Thermal Spray Association, What is thermal spray. http://www.thermalspray.org